

**Developing methods for profiling of cathinone derivatives
and elucidation of their metabolites formed in rat and
human hepatocytes**

A thesis presented for the degree of Doctor of Philosophy in Pharmaceutical
Sciences

By

Osama I. G. Khreit

Department of Pharmaceutical Science,
Strathclyde Institute of Biomedical and Pharmaceutical Science,
University of Strathclyde
161 Cathedral Street
Glasgow G4 0RE

2013

Author's declaration

The copyright of this thesis belongs to the author under the terms of the United Kingdom Copyrights Act as qualified by University of Strathclyde Regulations 3.50. Due acknowledgement must always be made to the use of any material contained in, or derived from this thesis.

(“And say: “My Lord! Increase me in knowledge.”)

Al Qur’an Surah 20: Verse 114

Abstract

The recent global increase in the abuse of 4'-methylmethcathinone (mephedrone, 3a) and related compounds has led to a requirement for full chemical characterisation of these products. In this thesis the synthesis and characterisation of the hydrobromide salts of two mephedrone derivatives: 4'-methyl-*N*-ethylcathinone (4-MEC, 3c) and 4'-methyl-*N*-benzylcathinone (4-MBC, 3d) is reported. These compounds were previously identified in samples of the “*legal high*” NRG-2. Additionally, the first fully validated chromatographic methods for the detection and quantitative analysis of these substances both in their pure form, and in the presence of a number of common adulterants used in illicit drug manufacture are reported.

(±)-mephedrone [4-MMC, 3a] is a synthetic “*legal high*”, with a classical cathinone structure similar to methcathinone. The *in vitro* metabolism of 4-MMC (3a) was investigated in freshly Sprague-Dawley rat hepatocytes to characterize the associated Phase I and II metabolites, 2×10^6 cells mL⁻¹ were incubated with 4-MMC (3a) The reaction mixture analysed on a (ZIC[®]-HILIC) column using LC-MS and LC-MS² on Orbitrap instruments; 4-MMC yielded seventeen metabolites. These metabolites were structurally characterized on the basis of accurate mass analyses and LCMS² fragmentation patterns and the major metabolic routes for 4-MMC(3a) determined to be *via* (i) oxidation of the 4'-methyl group and (ii) reduction of the β-keto moiety, with a range of Phase II metabolites also being formed including several glucuronides and acetates. The biotransformation of a modified 4'-trifluoromethyl-derivative (4-TFMMC, 3b) was also studied and showed significant differences in its metabolism compared to 4-MMC (3a). Key pharmacokinetic parameters for both drugs have been calculated [biological half-lives ($t_{1/2}$) for 4-MMC (3a) = 61.9 minutes and for 4-TFMMC = 203.8 minutes] and these data may aid in the understanding of *in vivo* metabolism and the likely pharmacokinetic effects of chemical/structural modifications within this class of controlled substances. The same procedure was carried out with 4'-methyl-*N*-ethylcathinone [4-MEC (3c)] and similar pathways were observed.

Cryopreserved human hepatocytes (0.5×10^6 cells mL⁻¹) were incubated with 4-MMC (3a) and 4-TFMMC (3b) to investigate the metabolic pathways in human cells. Using

the same analytical techniques, it was found that the metabolic pathways of *in vitro* cryopreserved human hepatocytes for 4-MMC (3a) and 4-TFMMC (3b) were similar to those of rat hepatocytes. However, human hepatocytes demonstrated slower metabolism and some metabolites were absent compared to the rat hepatocytes.

Table of Contents

<i>Author's declaration</i>	<i>I</i>
<i>Abstract</i>	<i>III</i>
<i>List of Tables</i>	<i>XII</i>
<i>List of Schemes</i>	<i>XIV</i>
<i>List of Figures</i>	<i>XV</i>
<i>Published and Proposed Contributions from this work</i>	<i>XX</i>
<i>Glossary</i>	<i>XXII</i>
<i>Acknowledgements</i>	<i>XXVI</i>
Chapter 1: General Introduction	1
1.1 Recreational Drug Use	1
1.2 Misuse of Drugs Act 1971	2
1.3 What are Legal Highs?	4
1.4 Legal Highs	5
1.6 Cathinone/methcathinone derived Legal Highs	8
1.6.1 Chemical structure of cathinone	11
1.6.2 Mechanisms of action of cathinone	17
1.6.3 Pharmacology of cathinone	19
1.5 Analytical methods for the detection and quantification of Cathinones ...	22
1.5.1 Presumptive test of cathinones	22
1.5.2 Analytical techniques.....	23
1.7 Identification of metabolic pathways of cathinone derivatives	31
1.8 The role of the liver in drug metabolism	37
1.9 Common Phase I and Phase II Metabolism Pathways	39
1.10 Instrumentation	42
1.10.1 High performance liquid chromatography system.....	42
1.10.2 Mass chromatography.....	45

1.10.3 Gas chromatography –mass chromatography	51
1.11 <i>In Silico</i> tools for data processing	52
1.11.1 SIEVE software	52
1.11.2 MetWorks (Thermo Fisher Scientific).....	54
1.11.3 ToxID Software	56
1.12 Metabolite detection methods.....	57
1.13 Aims and Objectives.....	61
<i>Chapter 2: Synthesis, full chemical characterisation and development of a validated HPLC method for the quantification of components found in the evolved “Legal high” NRG-2.....</i>	<i>62</i>
2.1 Introduction.....	62
2.2 Experimental.....	64
2.2.1 Synthesis of (±)-4'-methyl- <i>N</i> -methylcathinone hydrobromide (4-MMC, 3a)	66
2.2.2 Synthesis of (±)-4'-methyl- <i>N</i> -ethylcathinone hydrobromide (4-MEC, 3c).....	66
2.2.3 Synthesis of (±)-4'-methyl- <i>N</i> -benzylcathinone hydrobromide (4-MBC, 3d)	67
2.2.4 HPLC Instrumentation.....	68
2.2.5 Mobile Phase preparation	69
2.2.6 Preparation of Standard samples for HPLC.....	69
2.2.7 Analytical method validation.....	71
2.2.8 Using AT-IR spectroscopy to characterise NRG2, 4-MEC (3c) and 4-MBC (3d) samples	72
2.2.9 Ultraviolet-Visible Absorption measurements of 4-MEC (3c), 4-MBC (3d) and Nicotinamide	73
2.2.10 Liquid chromatography–electrospray mass spectrometry analysis	74
2.2.11 Nuclear Magnetic Resonance Spectroscopy	74
2.3 Results and discussion.....	75
2.3.1 The synthesis of reference substances	75
2.3.2 Structural elucidation	75

2.3.3 The HPLC development/analysis work	90
2.3.4 Re-development and validation of a HPLC method for the separation and identification ten of NRG-2 samples containing Cathinone derivatives and potential adulterants.....	100
2.4 Conclusions	114
<i>Chapter 3: Elucidation of the Phase I and Phase II metabolic pathways of (±)-4'-methylmethcathinone (4-MMC), (±)-4'-(trifluoromethyl) methcathinone (4-TFMMC) and (±)-4'-methyl-N-ethylcathinone (4-MEC) in rat liver hepatocytes using LC-MS and GC-MS</i>	<i>115</i>
3.1 Introduction	115
3.2 Experimental.....	119
3.2.1 Chemicals and Materials.....	119
3.2.2 Synthesis of (±)-4'-(trifluoromethyl) methcathinone hydrochloride (3b, 4-TFMMC) and ((±)-4'-(methyl) methcathinone hydrochloride (3a, 4-MMC)...	120
3.2.3 Biotransformation of 4-MMC (3a), 4-TFMMC (3b) and 4-MEC (3c) in Sprague-Dawley rat hepatocytes	122
3.2.4 Instrumentation	122
3.2.5 Solutions	124
3.2.6 Preparation of hepatocyte perfusion solutions.....	125
3.2.7 Isolation of hepatocytes	128
3.2.8 Viability and total live cell count.....	130
3.2.9 Incubation of 4-MMC (3a), 4-TFMMC (3b) and 4-MEC (3c) with freshly isolated rat hepatocytes	131
3.2.10 Hepatocyte incubation samples extracted by protein crash plates.....	133
3.2.11 Effects of 4-MMC and 4-TFMMC on Hepatocyte Viability.....	134
3.2.12 Effects of 4-MEC on Hepatocyte Viability	135
3.2.13 GC-MS Procedure for Identification of 4-MMC Metabolites.....	136
3.3 Results and Discussion	137
3.3.1 Synthesis of 4-MMC (3a), 4-TFMMC (3b).....	137
3.3.2 Using Multiple Mass Defect Filters for metabolite identification.....	137
3.3.3 Biotransformation of 4-MMC (3a) in Sprague-Dawley rat hepatocytes .	140

3.3.4 Biotransformation of 4-TFMMC (3b) in Sprague-Dawley rat hepatocytes	145
3.3.5 Biotransformation of 4-MEC (3c) in Sprague-Dawley rat hepatocytes ..	148
3.3.6 Metabolic profiling of 4-MMC (3a) and 4-TFMMC (3b)	153
3.3.7 Metabolic profiling of 4-MEC (3c)	157
3.3.8 LC/MS ⁿ	159
3.4 Structural elucidation of Hydroxylated metabolite of mephedrone by gas chromatography–mass spectrometry	162
3.4.1 GC-MS identification of metabolites.....	162
3.5 Conclusions	165
<i>Chapter 4: Metabolism of mephedrone and 4-TFMMC using cryopreserved human hepatocytes and analysed by LC-MS and LC-MS²</i>	<i>167</i>
4.1 Introduction	167
4.2 Chemicals and Materials	170
4.2.1 Chemicals.....	170
4.2.2 Incubation materials.....	170
4.2.3 Analytical materials and Equipment.....	171
4.3 Preparation of drug stock solutions.....	171
4.3.1 Stock solutions	171
4.4 Method and incubation protocol.....	171
4.4.1 Thawing and plating protocol	171
4.4.2 Viability of hepatocytes using Trypan Blue exclusion	172
4.4.3 The viability calculation	173
4.4.4 Incubation protocol	173
4.4.5 Effects of 4-MMC (3a) and 4-TFMMC (3b) on viability of cryopreserved human hepatocytes.....	175
4.4.6 Sample preparation for LC-MS	176
4.5 Results and discussion.....	177
4.5.1 Effects of cryopreservation of human hepatocytes on drug-metabolizing enzymes	177

4.5.2 Biotransformation of 4-MMC (3a) and 4-TFMMC (3b) in Cryopreserved human hepatocytes.....	181
4.5.3 Metabolic profiling of 4-MMC (3a) and 4-TFMMC (3b) in cryopreserved human hepatocytes.....	188
4.5.4 Comparison of major Phase I and Phase II metabolism reactions in Rat and Cryopreserved Human Hepatocytes	193
4.6 Conclusions	197
<i>Chapter 5: Summary and suggestions for Future work</i>	<i>199</i>
5.1 Summary	199
5.2 Future work	204
5.3 Final comments.....	205
<i>References.....</i>	<i>206</i>
<i>Appendices.....</i>	<i>220</i>
Appendix 1:	220
1.1 Scheme for the proposed fragmentation of metabolite13, fragmentation can be formed a conjugated indole.....	220
1.2 Scheme for the proposed fragmentation of metabolite14, fragmentation can be formed a conjugated indole.....	221
1.3 Scheme for the proposed fragmentation of metabolite16, fragmentation can be formed a conjugated indole.....	221
1.4 Scheme for the proposed fragmentation of metabolite35, fragmentation can be formed a conjugated indole.....	221
1.5 Scheme for the proposed fragmentation of metabolite36, fragmentation can be formed a conjugated indole.....	223
1.6 Scheme for the proposed fragmentation of metabolite43, fragmentation can be formed a conjugated indole.....	224
1.7 Scheme for the proposed fragmentation of metabolite48, fragmentation can be formed a conjugated indole.....	225
Appendix 2:	226

2.1 2D [¹ H, ¹ H] COSY NMR spectrum of (±)-4'-methyl-N-ethylcathinone hydrobromide.....	226
2.2 2D [¹ H, ¹ H] COSY NMR spectrum of (±)-4'-methyl-N-benzylcathinone hydrobromide.....	227
2.3 2D [¹ H, ¹ H] COSY NMR spectrum (expanded) of (±)-4'-methyl-N-benzylcathinone hydrobromide.....	228
Appendix 3: Calibration curve of common NRG-2 ingredients and adulterants injected six times at different concentrations.....	229
3.1 Calibration curve of 4-FMC (4c) (0.5 – 10 µg/mL)	229
3.2 Calibration curve of caffeine (0.5 – 10 µg/mL).....	229
3.3 Calibration curve of 4-MMC (3a) (0.5 – 10 µg/mL)	230
3.4 Calibration curve of 4-MEC (3c) (0.5 – 10 µg/mL)	230
3.5 Calibration curve of MDPV (7c) (2 – 40 µg/mL).....	231
3.6 Calibration curve of benzocaine (0.5 – 10 µg/mL).....	231
3.7 Calibration curve of 4-MBC (3d) (0.5 – 10 µg/mL).....	232
Appendix 4 :	233
4.1 ¹ H-NMR spectrum (d ₆ -DMSO, 60 °C) of (±)-4'-(trifluoromethyl) methcathinone hydrochloride (3b).....	233
4.2 ¹³ C-NMR spectrum (d ₆ -DMSO, 60 °C) of (±)-4'-(trifluoromethyl) methcathinone hydrochloride (3b).....	233
4.3 Expanded ¹³ C-NMR spectrum (d ₆ -DMSO, 60 °C, 110 – 140 ppm) of (±)-4'-(trifluoromethyl) methcathinone hydrochloride (3b).....	234
4.4 ¹⁹ F-NMR spectrum (d ₆ -DMSO, 60 °C) of (±)-4'-(trifluoromethyl) methcathinone hydrochloride (3b).....	234
4.5 HSQC spectrum (d ₆ -DMSO, 60 °C) of (±)-4'-(trifluoromethyl)methcathinone hydrochloride (3b)	235
4.6 HMBC spectrum (d ₆ -DMSO, 60 °C) of (±)-4'-(trifluoromethyl) methcathinone hydrochloride (3b).....	236
4.7 ATR-FTIR spectrum of (±)-4'-(trifluoromethyl)methcathinone hydrochloride (3b).....	236
4.8 (a) LRMS and (b) HRMS spectra of (±)-4'-(trifluoromethyl)methcathinone hydrochloride (3b)	237

4.9 UV spectra of (\pm)-4'-(trifluoromethyl)methcathinone hydrochloride (3b) in (a) EtOH: 3b, $c = 2.0 \times 10^{-3}$ g/100 mL; (b) H ₂ O: 3b, $c = 2.0 \times 10^{-3}$ g/100 mL; (c) 0.1 M aqueous HCl: 3b, $c = 2.0 \times 10^{-3}$ g/100 mL; (d) 0.1 M aqueous NaOH: 3b, $c = 2.0 \times 10^{-3}$ g/100 mL.	237
Appendix 5	238
Schematic setup of the perfusion equipment (Obtained from Dr. Mark Jairaj Thesis 2002).....	238

List of Tables

Table 1. The penalties for possession of and dealing in illicit drugs depends on the class of drug involved	3
Table 2. Cases of toxicity due to self-reported mephedrone consumption	9
Table 3. Name of the cathinone derivatives	13
Table 4. Legal high products bought on UK-based websites	26
Table 5. Chemical reactions of Phase I and II metabolism	39
Table 6. Conjugation reactions of Phase II metabolism	41
Table 7. Example of common Phase I and II metabolism.	60
Table 8. ¹ H (400 MHz), ¹³ C (100 MHz) NMR spectral data and ¹ H- ¹³ C long-range correlations of (±)-4'-methyl- <i>N</i> -ethylcathinone.HBr (4-MEC, 3c)	80
Table 9. ¹ H (400 MHz), ¹³ C (100 MHz) NMR spectral data and ¹ H- ¹³ C long-range correlations of (±)-4'-methyl- <i>N</i> -benzylcathinone.HBr (4-MBC, 3d)	81
Table 10. Ultraviolet spectral data of (±)-4'-methyl- <i>N</i> -ethylcathinone.HBr (4-MEC) (3c) and (±)-4'-methyl- <i>N</i> -benzylcathinone.HBr (4-MBC) (3d)	90
Table 11. Summary of validation data for the quantification of (±)-mephedrone.HBr(3a), (±)-4'-methyl- <i>N</i> -ethylcathinone.HBr (4-MEC)(3c) and (±)-4'-methyl- <i>N</i> -benzylcathinone.HBr (4-MBC)(3d)	93
Table 12. Summary of validation data for the quantification of (±)-mephedrone.HBr (4-MMC) (3a), (±)-4'-methyl- <i>N</i> -ethylcathinone.HBr (4-MEC) (3c) and (±)-4'-methyl- <i>N</i> -benzylcathinone.HBr (4-MBC) (3d)	95
Table 13. Gradient program of methods (M1, M2 and M3)	105
Table 14 : Summary of validation data for the quantification of seven compounds	109
Table 15 : HPLC quantitation results of 10 NRG-2 products were purchased from the UK-based website	113
Table 16. Viability of hepatocytes (n=3) during the 2 hour treatment period with 100 μM 4-MMC (3a) and 4-TFMCC (3b).	135
Table 17. Viability of hepatocytes (n=3) during the 2 hour treatment period with 100 μM 4-MEC (3c).	135
Table 18. LC-MS Exactive Orbitrap data for metabolites of 4-MMC (3a) incubated with Sprague-Dawley rat liver hepatocytes (120 min)	141

Table 19. LC-MS Exactive Orbitrap data for metabolites of 4-TFMMC (3b) incubated with Sprague-Dawley rat liver hepatocytes (120 min).....	145
Table 20 : LC-MS Exactive Orbitrap data for metabolites of 4-MEC (3c) incubated with Sprague-Dawley rat liver hepatocytes (120 min)	151
Table 21 Personal and medical details of donors from whom hepatocytes were obtained.....	170
Table 22. Count viability of cryopreserved hepatocytes during the 2 hour incubation (n=4).....	175
Table 23. Profile activities of range of Phase I and Phase II reactions measured in hepatocytes isolated from two donors.....	177
Table 24: Expression of 13 CYP enzymes determined in the donor hepatocytes used in this study	179
Table 25 : LC-MS Exactive Orbitrap data for biotransformation of 4-MMC (3a) incubated with human hepatocytes (120 min)	184
Table 26. LC-MS Exactive Orbitrap data for biotransformation of 4-TFMMC (3b) incubated with human hepatocytes (120 min)	187
Table 27. Comparison the K_{met} and half-life for both 4-MMC and 4-TFMMC with human and rat hepatocytes.	193

List of Schemes

Scheme 1. Proposed scheme of Phase I metabolism of Benzedrone, Flephedrone (4c), Methedrone (9b) and Methylethcathinone (3c).....	35
Scheme 2. Proposed scheme of Phase I metabolism of 3,4-methylenedioxy-N-benzylcathinone, butylone (7b), ethylone (6b), methylone (5b) and pentylone (8b).....	36
Scheme 3. Proposed scheme of phase I metabolism of [a] dimethylcathinone (4d), and [b] naphyrone (5d).....	37
Scheme 4. <i>Reagents and Conditions:</i> (a) Br ₂ / HBr (48 % in water) / CH ₂ Cl ₂ / rt / 1h (99.6 %); (b) MeNH ₂ .HCl / NEt ₃ / CH ₂ Cl ₂ / rt / 24h; (c) EtNH ₂ .HCl / NEt ₃ / CH ₂ Cl ₂ / rt / 24h; (d) BnNH ₂ / CHCl ₃ / Δ / 24h; (e) HBr (33 % in AcOH) / AcOH / rt / 1h....	63
Scheme 5. Proposed fragmentation of 4'-methyl methyl-N-ethylcathinone.HBr (4-MEC, 3c) under ESI-MS conditions.	86
Scheme 6. Proposed fragmentation of 4'-methyl methyl-N-benzylcathinone.HBr (4-MBC, 3d) under ESI-MS conditions.....	87
Scheme 7. <i>Reagents and Conditions:</i> (a) Br ₂ / HBr (48 % in water) / CH ₂ Cl ₂ / rt / 1h (2a, 99.6 %; 2b, 99.8%); (b) MeNH ₂ .HCl / NEt ₃ / CH ₂ Cl ₂ / rt / 24h; (c) HCl (4 M in 1, 4-dioxane) / EtOH / rt / 1h	116
Scheme 8. Proposed scheme for the Phase I and II metabolism of (±)-mephedrone (4-MMC, 3a) in Sprague-Dawley rat liver hepatocytes.	142
Scheme 9. Proposed scheme for the Phase I and II metabolism of (±)-4'-trifluoromethyl)methcathinone (4-TFMMC, 3b) in Sprague-Dawley rat liver hepatocytes.....	146
Scheme 10. Proposed scheme for the Phase I and II metabolism of (±)-4'-methyl-N-ethylcathinone (4-MEC, 3c) in Sprague-Dawley rat liver hepatocytes	152
Scheme 11. Proposed scheme for the Phase I and II metabolism of (±)-mephedrone (4-MMC, 3a) in cryopreserved human hepatocytes.....	185
Scheme 12. Proposed scheme for the Phase I and II metabolism of (±)-4'-trifluoromethyl) methcathinone (4-TFMMC, 3b) in cryopreserved human hepatocytes.....	188

List of Figures

Figure 1. The number of new psychoactive substances reported via EWS from 2005 to 2011.....	5
Figure 2. Bupropion (9a) Chemical structure.	10
Figure 3. Chemical structure of MDMA (ecstasy) (1e) and Methylone (5b).	11
Figure 4. The relationship between cathinone and amphetamine	11
Figure 5. Chemical structure of some Alkylation derivatives of cathinone.....	12
Figure 6. Common sites for structure variation of cathinone, at R ¹ - R ⁵	13
Figure 7. A diagram of central nervous system chemical synapse	18
Figure 8. Chemical structure of methcathinone (4b).	21
Figure 9. Chemical ionisation and electron impact ionisation were obtained under GC conditions for three trifluoromethyl ring-substituted methcathinone compounds.....	25
Figure 10. GC separation of cathinones and <i>iso</i> -cathinones	28
Figure 11. Chemical structure of found in four capsules: (3a) mephedrone (6c) 2-fluoromethamphetamine, (6a) α -phthalimidopropiophenone and (7a) <i>N</i> -ethylcathinone	28
Figure 12. Chromatograms showed the correlation between the separation and the type of substituent nitrogen atoms of the 24 racemic cathinones	31
Figure 13. Proposed metabolic pathways for methylone (bk-MDMA) (5b), ethylone (bK-MDEA) (6b) and butylone (bk-MBDB) (7b)	33
Figure 14. Schematic diagram of a basic HPLC.	43
Figure 15. A Low pressure mixing system (one pump).....	44
Figure 16. High pressure mixing system (two pumps)	44
Figure 17. A scheme of ESI mechanism.....	47
Figure 18. Scheme of electron impact ionisation (EI)	48
Figure 19. Decomposition of a molecule under Electron Impact ionisation.....	49
Figure 20. Scheme of LTQ Orbitrap mass spectrometer	50
Figure 21. Schematic layout of Orbitrap bench-top mass spectrometer (Exactive) ..	51
Figure 22. Frame parameter using to frame peaks in three dimensional axes	53
Figure 23. Application of Sieve Software to identifying the difference between two sample groups.	54

Figure 24. MetWorks software work flow (a) seven-step procedure of Networks and (b) Multiple Mass Defect Filters (MMDF)	56
Figure 25. ToxID interface used to load LC-MS raw data	57
Figure 26. (a) ^1H NMR spectrum and (b) ^{13}C NMR spectrum of (\pm)-4'-methyl- <i>N</i> -ethylcathinone.HBr (4-MEC, 3c).....	77
Figure 27: 2D [^1H , ^{13}C] HMBC NMR spectrum of (\pm)-4'-methyl- <i>N</i> -ethylcathinone hydrobromide (4-MEC, 3c).....	78
Figure 28 : 2D [^1H , ^{13}C] HMQC NMR spectrum of (\pm)-4'-methyl- <i>N</i> -ethylcathinone hydrobromide (4-MEC, 3c).....	79
Figure 29: (a) ^1H NMR spectrum and (b) ^{13}C NMR spectrum of (\pm)-4'-methyl- <i>N</i> -benzylcathinone.HBr (4-MBC, 3d).....	82
Figure 30: 2D [^1H , ^{13}C] HMBC NMR spectrum of (\pm)-4'-methyl- <i>N</i> -benzylcathinone hydrobromide (4-MBC, 3d).	84
Figure 31: 2D [^1H , ^{13}C] HMQC NMR spectrum of (\pm)-4'-methyl- <i>N</i> -benzylcathinone hydrobromide (4-MBC, 3d).	84
Figure 32. HRESIMS spectra of (a) (\pm)-4'-methyl- <i>N</i> -ethylcathinone.HBr (4-MEC ,3c) and (b) (\pm)-4'-methyl- <i>N</i> -benzylcathinone.HBr (4-MBC, 3d).	86
Figure 33: ATR-FTIR spectrum of (\pm)-4'-methyl- <i>N</i> -ethylcathinone.HBr (4-MEC, 3c).....	88
Figure 34. ATR-FTIR spectrum of (\pm)-4'-methyl- <i>N</i> -benzylcathinone.HBr (4-MBC, 3d).	88
Figure 35. UV spectra of (\pm)-4'-methyl- <i>N</i> -ethylcathinone.HBr (3c, —) and (\pm)-4'-methyl- <i>N</i> -benzylcathinone.HBr (3d, ---).....	89
Figure 36 : Representative chromatograms of solutions containing: (\pm)-mephedrone.HBr (3a, 5 $\mu\text{g mL}^{-1}$); (\pm)-4'-methyl- <i>N</i> -ethylcathinone.HBr (4-MEC) (3c, 5 $\mu\text{g mL}^{-1}$); (\pm)-4'-methyl- <i>N</i> -benzylcathinone.HBr (4-MBC) (3d, 5 $\mu\text{g mL}^{-1}$)	91
Figure 37: Representative chromatograms of solutions containing: (\pm)-mephedrone.HBr (4-MMC) (3a, 5 $\mu\text{g mL}^{-1}$); (\pm)-4'-methyl- <i>N</i> -ethylcathinone.HBr(4-MEC) (3c, 5 $\mu\text{g mL}^{-1}$); (\pm)-4'-methyl- <i>N</i> -benzylcathinone.HBr (4-MBC) (3d, 5 $\mu\text{g mL}^{-1}$).....	92
Figure 38. Representative chromatograms of solutions containing: (a) (\pm)-mephedrone.HBr (4-MMC) (3a, 5 $\mu\text{g mL}^{-1}$); (b) (\pm)-4'-methyl- <i>N</i> -ethylcathinone.HBr	

(4-MEC) (3c, 5 $\mu\text{g mL}^{-1}$); (c) (\pm)-4'-methyl- <i>N</i> -benzylcathinone.HBr (4-MBC) (3d, 5 $\mu\text{g mL}^{-1}$) and (d) caffeine (5 $\mu\text{g mL}^{-1}$); (\pm)-mephedrone.HBr (4-MMC) (3a, 5 $\mu\text{g mL}^{-1}$), (\pm)-4'-methyl- <i>N</i> -ethylcathinone.HBr (4-MEC) (3c, 5 $\mu\text{g mL}^{-1}$), benzocaine (5 $\mu\text{g mL}^{-1}$) and (\pm)-4'-methyl- <i>N</i> -benzylcathinone.HBr (4-MBC) (3d, 5 $\mu\text{g mL}^{-1}$)	96
Figure 39. LC-MS analysis of three NRG-2 products.	97
Figure 40. ^1H NMR spectra of (a) NRG-2-A; (b) NRG-2-B and (c) NRG-2-C.	98
Figure 41. Representative chromatograms of solutions containing: (a) NRG-2-A (10 $\mu\text{g mL}^{-1}$); (b) NRG-2-B (10 $\mu\text{g mL}^{-1}$) and (c) NRG-2-C (10 $\mu\text{g mL}^{-1}$)	100
Figure 42. Representative chromatograms of solutions containing seven compounds (10 $\mu\text{g mL}^{-1}$)	102
Figure 43 : Representative chromatograms of solutions containing seven compounds (10 $\mu\text{g mL}^{-1}$)	103
Figure 44 : Representative chromatograms of solutions containing seven compounds (10 $\mu\text{g mL}^{-1}$)	103
Figure 45. Gradient HPLC chromatogram of the mixture of 7 standard samples at eluting gradient condition [M1; 30% MeOH(0 min) \rightarrow 40 % MeOH (7-15 min) \rightarrow 30% MeOH (18 min) \rightarrow ext. 30% MeOH (40 min)]	104
Figure 46. Gradient HPLC chromatogram of the mixture of 7 standard samples under gradient conditions (M2):30% MeOH (0 min) \rightarrow 46 % MeOH (4-10 min) \rightarrow 30% MeOH (20 min)]	106
Figure 47. Gradient HPLC chromatogram of optimised separation of the mixture of seven standard samples with eluting gradient conditions M3: 30% MeOH (0 min) \rightarrow 60 % MeOH (7 -12min) \rightarrow 30% MeOH (18 min)]	107
Figure 48. Representative chromatograms of solutions containing: (1) NRG-2-1 (10 $\mu\text{g mL}^{-1}$); (2) NRG-2-2 (10 $\mu\text{g mL}^{-1}$) ; (3) NRG-2-3 (10 $\mu\text{g mL}^{-1}$) ; (4) NRG-2-4 (10 $\mu\text{g mL}^{-1}$) ; (5) NRG-2-5 (10 $\mu\text{g mL}^{-1}$) ; (6) NRG-2-6 (10 $\mu\text{g mL}^{-1}$) ; (7) NRG-2-7 (10 $\mu\text{g mL}^{-1}$) ; (8) NRG-2-8 (10 $\mu\text{g mL}^{-1}$) ; (9) NRG-2-9 (10 $\mu\text{g mL}^{-1}$) ; (10) NRG-2-10 (10 $\mu\text{g mL}^{-1}$) obtained using gradient condition [30% methanol (0 min) \rightarrow 60 % methanol (7 -12min) \rightarrow 30% methanol (18 min)]	112
Figure 49. ZIC –HILIC column provides an ideal mechanism for the analysis of polar compounds	119
Figure 50. Apparatus used in perfusion technique	129

Figure 51. Diagram of surgical incisions	129
Figure 52. Rotor incubator apparatus.....	131
Figure 53. Schematic diagram illustrating isolation, incubation and extraction process of 4-MMC (3a), 4-TFMMC (3b) and 4-MEC (3c)	133
Figure 54 : Vacuum manifold which was used with the protein crash filter.	134
Figure 55. Application of Metwork software for the identification of 4-MMC (3a) metabolites in rat Hepatocytes	138
Figure 56. Application of Metwork software for the identification of 4-TFMMC(3b) metabolites in rat Hepatocytes	139
Figure 57. Application of Metwork software for the identification of 4-MEC (3c) metabolites in rat Hepatocytes	139
Figure 58. Extracted ion chromatograms of the minor metabolites (10, 11, 15, 19 and 22) of (±)-mephedrone (4-MMC, 3a).....	144
Figure 59. Extracted ion chromatograms of the minor metabolites (27, 29, 30 and 33) of (±)-4'-(trifluoromethyl) methcathinone (4-TFMMC, 3b)	147
Figure 60. Representative chromatogram obtained using Exactive LC/MS with sample of 4-MEC(3c) incubated in KH buffer	149
Figure 61. LC-MS analysis of the main 4-MEC metabolite	150
Figure 62 : Relative amounts of metabolites of (±)-mephedrone (4-MMC, 3a) formed after incubation with Sprague-Dawley rat liver hepatocytes (n = 3)	153
Figure 63. Relative amounts of metabolites of (±)-4'-(trifluoromethyl) methcathinone (4-TFMMC, 3b) formed after incubation with Sprague-Dawley rat liver hepatocytes (n = 3).....	154
Figure 64. Plot of the rate of decrease of (±)-mephedrone (4-MMC, 3a) and (±)-4'-(trifluoromethyl) methcathinone (4-TFMMC, 3b) concentrations during incubation with Sprague-Dawley rat liver hepatocytes (n = 3).	155
Figure 65. Relative amounts of metabolites of (±)-4'-methyl-N-ethylcathinone (4-MEC, 3c) formed after incubation with Sprague-Dawley rat liver hepatocytes	158
Figure 66 : Plot of the rate of decrease of (±)-4'-methyl-N-ethylcathinone concentration (3c, 4-MEC) during incubation with Sprague-Dawley rat liver hepatocytes (n = 3).....	159

Figure 67. MS ² fragmentation obtained on LTQ Orbitrap of hydroxylated mephedrone and hydroxylated 4-TFMMC.	160
Figure 68. Scheme for the proposed fragmentation of metabolite 31.....	161
Figure 69. EI mass spectra, structure and predominant fragmentation patterns of (a) 4-MMC (3a) (b) metabolite (7) (c) metabolite (16).	164
Figure 70. Counting hepatocytes using a Haemocytometer.....	172
Figure 71. The layout of 24-well plates	174
Figure 72 : CYP2D6 distribution in human hepatocytes of 196 donors	180
Figure 73. Selected ion chromatograms from LC-MS analysis and mass spectra of 4-MMC (3a) and 4-TFMMC (3b).	182
Figure 74. Relative amounts of metabolites of (±)-mephedrone (4-MMC, 3a) formed after incubation with human hepatocytes (n = 4).....	190
Figure 75. Relative amounts of metabolites of (±)-4 ⁷ -(trifluoromethyl) methcathinone (4-TFMMC, 3b) formed after incubation with human hepatocytes (n = 4).....	191
Figure 76. Plot of the rate of decrease of (±)-mephedrone (4-MMC, 3a) and (±)-4 ⁷ -(trifluoromethyl) methcathinone (4-TFMMC, 3b) concentrations during incubation with cryopreserved human hepatocytes (n = 4).	192
Figure 77. Extracted ion chromatograms of m/z 222.1224.....	195

Published and Proposed Contributions from this work

Khreit, O. I. G., C. Irving, et al. (2012). "Synthesis, full chemical characterisation and development of validated methods for the quantification of the components found in the evolved "legal high" NRG-2." *Journal of Pharmaceutical and Biomedical Analysis* 61(0): 122-135.

Khreit, O. I. G., M. H. Grant, et al. "Elucidation of the Phase I and Phase II metabolic pathways of (\pm)-4'-methylmethcathinone (4-MMC) and (\pm)-4'-(trifluoromethyl)methcathinone (4-TFMMC) in rat liver hepatocytes using LC-MS and LC-MS²." *Journal of Pharmaceutical and Biomedical Analysis* 72(2013)177-185.

Khreit, O. I. G., M. H. Grant, Henderson C., Wallace G., Jackson J. P., Watson D. G., Sutcliffe, O. B. "Elucidation of the Phase I and Phase II metabolic pathways of (\pm)-4'-methylmethcathinone (4-MMC) and (\pm)-4'-(trifluoromethyl)methcathinone (4-TFMMC) in cryopreserved human hepatocytes using LC-MS and LC-MS² ". (In prep.)

Glossary

3-BMAP	1-(3-Bromophenyl)-2-(methylamino)propan-1-one
μM	micromolar
μm	micrometer
4-FMC	4-Fluoromethcathinone
4-MBC	(±)-4'-methyl-N-benzylcathinone
4-MEC	(±)-4'-methyl-N-ethylcathinone
4-MMC	(±)-4'-methyl-N-methylcathinone (mephedrone)
4-TFMCC	(±)-4'-(trifluoromethyl) methcathinone
ACMD	Advisory Council on Misuse of Drugs
ADME	The absorption, distribution, metabolism, and excretion
amu	Atomic mass unit
APCI	Atmospheric Pressure Chemical Ionization
ATR-FTIR	Attenuated Total Reflectance- FTIR
bk	Beta-keto
bk-MBDB	β-keto-N-methyl-3, 4-benzodioxolylbutanamine (Butylone)
bk-MDEA	3, 4-Methylenedioxyethcathinone (Ethylone)
bk-MDMA	3, 4-Methylenedioxymethcathinone (Methylene)
BSA	Bovine Serum Albumin
CID	Collision induced dissociation
cm	centimeter
CYP	Cytochrome P 450
d6-DMSO	dimethyl sulfoxide (Deuterated DMSO)
EMCDDA	The European Monitoring Centre for Drugs and Drug Addiction
ESI	Electrospray Ionisation

EU	European Union
Europol	European police office
eV	electronvolt
EWS	The EU early-warning system
FMO	Flavin-containing monooxygenase
FTIR	Fourier Transform Infrared Spectroscopy
g	gram
GC-EI/CI-ion trap MS	Gas Chromatography-Electron Impact/chemical ionisation-ion trap Mass Spectrometry
GST	Glutathione-S-Transferase
HBSS	Hank's balanced salt solution
HEPES	N-[2-hydroxyethyl]piperazine-N'-[2-ethanesulphonic acid]
HLM	Human liver microsomes
HMBC	Heteronuclear Multiple Bond Coherence
HMQC	Heteronuclear Multiple Quantum Coherence
HPLC	High performance- Liquid Chromatography
HRESIMS	High resolution Electrospray Mass Spectrometry
i-PAP	12-(iso-propylamino)-1-phenylpropan-1-one
IR	Infrared
IU	International Unit
kV	Kilovolts
L	Liter
LCD	Lysergic Acid Diethylamide
LC-ESI-MS	Liquid Chromatography-Electrospray Ionisation -Mass Spectrometry
LC-MS	Liquid chromatography-Mass Spectrometry
LIT	Liner Ion Trap

LRMS	Low resolution mass spectrometry
MABP	α -methylamino-butyrophenone
MDMA	3, 4-methylenedioxy-N-methylamphetamine
MDPBP	3, 4-Methylenedioxy- α -pyrrolidinobutyrophenone
MDPV	Methylenedioxypropylvalerone
MDZ	Midazolam
MeOH	Methanol
mg	Milligram
mL	milliliters
mM	millimolar
mm	millimetre
MMDF	Multiple Mass Defect Filters
MOA	Monoamine oxidases
MOPPP	4-methoxy- α -pyrrolidinopropiophenone
MPBP	4-Methyl- α -pyrrolidino-butyrophenone
MPHP	4-Methyl- α -Pyrrolidinohexiophenone
MPPP	4-Methyl- α -pyrrolidinopropiophenone
Mpt.	Melting point
NADPH	Nicotinamide adenine dinucleotide phosphate-oxidase
NMR	Nuclear Magnetic Resonance Spectroscopy
PBS	Phosphate buffered saline
pmol	picomole
ppm	Part per million
psi	Pounds per square inch
RPM	Revolutions per minute
RSD	Relative standard deviation
rt	Room temperature

SD	Standard Deviation
SEM	Standard error of the mean
SNP	Single-nucleotide polymorphism
t-BAP	2-(tert-butylamino)-1-phenylpropan-1-one
TEST	Testosterone
UDP	Uridine diphosphate
UV	Ultra-Violet
ZIC-HILIC	Zwitterionic-Hydrophilic interaction liquid chromatography
α -PBP	α -Pyrrolidinobutiophenone
α -PVP	α -Pyrrolidinopentiophenone
β k-PMMA	4-Methoxymethcathinone (Methedrone)
β -naphyrone	1-naphthalen-2-yl-2-pyrrolidin-1-yl-pentaon-1-one

Acknowledgements

First of all, I thank my dear God for the blessings and unconditional love he has given me and my supervisors daily.

Second, I would like to express my deepest and sincerest gratitude to my supervisors Dr. David Watson, Professor Helen Grant, Professor Alexander Gray, and the first person who actually pushed me into this work: Dr. Oliver Sutcliffe who has been spending a lot of efforts and time on supervising me. I also have benefited from their guidance, great kindness and patience, and I wish to say a heartfelt thank you to all of them.

Thirdly, I would also like to thank technical staff, Ms Catherine Henderson (Bioengineering Lab) who has spent huge efforts in the field of hepatocytes preparations and incubations, Dr. Tang Zhang and Dr. Gavin Blackburn who helped me with their time with Mass spectrometry techniques. Many thanks also to Dr. John Igoli for his help in the NMR interpretation.

A special gratitude goes to my beloved family for their support .I thank my parents and brothers(especially to Akram) for their whole hearted love and encouragement, my wife and four kids , for their cooperation, without them , I do not think I could have finished the thesis on time.

My sincere thanks also go to all of closest classmate and co-workers in the laboratory, for their cooperation, assistance and helpful discussions.

Chapter 1: General Introduction

1.1 Recreational Drug Use

In the last few years, a number of synthetic substances, so-called legal recreational drugs, have become available on internet websites or in high street shops. These chemical substances, which have a structural similarity to many drugs of abuse (for example amphetamine) are claimed to be legal and can be used for the purpose of entertainment, pleasure and euphoria. However, many of the substances which are sold on the market have not been fully evaluated in terms of their biological activity and toxicology as such as the long term adverse effects on both health and society remain unknown. As the use of recreational drugs is now a major activity amongst young people in the UK, the reasons for users taking different drugs have been investigated [1]. The most popular reasons for using commonly abused recreational drugs such as ecstasy, amphetamine, cocaine and LSD are to keep users awake when out with friends, to promote an activity, to feel euphoric, to remain vigilant, and to feel intoxicated. The researchers concluded that the primary motivation for the use of these drugs was to experience their effects and promote social activity. It could be argued that the motivation for recreational drug use is different from that of a dependent user whose decision to use is motivated by addiction [1].

Siegel argues that it is human instinct to look for mind-altering substances (psychoactive substances) as a natural part of their biology and that they function as part of the human desire to satisfy hunger and thirst, and the need for housing, thus pursuit of intoxication by using mind-altering substances is considered to be the "Fourth Drive" after hunger, thirst and sexual activity [2].

In recent years, the method of supply for recreational drugs in the UK has changed, with increasing use of the internet to buy these drugs. The popular substances are referred to as "legal highs", which are widely used as recreational drugs. In addition, compounds being used as recreational drugs have also changed and drugs such as cathinones, piperazines and synthetic cannabinoids are being seen as convenient, cheap, and legal alternatives to illegal recreational substances. However, some of

these compounds were banned in the UK under the revision of Misuse of Drugs Act 1971, such as substituted cathinones which were banned in 2010, due to significant toxicity being associated with their use. In 2010, Davies *et al.* published a paper in which they described that piperazine (e.g. 1-methyl -4-benzylpiperazine (MBZP); 1-[3-trifluoromethyl) phenyl] piperazine (TFMPP); Chlorophenylpiperazine (CPP)) and cathinone based compounds (e.g. Mephedrone (4-MMC,3a) ; 3-Fluoromethcathione (3-FMC)) were widely available for purchase via the internet as legal high substances in 2009 in the UK over a six month time period, and their popularity has since increased dramatically. Many active ingredients of these compounds are changing, so that they remain legally purchased as recreational drugs in the UK because legislation cannot keep up with the development of new agents[3].

1.2 Misuse of Drugs Act 1971

The United Kingdom Parliament established an act for controlled and misused substances called the Misuse of Drugs Act in 1971, which represented work similar to the obligations under United Nations treaties which included the convention on Narcotic Drugs of 1961 [4], convention on Psychotropic Substances of 1971[5], and convention against Illicit Traffic in Narcotic Drugs and Psychotropics of 1988 [6]. The Misuse of Drugs Act states that it is an offence to possess a controlled drug ,to possess with intention to supply a controlled drug ,to offer or to supply a controlled drug , or to give permission to use a house or office to people who are taking a controlled drug [7].

According to this Act controlled drugs are classified under three categories, Class A, Class B, and Class C, and five schedules. Table 1 shows that the ranges of penalties for possession of a controlled drug, or possession with propose to supply are classified in a different way within each class of drug. Class A includes substances such as: ecstasy, heroin, cocaine, magic mushrooms, Class B such as: amphetamine, cannabis, pholcodine, and Class C such as: tranquilisers, ketamine and some painkillers. Therefore, the class A drugs are considered to be most dangerous and cause most harm ,thus this class attracts more serious penalties than the other two classes [7].

Table 1. The penalties for possession of and dealing in illicit drugs depends on the class of drug involved [7].

Offence	Class A	Class B	Class C
Possession	Up to seven years in prison / unlimited fine /both.	Up to five years in prison /unlimited fine /both.	Up to two years in prison /unlimited fine / both.
Dealing	Up to life in prison / unlimited fine / both.	Up to 14 years in prison / unlimited fine / both.	Up to 14 years in prison / unlimited fine / both.

Likewise, controlled drugs are also classified under five schedules as following:

Schedule 1: These substances are not used for medical purpose and are strictly controlled. They can only be supplied, or possessed under a special Home Office licence, for example ecstasy, cannabis, coca leaf, raw opium, magic mushrooms, mephedrone and all other cathinones.

Schedule 2 and 3: These substances are used for medical purpose under a doctor's prescription and are partly controlled. Schedule 2 drugs include amphetamines, cocaine, dihydrocodeine, Diconal[®] (Dipipanone and cyclizine tablets), heroin, methadone, morphine, opium in medicinal form, pethidine and Ritalin. Schedule 3 drugs include barbiturates, Rohypnol, temazepam and tranquillisers.

Schedule 4: These substances were recently divided into two parts. Part 1 includes minor tranquillizers which are illegal to possess without a prescription, and Part 2 includes anabolic steroids which can be legally possessed without a prescription but it is illegal to supply them to other people.

Schedule 5: The substances among this schedule are diluted or small dose preparations, non-injectable preparations of controlled drugs which are able to be sold over-the-counter at a pharmacy without a prescription and considered a minimal risk of misuse. They include some cough medications, anti-diarrhoea agents and mild painkillers, which are legally possessed by anyone without a prescription only from a

pharmacy, but the restriction of these substances is usually more often ignored than enforced.

In addition, under this Act a set of regulations called the Misuse of Drugs Regulations 2001, which came into force in 2002 were created. They provided the specific exemptions from the provisions of Misuse of Drugs Act 1971 permitted by a licence of the Secretary of State, which allow supply, production or possession of controlled drugs in compliance with the terms of the licence and with any conditions attached to licence. Furthermore, supply, possession and import or export of these kinds of controlled drugs under these licences is only for medical or scientific research purposes[8, 9].

1.3 What are Legal Highs?

"Legal highs" are compounds which contain psychoactive ingredients such as cathinone, piperazine and synthetic cannabinoids, and are abused by young people as psychostimulants at parties and clubs. Although the structure of the single chemical might be related to an illicit substance such as amphetamine, these products can be easily bought via the internet as "legal highs", often without legal control, and used as alternatives to the classical drugs of misuse, such as amphetamine, which is the most commonly abused drug worldwide[10-12]. Although most of the active ingredients of legal highs are controlled under the UK Misuse of Drugs Act 1971, after 16th April 2010 many of substances readily bought state on the websites or the packaging that they contain legal substances, and only after screening are they found to contain controlled substances. This fact is supported by Ramsey and co-workers who purchased six products from the internet and then analyzed them. Five of these products were found to contain at least one controlled substance. This illustrates that the purchasers of legal highs often receive limited or inaccurate information on the active ingredients for these products which are advertised as legal highs. In addition, some brand names of legal highs which can be bought from different website sources may contain different active ingredients. This would increase the risk of individuals purchasing legal highs that contain a controlled substances, as well as increasing the potential for significant toxicity associated with these substances [13].

Recently, a total of forty-nine new psychoactive substances were detected in the European Union in 2011 and reported via the information exchange mechanism. Figure 1 shows that the number of psychoactive substances reported via the EU early-warning system(EWS) in each year during the period from 2005 to 2011[14, 15], and the number of online shops advertising at least one of the psychoactive substances, increased from 314 in January 2011 to 690 in January 2012 [15].

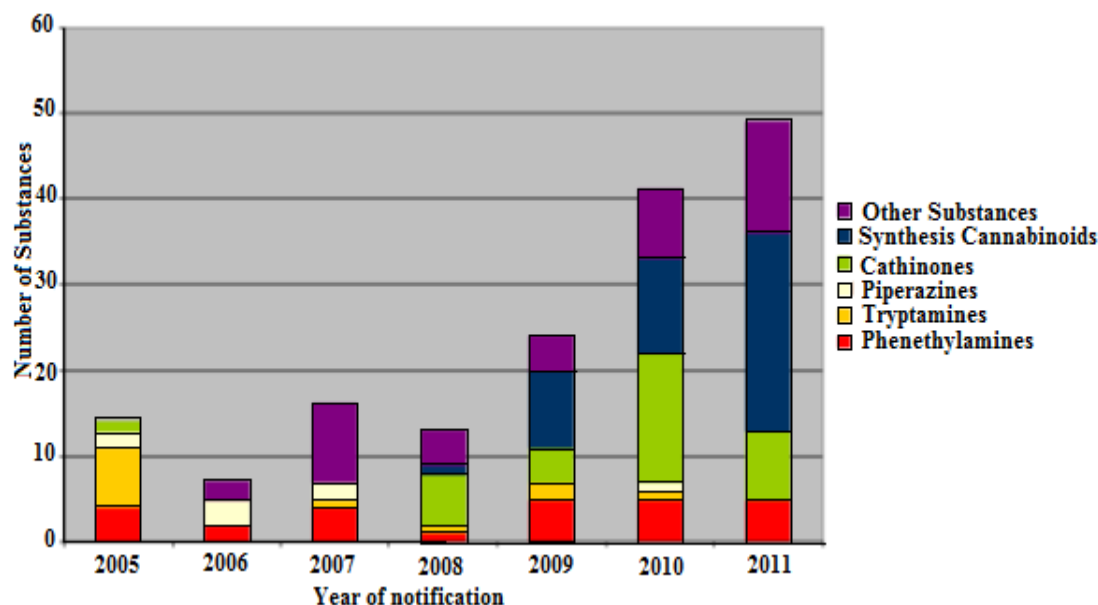


Figure 1.The number of new psychoactive substances reported via EWS from 2005 to 2011[15].

1.4 Legal Highs

Legal high substances have been designed as novel structures that create central nervous system activity, and are synthesized by adding or removing some functional groups from known pharmacologically active substances. These substances are usually sold over the internet and head shops (a retail outlet specializing in drug paraphernalia used for recreational drugs) in a variety of preparations (powders supplied in zip-lock plastic bags, capsules or tablets). Additionally, sometimes these substances are labeled “plant food”, “bath salts” or known as research only chemicals, since based on the literature, and drug discussion forums on the internet,

these substances are still an area of active research [13, 16, 17]. A number of studies have classified the legal high substances into four main chemical classes including ; cathinones , phenethylamines , tryptamines and piperazines [17].

Phenethylamines and tryptamines have increased in usage as recreational drugs after the famous books published by Alexander and Ann Shulgin titled “Phenethylamine I have known and Loved, 1991” and “Tryptamine I have known and Loved, 1997”. In addition, the ready availability of precursors and simple synthesis are suggested to be responsible for the increase in the use of these substances. Piperazine also emerged in the illegal drug market ten years ago, but the use of this drug is decreasing, and no new derivatives have been observed in the EU in the past two years [17]. In addition, cathinones were appearing at first in the EU in the middle of 2000s and bought via the internet and in certain head shops as “Legal highs”. They increased in use year by year, and have become more popular as recreational drugs.

Most potentially active substances are marketed as ‘legal’ due to the lack of documented evidence that has been provided. Thus, it is not possible to list every chemical under controlled substance legislation, and to list the substances that are misused according to drug legislation would require an extensive process[16, 17]. Despite the fact that using research chemicals within the illegal drug market is uncommon, and the persistency of the research generally brief, this research might be expressly raised when the consumers become intrigued about the related research[16]. Also, the proliferation of these new compounds emerges only after they are misused. Distribution of these new chemical products can be achieved easily via the internet, although there are differences in the legislation among the countries at the point of the supplier (Source) and the distribution system [16].

A report was presented by EMCDDA and Europol in 2011 that showed the list of new psychoactive substances in 2010 was dominated by synthetic cannabinoids and synthetic cathinones, as twenty-three and eight compounds of synthetic cannabinoids and cathinones respectively, formed two thirds of the total number of substances that were reported in 2011 [15].

Cathinones have been placed in the class C category under the UK's Misuse of Drugs Act 1971, however, in April 2010, many cathinone derivatives, such as mephedrone, were re-classified and placed in the class B category [18, 19].

There are other "legal highs", the pipradrol derivatives, which have appeared in the recreational drug market and these substances are a new class of synthetic stimulants closely related to pyrrolidine and piperidine compounds, the pipradrol derivatives also producing amphetamine like effects[14].

In addition, the information provided in internet sites to the user of legal highs on active substances that contain the legal highs is often limited and inaccurate, and does not remain constant over any time period [13, 20]. On the other hand, Davies and co-worker, during a six month survey, found that there was little variation in most of the legal highs which were supplied. However, there was variation in the content of active ingredients in a quarter of the products supplied and this is possibly responsible for significant toxicity and adverse effects associated with piperazine and cathinone[3].

Surveys of drug use among real clubbers, such as those conducted by Dick and Torrance[21], or Winstock [22], assessed the variation in contents of psychoactive substances such as legal highs. Dick and Torrance in 2010 have shown that 26% of respondents had used benzylpiperazine, and 41.7% had used mephedrone (cathinone derivatives). Winstock in 2011 found that use of mephedrone increased after it was banned in April 2010 as 61% of respondents used mephedrone (compared to 42% in 2010) and ketamine has fallen from 50.7% of respondents using it in 2010 to 41.2% in 2011[21, 22].

This thesis reports the analytical profile of a powder sample called NRG-2, which was marketed online, to investigate comments that were mailed on some drug discussion forums via the internet that showed users reporting these products to be safe and legal to use.

Samples of NRG-2 were obtained from an internet websites, where these materials was advertised as of 99.8% purity and labeled as plant food substances and "not for

human consumption”. In the current study it was found that substances with the same name of NRG-2, bought from several sellers contained various active ingredients.

1.6 Cathinone/methcathinone derived Legal Highs

The Khat plant “*Catha edulis*” can grow as a small shrub or tree. The cultivation of this tree in the Arabic peninsula begins as a bush, but in some countries, particularly in Africa, the small tree is cultivated and kept short by pruning it. Left in the wild, Khat is a high tree that can often reach twenty-five meters[23].

Most east African and Arabic peninsula people have used Khat as a stimulant by chewing the fresh leaves of the Khat, since the dry leaves are unusable and decompose into norpseudoephedrine and norephedrine [24-26].

The main stimulant effects in Khat leaves are suggested to be from the alkaloid compounds, which have stimulant properties and are present in its leaves. Present within the fresh leaves are cathines, cathinone, and norephedrine, however, the most potent central nervous system stimulant is cathinone which is extracted from the khat as a major active constituent. It is structurally similar to amphetamine-but has a less powerful pharmacological profile than amphetamine- and the difference is only that cathinone possesses a ketone oxygen at the beta-carbon position, cathinone is thus a beta-keto analogue of amphetamine [26, 27].

Over the past few years, new cathinone derivatives were designed and emerged on the illicit drug market in many countries around the world, because the cathinone chemical structure can be altered to yield a series of different cathinone derivatives which are closely structurally related to cathinone, these derivatives are known as the beta-keto designer drugs or cathinone derivatives. An example of this is the *N*-methyl cathinone derivative that is known as methcathinone (methamphetamine analogue) [28].

Synthetic cathinones are mainly seen in the UK being sold online and advertised as legal high products and data provided from UK forensic experts suggested that cathinone is regularly submitted as either white or brown powders. Although cathinone is advertised as high purity, some adulterants such as caffeine, benzocaine,

lignocaine, and paracetamol were detected and characterized in a small quantity of seized cathinones. Cathinones were identified with some controlled drug adulterants such as amphetamine, cocaine, ketamine, and benzylpiperazine[28].

In the UK, mephedrone, and the other cathinone derivatives, were classified as class B, Schedule I under the UK's Misuse of Drugs Act 1971, on 16th April 2010, primarily because severe and even deadly poisonings have been attributed to the consumption of mephedrone as it is a cathinone derivative which is consumed without any safety testing. Table 2 below shows twenty-five cases which were associated with toxicity caused by self-reported mephedrone consumption as a recreational drug (Data from Guys and St Thomas' hospital toxicology) [19, 28].

Table 2. Cases of toxicity due to self-reported mephedrone consumption [28].

Date of case	Number of cases
January-March 2009	2
April-June 2009	0
July-September 2009	8
October-December 2009	5
January 2010 -22 nd February 2010	10

The chemical name of mephedrone is 4-methylmethcathinone and it has so many synonyms such as 4-MMC (3a), Miaow, MMCat, Roxy, Mefedron (Poland), Krabba (Sweden), Bubbles, Meph, Rush, and called Meow Meow/Miaow Miaow in the UK especially in Brighton and Hove. In addition, mephedrone has quite a short history of human consumption and was known as a phenethylamine research chemical. Forum chatting about mephedrone appears to have launched it as a recreational material in or after 2007 [29].

In 2010, the 'Annual report of drug-related deaths in the UK' reported fifty-two cases of death in the UK and Islands, in which mephedrone was the leading cause of death; in thirty-eight cases out of the total number mephedrone was detected, and in two cases mephedrone was confirmed as the direct cause of death, however, in the

rest of the other cases mephedrone acted jointly with other substances or with some health issues[30].

The common modalities of intake of cathinone derivatives are orally or through the insufflation route, and they are regularly sold as tablets or free powder, except methcathinone which is administered by injection. Cathinone derivatives have been reported to produce psychological behavior effects such as anxiety, confusion, delusions, hallucinations, paranoia, psychosis, and to induce symptoms such as increased alertness, euphoria, feelings of stimulation, and sympathy. Also, there are many common side effects such as dehydration, erectile dysfunction, and severe discoloration of knees that can occur, due to damage to the vascular system, which is called “blueknees”. Cardiac dysrhythmia and drug induced paranoid states have also been reported [31-33].

On the other hand, a cathinone derivative called Bupropion (9a) (Figure 2; Table3) is used medically in the UK as a prescribed drug used as an antidepressant and as an aid to smoking termination. It is marketed under trade name Zyban[®], but it has not been detected in forensic analysis of seizures in the UK or reported as abused drug [28].

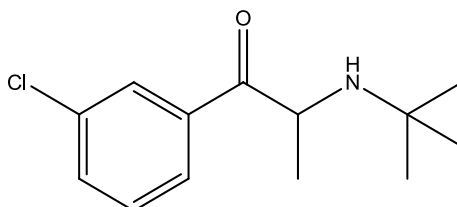


Figure 2. Bupropion (9a) Chemical structure.

Methylone (5b) was first synthesized in 1996 as a potential antidepressant drug, and recently encountered as one of the synthetic abused substances. It is related to the cathinone class as well as having a similar structure to MDMA (1e) (Figure 3) with the exception of the β -keto group which has been added to the beta-carbon position of the methylone structure. It may have encouraged the young people to use this drug as it was marketed as plant food. Before April 2010 β -keto compounds were not controlled under the Misuse of Drugs Act in the UK, then after that date it was

illegal, and classified as class B along with the other cathinones under revision of the Misuse of Drugs Act 1971 [34].

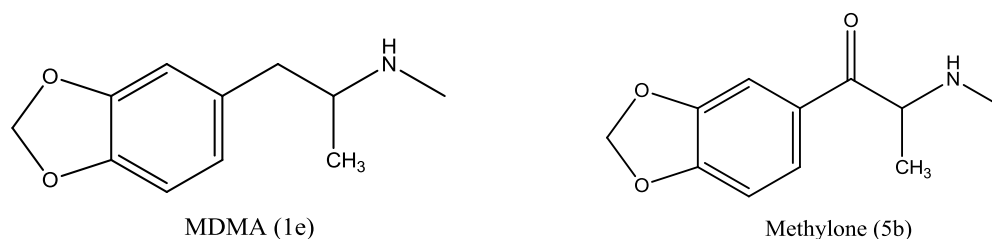


Figure 3. Chemical structure of MDMA (ecstasy) (1e) and Methylone (5b).

1.6.1 Chemical structure of cathinone

Another name for cathinone is alpha-aminopropiophenone which is the basic structure of all cathinone derivative compounds, and it is derived from phenethylamine. Cathinone is termed a natural amphetamine due to the relative relationship between the cathinone and amphetamine that is shown in Figure 4. Both contain phenethylamines, but the structural difference between cathinone (4a) and amphetamine is that cathinones can be considered as phenethylamine derivatives with a beta-keto group attached in beta-carbon position on the side chain [18, 31, 35].

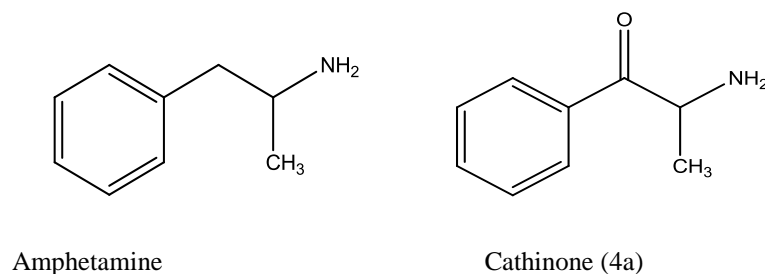


Figure 4. The relationship between cathinone and amphetamine [28].

Although in Figure 6, all R groups are hydrogen in the case of cathinone, the structure can be redesigned to produce the various cathinone derivatives. Figure 5 shows the added substituents to yield different cathinone derivatives. A series of related clusters of cathinone derivatives can be produced by adding one or more functional groups to the common sites to produce a series of cathinone derivatives. Chemical modification at position R¹ or R² by alkylation (methyl or ethyl group) results in a series of alkylation derivatives of cathinone. *N*-methyl produces

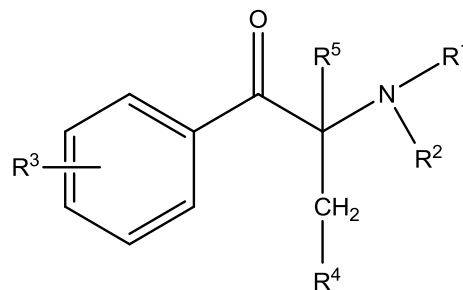


Figure 6. Common sites for structure variation of cathinone, at R¹ - R⁵ [28]

Table 3. Name of the cathinone derivatives, and their chemical structures obtained by substitutions of the generic cathinone structure of Figure (5) with the substituents shown in the table [31].

R ¹	R ²	R ³	R ⁴	R ⁵	Name of substance
H	H	H	H	H	2-amino-1-phenyl-1-propanone (cathinone)(4a)
NR ² R ³ = phthalimide		H	H	H	α-phthalimidopropiophenone (6a)
CH ₃	H	H	H	H	Methcathinone (ephedrone)(4b)
CH ₃	H	3-Br	H	H	1-(3-Bromophenyl)-2-(methylamino)propan-1-one (3-BMAP)

Table 3. Continued

R¹	R²	R³	R⁴	R⁵	Name of substance
CH ₃	CH ₃	H	H	H	<i>N,N</i> -Dimethylcathinone (metamfepramone)(4d)
C ₂ H ₅	H	H	H	H	<i>N</i> -Ethylcathinone (EC)(7a)
CH ₃	H	H	CH ₃	H	Buphedrone (MABP)(8a)
C ₂ H ₅	H	4-Methyl	H	H	4-Methyl- <i>N</i> -ethylcathinone (4-MEC) (3c)
CH ₃	H	4-Methyl	H	H	Mephedrone (4-MMC) (3a)
C ₂ H ₅	C ₂ H ₅	H	H	H	diethylcathinone (*Amfepramone)
t-Butyl	H	3-Cl	H	H	(±)-2-(<i>tert</i> -Butylamino)-1-(3-chlorophenyl)propan-1-one (*Bupropion)(9a)
Isopropyl	H	H	H	H	12-(iso-propylamino)-1-phenylpropan-1-one (i-PAP)
t-Butyl	H	H	H	H	2-(<i>tert</i> -butylamino)-1-phenylpropan-1-one (t-BAP)
CH ₃	H	3,4-Methylenedioxy	H	H	Methylone (βk-MDMA) (5b)

Table 3. Continued

R¹	R²	R³	R⁴	R⁵	Name of substance
C ₂ H ₅	H	3,4-Methylenedioxy	H	H	Ethylone (βk-MDEA)(6b)
CH ₃	H	3,4-Methylenedioxy	CH ₃	H	Butylone (βk-MBDB)(7b)
C ₂ H ₅	H	3,4-Methylenedioxy	CH ₃	H	Pentylone (βk-MBDP)(8b)
CH ₃	H	4-Methoxy	H	H	Methedrone (βk-PMMA)(9b)
CH ₃	H	4-F	H	H	Flephedrone (4-FMC)(4c)
CH ₃	H	3-F	H	H	3-Fluoromethcathinone (3-FMC)(5c)
CH ₃	H	2-F	H	H	2-Fluoromethcathinone (2-FMC)(6c)
(Pyrrolidine)		H	H	H	α-Pyrrolidinopropiophenone (PPP)
(Pyrrolidine)		4-Methyl	H	H	4'-Methyl- α-pyrrolidinopropiophenone (MPPP)
(Pyrrolidine)		4-MeO	H	H	4'-methoxy-α-pyrrolidinopropiophenone (MOPPP)

Table 3. Continued

R¹	R²	R³	R⁴	R⁵	Name of substance
(Pyrrolidine)		4-Methyl	Propyl	H	4'-Methyl- α -pyrrolidinohexiophenone (MPHP)
(Pyrrolidine)		4-Methyl	C ₂ H ₅	H	4-Methyl- β -ketone-prolintane (*Pyrovalerone)
(Pyrrolidine)		H	CH ₃	H	α -Pyrrolidinobutiophenone (α -PBP)
(Pyrrolidine)		H	C ₂ H ₅	H	α -Pyrrolidinopentiophenone (α -PVP)
(Pyrrolidine)		4-Methyl	CH ₃	H	4'-Methyl- α -pyrrolidinobutiophenone (MPBP)
(Pyrrolidine)		4-Methyl	H	CH ₃	4-Methyl- α -pyrrolidino- α -methylpropiofenone
(Pyrrolidine)		3,4-Methylenedioxy	H	H	3',4'-Methylenedioxy- α -pyrrolidinopropiophenone (MDPPP)
(Pyrrolidine)		3,4-Methylenedioxy	C ₂ H ₅		Methylenedioxyprovalerone (MDPV)(7c)
(Pyrrolidine)		3,4-Methylenedioxy	CH ₃	H	3',4'-Methylenedioxy- α -pyrrolidinobutyrophenone (MDPBP)
(Pyrrolidine)		Benzyl	C ₂ H ₅	H	β -naphyrone (5d)

*Used medically as a prescribed drug.

1.6.2 Mechanisms of action of cathinone

The main effects of cathinone are that it has been shown to increase the release of dopamine, noradrenaline, and serotonin in the central nervous system [31]. Dopamine is a catecholamine that functions as a neurotransmitter to send signals to other nerve cells. It has a particular role in mediating reward-motivated behaviour, and many addictive drugs act through increasing the effects of dopamine. Dopamine is linked to several personality traits including reward-seeking behaviour and extraversion. Noradrenaline is also a catecholamine with a role as a neurotransmitter. It is released from neurons and affects attention and responses in the brain and increasing the brain's oxygen supply. Serotonin is a monoamine neurotransmitter that works in the central nervous system. High levels of serotonin lead to feelings of well-being and happiness.

The action of cathionines is similar to amphetamine. Amphetamines act by increasing the concentration of dopamine and noradrenaline in the synaptic cleft of CNS synapse, leading to increased binding of post-synaptic membrane receptors of dopaminergic and noradrenergic neurons, This is illustrated in Figure 7 and includes amphetamine binding to monoamine oxidase enzyme in dopaminergic neurons to prevent the degradation of dopamine. Amphetamine can also interact with dopamine containing synaptic vesicles resulting in the release of free dopamine into the nerve terminal[36].

Cathionines also increases activity in the dopaminergic neurons [23]. Increased release of monoamines such as dopamine and serotonin is achieved through an inhibitory effect on the monoamine oxidase enzyme (MAO) [23]. Some studies have found that cathinone is more potent in this respect than racemic amphetamine.

A number of studies have also discovered that the storage sites of noradrenaline in sympathetic neurones were affected by introducing cathinone or amphetamine. Therefore, cathinone or amphetamine show inhibitory effects on the uptake of noradrenaline [35, 37, 38].

Sparago *et al.* evaluated neurotoxic and pharmacologic properties of the enantiomers of methcathinone (4b) , they assessed the neurotoxic potential toward brain

dopamine and serotonin neurons by measuring dopamine and serotonin axonal markers using means of silver degeneration methods, and pharmacologic effects were evaluated by measuring locomotor stimulation. Methcathinone (4b) produced dose-related neurotoxic and locomotor stimulant effects which depends on the species and enantiomer. In mice, although both enantiomers produced toxic effects on dopamine neurons, the R (+)-methcathinone was more potent, and neither enantiomer produced long-term effects on serotonin neurons. But in behavioral studies, both enantiomers increased mouse locomotor activity, however, the S (-)-methcathinone was more potent, which suggests that methcathinone's neurotoxic and locomotor stimulant effects may be separable. In the rat, both enantiomers produced toxic effects on dopamine neurons, only S (-)-methcathinone produced toxic effects on serotonin neurons, and both enantiomers produced comparable locomotor stimulant effects. These results indicate that methcathinone has the potential to damage dopamine and serotonin neurons, and methcathinone(4b) confers serotonin toxic activity onto cathinone(4a), however cathinone (4a) is known to lack of serotonin neurotoxic activity[39].

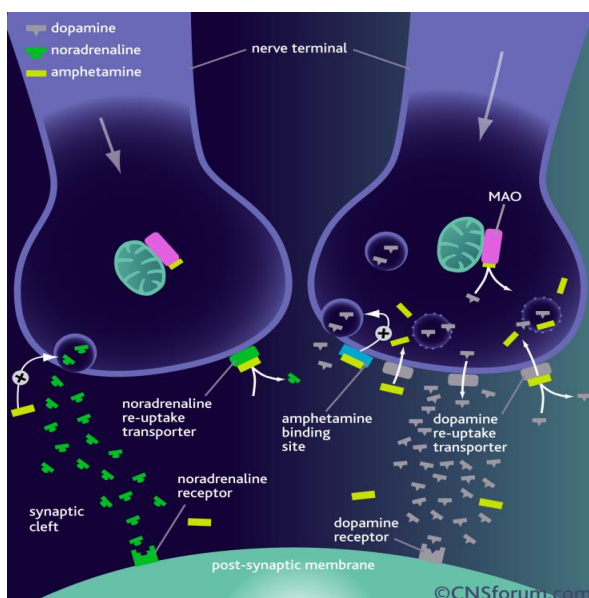


Figure 7. A diagram of central nervous system chemical synapse (which allows nerve cell to pass a chemical signals to another cell) illustrated the mechanism of action a high dose of amphetamine[36, 40].

Initial pharmacological work on cathinone was undertaken by Kalix and Braenden, who studied the effect of cathinone on the serotonergic pathway in a rat brain region (corpus striatum) to find out whether the cathinone could mimic the actions of amphetamine. The rat tissue was pre-labelled with ^3H -serotonin. Three times the cathinone concentration was needed to produce a similar level of effect as a concentration of amphetamine. Also Kalix and coworkers found in several brain regions, (nucleus accumbens, striatum and caudate nucleus) , which were pre-labelled with ^3H -dopamine, that cathinone could stimulate the release of radioactive label from those regions[23, 41].

In 1990, Pehek *et al.* demonstrated that cathinone and amphetamine loaded into rat tissue and then measured by *in vitro* microdialysis probes increased the levels of dopamine in the anterior caudate putamen and nucleus accumbens of the brain of rat [26, 42].

A considerable amount of behavioural investigation on the effects of cathinone and amphetamine has been published. Some of these studies were carried out in mice and rats, by pre-treatment with agents showing strong central anti-dopaminergic action such as haloperidol and spiroperidol, the results showed a reduction of alertness, locomotor activity, grooming, licking, and biting, after cathinone or amphetamine were present. Their results proposed that the stimulating properties of khat leaves are due to the presence of cathinone with amphetamine-like effects [26, 43, 44].

On the other hand, Babayai *et al.* investigated the effect of cathinone on the visual differentiation of cats, and reported interesting findings that affinity of cathinone for serotonin receptors was higher than that of amphetamine by about four times and they suggested it may be due to the activation of the serotonin pathways, which have a more important role in the action of cathinone compared to that of amphetamine. This hypothesis is supported by observations that the short-term and prolonged visual stimuli were increased when the serotonergic system is activated, and decreased when the dopaminergic system is activated [45].

1.6.3 Pharmacology of cathinone

The spectrum of effects seen after consumption of the Khat plant were clearly known as pharmacological effects, including central effects such as increased

alertness, euphoria, sensual stimulation, anorexia and hyperthermia, also peripheral effects including increased heart rate, breathing rate and blood pressure [37, 46, 47]. Cathinone was isolated from Khat and was considerably more potent than other alkaloids in khat leaves, and thus several studies were undertaken to determine whether cathinone was responsible for khat stimulating properties. Valterio (1982) found that the stimulating effects of khat leaves are due to the presence of cathinone, and the results showed increasing stimulation of the locomotor activity of mice characterized by a dose-response curve of an inverted -U shape similar to that of amphetamine [44]. In a clinical experiment, fresh leaves and alkaloid-free leaves as placebo were compared in six drug-naïve volunteers and the plasma concentration of cathinone after ingestion was found to be 127 ng mL^{-1} (± 53 SD) after 127 ± 30 minutes. The cathinone caused cardiovascular effects similar to those observed with amphetamine [48]. Cathinone is known to be a natural analogue of amphetamine, producing similar central nervous system stimulation. As a result, similar clinical effects to amphetamine could be postulated [35].

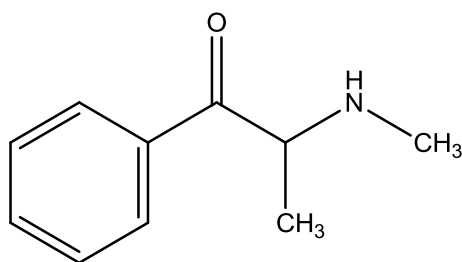
Although cathinone is metabolized rapidly during the first passage through the liver, unchanged cathinone is found in urine at about 2%. The majority of the metabolites were excreted in norephedrine metabolite form. The rate of inactivation of the metabolites has been shown to be the same as the rate of the absorption [35].

In the leaves of khat, isolated (S)-cathinone isomer from the Khat leaves have revealed that substance is found to be more potent constituent as a stimulant of the central nervous system than its enantiomer, and its pharmacological profile has been shown, in both *in vitro* and *in vivo* studies, to be very similar to that of amphetamine [23, 49, 50]. Cathinones and amphetamines have both reuptake inhibition activity and monoamine releasing activity; each of them has a different relative binding potency to monoamine (dopamine, serotonin and noradrenaline) receptors. The potency of cathinones is mostly lower than that of amphetamines because cathinones have a β -keto group in their structure making them slightly more polar, and thus less capable of crossing the lipid blood brain barrier [51].

Methcathinone was synthesized for the first time in Germany in 1928, and used as an anti-depressant in the Soviet Union during the 1930s and 1940s [52]. Studies carried

out on rat brain tissue preloaded by H^3 dopamine showed that methcathinone caused release of dopamine from this tissue. Gygi investigated the reduction in the concentration of dopamine and serotonin in the different rat brain regions after methcathinone administration. This was due to a decrease in the activities of neurotransmitter biosynthetic enzymes tyrosine hydroxylase (tyrosine 3-monooxygenase) and tryptophan hydroxylase, and as a result they suggested that methcathinone is a substrate of dopamine and serotonin uptake transporters. In addition, compared with other stimulants of abuse, methcathinone appears to be similar to methamphetamine in terms of effects on monoamine systems [53].

Methcathinone (4b), shown in Figure 8, is a derivative of cathinone which occurs naturally in the Khat plant (*Catha edulis*) [54]. It has potential toxic effects on dopamine and serotonin neurons [39], and neurotoxicity produced by transport of methcathinone into the neurone gave evidence that methcathinone is a substrate for dopamine and serotonin transporters [55].



Methcathinone

Figure 8. Chemical structure of methcathinone (4b).

Intravenous injection of methcathinone (4b) by drug-addicted people from Russia, Ukraine, and Estonia has been reported to cause symptoms similar to those seen in patients with Parkinson's Disease due to a rise in manganese levels. This is thought to occur due to potassium permanganate that is used as an oxidant agent during self-synthesis of methcathinone by the patients who had contributed in this study. It is prepared from pseudoephedrine hydrochloride using potassium permanganate as a potent oxidant which is elevated manganese levels. Also both instructions on the synthesis and ingredients of this kind of methcathinone are available in the internet [56].

1.5 Analytical methods for the detection and quantification of Cathinones

Recently, the supply of abused drugs has increased dramatically on the European illegal drug market and secret drug laboratory operators have attempted to avoid controlled substance laws and legal regulations by making “designer” compounds similar to current drugs of abuse, including methamphetamine, ecstasy (1e), and cathinone derivatives. “Legal highs” containing cathinone derivatives have produced severe side effects in users across the world. Therefore, the analysis of these drugs has become of intense interest from a point of view of legislation, medication and toxicity.

1.5.1 Presumptive test of cathinones

Presumptive tests, based on a colour reaction, are known as fast screening procedures that can be designed to indicate that the drug classes are either present or absent in the test sample, however, they cannot identify a specific substance within that class, and the interpretation of colour should be carried out with care because some samples may have a difference in purity, and may contain unrelated materials.

Recently, this test is more often used as a field test, as a first screening test and confirmatory tests must always be carried out in laboratories and the results combined with those from the first screening tests. The advantage of the colour test is that it is an easy and rapid chemical test, and a few different reagents typically work for testing of cathinone and its derivatives. *Chen reagent* can react with cathinone and methcathinone and the colour gradually turns to yellow or orange, and methcathinone can also react with *Simon reagent* changing the colour to form a slightly blue, ring like precipitate. Neither cathinone nor methcathinone react with *Marquis reagent* and do not give a coloured reaction. It gives an orange/ brown colour change if a substance is present from the class of amphetamines. The ACMD have stated that “there are currently no colorimetric field tests available to identify all of the cathinone derivatives, although some chemical tests, such as the Simon’s test and Chen test may be used to give an indication of a small number of cathinones” [28, 57].

1.5.2 Analytical techniques

GC-MS has successfully been used to characterize some of the most popular legal highs available, and some of these products were found to contain the cathinone derivatives. A gas chromatographic-mass spectrometric method for detection of cathinone and methcathinone in urine has been developed; Paul and Cole reported that cathinone and methcathinone in selected urine specimens can be detected by a procedure similar to that used for amphetamine and methamphetamine and it can detect all of them simultaneously. To confirm that detected drugs were not metabolites of over-the-counter medication (OTC), cathinone (4a) and methcathinone (4b) were analysed in urine specimens that were collected from individuals who had ingested phenylpropanolamine and pseudoephedrine and then did not produce keto-amines as metabolic products after ingestion these OTC medications. During the extraction process for urine specimens, periodate oxidation that can degrade the OTC medications, was avoided because cathinone and methcathinone were totally lost by the oxidation. The overall recoveries were detected by adding internal standards at the beginning and end of the extraction process, and were 82% for amphetamine, 85% methamphetamine, 86% cathinone, and 78% methcathinone. For GC-MS detection, 4-carbethoxyhexafluorobutyryl chloride (4-CB) derivatives exhibited better ion selection and chromatographic resolution than derivatization by heptafluorobutyric anhydride. When the method was applied to test urine specimens, the samples that tested positive for cathinone also contained phenylpropanolamine, and those tested positive for methcathinone also contained ephedrine and pseudoephedrine, suggesting that the associated compounds are metabolites of cathinone and methcathinone [58].

The identification of cathinone (4a) and methcathinone (4b) was based on comparing retention times and relative ion abundances with that of reference compounds, and then deuterated internal standards for both amphetamine and methamphetamine were used to measure the concentration of cathinone and methcathinone respectively[58].

One of the difficulties encountered during identification of unreported cathinone derivatives is the deficit in commercially available reference standards, especially

when dealing with unknown derivatives or isomers. This prerequisite was addressed by Brandt and co-workers' studies by preparing three trifluoromethyl ring-substituted methcathinone compounds with CF₃ substituent at 2-, 3-,4-position of the aromatic ring, and then characterizing them using infrared technique (ATR-FTIR), NMR (¹H and ¹³C), and Gas chromatography –Mass spectrometry (GC-EI/CI-ion trap MS). Differentiation between the 2-, 3-, 4- isomers was possible by ATR-FTIR, and the separation of those three isomers was feasible under the GC conditions used and is represented in Figure 9. The loss of water from the [M+H]⁺ ion under chemical ionisation interface (CI) conditions resulted in a fragment at *m/z* 214 in addition to one at *m/z* 58, and under Electron Impact (EI) yielded more fragments including α-cleavage of M⁺ yielding *m/z* 173 followed by loss of neutral fragment CO yielding fragment at *m/z* 145. Further fragmentation may have occurred which gave rise of *m/z* 56 (Figure 9) [59].

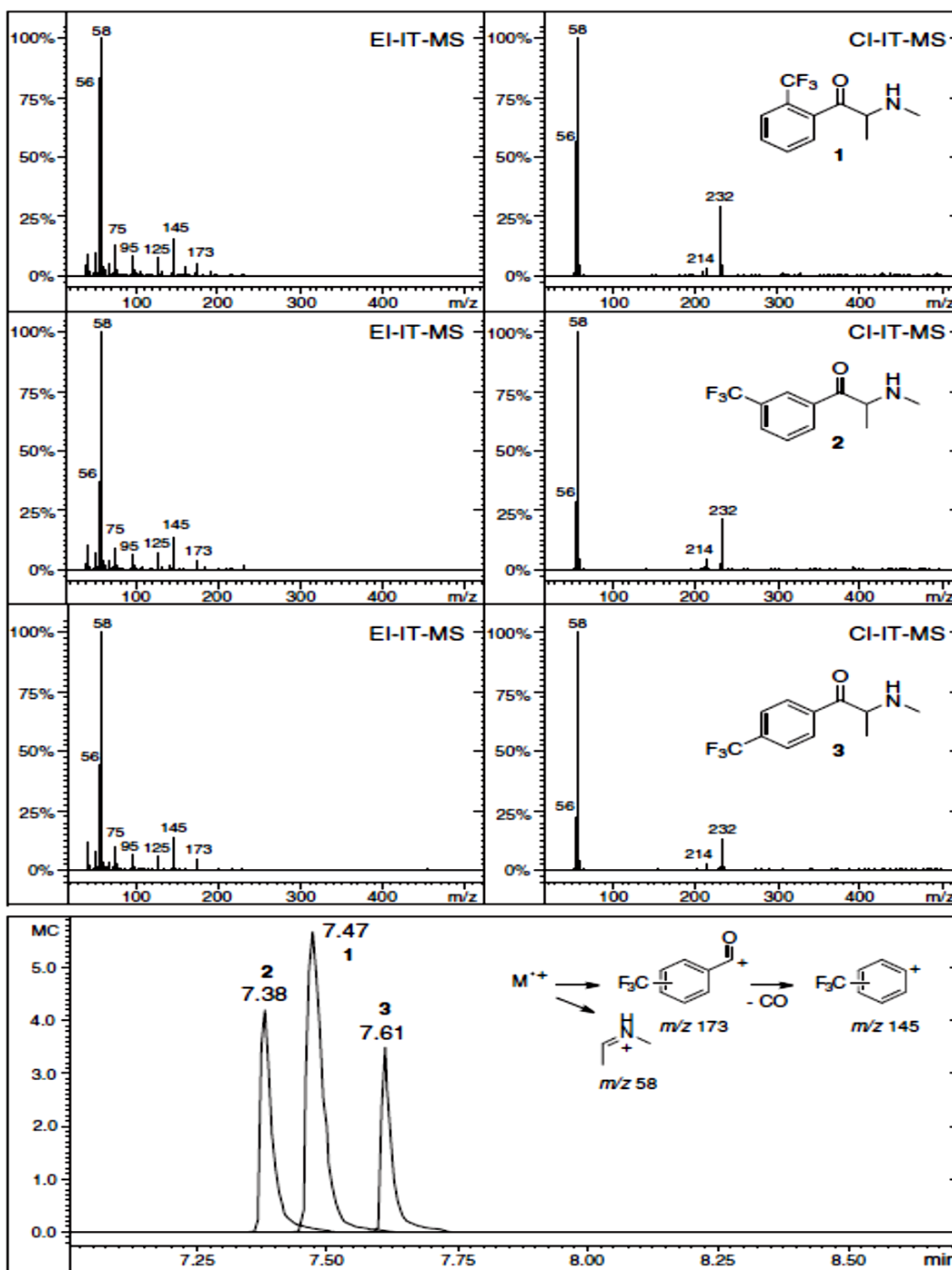


Figure 9. Chemical ionisation and electron impact ionisation were obtained under GC conditions for three trifluoromethyl ring-substituted methcathinone compounds [59].

As described above several cathinone derivatives have gained popularity as named legal highs which are available on internet websites and some high street shops.

Brandt *et al.* reported that twenty-four legal high products were bought from eighteen internet websites during a period of six weeks following the ban of mephedrone and the other cathinone derivatives in April 2010, and then analysed using Gas Chromatography-ion trap mass spectrometry and nuclear magnetic resonance spectroscopy and compared with reference standards. In particular, Table 4 shows that compounds detected in the purchased products were as a single cathinone in some products and cathinone mixtures in other products. Generally, the content of all samples included 4-methyl-*N*-methcathinone (mephedrone) (4-MMC; 3a), 4-methyl-*N*-ethylcathinone (4-MEC; 3c), butylone (7b), 4-fluoromethcathinone (flephedrone) (4c) and 3, 4-methylenedioxypropylone (MDPV) (7c), as well as some adulterants such as, caffeine, Benzocaine, lidocaine, and procaine. 70% of products which were labelled as NRG-1 or NRG-2 and claimed to consist of legal chemicals such as naphyrone (5d) actually contained a mixture of cathinone derivatives that were banned in April 2010, apart from only one sample of NRG-1 that seemed to contain only naphyrone (5d) which was a legal substance [19].

Table 4. Legal high products bought on UK-based websites during a period of study of 6 weeks following the ban of mephedrone on 16th April 2010 [19].

Website	Product number	Label	Compound detected
1	1	NRG-1	Butylone + MDPV
2	2	NRG-1	Flephedrone (4-fluoromethcathinone)
3	3	NRG-1	Flephedrone+ MDPV
4	4	NRG-2	4-Methyl- <i>N</i> -ethylcathinone
5	5	NRG-1	Flephedrone+ MDPV
6	6	NRG-1	Caffeine (+ mephedrone traces)
7	7	NRG-1	Naphyrone
8	8	NRG-1	Butylone + MDPV
9	9	MDAI	Inorganic material
10	10	NRG-1	Mephedrone
11	11	NRG-1	Inorganic material
11	12	NRG-2	Mephedrone + benzocaine

Table4. Continued

Website	Product number	Label	Compound detected
12	13	NRG-1	Mephedrone
12	14	NRG-2	Mephedrone
12	15	DMC	Caffeine + lidocaine
12	16	MDAI	Mephedrone
13	17	NRG-2	4-Methyl- <i>N</i> -ethylcathinone
14	18	NRG-1	Caffeine
14	19	NRG-2	Benzocaine + caffeine
15	20	NRG-2	4-Methyl- <i>N</i> -ethylcathinone
16	21	NRG-2	4-Methyl- <i>N</i> -ethylcathinone
16	22	Granules	Mephedrone
17	23	NRG-1	Procaine (+ mephedrone traces)
18	24	NRG-1	Caffeine

In addition, as most commonly available cathinone derivatives in the recreational market contain mephedrone, there are many published methods for identification and quantification of mephedrone in the forensic and toxicological field. McDermott *et al.* recently reported that GC-MS enables fast separation of iso-cathinones that are found in seized samples which include mephedrone and iso-mephedrone, as well as extra compounds of ethcathinone and iso- ethcathinone which were detected in seized samples (Figure 10). They analysed cathinone derivatives by GC using a 100% methylsilicone phase which is very popular due to its low polarity that can provide separation of mephedrone and ethcathinone isomers with good efficiency. They also used NMR and IR techniques to support these findings[60].

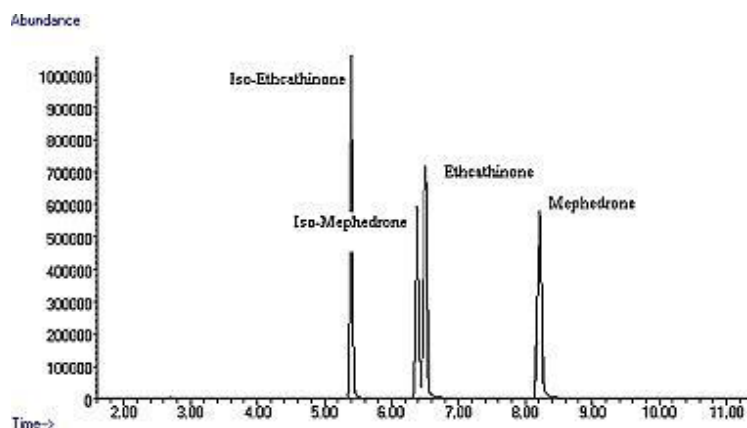


Figure 10. GC separation of cathinones and *iso*-cathinones [60].

Camilleri *et al.* in August 2007, characterised materials of four capsules containing a white powder which were delivered to Adelaide Hospital in South Australia and the active ingredients found included 4-methylmethcathinone (mephedrone, 3a), 2-fluoromethamphetamine (6c), α -phthalimidopropiophenone (6a) and *N*-ethylcathinone (7a) (Figure 11), all of which were not under the regulations of South Australia controlled substance. They presented GC-MS, NMR, and vapour- and condensed-phase IR analysis to examine whether these substances would fulfil the legal clarification of these substances in South Australia and explored possible challenges for a forensic analyst for categorizing these substances as controlled substance analogues [16].

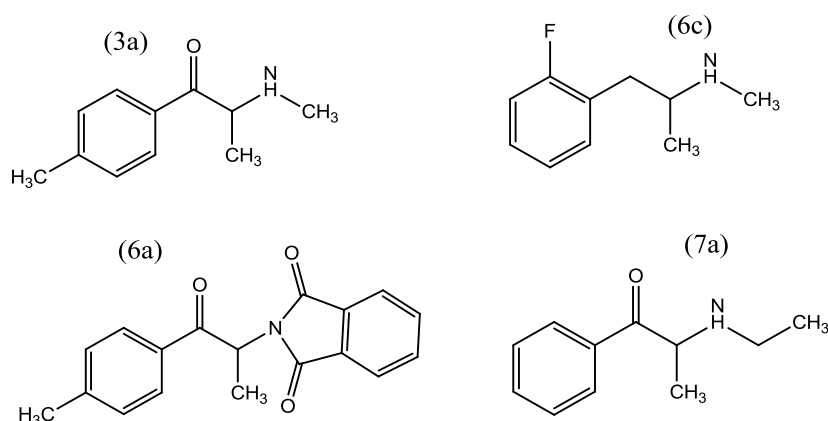


Figure 11. Chemical structure of found in four capsules: (3a) mephedrone (6c) 2-fluoromethamphetamine, (6a) α -phthalimidopropiophenone and (7a) *N*-ethylcathinone [16].

In recent years, liquid chromatography coupled to mass spectrometry has become increasingly important in identification and quantification of cathinone derivatives in the field of forensic and toxicology. Studies such as those carried out by Sorensen have shown that Liquid Chromatographic-Mass Spectrometry was developed and validated to identify and quantify cathinone derivatives as well as ephedrine in live patients and post-mortem blood samples. The column used in analysis of cathinone derivatives was an ethyl-linked phenyl phase, which enabled a good efficiency in separation of many structural isomers due to the low hydrophobicity of the phenyl phases. In addition, the interaction between π electrons from the benzene ring of the analytes and the π electrons of the phenyl ring of stationary phase can provide a unique selectivity. Electrospray ionisation was utilised in positive ion mode for all substances[61].

Ammann *et al.* determined twenty-five cathinone derivative substances and their related ephedrine in blood samples using a liquid chromatography-tandem mass spectrometry (LC-MS-MS) method operated in electrospray positive ionization multiple reaction monitoring mode after extracting the blood samples using a liquid-liquid extraction method using 1 mL of 1-chlorobutane containing 10% of isopropanol. The method which was used was validated. The cathinone derivative fragments were characterized based on GC-EI-MS and LC-ESI-MS techniques, therefore parent ions of cathinone derivatives were hard to observe by EI whereas the protonated molecular ions were clearly obtained by ESI. Two major α -cleavage fragmentation patterns were observed when EI mode was used, which were very useful in identification [17, 62].

Santali *et al.* developed and validated a qualitative and quantitative HPLC method for analysis of mephedrone as a pure substance and in the presence of common diluents and adulterants which are used in illicit drug manufacture such as paracetamol, caffeine, methylone (5b), lidocaine, ketamine, diamorphine (Heroin), cocaine, and benzocaine. Their data were obtained using ACE C18 column (150×4.6 mm i.d., particle size: 3 mm) which was fitted with guard column (ACEC18), and the column temperature was maintained with programmable controller at 22 °C. This method was performed using a variable wavelength UV absorbance detector at 258 nm, for pure substances and PDA-UV absorbance detector for detection of

adulterants methods. The mobile phase was prepared by separately mixing organic modifier (methanol) and aqueous ammonium formate buffer (10mM; pH 3.5) at 40:60; for pure substances 30:70 for the internal standard (nicotinamide) method and 28:62 for the adulterants method. Several techniques such as IR, NMR, UV and MS have been used to support the structural elucidation of two salt forms of 4-methylmethcathinone racemic (hydro- bromide and chloride salts) [63]. In addition, Gibbons *et al.* purchased material from a website and analysed it by extensive one- and two-dimensional NMR experiments, and high resolution mass spectrometry (HRMS), supported by elemental analysis to determine whether mephedrone was present as a free base or as a salt. They found results corresponding to the hydrochloride salt form and measured optical rotation which indicated that mephedrone was racemic in nature with high purity [18].

Since all the cathinone derivatives are chiral and the stimulant potency of the enantiomers of these compounds is thought to be different, a chiral analytical method for separation of a set of twenty-four cathinone derivatives has been developed using a HPLC methods. For chiral analysis the column used consisted of a normal phase stationary phase [(S)- α -methylbenzylcarbamate], using hexane, isopropanol, and triethylamine as a mobile phase under isocratic conditions. The ratio of the three mobile phases was optimised during the method development and final ratio was (97:3:0.1) of hexane, isopropanol, and triethylamine respectively. With a wavelength of 254 nm, nineteen out of twenty-four substances were successfully separated into their enantiomers (e.g. Figure 12- a). A correlation between the separation results and substituent nitrogen atoms of the cathinone showed that the other five compounds that were not baseline separated contained a tertiary amine group. One of the five, *N*-dimethylbutylone, was partially separated (e.g. Figure 12- b), but the other 4 compounds which all contained a tertiary amine, including a pyrrolidine, were not separated at all (e.g. Figure 12- c) [64].

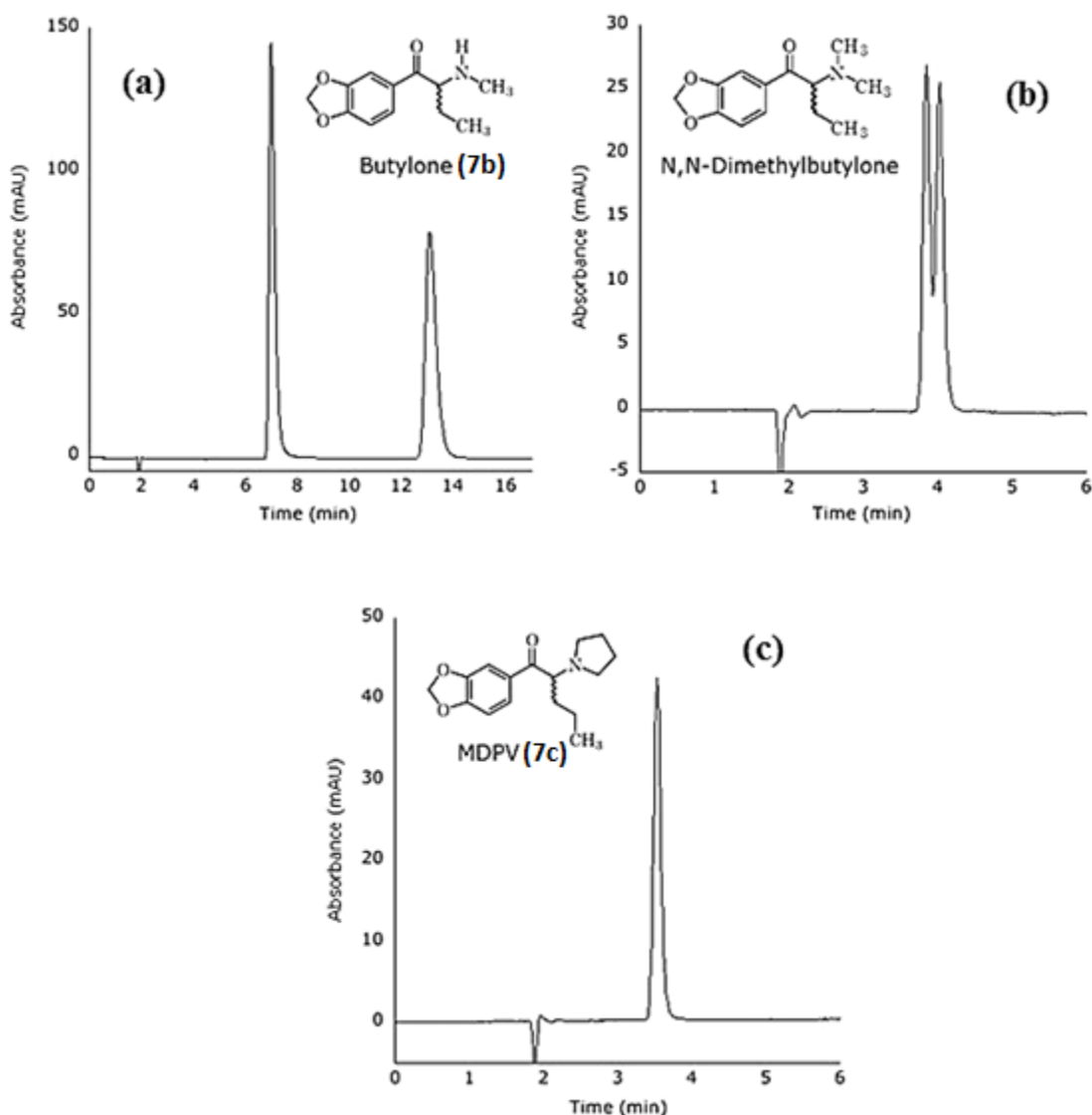


Figure 12. Chromatograms showed the correlation between the separation and the type of substituent nitrogen atoms of the 24 racemic cathinones: (a) cathinone derivatives were successfully separated into their enantiomers (e.g. butylone; 7b); (b) cathinone derivatives were partially separated (e.g. N, N-Dimethylbutylone) ;(c) cathinone derivatives were not separated into their enantiomers (e.g. MDPV; 7c) [64].

1.7 Identification of metabolic pathways of cathinone derivatives

Recently, as discussed above a series of new cathinone derivatives, called beta-ketos, appeared on the black market, and a number of studies have investigated the

metabolism of these cathinone derivatives, such as mephedrone (4-MMC; 3a) , methylone (5b), butylone (7b) and ethylone (6b) [65, 66].

In 2010, Meyer *et al.* published a paper in which they identified metabolic pathways of mephedrone in rat and human urine specimens by GC/MS, and the phase I metabolic pathways were proposed as: *N*-demethylation to produce a primary amine (normephedrone), reduction of the keto moiety to the corresponding alcohol and oxidation of the tolyl moiety to the resultant alcohol and carboxylic acid, to produce hydroxytolyl mephedrone and 4-carboxy-mephedrone respectively. However, phase II metabolism was not detected due to utilising enzymatic hydrolysis (glucuronidase and arylsulfatase) within the sample preparation process [67]. Recently, *in vitro* metabolism studies were carried out by Pedersen *et al.* in human liver microsomal preparations containing cytochrome enzymes. They also investigated the metabolism of mephedrone *in vivo* in four forensic traffic cases where mephedrone was detected and blood samples were available and analysed for all cases, and a urine sample which was available for only one case [68]. All metabolites were detected or quantified by an ultra-performance liquid chromatography-tandem mass spectrometer (UPLC-MS-MS) and an ultra-performance liquid chromatography-time of flight mass spectrometer (UPLC-TOF/MS). The fragmentation pattern of all metabolites was detected by ultra-liquid chromatography- quadrupole time of flight/mass spectrometry (UPLC-QTOF/MS^E). Hydroxytolyl-mephedrone and normephedrone were detected *in vitro*, and they found that CYP2D6 was the main responsible enzyme for *in vitro* Phase I metabolism of mephedrone. In the traffic cases the two above metabolites were detected *in vivo* as well as 4-carboxy-dihydro-mephedrone , dihydro-mephedrone and 4-carboxy-mephedrone [68].

Metabolic pathways of methylone (bk-MDMA) (5b) (Figure 13, scheme 2) were investigated using rat and human urine specimens and two techniques of gas chromatography-mass spectrometry (GC-MS) and liquid chromatography-ESI-mass spectrometry have been employed. The urine was collected from the human subject at approximately 36 hour after intake, and collected from the rat in a vessel 24 hour after a single intraperitoneal dose of 5mg kg⁻¹. In both human and rat urine, the majority of metabolic pathways were identified including *N*-demethylation to the

respective primary amine, methylenedioxcathinone (MDC), which was found to be moderately conjugated, and the second major pathway was demethylation followed by *O*-methylation in the 3-OH group of the aromatic ring forming the corresponding 3-hydroxy-4-methoxymethcathinone (3-OH-4-MeO-MC) or in position 4-OH in the aromatic ring to the corresponding 4-hydroxy-3-methoxymethcathinone (HMMC). They were mostly conjugated. After quantification studies, the authors found that MDC and (3-OH-4-MeO-MC) metabolites of methylone (5b) are minor in human urine samples, whereas HMMC(4-OH-3-MeO-MC) was found to be the most abundant metabolite [65].

The metabolites of both ethylone (bk-MDEA) (6b) and butylone (bk-MBDB) (7b) which are members of a new cathinone chemical class called the beta-ketos (bk) were detected in an abuser's urine using GC-MS and LC-MS techniques and the structures of their major metabolites were confirmed by synthesised reference standards. The major metabolic pathways for ethylone (6b) and butylone (7b) are shown in Figure 13, and the same pathways were determined for both bk-MDEA (6b) and bk-MBDB (7b) which mainly undergo demethylation followed by *O*-methylation, *N*-dealkylation and also reduction of keto moiety[69-71].

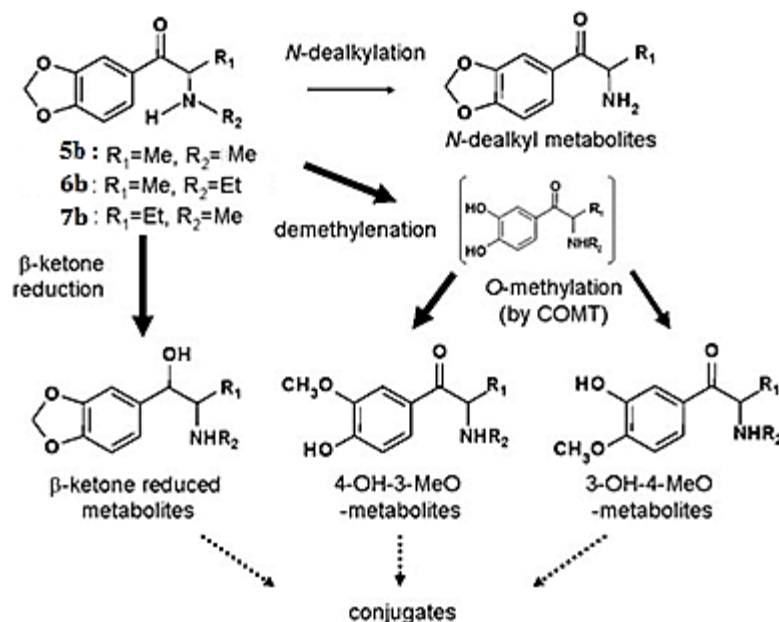
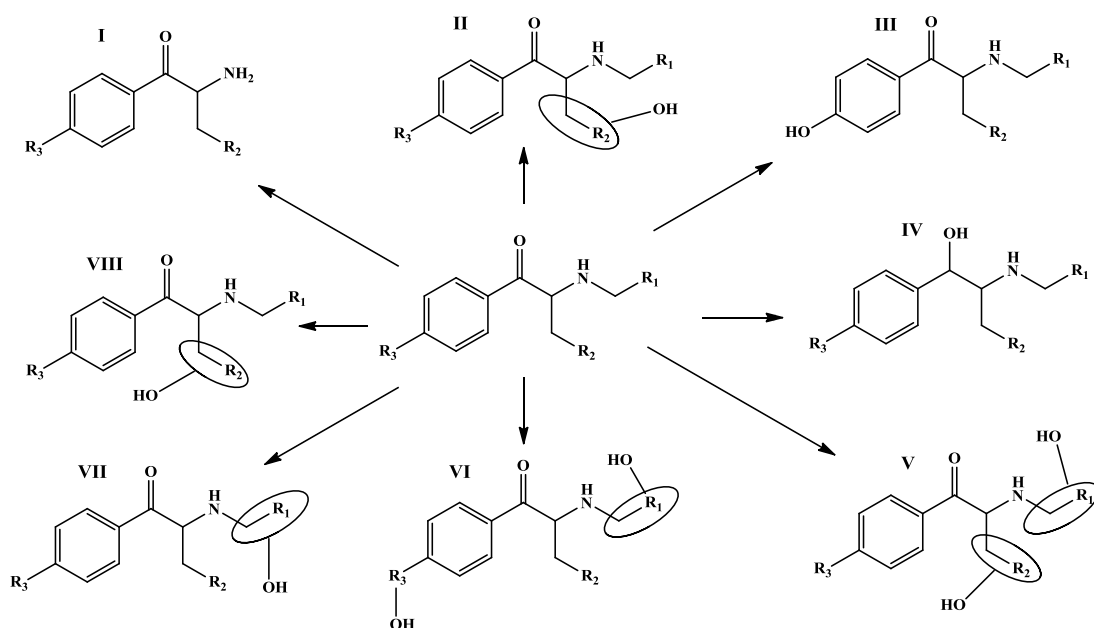


Figure 13.Proposed metabolic pathways for methylone (bk-MDMA) (5b), ethylone (bk-MDEA) (6b) and butylone (bk-MBDB) (7b) [70, 71].

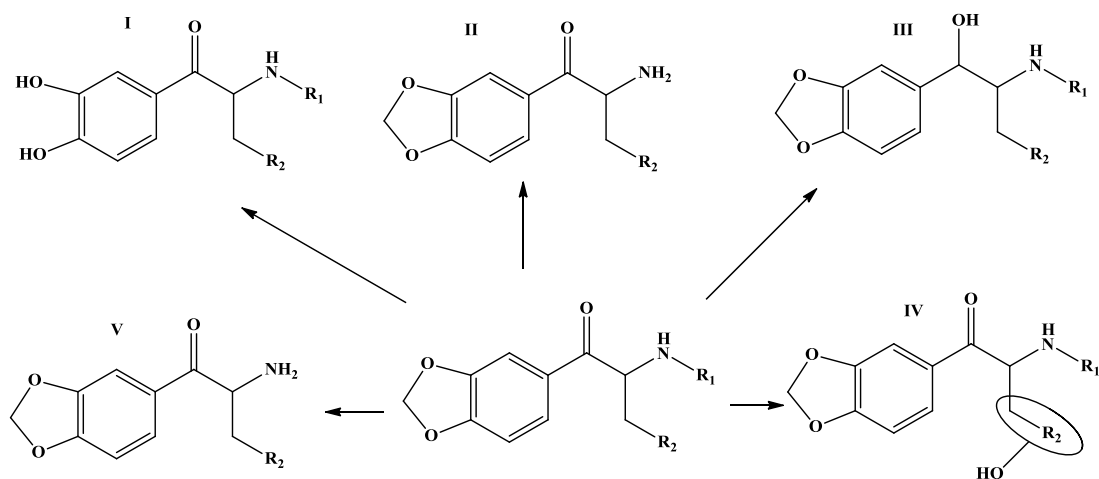
Recently, researchers have shown that human liver microsomes (HLM) can be used to investigate metabolic pathways of eleven cathinones, the metabolic pathways of eight of them had not previously been reported. An automated online extraction method of high performance liquid chromatography combined with mass spectrometry (LC-MSⁿ) was developed for HLM experiments[72].

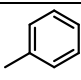
A screening method was developed, the method provided a straightforward approach to identifying the Phase I metabolic pathways for eleven cathinones which included dealkylation, hydroxylation, reduction of the keto group, and demethylenation in cathinone derivatives that have a methylenedioxy moiety. The proposed schemes of phase I metabolism of cathinone derivatives that were detected in eleven cathinone samples are shown in Scheme 1, 2 and 3. The detection was carried out using LXQ linear ion trap with an APCI interface used as ionisation source and controlled by XCalibur software (Version 2.0.7 SP1). Extraction was carried out by employing two columns in series, a Cyclone and C18 XL column were used as extraction columns, and a Betasil Phenyl/Hexyl column was used for chromatographic separation, the combination of all these columns were managed inline and separated again through two six-port switching valves controlled by Aria software. Amongst the eleven cathinones detected, only butylone (7b), ethylone (6b), and methylone (5b) have had their metabolic pathways already published. Meyer *et al.* also has identified those metabolites for methylone (5b) and butylone (7b) in urine using their standard toxicological GC-MS screening procedure. For ethylone (6b) and butylone (7b) their metabolites have also been detected by Zaitso *et al.* as described above [71-73].



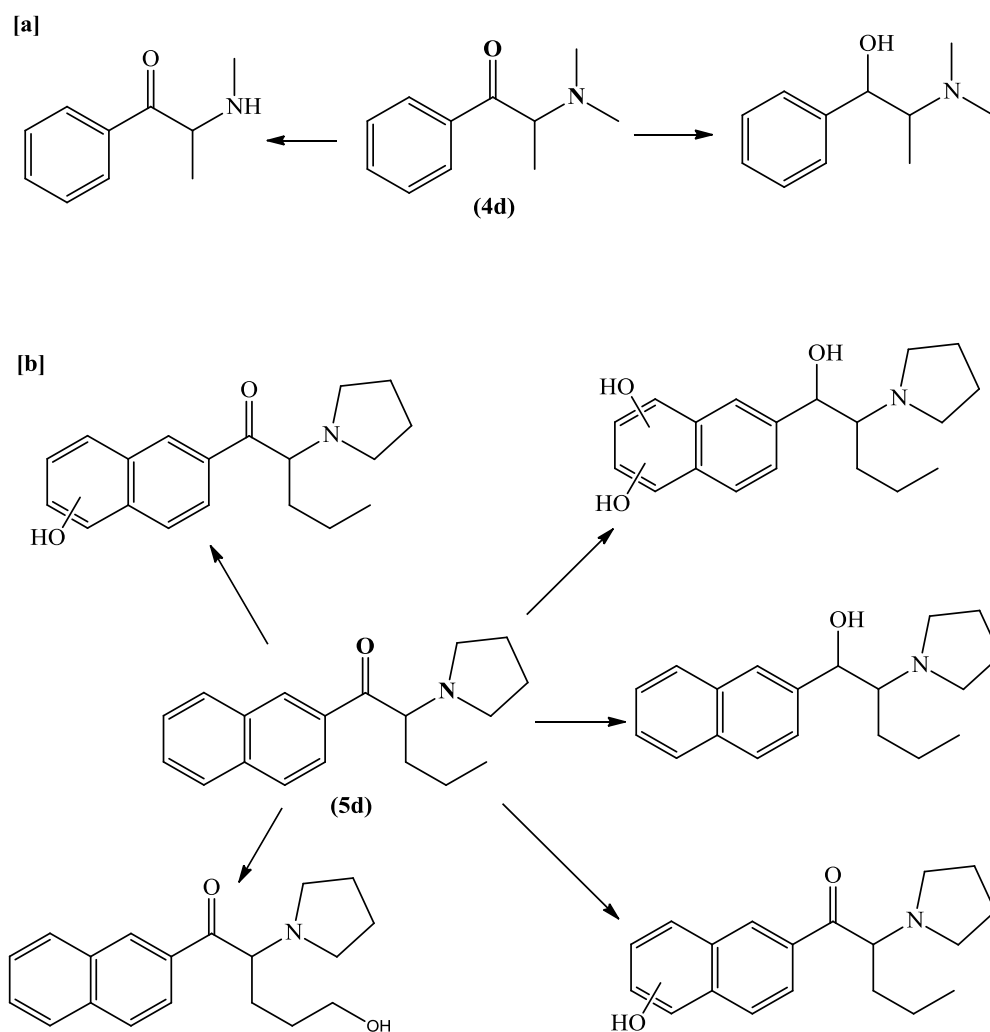
Name of cathione	R1	R2	R3	Metabolites detected
Benzedrone (3d)		H	CH ₃	I,II,V,VI,VII,VIII
Flephedrone (4c)	H	H	F	I,II
Methedrone (9b)	H	H	OCH ₃	I,III
Methylethcathinone (3c)	CH ₃	H	CH ₃	I,II,IV

Scheme 1. Proposed scheme of Phase I metabolism of Benzedrone, Flephedrone (4c), Methedrone (9b) and Methylethcathinone (3c) [72].



Name of cathinone	R1	R2	Metabolites detected
3,4-Methylenedioxy- <i>N</i> -benzylcathinone		H	I,II,III
Butylone (7b)	CH ₃	CH ₃	I,II,IV
Ethylone (6b)	CH ₂ CH ₃	H	I,II,IV
Methylone (5b)	CH ₃	H	II,III,IV
Pentylone (8b)	CH ₃	CH ₂ CH ₂ CH ₃	I,II,III,V

Scheme 2. Proposed scheme of Phase I metabolism of 3,4-methylenedioxy-*N*-benzylcathinone, butylone (7b), ethylone (6b), methylone (5b) and pentylone (8b) [72].



Scheme 3. Proposed scheme of phase I metabolism of [a] dimethylcathinone (4d), and [b] naphyrone (5d) [72].

1.8 The role of the liver in drug metabolism

In this study, although we recognize that the liver might not be the only target organ for the metabolism of cathinones, it is likely to be a major site of metabolism of the drug, and we have therefore chosen to study the metabolism of cathinone derivatives in isolated rat and human hepatocytes.

The liver is considered as one of the largest organs in the body, for example, in humans it is reported to be approximately 5% of the total body weight at birth, and 2.5% in the adult [74].

Although, metabolism may occur in many organs such as the intestinal mucosa, the liver is the most important organ for metabolism and detoxification of drugs, and contains a significant amount of the major drug metabolic enzymes for Phase I oxidative and Phase II conjugative pathways[75, 76].

The major function of the liver is to take up substrates from the intestine and transform them into water-soluble metabolites by a procedure which is known as first-pass metabolism, and then to distribute them into the blood for excretion into the urine, or excrete them directly into the bile. Metabolism involves a sequential process of oxidation – conjugation reactions commonly known as metabolic detoxification[74, 76].

The composition of the liver tissue is divided into parenchymal and nonparenchymal cells. The parenchymal cells are known as hepatocytes, and they are in the majority in the liver being approximately 60% and 80% by cell number and weight, respectively. These cells are mostly used for toxicological and metabolic studies. The nonparenchymal cells include: endothelial cells, which line the sinusoidal space, Kupffer cells which are responsible for the scavenging of endotoxins released from the bacterial flora in the gut, and lipocytes (Hepatic stellate cells) which serve as vitamin A-storing cells[76].

In vitro preparations such as hepatocyte suspensions provide a ready source of drug metabolites under the correct incubation conditions, since they can offer the full complement of drug-metabolising enzymes and cofactors present *in vivo*. In addition, isolation of hepatocytes is becoming widely used as an *in vitro* model for studying metabolism of xenobiotics [77]. Initial attempts to isolate hepatocytes by introducing enzymes (such as collagenase and hyaluronidase) as dissociating agents to liver slices were not very successful and yielded cells with poor viability and functionality. In 1969, Berry and Friend established a liver perfusion technique in which the liver of laboratory animals is perfused with collagenase in a recirculating system and this produced high viability cells. In rat liver, Moldeus *et al.* in 1978 carried out the perfusion by cannulating the hepatic portal vein and the liver was perfused with collagenase in a circulating system [78].

In addition, hepatocytes can be used to study integrated hepatic metabolism (Phase I and Phase II) during 2 hours of incubation with the substrates. Collagenase, a connective tissue degradation enzyme, is used to disperse the cells from the tissue.

1.9 Common Phase I and Phase II Metabolism Pathways

Drug therapy is complicated by drug metabolism, because the metabolites may have different properties from the parent drug that might lead to loss of its specific activities, or the metabolite may prove to be toxic, for example, the metabolites formed from paracetamol can cause liver toxicity[79].

The pathways by which drugs may be metabolised are many and they can be divided into two phases: Phase I which is considered as functionalization reactions and Phase II which is considered as conjugative reactions. The reactions of Phase I metabolism can be thought of as a preparation stage for the drug to allow it to pass through Phase II reactions. However, compounds which already have functional groups such as those mentioned in Table 6 can be conjugated directly, and transformed to Phase II metabolites without going through Phase I. The major metabolic reactions of Phase I and Phase II metabolism are listed in Table 5 [80].

Table 5. Chemical reactions of Phase I and II metabolism [81].

Phase I	Phase II
Oxidation	Glucuronidation/ Glucosidation
Reduction	Sulfation
Hydrolysis	Methylation
Hydration	Acetylation
Dethioacetylation	Amino acid conjugation
Isomerisation	Glutathione conjugation
	Fatty acid conjugation
	Condensation

Phase I metabolic reactions have three main reactions including: oxidation, reduction, and hydrolysis. Oxidation is important and diverse reactions are performed by either the microsomal mixed-function oxidase system (cytochrome P 450-dependent) or nonmicrosomal enzymes (e.g. L-monoamine oxidases MAOs). The CYP 450 enzyme system is located in the endoplasmic reticulum of various cells, particularly in organs such as lung, liver, kidney, and gut, and can carry out many different reactions of Phase I metabolism including dealkylation, aliphatic and aromatic hydroxylation, dehalogenation and epoxidation. All these reactions include the incorporation of an oxygen atom into the molecule, with the help of coenzyme (NADPH), and the CYP -450 enzyme system.

Hepatic microsomal enzymes require a coenzyme (NADPH) to catalyse the reduction metabolic reactions, but generally oxygen inhibits these reactions. Compounds that can undergo reduction include azo-compounds (nitrogen-nitrogen double bonds), nitro-compounds (nitrogen group; NO₂), epoxides, heterocyclic ring compounds, and halogenated hydrocarbons. This reaction can frequently result in activation of a substrate rather than detoxification [80, 82].

Large chemicals such as esters, amides, hydrazides and carbamates can readily be hydrolysed by various enzymes in plasma or in liver, and the specific form of hydroxylation is hydration in which water is added to compounds without causing any dissociation of these compounds. For example, hydration of epoxides is carried out by epoxide hydrolase enzyme.

As discussed above the key function of Phase I metabolism is preparing the compounds to undergo Phase II metabolism and then Phase II normally produces water-soluble compounds that can easily be excreted in bile fluid or urine. Phase I products are considered as intermediate metabolites which contain a reactive chemical group such as hydroxyl(-OH), amino(-NH₂) and/or carboxyl (-COOH) that is ready to conjugate with endogenous substrates and this results in Phase II metabolites[80]. Table 6 lists the primary Phase II reactions (conjugation reactions) which are catalysed by various groups of transferase enzymes and a variety of functional groups which can react to form the conjugation products[81].

Table 6. Conjugation reactions of Phase II metabolism [81].

Reaction	Enzyme	Functional group
Glucuronidation	UDP -Glucuronosyltransferase	-OH , -COOH , -NH ₂ , -SH
Glycosidation	UDP-Glycosyltransferase	-OH , -COOH , -SH
Sulfation	Sulfotransferase	-NH ₂ , -SO ₂ NH ₂ , -OH
Methylation	Methyltransferase	-OH , -NH ₂
Acetylation	Acetyltransferase	-NH ₂ , - SO ₂ NH ₂ , -OH
Amino acid conjugation		-COOH
Glutathione conjugation	Glutathione-S-transferase	Epoxide ,Organic halide
Fatty acid conjugation		-OH
Condensation		Various

Glucuronidation is one of the most important Phase II reactions, there are 4 general classes of glucuronides (O, N, S, and C), and the site of glucuronidation reactions for substrates having one or more of functional groups are shown in the above Table 6. The glucuronide conjugation of some compounds, especially in children is often not developed completely, thus the drugs may accumulate and cause serious toxicity [75].

Sulfation reactions are less dominant than glucuronidation reactions, probably due to the low availability of the activated form of inorganic sulphate in animal cells and the kinetics of the transferase enzymes. Phenols are considered as the most common substrate that can undergo sulfation reactions [75, 81, 83].

The glutathione conjugation pathway is different from the other Phase II metabolism conjugation. The functional element of glutathione is the cysteinyl moiety, which consists of the reactive nucleophilic thiol group (-SH) that attacks electrophilic

substrates. Glutathione conjugation plays the major role in detoxifying many reactive compounds such as radicals, metals, and other electrophilic compounds. Although this reaction is catalysed by a family of glutathione-S-transferase enzymes, the reaction may also occur non-enzymatically with more reactive electrophiles, and does not require energy to be supplied [84, 85].

The evidence shows that drug metabolism has significant importance when drugs which have a chiral centre are used. When a drug which is a mixture of two enantiomers is used, the metabolic enzymes in the process of drug metabolism could differentiate between one enantiomer and the other, and the metabolic reaction may occur at different rates between one enantiomer and the other [79].

In many cases Phase II metabolism occurs after Phase I, but in addition compounds having undergone Phase II metabolism may then undergo further Phase I metabolism. In general, Phase II metabolism generally produces polar metabolites that are more easily excreted, and can lead to a reduction of toxicological activities [86].

1.10 Instrumentation

1.10.1 High performance liquid chromatography system

HPLC is the physical separation technique widely used for the quantitation of drugs in formulations. A block diagram of the basic components of high performance liquid chromatograph system is demonstrated in Figure 14.

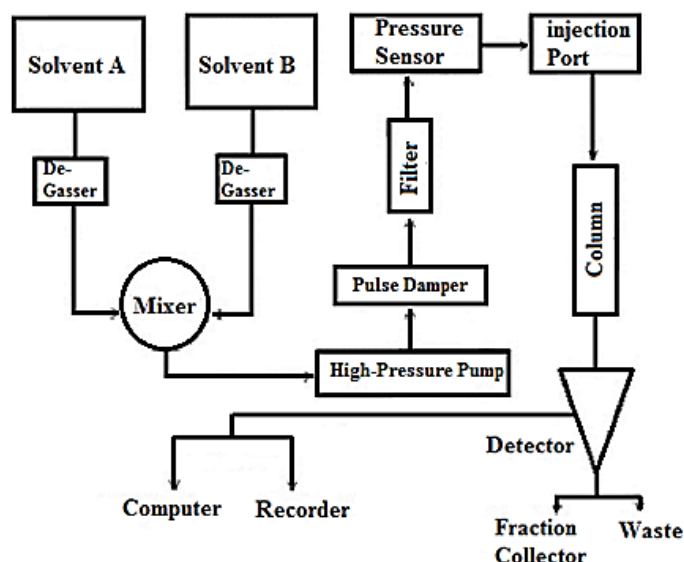


Figure 14. Schematic diagram of a basic HPLC.

The components within a HPLC system are interconnected by short segments of transfer tubing that traditionally can be made from stainless steel or polyetheretherketone (PEEK[®]) with very tiny internal diameter (0.1 mm). The column is usually made from a stainless steel tube with an internal diameter from 0.5 to 5 mm and 3 to 25 cm in length. The average size of particle diameter of stationary phase packing is typically manufactured between 3-10 μm and that can provide high efficiency columns. A high pressure pump is used to deliver solvents (mobile phase) through the system. It can pump a solvent up to a pressure of 4000 psi and can provide a flow rate of 0 to 10 mL min^{-1} , however, certain manufacturers produce micro-columns which have internal diameter such as 0.3 mm, the flow rate of the mobile phase of these columns should not go over a few $\mu\text{L min}^{-1}$.

In addition, HPLC systems may include one or several pumps. A single pump is adequate when the isocratic mode is used as the mobile phase has fixed composition, however, in the case of gradient elution when the mobile phase varies with time, two systems can be chosen: Figure 15 shows a system that can electronically activate a proportioning valve to elute the solvents at a programmed composition into a single pump (using a low pressure mixing chamber located before the pump), and Figure 16 shows a system that uses two pumps to deliver the proportions of solvents required. The flow from each pump is determined by the system controller, and the

mixing is done in a tee that is located before the column and after the pumps in the high pressure side of the pumps (using a high pressure mixing chamber) [87].

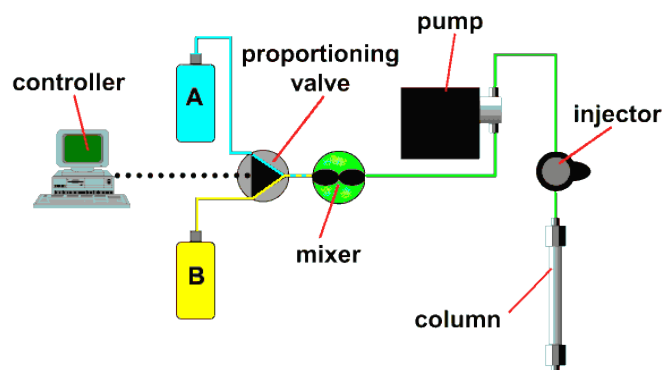


Figure 15.A Low pressure mixing system (one pump) [88].

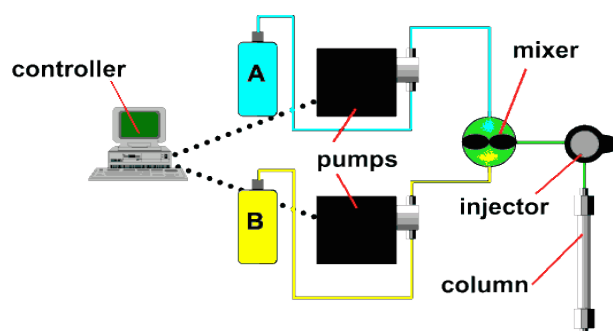


Figure 16.High pressure mixing system (two pumps) [88].

Silica gel represents the basic material used to pack HPLC columns which is a straight phase packing, and octadecylsilane- coated (ODS- coated) silica gel which is a reverse-phase packing. Both are considered as the most commonly used packing for chromatography applications, although in recent times some stationary phases based on organic polymers have become available.

A small volume (from 10 to 500 μL) of sample can be injected into the system and passed through the column, however, more advanced instruments may have automatic sample injection. The output of the column as a mobile phase with analyte can be fed to a detector or different fractions can be collected using a waste fractions collector. The detector is usually a UV-visible detector, although a wide range of

detectors is available, such as MS which is discussed later in this chapter, a data capture system which is an advanced instrument is a PC with software suitable for processing chromatographic data.

The analytes that need to be separated are loaded onto the column via a loop valve and then distributed between mobile phase and stationary phase, and the separation occurs according to the relative length of time spent in stationary phase. The time during which a compound is retained in the column depends mainly on its polarity in the case of silica gel stationary phase packings, and in the case of ODS- silica gel (Reversed phase) that mainly depends upon its lipophilicity. Most drug molecules have both polar and lipophilic groups, and the other factor to be taken into account is the nature of mobile phase which can also play a role in the degree of retention of compounds. For example, with a more polar mobile phase in the case of silica gel compounds elute more quickly from the column, and with more non-polar mobile phase, compounds elute more quickly from the reverse phase column such as ODS silica gel [89].

The most commonly used technique is reversed-phase chromatography, and generally three organic solvents are used as the mobile phase in this technique: Methanol, acetonitrile, and tetrahydrofuran. These solvents are the most different in their chromatographic selectivity and they are fully miscible with water, because solvent miscibility is very important. An LC system cannot work with combinations of solvents which are immiscible. The composition of mobile phase in the HPLC system can be combinations of two solvents that are usually one organic solvent and water. This is referred to as a binary mobile phase. In combinations of three solvents such as two organic solvents and water (three solvents), these are referred to as a ternary mobile phase [89, 90].

1.10.2 Mass chromatography

Mass spectrometry can be divided into two fundamental processes, ion generation and ion separation; some of these methods are discussed below, therefore the basic components of any mass spectrometer are made up of three separate systems

including : an ion source such as Electron Impact (EI) , chemical ionisation (CI) and Electrospray (ESI), and the second is a mass analyser such as Time-of-flight, Quadrupole, and Orbitrap , and finally the third is the detector such as Photomultiplier and Electron multiplier [91].

1.10.2.1 Ion generation

Recently, the two most important ion generation methods have become Electrospray ionisation and Electron impact, although there are about 12 methods for generation of ions prior to mass spectrometric separation.

1.10.2.1.1 Electrospray Ionisation (ESI)

Electrospray ionisation is widely ionisation technique used as Liquid chromatography – mass spectrometer interface, this technique has been continued in development for twenty years but the basic mechanism principles have remained basically the same as that seen in Figure 17. Positive ion ESI (PESI) is soft ionisation process which produces very little fragmentation and that can be considered as its main disadvantage, but it is most sensitive to use PESI with substance containing an amine group which can be detected at concentrations below 1 ng mL^{-1} , however, compounds with amide and phosphate groups can also be detected[92]. The analytes and solvent flow passes through the electrospray needle following liquid chromatography or direct injection from a syringe pump. The needle has a high negative or positive potential that is typically of 3.0-4.5 kV and all molecules inside the needle have surface charges the same as the charge on the needle that depending on the ion polarity of interest. Once the droplets leave the needle they first form a Taylor cone as shown in Figure 17. The cone bursts away into a fine spray and then solvent evaporation occurs, the size of droplets shrinks until they reach a limit where the surface tension can no longer bear the charge within the droplet, and then at that point a “Coulombic explosion” happens and the droplet forms a series of smaller droplets. The shrinking process and coulombic explosion can repeated several times until individual analyte molecules charged with single or multiple charges are formed [89].

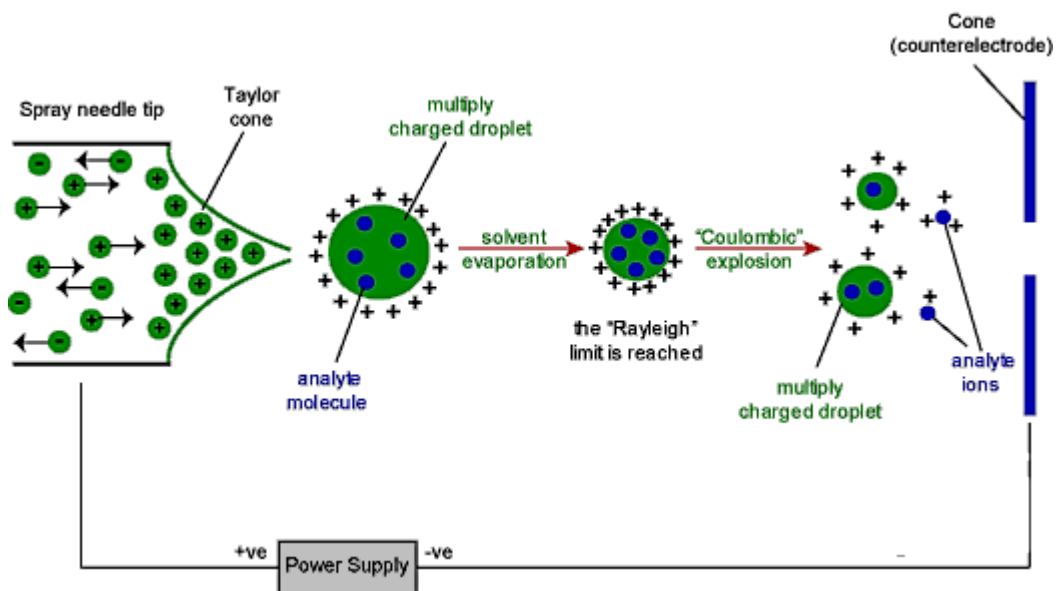


Figure 17.A scheme of ESI mechanism [93].

Generally, Negative ion ESI (NESI) is less sensitive than PIESI although there some compounds that can be detected only in negative ion mode such as neutral sugars and organic acids. Compounds such as amino acids can bear either a positive or negative charge and can be detected in both positive and negative modes [92]. Practically, mobile phases containing simply acetic acid or formic acid tend to produce a better sensitivity in positive ion mode than mobile phases containing the ammonium ion since the electrolyte additive in mobile phase that can suppress other positively charged ions in the sample by competing with analyte to produce gas phase ions. Also in negative ion mode mobile phases such as trifluoroacetic acid, since it is a stronger acid than most organic acids , can suppress the other negatively charged ions[89].

ESI was chosen in the current study due to suitability of this technique for a wide range of compounds compared to the other technique such as APCI. It is best suited for mid-to high molecular weight polar or ionic analytes and also applicable to less volatile compounds which have a molecular weight greater than 1000 Da that cannot be readily ionised in the gas phase [94].

1.10.2.1.2 Electron Impact (EI)

The original sort of ionisation utilised in mass spectrometry was electron impact ionisation (EI) and it is considered to be a hard ionisation technique. It is commonly used in combination with gas chromatography mass spectrometry (GC-MS). EI uses high-energy electrons at 70eV and at this voltage ionisation and fragmentation become very reproducible between different types of ionisation source. This enables EI to generate mass spectral “fingerprints” for molecules which contain many fragments due to the breaking of the bonds within the analyte.

A rhenium or tungsten filament is heated in vacuum atmosphere in order to generate free electrons which are accelerated within a restricted source toward a positive target. The unionised analyte is introduced into the instrument between the filament and the target through a number of separation techniques including GC and direct injection via a heated probe and is then are bombarded by electrons (See Figure 18) [89].

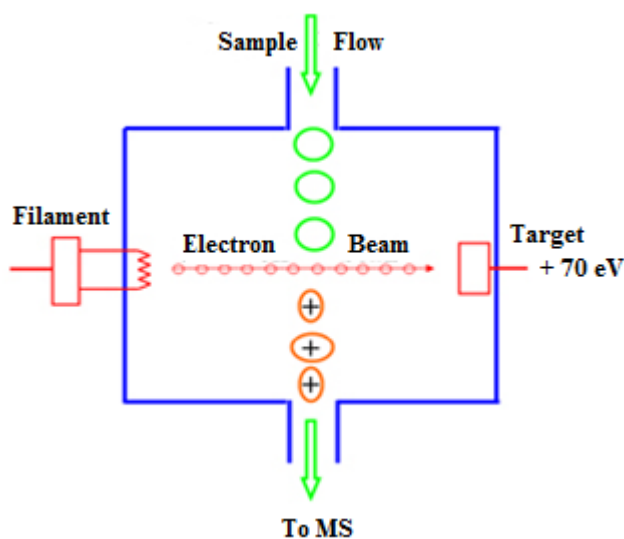


Figure18 . Scheme of electron impact ionisation (EI) [95].

EI is still very commonly used in standard chemical detection but is not appropriate where the molecules being analysed are very involatile or unstable. Figure 19 shows a general scheme of type of molecular fragmentation that is allowed under EI conditions. M^+ denotes the molecular ion of an analyte which bears one positive charge due to losing one electron. It may lose a radical and this is considered as

straightforward fragmentation since no rearrangement has been involved. The radical removes an unpaired electron from M^+ resulting in formation of a cation A^+ . The cation can go on to lose any number of neutral fragments (N), such as CO_2 or H_2O , to produce further cations such as D^+ . The fragmentation process can occur in a different order and that neutral fragments can be lost first and since the ion still has an unpaired electron B^+ it can lose a radical later to produce cation C^+ [89, 91].

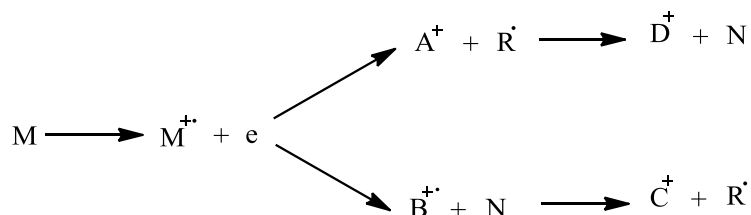


Figure 19. Decomposition of a molecule under Electron Impact ionisation.

1.10.2.1 Ion separation methods

1.10.2.1.1 The Orbitrap Mass spectrometer

A new approach to Fourier transform mass spectrometry is the Orbitrap analyser which uses an electrostatic field to trap ions rather than the magnetic field used in ion cyclotron resonance FT instruments. One of the systems commercially utilizing the Orbitrap analyser is available as a hybrid linear ion trap/Orbitrap mass spectrometer (LTQ Orbitrap). Figure 20 shows scheme layout of the LTQ Orbitrap which consists of three major parts. The first part of LTQ system after the ionisation source is a linear ion trap which can produce MS and MS^n spectra. The ions are then focused in a quadrupole called the C-trap due to it is like letter C shape. Finally the ions injected into the third trap which is the Orbitrap. The ions tangentially cycle around an inner electrode and are trapped by applying a suitable voltage between outer and inner electrodes. The mass spectrum is obtained by measuring the image current after Fourier transformation. The frequency spectrum is translated into a mass spectrum using a two-point calibration then finally processed using Xcalibur software. The

Orbitrap can provide mass accuracy ≤ 3 ppm and resolution that surpasses 100,000 [96-99].

Both the linear ion trap and the Orbitrap can be used as an analyser to detect ions and record spectra, it depends on the analysis requirements and mode used. The Orbitrap and the LIT can be operated independently or in combination. Accurate mass measurement can be performed in the Orbitrap and MS^2 and MS^3 experiments can be recorded with the LIT [97, 99].

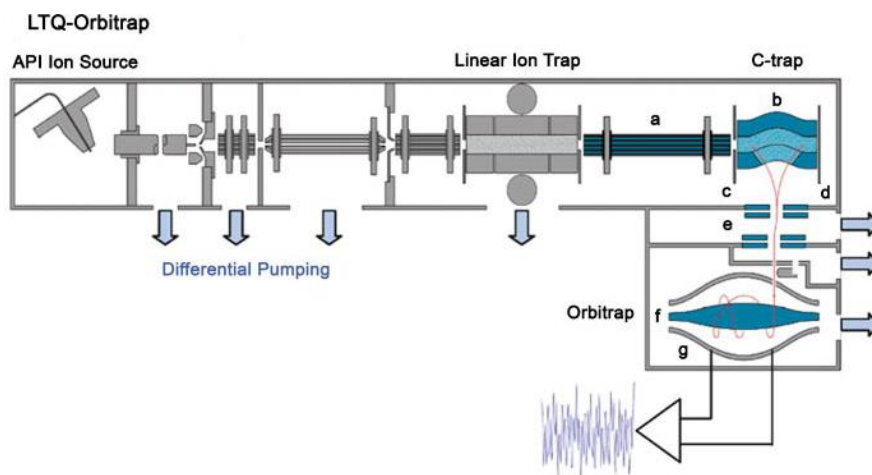


Figure 20. Scheme of LTQ Orbitrap mass spectrometer: (a) transfer Octopole; (b) C-trap (c) gate electrode (d) trap electrode (e) ion optics (f) inner electrode of Orbitrap (g) outer electrode of Orbitrap [95, 100].

The Orbitrap is also available in the other commercial instrumentation such as the Exactive which is an easy-to-use benchtop LC/MS system that can measure wide mass range spectra at high resolution and with minimum supervision. In Figure 21 the schematic layout of the Exactive high resolution instrument is shown. The Exactive does not have the capability of performing selected ion fragmentation using collision induced dissociation (CID) which the LTQ Orbitrap has [92, 99].

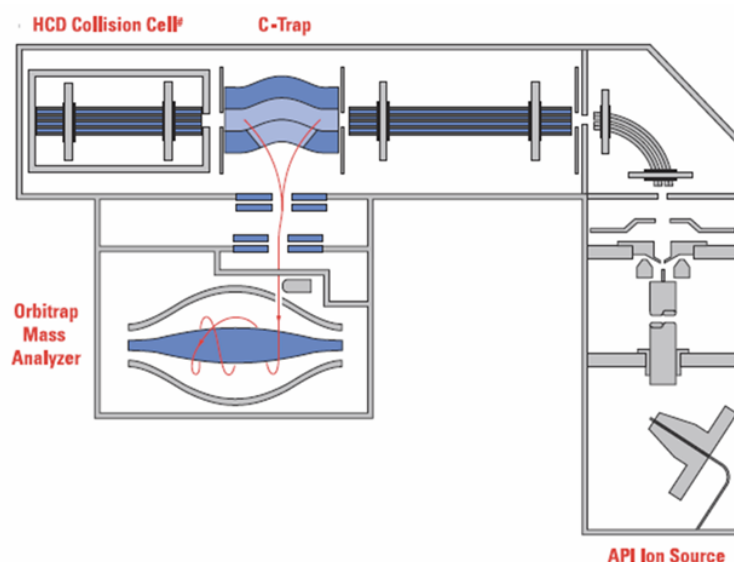


Figure 21. Schematic layout of Orbitrap bench-top mass spectrometer (Exactive, Thermo Fisher Scientific, Bremen, Germany) [100].

1.10.3 Gas chromatography –mass chromatography

Gas chromatography was early separation technique to be coupled to a mass spectrometer. Generally sample containing metabolites is derivatised and injected into a heated glass or quartz liner rather than direct into the capillary column. The injection can be carried out either manually or through the use of an autosampler. The reason for using a liner is because to the diameter of the capillary column is between 0.2 and 0.5 mm and direct injection can easily damage it. The analytes travel to the ionisation source and are ionised as discussed earlier by electron impact ionisation. In a quadrupole GC-MS system, a voltage is applied to the four rods of a quadrupole mass analyser creating an electric field, and each ion can follow a different path as it moves through the quadrupole. Only ions of specific m/z ratio, for a given voltage, can make their way through the quadrupole without hitting the rods. Hence a scanning method is used to detect a wide range of m/z ratios, which is known as total ion current (TIC) mode that is good for detection the unknown compounds. The GC-MS has to be connected to computer and data analysis software such as Xcalibur which generates a chromatogram and mass spectrum for each compound present within that analysis.

1.11 *In Silico* tools for data processing

1.11.1 SIEVE software

Thermo Scientific SIEVE software is the one of commercial software packages for processing LC-MS data. It aims to plot extracted ion chromatograms against the full scan range of mass spectrometer and is used for comparative analysis. In Figure 22 an example using this software is shown. The bin width for the ions was set as 0.02 amu and the extracted ion chromatograms in these bins are compared between two sample groups. It offers an easy-to-use automated key for measuring the large amounts of LC/MS data generated by the label-free sample analyses used.

Sieve software was employed in this study for data processing, particularly for alignment, peak detection and statistical analysis. Firstly, LC chromatograms are aligned by selected a Reference raw data file to evaluate the difference in retention time from LC run in the experiment, and then all peaks collected from all raw data files above a given threshold value T will be ordered by the intensity.

Figure 22 shows frames of 2.5 min x 0.02 amu that are defined based on the most intense peak, and define the next frame upon highest peak that does not overlap with previous frames.

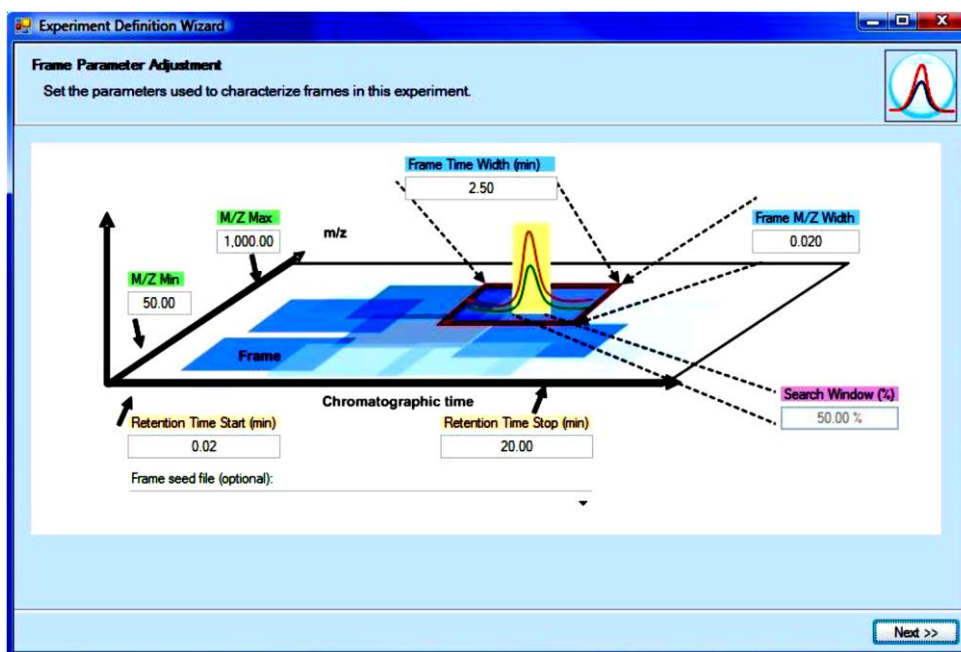


Figure 22. Frame parameter using to frame peaks in three dimensional axes; m/z versus retention time versus peak intensity.

The variances in the plots are highlighted and the exact masses of ions yielding the difference can be detected. This is illustrated in Figure 22 as the software has found a difference in the intensity peaks of desmethyl-MMC (7) which is metabolite of mephedrone formed after incubation with hepatocytes. The red plots for the exact ion at m/z 164.10 display the level of desmethyl-MMC (7) in the sample at 30 minute of incubation time and the blue plots show the level of the same metabolite after 120 minute of incubation time. Also this software can give a ratio for the mean peak areas as well as a P value. To calculate valid p -value, Sieve can be used analyse a minimum four LC/MS raw data files comparing two control files and two sample files. It can analyse up to 100 LC/MS raw data files in a single operation by comparing a 50 control files and 50 sample files. The quality of the chromatogram of alignments can affect the p -values obtained and with poor chromatogram alignments the p -value will not be accurate. As illustrated in Figure23 that the alignment of the chromatographic peaks of the different runs was good but not perfect. To avoid artifacts that can produced by poor peak alignment, the data have to be checked carefully in Sieve software.

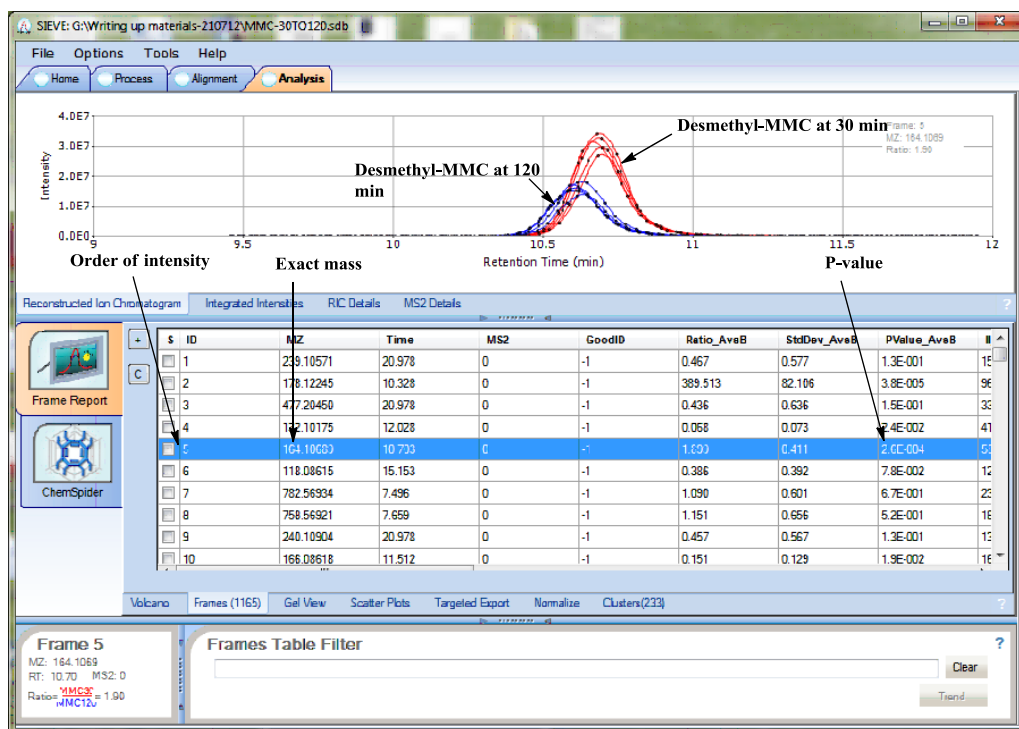


Figure 23. Application of Sieve Software to identifying the difference between two sample groups.

1.11.2 MetWorks (Thermo Fisher Scientific)

Thermo Fisher Scientific MetWorks™ 1.3 is a metabolite identification software for small molecules and their metabolites, it can integrate the acquisition features of the Xcalibur data system and can be used with a high degree of accuracy and assurance to find and characterise a variety of drug candidate metabolites. The results can be reviewed and edited, and at the end of workflow can produce a customized MetReport showing what metabolites have been detected.

MetWorks utilises liquid chromatography/mass spectrometry data to make the search for expected and unexpected metabolites easy and fast. The candidate drug and its metabolites can be calculated automatically and accurate mass analysis data will provide with ppm values using standard molecular formula. MetWorks Version 1.3 provides a new feature that increases the power limit of Multiple Mass Defect Filters (MMDF) as well as new brief summary report can be generated.

There are seven major steps of MetWorks procedure. First step is selecting and loading the acquired raw data (Xcalibur file used in this study) and then once an analyte name and elemental formula are enter in the analyte(s) dialog box, the application will calculate the exact m/z automatically. Metworks 1.3 also has new modification manager, a modification list based on drug structure and expected modification (Phase I and II). Searches can be based one or two modifications specified by the user and the software create custom lists of expected modifications. The other steps of workflow are shown in Figure 24-a. The output of the modification parameter MMDF interface displaying the distribution of parent drug and its possible metabolites on a mass defect plot is shown in Figure 24-b.

The values of mass defect filters are installed automatically at the top of dialogue box as shown in Figure 24-b. In addition, filter value can also be specified manually by allowed typing up to six values into the table. Adjusting the filter is easy by dragging the cursor up or down in the bottom panel where all the identified metabolites are marked by coloured triangles as well as rectangle for the parent compound. By clicking on a triangle, information related to this metabolite would be appear on small placeholders[101].

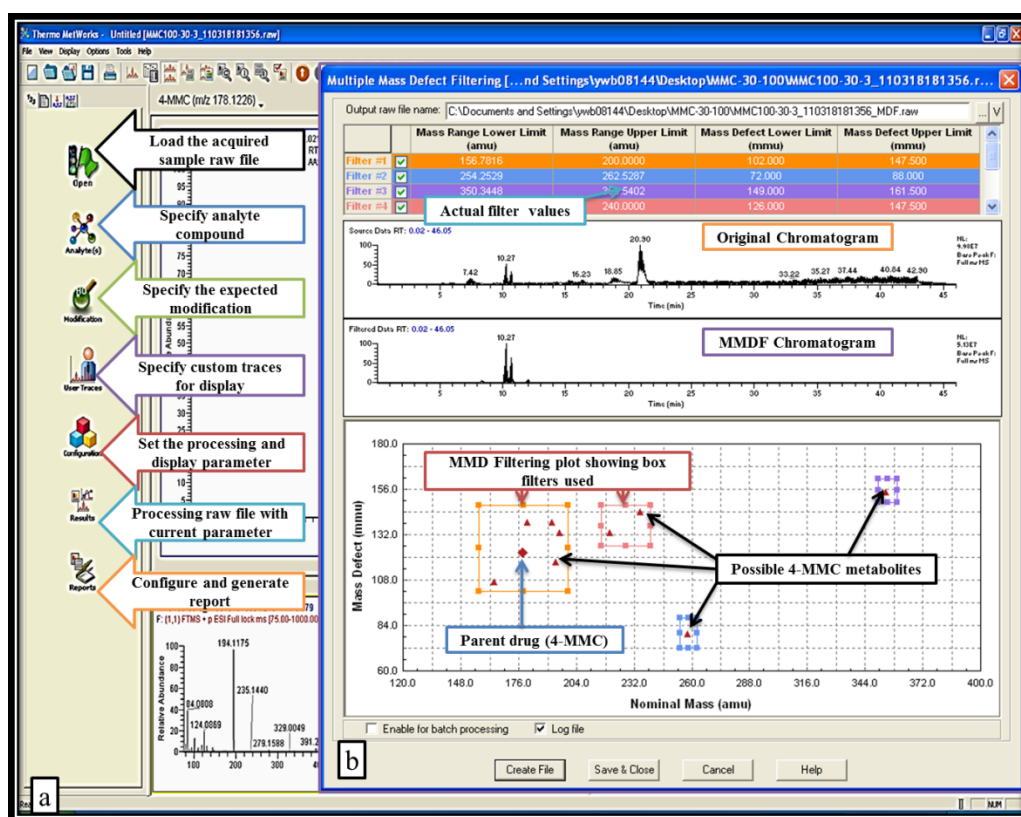


Figure 24. MetWorks software work flow (a) seven-step procedure of Networks and (b) Multiple Mass Defect Filters (MMDF) provide capabilities of data reduction and full data visualization.

1.11.3 ToxID Software

ToxID is versatile software that provides data processing and automated analyte identification in variety of LC-MS analyses. Xcalibur data files which are based on chromatographic retention time and MS spectra can be loaded into the manual user interface that is shown in Figure 25. Sample reports are then automatically generated, either summary report that lists all analytes found in the raw data file or a long report with more details for each analyte that is achieved in the summary report. The reports generated are based on screening methods and platforms, using the Excel ToxID configuration file (ToxID-Cofig.csv) as a template[102].

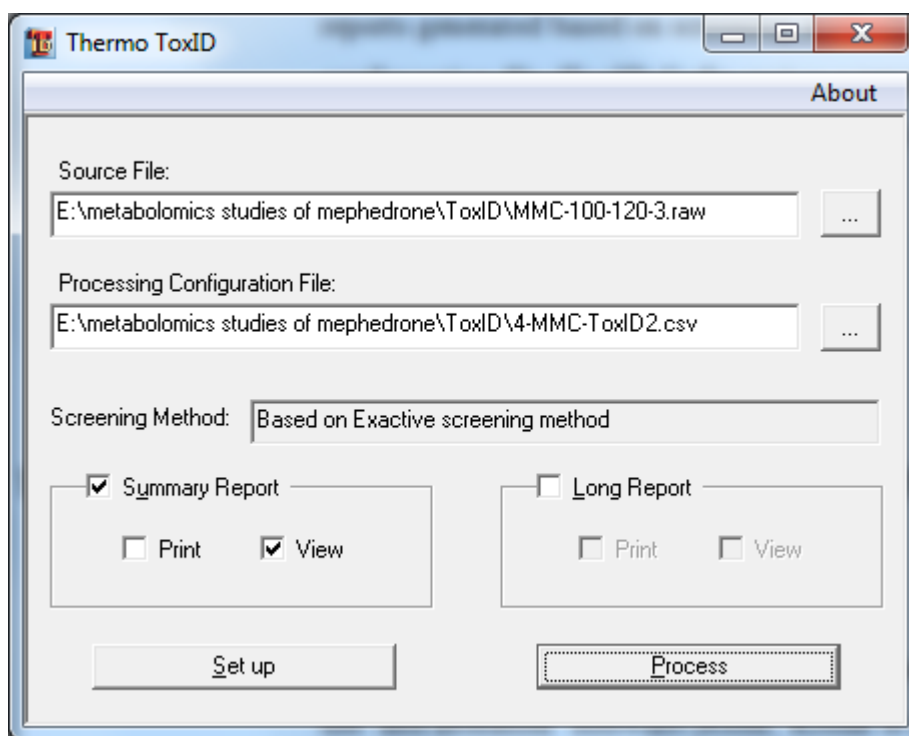


Figure 25. ToxID interface used to load LC-MS raw data such as Xcalibur.

In addition, another report can be generated automatically from this software in spreadsheet format which provides data that can be imported into a database. As a final point, all these reports will be saved in raw file folder using format included the name of source file, date, time and report type, but the spreadsheet file has no report type in its file name format. Depending on the experiments used, ToxID can be run in three ways. To process a single raw data file, to process an entire sequence or selected Data files.

In the current study ToxID was used with Thermo Scientific Xcalibur Data system to identify analytes according to accurate mass and retention time.

1.12 Metabolite detection methods

The past thirty years have seen increasingly rapid advances in the use of gas chromatography–mass spectrometry for identifying many drug metabolites. But because of the requirement for sample preparation such as derivatization which increases the time of analysis, and the limitation of molecular size, liquid

chromatography–mass spectrometry has become more popular for identifying the drug metabolites. An ESI interface is most commonly utilised because of its capability to produce gas-phase ions directly from the liquid phase. Tandem mass spectrometry is used to characterise compounds and their metabolites, and for many years it has been utilized to confirm the structure of unknown compounds and identify unknown metabolites of drug candidates. In recent years researchers have identified a variety of drug metabolites using different types of mass spectrometer, for example many pharmaceutical industries utilise QQQ mass spectrometers (triple quadrupole), because of the low cost and flexibility. However, new hybrid techniques such as the LTQ – Orbitrap provide some advantages over a QQQ spectrometer[103]. Some studies have described how the LTQ – Orbitrap mass spectrometer technique coupled with Liquid chromatography can provide high performance for fragmentation of small molecules and is capable of achieving a high resolution up to 150,000 with mass accuracy to 1ppm [104, 105].

To successfully characterize drug metabolites in complex matrices requires the use of sensitive and selective analytical techniques. Mass spectrometry can provide the required sensitivity and selectivity once combined with LC and the ESI ionisation technique. In a study by Brazzarola *et al.* of the mass spectrometric behaviour of ephedrine different ionisation conditions were used. They reported that EI (Electron Impact ionisation) showed limitations in the characterisation of these sort of substances, because of their low volatility, and they investigated the comparison of the results achieved by FAB(fast atom bombardment), ESI (electrospray ionisation) and APCI (atmospheric pressure chemical ionisation) ionisation techniques to identify several advantages of these new ionisation techniques which are commonly used in many pharmaceutical laboratories[106].

Mass spectrometer as mentioned above plays an important role in assessment of drug metabolism. The process of metabolite identification by MS can start by detection of a metabolite molecular ion. Subsequently the product ion scan is the major experiment that obtains structural elucidation information on the detected metabolite. MS-MS (MS^2) is considered the first step of a product ion scan, and following generation of product ions spectra from the fragment ions that were obtained from

the first step, which is defined as MS³ fragmentation, may be obtained. This helps to elucidate the structure of metabolites, and the sites of transformation from the differences in m/z ratios of the fragment ions arising from the parent compound and its metabolites [107].

As shown in Table 7, some of the common Phase I and Phase II metabolism (Transformation) reactions can be detected based on LC-MS techniques, those include targeted searches for parent precursor ion mass substitutes by a net transformation mass, monitoring for a metabolite ion (M+16, M-14) and neutral loss scans based on the parent fragmentation or common Phase II transformations such as loss of glucuronide[108].

To facilitate of drug metabolism detection, primary examination of metabolites may employ a list of targeted metabolism reactions based on the starting drug mass. The common chemical reactions of drug metabolism are converted to a list of target precursor ion m/z using the known mass shift of the chemical reaction which is shown in Table 7 , as well as the starting mass of the drug itself [108].

Table 7. Example of common Phase I and II metabolism[108].

Type of metabolism reaction	Net chemical reaction	Nominal m/z shift	Exact m/z Shift
Phase I			
Hydroxylation / N-oxidation/ S-Oxidation	+O	+16	+15.9949
Dihydroxylation	+2O	+32	+31.9898
Dehydrogenation or reduction	-H ₂	-2	-2.0156
Demethylation	-CH ₂	-14	-14.0156
Deethylation	-C ₂ H ₄	-28	-28.0312
Depropylation	-C ₃ H ₆	-42	-42.0468
Oxidative deamination	-NH ₃ ,+O	-1	-1.0316
Oxidative dechlorination	-Cl,+OH	-18	-17.9662
Oxidative defluorination	-F,+OH	-2	-1.9957
Hydration	+H ₂ O	+18	+18.0105
Oxidation of CH ₃ → COOH	-H ₂ ,+O ₂	+30	+29.9742
Phase II			
Glucuronidation	+C ₆ H ₈ O ₆	+176	+176.0321
Sulfation	+SO ₃	+80	+79.9568
Glutathione conjugation	+C ₁₀ H ₁₅ N ₃ O ₆ S	+305	+305.0681
	+C ₁₀ H ₁₇ N ₃ O ₆ S	+307	+307.0837
Cysteine-glycine conjugation	+C ₅ H ₁₀ N ₂ O ₃ S	+178	+178.0410
Cysteine conjugation	+C ₃ H ₇ NO ₂ S	+121	+121.0196
N-acetyl-cysteine conjugation	+C ₅ H ₉ NO ₃ S	+163	+163.0301
Glycine	+C ₂ H ₃ NO	+57	+57.0213
Glutamine	+C ₅ H ₁₀ N ₂ O ₃	+145	+145.0609
Taurine	+C ₂ H ₅ NO ₂ S	+107	+107.0038

1.13 Aims and Objectives

1. The first aim of this study was to develop fast analytical methods to identify and quantify novel cathinone derivatives both in their pure form and in the presence of common adulterants. These were evaluated using sources of samples of NRG-2 (These substances are legal high substances which were bought in the UK's black market). This step will include identification, and then the synthesis of pure substances with, full structural characterisation. Finally development of validation of analytical methods for cathinone derivatives in legal highs will be carried out.
2. The second aim is to characterize mephedrone metabolites, as well as those of a new designer cathinone called 4-MEC, found in the most of the NRG-2 street samples. In order to identify the metabolic pathways for these compounds and determine whether or not any potentially reactive or potential toxic metabolites are formed *in vitro* in human and rat hepatocytes. These *in vitro* studies were carried out in order to detect the major pathways of drug metabolism, especially Phase II pathways, which had not been observed before, and to understand the toxicity of the drugs, and the role of metabolism in this toxicity.

Our specific objectives in the second aim were:

- To develop a toxicological screening procedure based on identified metabolites using ESI- LC-MS
- To gain some insight into how small structural alterations might affect metabolism by studying the metabolism of the 4-trifluoromethyl analogue of mephedrone.
- To perform MS/MS experiments, by using an LTQ Orbitrap to achieve further structural information.
- To use GC-MS to gain additional information on the metabolites formed.

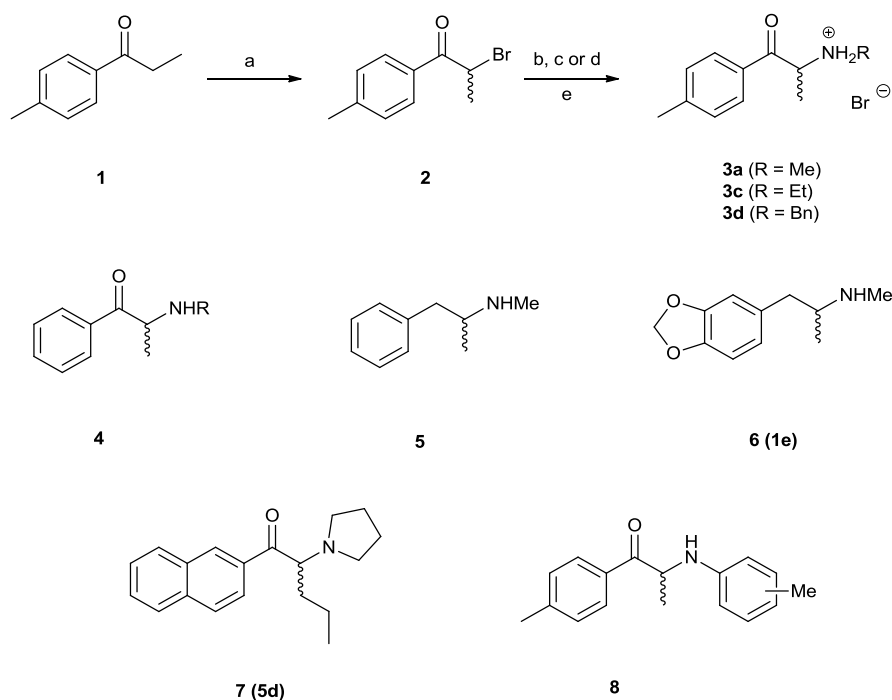
Chapter 2: Synthesis, full chemical characterisation and development of a validated HPLC method for the quantification of components found in the evolved “Legal high” NRG-2

2.1 Introduction

In the last few years there has been a striking increase in the sale of “*legal highs*” [20]. These chemicals may be bought through the internet at low cost and are sometimes pure compounds which display highly similar chemical structures to existing controlled substances within the phenethylamine class.

(±)-4'-Methylmethcathinone or (±)-mephedrone (**3a**, 4-MMC) [11, 16, 31, 63, 109-115] is a synthetic β -ketoamphetamine that is structurally similar to methcathinone (**4**, R = Me), related to cathinone (**4**, R = H), a psychoactive compound found in Khat. (±)-Mephedrone has recently emerged in drug seizures, as a “*legal high*” replacement for controlled stimulants, including amphetamines such as methamphetamine (**5**) and MDMA (**6**; **1e**) (Scheme 4). (±)-Mephedrone is now a substance controlled by legislation in the United Kingdom, Germany, Norway, Sweden, the Netherlands, Finland, Romania, Republic of Ireland, Denmark, Canada and Israel. Since the legislative change, a number of evolved “*legal high*” products, such as NRG-1 (naphyrone, **7**; **5d**) and NRG-2, which are advertised to contain legal mephedrone substitutes, have become available. However, many of these have been reported to contain structurally related cathinone derivatives that are themselves controlled substances [19, 116, 117].

This research has thrown up many questions in characterization and analysis of NRG-2 as a “*legal high*” product. The identification of the above compounds was first performed by HPLC and then further identification and confirmation was carried out by Dr Sutcliffe using NMR spectroscopy. In this chapter the synthesis of standard substance and full characterisation of these standards has been carried out.



Scheme 4. Reagents and Conditions: (a) Br₂ / HBr (48 % in water) / CH₂Cl₂ / rt / 1h (99.6 %); (b) MeNH₂.HCl / NEt₃ / CH₂Cl₂ / rt / 24h; (c) EtNH₂.HCl / NEt₃ / CH₂Cl₂ / rt / 24h; (d) BnNH₂ / CHCl₃ / Δ / 24h; (e) HBr (33 % in AcOH) / AcOH / rt / 1h (67.4 % (4-MMC, 3a), 41.5 % (4-MEC, 3c) and 27.2 % (4-MBC, 3d) from 2).

The prevalence of these cathinone-derived “legal high” drugs has given rise to both legal and analytical challenges in the identification of these substances. Thus, robust analytical profiling and the development of validated methods of testing are required. Although two groups have previously reported the detection and selected analytical information (such as NMR [19, 116], MS [19, 116] and IR [116] data) of (±)-4'-methyl-*N*-ethylcathinone (**3c**, 4-MEC) in samples of NRG-2[19] and bulk powders seized by law enforcement agencies[116], however, there has been no comprehensive analytical profiling of a pure reference sample or the development of a validated chromatographic method for this substance. This chapter seeks to address this matter by presenting the complete chemical synthesis, key physicochemical parameters (Log P, pK_a) and full structural elucidation of (±)-4'-methyl-*N*-ethylcathinone (**3c**) by NMR, IR, UV and MS. Additionally, we report the synthesis and characterisation of a novel structurally-related derivative (±)-4'-methyl-*N*-benzylcathinone (**3d**, 4-MBC), which has been identified in seized samples of NRG-2. A fully validated chromatographic method for the detection and quantitative

analysis of these two substances, both in their pure form and in the presence of common adulterants is presented and evaluated using sources samples of NRG-2.

In 2010, Brandt *et al.* published a paper in which they reported that wide range of “legal high” products had been purchased online from eighteen UK – based websites through six weeks after mephedrone had been banned. Seven samples labelled as NRG-2 were analysed. Four of the NRG-2 samples were found to contain the expected 4-MEC (3c) only, but the remaining three NRG-2 appeared to be consisted of mephedrone alone, a mephedrone / benzocaine mixture, or benzocaine / caffeine mixture, MDPV. But 4-MBC (3d) were absent in these samples [19, 117]. In the current study, the results obtained from the analysis of ten NRG-2 samples indicated the presence of 4-MBC (3d) and MDPV in some of these samples. Thus, re-development and re-validation of a HPLC method for separation of a wide range of substituted cathinones was carried out.

Isocratic methods were examined prior to gradient mobile phase elution but were found unacceptable due to the difficulty of separating the seven compounds in the mixture in one run.

Thus a gradient method was developed in order to control the retention time and the resolution of analytes which had a wide range of polarity [118].

2.2 Experimental

All reagents were of commercial quality (obtained from Sigma-Aldrich, Gillingham, UK or Alfa-Aesar, Heysham, UK) and used without further purification. Solvents were dried, where necessary, using standard procedures.

(±)-4'-Methyl-2-bromopropiophenone (**2**) and (±)-4'-methylmethcathinone hydrobromide (**3a**, 4-MMC) were prepared using the methods reported previously by Santali *et al.* who used method reported by Kalendra *et al.* with following modification, by adding one drop of hydrobromic acid (48% aqueous solution) and one drop of bromine to a solution of 4-methylpropiofenone (**1**, 14.8 g, 100 mmol) in dichloromethane (50 mL). The mixture was stirred at room temperature while waiting for the bromine colour was disappeared (circa. 30 s), and then introduced dropwise with stirring additional bromine drops (5.1 mL, 100 mmol total including the original drop). The Stirring was continued for 1 h and then concentrated in vacuo

to reveal dark orange oil which solidified on standing. The crude product was recrystallised from diethyl ether to afford (\pm)-4-methyl-2-bromopropiophenone (**2**) (22.6 g, 99.6%) as colourless crystals [63, 119].

^1H and ^{13}C NMR spectra were acquired on both JEOL AS-400 (JEOL, Tokyo, Japan) and Bruker Avance 400 (Bruker, Karlsruhe, Germany) NMR spectrometers operating at a proton resonance frequency of 400 MHz. Infrared spectra were obtained in the range 4000-400 cm^{-1} using a ThermoScientific Nicolet iS10ATR-FTIR instrument (ThermoScientific, Rochester, USA). Mass spectra were recorded on a ThermoScientific LTQ ORBITRAP mass spectrometer (ThermoScientific, Rochester, USA) using electrospray ionisation. Ultraviolet spectra were obtained using a Unicam 300 UV spectrophotometer (ThermoScientific, Rochester, USA). Thin-Layer Chromatography (TLC) was carried out on aluminium-backed SiO_2 plates (Merck, Darmstadt, Germany) and spots were visualised using ultra-violet light (254 nm). Microanalysis was carried out using a PerkinElmer 2400 Series II elemental analyser (PerkinElmer, San Jose, USA). Melting points were determined using differential scanning calorimetry (DSC; Netzsch STA449 C, Netzsch-Gerätebau, Wolverhampton, UK). Optical rotation values $[\alpha]_{\text{D}}^{22}$ (10^{-1} deg $\text{cm}^2 \text{g}^{-1}$) were performed on a Bellingham & Stanley ADP-220 polarimeter (Bellingham & Stanley, Tunbridge Wells, UK). Log P and pK_a values were determined on a Sirius T3 instrument (Sirius Analytical Instruments, Forest Row, UK). Calculated Log P and pK_a values were determined using Pipeline Pilot software, Vers. 7.5 (Accelrys, San Diego, USA). Sample of NRG-2 were purchased from different internet sources, a reference standard for 4-MMC (3a), 4-MEC (3c) and 4-MBC (3d) were synthesized in house in the SIBPS laboratories at University of Strathclyde, UK.

HPLC grade methanol was obtained from Fisher Scientific (Leicestershire, UK). Ammonium formate and formic acid (laboratory reagent grade) were purchased from BDH laboratory supplies (England), Uracil was obtained from Sigma Aldrich (USA), Caffeine and Benzocaine were purchased from Sigma Aldrich (Germany).

2.2.1 Synthesis of (±)-4'-methyl-N-methylcathinone hydrobromide (4-MMC, 3a)

The title compound was prepared using the method reported by Sutcliffe *et al.* [63] with the following modifications: To a suspension of (±)-4'-methyl-2-bromopropiophenone (**2**, 4.54 g, 20 mmol) and methylamine hydrochloride (1.35 g, 20 mmol) in dichloromethane (40 mL) was added triethylamine (5.58 mL, 40 mmol). The mixture was stirred at room temperature overnight and then acidified (pH ~ 1) with 6 M hydrochloric acid (50 mL). The aqueous layer was washed with dichloromethane (3 × 50 mL), basified (pH ~ 10) with 5 M sodium hydroxide (*circa.* 100 mL) and then re-extracted with dichloromethane (3 × 50 mL). The combined organic fractions were dried (MgSO₄) and concentrated *in vacuo* to give a viscous yellow oil. The oil was dissolved in glacial acetic acid (2ml), treated with hydrobromic acid (33% solution in acetic acid, 5 mL) and stirred at room temperature for 1 h. The mixture was diluted with diethyl ether (100 mL) and stirred until a pale beige solid formed (*circa.* 30 min). The crude product was filtered, washed with diethyl ether and recrystallised from acetone to afford (±)-4'-methyl-N-methylcathinone hydrobromide (1.74 g, 67.4% from **2**) as an off-white powder (All data analysis was reported and presented in Santali and co-worker studies and all synthesis experiments were done by Dr. Oliver Sutcliffe)[63].

2.2.2 Synthesis of (±)-4'-methyl-N-ethylcathinone hydrobromide (4-MEC, 3c)

The title compound was prepared using the method reported by Sutcliffe *et al.* [63] with the following modifications: To a suspension of (±)-4'-methyl-2-bromopropiophenone (**2**, 4.54 g, 20 mmol) and ethylamine hydrochloride (1.63 g, 20 mmol) in dichloromethane (40 mL) was added triethylamine (5.58 mL, 40 mmol). The mixture was stirred at room temperature overnight and then acidified (pH ~ 1) with 6 M hydrochloric acid (50 mL). The aqueous layer was washed with dichloromethane (3 × 50 mL), basified (pH ~ 10) with 5 M sodium hydroxide (*circa.* 100 mL) and then re-extracted with dichloromethane (3 × 50 mL). The combined organic fractions were dried (MgSO₄) and concentrated *in vacuo* to give a viscous yellow oil. The oil was dissolved in glacial acetic acid (2 mL), treated with hydrobromic acid (33 % solution in acetic acid, 5 mL) and stirred at room

temperature for 1 h. The mixture was diluted with diethyl ether (100 mL) and stirred until a pale beige solid formed (*circa.* 30 min). The crude product was filtered, washed with diethyl ether and recrystallised from acetone to afford (\pm)-4'-methyl-N-ethylcathinone hydrobromide (2.26 g, 41.5 % from **2**) as a colourless powder. Mpt. (acetone) 206.08 °C; R_f [SiO₂, EtOAc:*n*-hexane (1:3)] = 0.10; [α]_D²² = 0 (c = 0.5 g 100 mL⁻¹, MeOH); found: C, 52.90; H, 6.65; N, 4.95. C₁₂H₁₈BrNO requires C, 52.95; H, 6.67 and N, 5.15 %; UV (EtOH): λ_{\max} = 260.0 nm (A = 0.693, c = 1.02 x 10⁻³ g 100 mL⁻¹); IR (ATR-FTIR): 2735.4 (NH₂⁺), 1687.3 (C=O), 1605.4 cm⁻¹ (C=C); ¹H NMR (400 MHz, 60 °C, *d*₆-DMSO) $\delta^1\text{H}$ (ppm) = 8.92 (2H, br s, CH(NH₂⁺CH₂CH₃)CH₃); 7.98 (2H, d, *J* = 8.4 Hz, AA'BB'), 7.41 (2H, d, *J* = 8.4 Hz, AA'BB'), 5.21 (1H, q, *J* = 6.8 Hz, CH(NH₂⁺CH₂CH₃)CH₃), 3.04 (2H, dq, *J* = 12.4, 7.2 Hz, CH(NH₂⁺CH₂CH₃)CH₃), 2.42 (3H, s, ArCH₃), 1.53 (3H, d, *J* = 7.2 Hz, CH(NH₂⁺CH₂CH₃)CH₃) and 1.28 ppm (3H, t, *J* = 7.2 Hz, CH(NH₂⁺CH₂CH₃)CH₃); ¹³C NMR (100 MHz, 60 °C, *d*₆-DMSO) $\delta^{13}\text{C}$ (ppm) = 195.5 (C=O, C1), 145.2 (ArC, C4'), 130.2 (ArC, C1'), 129.4 (2 × ArC, C3'/C5'), 128.6 (2 × ArCH, C2'/C6'), 56.5 (CHCH₃, C2), 40.2 (NH₂⁺CH₂CH₃, C4); 20.9 (ArCH₃, C7'), 15.7 (CHCH₃, C3) and 10.8 ppm (NH₂⁺CH₂CH₃, C5); LRMS (ESI+, 70 eV): *m/z* = 192 (34%, [M+H]⁺), 174 (100), 159 (30), 145 (57), 131 (16), 119 (25) and 91 (6); HRMS (ESI+, 70 eV) calculated for [M+H] C₁₂H₁₈NO: 192.1383, found: 192.1381.

2.2.3 Synthesis of (\pm)-4'-methyl-N-benzylcathinone hydrobromide (4-MBC, **3d**)

The title compound was prepared using the method for (**3c**) with the following modifications: To a solution of (\pm)-4'-methyl-2-bromopropiophenone (**2**, 4.54 g, 20 mmol) in chloroform (40 mL) was added benzylamine (4.36 mL, 40 mmol). The mixture was heated at reflux overnight, cooled, filtered and then acidified (pH ~ 1) with 6 M hydrochloric acid (50 mL). The aqueous layer was washed with chloroform (3 × 50 mL), basified (pH ~ 10) with 5 M sodium hydroxide (*circa.* 100 mL) and then re-extracted with chloroform (3 × 50 mL). The combined organic fractions were dried (MgSO₄) and concentrated *in vacuo* to give a viscous orange oil. The crude product was purified by gravity column chromatography [SiO₂, EtOAc:*n*-hexane (1:6)] to give a yellow oil. The oil was dissolved in glacial acetic acid (2 mL), treated

with hydrobromic acid (33 % solution in acetic acid, 5 mL) and stirred at room temperature for 1 h. The mixture was diluted with diethyl ether (100 mL) and stirred until a pale beige solid formed (*circa.* 30 min). The crude product was filtered, washed with diethyl ether and recrystallised from acetone to afford (\pm)-4'-methyl-N-benzylcathinone hydrobromide (1.82 g, 27.2 % from **2**) as an off-white powder. Mpt. (acetone) 219.48 °C; R_f [SiO₂, EtOAc:*n*-hexane (1:3)] = 0.11; $[\alpha]_D^{22} = 0$ ($c = 0.5$ g 100 mL⁻¹, MeOH); found: C, 61.06; H, 6.03; N, 3.99. C₁₇H₂₀BrNO requires C, 61.09; H, 6.03 and N, 4.19 %; UV (EtOH): $\lambda_{max} = 260.0$ nm ($A = 0.498$, $c = 1.04 \times 10^{-3}$ g 100 mL⁻¹); IR (ATR-FTIR): 2770.6 (NH₂⁺), 1683.9 (C=O), 1604.5 cm⁻¹ (C=C); ¹H NMR (400 MHz, 60 °C, *d*₆-DMSO) δ^1H (ppm) = 9.40 (2H, br s, CH(NH₂⁺CH₂Ph)CH₃); 7.93 (2H, d, $J = 8.2$ Hz, AA'BB'), 7.55 – 7.57 (2H, m, Ar-H), 7.45 – 7.41 (5H, m, Ar-H and AA'BB' overlapping signals), 5.27 (1H, q, $J = 7.2$ Hz, CH(NH₂⁺CH₂Ph)CH₃), 4.21 (2H, dd, $J = 7.2, 12.8$ Hz, CH(NH₂⁺CH₂Ph)CH₃), 2.42 (3H, s, ArCH₃) and 1.53 ppm (3H, d, $J = 7.2$ Hz, CH(NH₂⁺CH₂Ph)CH₃); ¹³C NMR (100 MHz, 60 °C, *d*₆-DMSO) $\delta^{13}C$ (ppm) = 195.1 (C=O, C1), 145.2 (ArC, C4'), 131.5, (ArC, C5), 130.2 (ArC, C1'), 129.8 (2 × ArCH, C7/C9), 129.4 (2 × ArCH, C3'/C5'), 128.8 (ArCH, C8), 128.6 (2 × ArCH, C2'/C6'), 128.3 (2 × ArCH, C6/C10), 57.0 (CHCH₃, C2), 48.7 (NH₂⁺CH₂Ph, C4), 20.9 (ArCH₃, C7') and 15.7 ppm (CHCH₃, C3); LRMS (ESI+, 70 eV): $m/z = 254$ (34%, [M+H]⁺), 236 (10), 146 (7), 119 (3) and 91 (100); HRMS (ESI+, 70 eV) calculated for [M+H] C₁₇H₂₀NO: 254.1539, found: 254.1537.

2.2.4 HPLC Instrumentation

Reversed phase high-performance liquid chromatography was performed with an integrated Agilent HP Series 1100 Liquid Chromatograph (Agilent Technologies, Wokingham, UK) fitted with an in-line degasser, 100-place autoinjector and single channel, tunable UV absorbance detector (264 nm). Data analysis was carried out using ChemStation for LC (Ver. 10.02) software (Agilent Technologies, Wokingham, UK). The flow rate was 0.8 mL min⁻¹ with an injection volume of 10 μ L. Six replicate injections of each calibration standard were performed. The stationary phase (ACE 3 C₁₈, 150 mm x 4.6 mm i.d., particle size: 3 μ m) used in the

study was obtained from HiChrom Limited (Reading, UK). The column was fitted with a guard cartridge (ACE 3 C₁₈) and maintained at an isothermal temperature of 22 °C with an Agilent HP Series 1100 column oven with a programmable controller (Agilent Technologies, Wokingham, UK).

2.2.5 Mobile Phase preparation

Preparation of aqueous ammonium formate buffer (10 mM, pH 3.5 ± 0.02): 1.30 g of ammonium formate was dissolved in 1.8 L ultra-pure deionised water and the pH of the solution adjusted by dropwise addition of formic acid (98 – 100%) to pH 3.5 (± 0.02). The mixture was transferred to a 2 L clear glass volumetric flask and diluted to volume with ultra-pure deionised water. The mobile phases were prepared by separately mixing volumes of the formate buffer and organic modifier in the appropriate proportions denoted in Section 2.3. Prior to use, all mobile phases were vacuum filtered through a 0.45 mm pore filter paper and degassed for 10 minutes at 25 °C using an ultrasonic bath.

2.2.6 Preparation of Standard samples for HPLC

2.2.6.1 Development of a Method for the Analysis of 4-MMC, 4-MEC and 4-MBC

Calibration standards (pure substances): 2.0 mg 4-MMC (3a), 4-MEC (3c), 4-MBC (3d) were weighed accurately into separate 100.0 mL clear glass volumetric flasks and diluted to volume with mobile phase to give solutions containing the components at 20.0 µg mL⁻¹. These solutions were then further diluted with mobile phase to give calibration standards containing 10.0 µg mL⁻¹, 5.0 µg mL⁻¹, 2.5 µg mL⁻¹, 1 µg mL⁻¹ and 0.5 µg mL⁻¹ of each analyte.

Calibration standards (adulterants study): 2.0 mg of each component (caffeine, 4-MMC (3a), 4-MEC (3c), benzocaine, 4-MBC (3d), sucrose, glucose, mannitol and lactose) were weighed accurately into 100.0 mL clear glass volumetric flask and diluted to volume with mobile phase to give solutions containing all components at 20.0 µg mL⁻¹. This solution was then further diluted with mobile phase to give

calibration standards containing $10.0 \mu\text{g mL}^{-1}$, $5.0 \mu\text{g mL}^{-1}$, $2.5 \mu\text{g mL}^{-1}$, $1 \mu\text{g mL}^{-1}$ and $0.5 \mu\text{g mL}^{-1}$ of each analyte.

Test solutions: Three samples of NRG-2 were obtained from three independent Internet vendors as white crystalline powders in clear zip-lock bags. 10.0 mg of each substance was weighed (in duplicate) accurately into a 100.0 mL clear glass volumetric flask and diluted to volume with mobile phase. This solution was then further diluted (1:10) with mobile phase to give the test solution.

2.2.6.2 Development of a HPLC Method for the Analysis of 4-FMC and MDPV

Flephedrone(4-FMC) and Methylenedioxypropylvalerone (MDPV) pure substances which used in this Section were synthesised using the method reported by Camilleri *et al.* [16]with modification.

After the development of the method was finished, seven solutions of individual compounds were prepared, the stock solutions that were used for all compounds were $10 \text{ mg } 100 \text{ mL}^{-1}$, some samples such as the benzocaine were ultrasonicated for *circa* 2 minutes to dissolve the analyte before being made up to 100 mL, and further diluted was taken place by transferred 10 mLs of stock solutions into 100 mL volumetric flasks and made them up to 100 mL with HPLC grade water. The samples individually were injected with final concentration of $10 \mu\text{g mL}^{-1}$.

Hence, each of six analytes (mephedrone (4-MMC,3a) , (\pm)-4'-methyl-*N*-ethylcathinone hydrobromide (4-MEC ; 3c), 4-fluoromethcathinone (flephedrone , 4-FMC) , (\pm)-4'-methyl-*N*-benzylcathinone (4-MBC; 3d) , Caffeine and Benzocaine) were weighted accurately *circa* 10 mg into a 100 mL volumetric flask then HPLC water was added , the mixture solution was ultrasonicated before made up to 100 mL, further diluted carried out by transferred 10 mL of this solution into 100 mL volumetric flask to give concentration of $10 \mu\text{g mL}^{-1}$ of intermediate solution then water was added , 4.0 mg of MDPV was added to the intermediate solution before being diluted to 100 mL to give final intermediate solution containing $10 \mu\text{g mL}^{-1}$ of the six compounds and $40 \mu\text{g mL}^{-1}$ of MDPV, finally this mixture solution further diluted has been done to prepare standard solutions containing *circa* $0.5 \mu\text{g mL}^{-1}$, 1.0

$\mu\text{g mL}^{-1}$, $2.5 \mu\text{g mL}^{-1}$, and $5.0 \mu\text{g mL}^{-1}$ of six compounds ($2 \mu\text{g mL}^{-1}$, $4.0 \mu\text{g mL}^{-1}$, $10 \mu\text{g mL}^{-1}$, $20 \mu\text{g mL}^{-1}$ of MDPV) using serial dilutions of the intermediate solution.

A mixture of the seven substituted cathinone samples and adulterants (mephedrone (4-MMC, **3a**), (\pm)-4'-methyl-*N*-ethylcathinone hydrobromide (4-MEC, **3c**), 4FMC, (\pm)-4'-methyl-*N*-benzylcathinone (4-MBC, **3d**), methylenedioxypropylvalerone (MDPV), Caffeine and Benzocaine) was made up and run through the HPLC.

Test solutions: Ten samples of NRG-2 were obtained from three independent Internet vendors as white crystalline powders in clear zip-lock bags. Stock solution that used of all samples are $100 \mu\text{g mL}^{-1}$ (in duplicate), and further diluted was taken place by transferred 10 mL of stock solution into 100 mL volumetric flask and made it up to 100 mL with HPLC grade water. The samples were injected in duplicate with final concentration of $10 \mu\text{g mL}^{-1}$ of powder assayed.

2.2.7 Analytical method validation

The relative response factor was obtained from the following equation:

$$\text{Relative response factor (RRF)} = (\text{Area of component}) / (\text{Area of reference})$$

The result from the above equation was used to calculate the corrected peak area:

$$\text{Corrected peak area} = \text{RRF} \times \text{Area of component}$$

The mixture solution which used to calculate the RRF prepared by weighted accurately circa 10 mg of seven compounds into a 100 mL volumetric flask, then HPLC water was added, the mixture solution was ultrasonicated before made up to 100 mL, further diluted carried out by transferred 10 mL of this solution into 100 mL volumetric flask to give final concentration $10 \mu\text{g mL}^{-1}$ of mixture in water.

In this study, from the practical part of view, HPLC method development was achieved with a good resolution between analytes in the mixture. The following equation was used:

$$\text{Resolution (Rs)} = 1.18 (t_{Rb} - t_{Ra}) / (W_{b0.5} + W_{a0.5})$$

Where t_{Rb} , t_{Ra} = the retention time of analyte b and a respectively.

$W_{b0.5}$, $W_{a0.5}$ = the peak widths of peak at half height.

A term called the capacity factor, k' , is often used to describe the migration rate of an analyte on a column. The capacity factor (retention factor) equation was used for each analyte is defined as [89]:

$$k' = t_R - t_0 / t_0$$

The retention time (t_R) were determined from inject the mixture of seven analytes and each analyte in a sample was have a different retention time. The time taken for the Uracil solution ($50\mu\text{g mL}^{-1}$) to pass through the column is called t_0 , the capacity factor then calculated for each analyte.

The limit of detection (LOD) and limit of quantification (LOQ) were calculated by using the expression $3.3\sigma / s$ and $10\sigma / s$ respectively. (Where σ = standard deviation of y-intercepts of regression lines for calibration curves generated using samples containing the analyte in the range of limit of detection, s = slope of the calibration curve of analyte).

2.2.8 Using AT-IR spectroscopy to characterise NRG2, 4-MEC (3c) and 4-MBC (3d) samples

A Thermo Scientific Nicolet iS 10 FT-IR spectrometer with an iTR accessory was used to obtain the spectrum from each sample in less than one minute, OMNIC Series software was used.

A small amount of the sample powder was placed on the ATIR analyzer crystal, which accurately forces the powder down against the crystal using the pressure applicator.

2.2.9 Ultraviolet-Visible Absorption measurements of 4-MEC (3c), 4-MBC (3d) and Nicotinamide

Ultraviolet absorbance spectra were measured using a Unicam UV Visible Spectrometer (UV 300) (Thermo Spectronic, Cambridge).

The samples and references were used as described above, and Hydrochloric acid was purchased from BDH laboratory supplies (Poole, England), sodium hydroxide purchased from sigma –Aldrich Co. Ltd (UK), and Ethanol was obtained from Sigma-Aldrich Chemie (USA). Data processing was done using Vision 32 1.05 software.

(±)-4'-methyl-*N*-ethylcathinone hydrobromide [4-MEC, 3c] and (±)-4'-methyl-*N*-benzylcathinone hydrobromide [4-MBC , 3d] (5.0 mg of each) were twice weighed accurately and separately transferred into 50 mL volumetric flasks. As a result, two stock solutions of each sample containing 0.1mg mL⁻¹ were prepared. One flask of each sample was dissolved and made up to volume with water (stock solution 1), and the other was dissolved in 50 mL of ethanol (stock solution 2).

From stocks solutions 1; 3 x 5 mL of stock solution were transferred into separate three 50 mL volumetric flasks for each sample standard and added into the first flask 5 mL of 1M HCl and made up to 50 ml of water to made two solutions, each of which having 10 µg mL⁻¹ of 4-MEC (3c) or 4-MBC (3d) with 0.1M HCl (Acidic solutions). And the second flasks added 5 mL of 1M NaOH to make solutions 10 µg mL⁻¹ of 4-MEC (3c) or 4-MBC (3d) with 0.1 M NaOH (basic solutions), the third flasks just had 5 mL transferred into them and were then made up to 50 mL with water (Neutral solutions).

From the second stock solutions of 4-MEC (3c) and 4-MBC (3d) ; 5 mL of each stock solution was transferred into separate 50 mL volumetric flasks and made up to mark with ethanol in order to prepare the final solutions, which consisted of 10 µg mL⁻¹ of 4-MEC (3c) or 4-MBC (3d) in ethanol.

The ultraviolet spectra are obtained using a 1 cm cell (Cuvette) and by scanning from 220 nm to 400 nm at scan speed 120 nm min⁻¹; bandwidth(1.5); and a data interval of (0.5).

2.2.10 Liquid chromatography–electrospray mass spectrometry analysis

Liquid chromatography-mass spectrometry data were acquired using a Finnigan LTQ Orbitrap instrument (Thermo-Fisher Corporation, Hemel Hempstead, UK). Sample analysis was carried out in positive ion (ESI) detection mode. The mass scanning range was 50 – 1250 m/z , while the capillary temperature was 250 °C and the sheath and auxiliary gas flow rates were 30 and 10, respectively (units not specified by the manufacturer). The LC-MS system (controlled by Xcalibur Ver. 2.0, Thermo-Fisher Corporation, Hemel Hempstead, UK) was run in binary gradient mode. Solvent A was aqueous ammonium formate buffer (10 mM, pH 3.5 ± 0.02) and solvent B was methanol; the flow rate was 0.3 mL min⁻¹. An ACE 3 C₁₈ (150 mm × 4.6 mm i.d., particle size: 3 μm) column (HiChrom Limited, Reading, UK) was used for all analyses. The gradient programme was as follows: 10 % B (0 minute) to 60 % B at 7 minute to 60 % B at 20 minute to 10 % B at 25 minute.

2.2.11 Nuclear Magnetic Resonance Spectroscopy

¹H , ¹³C , HMBC and HMQC spectra were recorded in a JEOL-AS-400 instrument operating at 400 MHz (¹H) and 100 MHz (¹³C). Chemical shifts are shown as (δ) and were measured in ppm (parts per million) and coupling constants (J) are reported in Hz. The spectra obtained at 60 °C in *d*₆-DMSO which obtained from Sigma-Aldrich Chemie (USA). Data processing was done using Topspin 2.0 software. Approximately 10mg of all standards and NRG-2 samples were weighed out into different sample vials. Then, accurately 600μL of *d*₆-DMSO was added to all sample vials and samples were solubilised by rigorous agitation. There were some samples were not dissolved completely. Hence UV-ultrasonic bath was used to increase the solubility. The prepared NRG-2 sample solutions were admitted into properly labelled NMR sample tubes (Wilmad, P-535) by using Pasteur pipettes. The remaining undissolved particles in sample solutions were removed by using cotton filter plugs inside Pasteur pipettes.

2.3 Results and discussion

2.3.1 The synthesis of reference substances

Reference samples of the two mephedrone derivatives (\pm)-4'-methyl-*N*-ethylcathinone (**3c**, 4-MEC) and (\pm)-4'-methyl-*N*-benzylcathinone (**3d**, 4-MBC) were prepared as their corresponding hydrobromide salts. The synthesis of both racemic target compounds was achieved using a modification of the previously reported method from (\pm)-4'-methyl-2-bromopropiophenone (**2**) in 41.5 % and 27.2 % yield respectively (Scheme4) [63]. Both compounds were obtained as stable, colourless to off-white powders after recrystallisation from acetone and exhibited an optical rotation $[\alpha]_D^{22}$ of 0 ($c = 0.5 \text{ g } 100 \text{ mL}^{-1}$, MeOH). The purity of the derivatives was confirmed by elemental analysis. Analysis of (4-MEC, **3c**) revealed 52.90 % (C), 6.65 % (H) and 4.95 % (N) which corresponded very closely to the theoretical percentage for the hydrobromide salt (52.95 % (C), 6.67 % (H) and 5.15 % (N)). Similarly (4-MBC, **3d**) gave 61.06 % (C), 6.03 % (H) and 3.99 % (N) which was in agreement with its expected theoretical compositions (61.09 % (C), 6.03 % (H) and 4.19 % (N)). The melting points for 4-MEC (**3c**) and 4-MBC (**3d**) were determined by differential scanning calorimetry (DSC) and gave sharp melting points at 206.08 and 219.48 °C respectively. Additionally, the pK_a and Log P values (**3c**, $pK_a = 8.88$; Log P = 2.38; **3d**, $pK_a = 7.44$; Log P = 4.64) were determined for each derivative using a Sirius T3 instrument and are in good agreement with the calculated values (**3c**, $pK_a = 8.41$; Log P = 2.36; **3d**, $pK_a = 5.95$; Log P = 3.59) determined by Pipeline Pilot software (Accelrys, Vers. 7.5).

2.3.2 Structural elucidation

The ^1H NMR spectrum of (\pm)-4'-methyl-*N*-ethylcathinone (4-MEC, **3c**) (obtained at 60 °C in d_6 -DMSO 1 , Figure 26a) showed the characteristic AA'BB' aromatic system for an unsymmetrically *para*-disubstituted aromatic system ($\delta^1\text{H} = 7.98 \text{ ppm}$,

¹ All ^1H -NMR spectra were recorded at 60 °C to ensure that the signal for the protons situated on the chiral centre (C2, *circa.* 5.2 – 5.3 ppm) which broadens and coalesces at ambient temperature was fully resolved. The chemical shifts of all signals were observed to be consistent at both ambient (25 °C) and high (60 °C) temperatures. For consistency the ^{13}C -NMR spectra were obtained under analogous conditions. Samples were filtered prior to analysis.

AA'BB', 2H, d, $J = 8.4$ Hz; $\delta^1\text{H} = 7.41$ ppm, AA'BB', 2H, d, $J = 8.4$ Hz), a deshielded one-hydrogen quartet at $\delta^1\text{H} = 5.21$ ppm ($\text{CH}(\text{NH}_2^+\text{CH}_2\text{CH}_3)\text{CH}_3$, $J = 6.8$ Hz), a deshielded two-hydrogen doublet of quartets at $\delta^1\text{H} = 3.04$ ppm ($\text{CH}(\text{NH}_2^+\text{CH}_2\text{CH}_3)\text{CH}_3$, $J = 12.4, 7.2$ Hz), characteristic of an A_3X_2 system with additional geminal coupling of the prochiral hydrogens proximal to the chiral centre, a slightly deshielded methyl singlet attributable to the methyl group attached to the aromatic ring (ArCH_3 , $\delta^1\text{H} = 2.42$ ppm), a methyl doublet ($\text{CH}(\text{NH}_2^+\text{CH}_2\text{CH}_3)\text{CH}_3$, $\delta^1\text{H} = 1.53$ ppm, $J = 7.2$ Hz) and finally a three-hydrogen A_2X_3 triplet ($\text{CH}(\text{NH}_2^+\text{CH}_2\text{CH}_3)\text{CH}_3$, $J = 7.2$ Hz) at $\delta^1\text{H} = 1.28$ ppm. Unlike the previously reported spectra (which were run in D_2O [19, 116]) a broad signal at $\delta^1\text{H} = 8.92$ ppm was consistently observed and corresponded to the ammonium salt protons. It was noted that in D_2O (4-MEC, **3c**) gave rise to an NMR spectrum consistent with that obtained by Brandt *et al.* [19] and Jankovics *et al.* [116] where the signal for the ammonium salt protons is absent due to rapid exchange with the solvent confirming that the synthesised (\pm)-4'-methyl-*N*-ethylcathinone sample is identical to the material obtained by the other researchers.

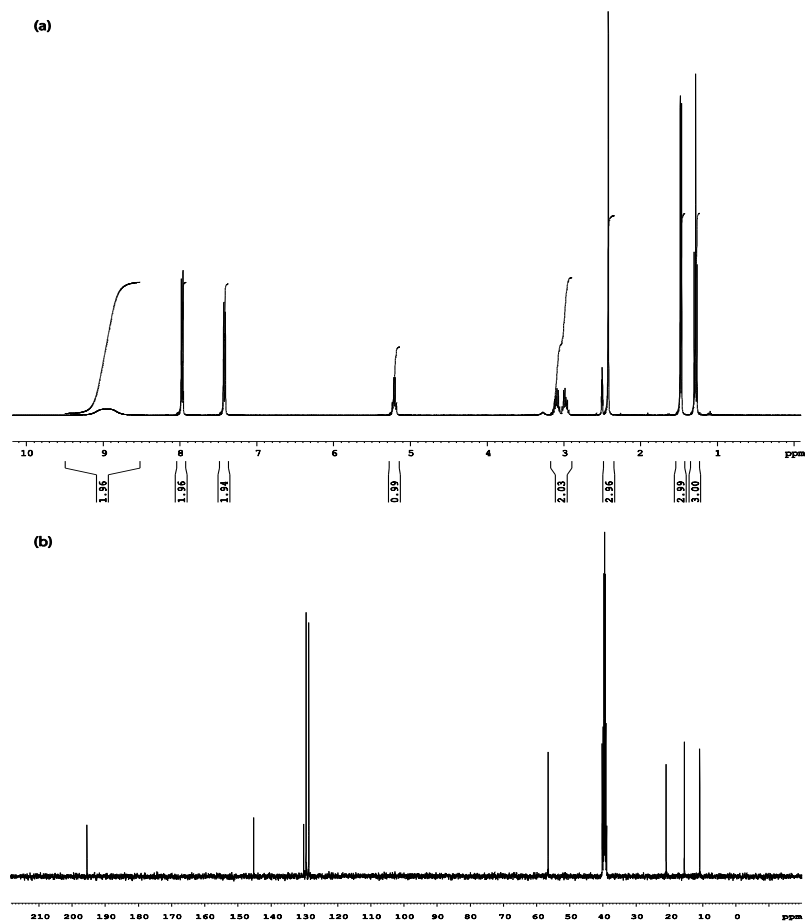


Figure 26. (a) ¹H NMR spectrum (400 MHz, *d*₆-DMSO, 60 °C) and (b) ¹³C NMR spectrum (100 MHz, *d*₆-DMSO, 60 °C) of (±)-4'-methyl-*N*-ethylcathinone.HBr (4-MEC, **3c**).

The ¹³C NMR spectrum (obtained at 60 °C in *d*₆-DMSO, Figure 26-b) supports the assertion that the sample of 4-MEC (**3c**) is predominantly pure with ten distinct carbon signals. Full spectral analysis using both 2D [¹H, ¹³C] HMQC and HMBC methods (Figures 27-28) allowed unambiguous assignment of all carbon and hydrogen resonances. For 4-MEC (**3c**) the *N*-CH₂CH₃ resonance ($\delta^1\text{H} = 1.28$ ppm, C5) gave a ²*J* correlation to C4 ($\delta^1\text{H} = 3.04$ ppm) which in turn gave a ³*J* correlation to C2. This characteristic pattern for the *N*-ethyl group was further confirmed through 2D [¹H, ¹H] COSY NMR data (Appendix 2). The resonance for C2 is in turn coupled to the methyl doublet (C3) and in the 2D [¹H, ¹³C] HMBC NMR spectrum

the protons of the methyl resonance ($\delta^1\text{H} = 1.53$ ppm) are coupled to a deshielded carbon ($\delta^{13}\text{C} = 195.5$ ppm, C1) completing the assignment of the 2-aminoethylpropan-1-one side chain. Further couplings in the 2D [^1H , ^{13}C] HMBC NMR spectrum between H2'/H6' and C1 (3J) supports placement of the propan-1-one side chain at C1' on the aromatic nucleus (between C6' and C2') and correlations between H2'/H6' and H3'/H5' confirmed the AA'BB' aromatic system. The methyl singlet at $\delta^1\text{H} = 2.42$ ppm (C7') exhibits a 3J [^1H , ^{13}C] HMBC correlation to C3'/C5' and a 2J correlation to C4' concluding the assignment of all resonances (Table 8).

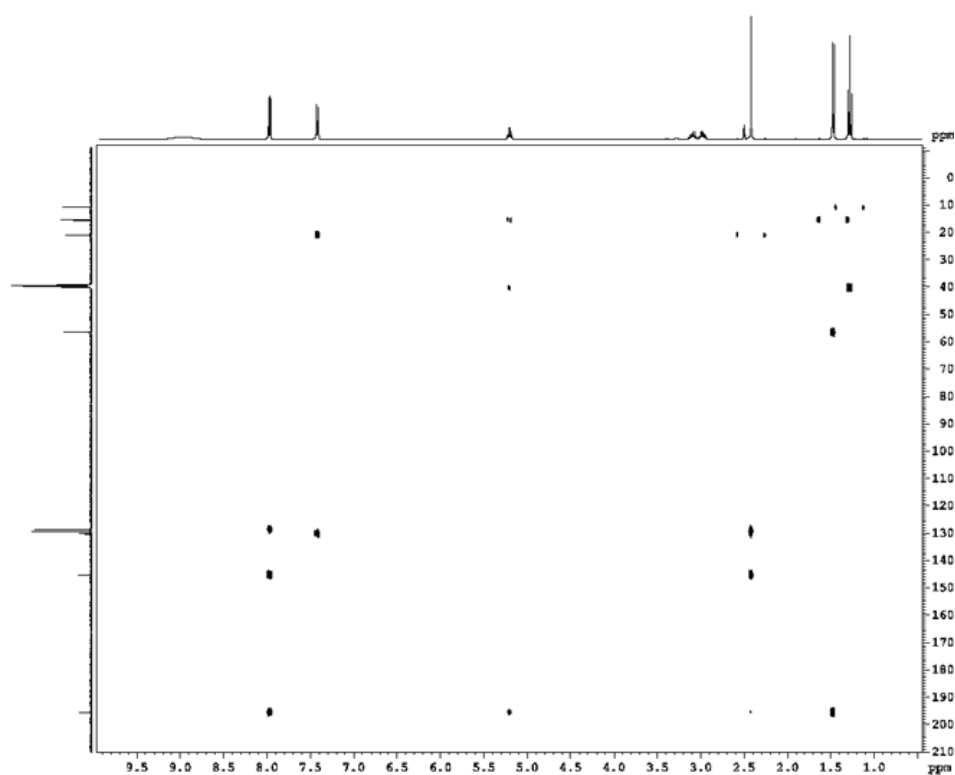


Figure 27: 2D [^1H , ^{13}C] HMBC NMR spectrum of (\pm)-4'-methyl-N-ethylcathinone hydrobromide (4-MEC, 3c).

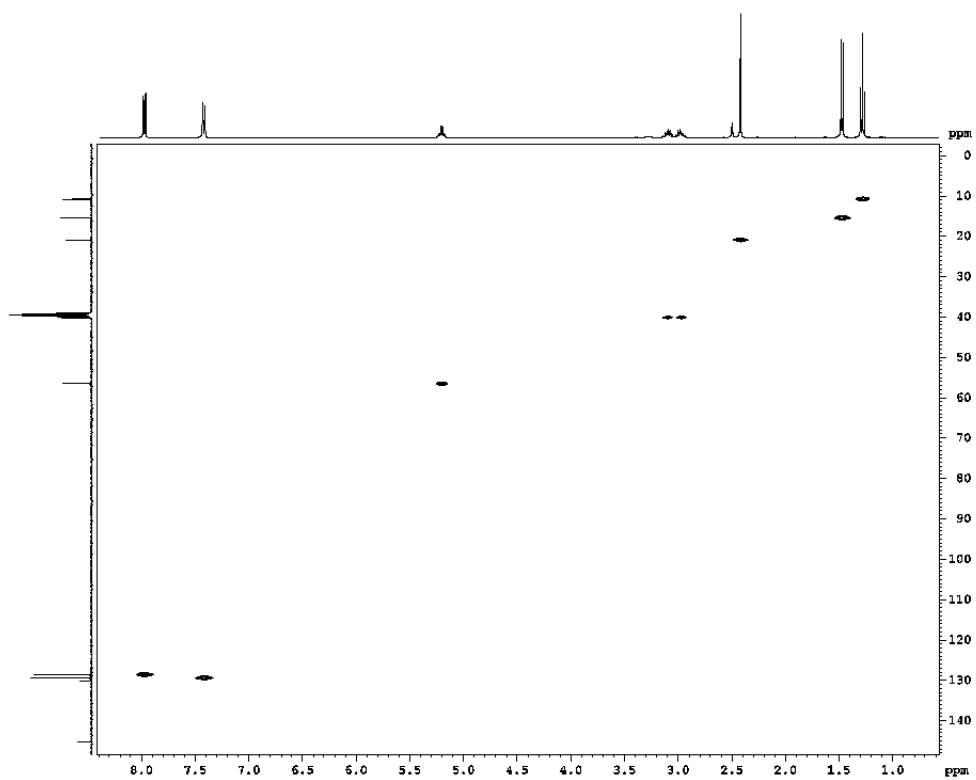
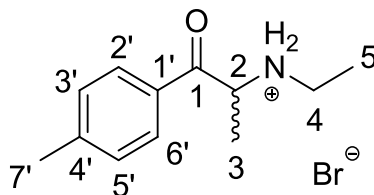


Figure 28 : 2D [^1H , ^{13}C] HMQC NMR spectrum of (\pm)-4'-methyl-N-ethylcathinone hydrobromide (4-MEC, 3c).

Table 8. ^1H (400 MHz), ^{13}C (100 MHz) NMR spectral data and ^1H - ^{13}C long-range correlations of (\pm)-4'-methyl-*N*-ethylcathinone.HBr (4-MEC, **3c**) in d_6 -DMSO. Chemical shifts (δ) in ppm; Coupling constants (J) in Hz.

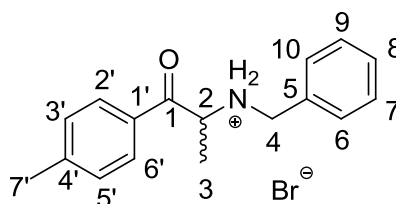


Position	^1H	^{13}C	2J	3J
1	-	195.5	-	-
2	5.21 q, $J = 6.8$	56.5	C1, C3	NCH_2CH_3
3	1.53 d, $J = 7.2$	15.7	C2	C1
4	3.04 dq, $J = 12.4, 7.2$	40.2	-	C2
5	1.28 t, $J = 7.2$	10.8	C4	-
1'	-	130.2	-	-
2'/6'	7.98 d, $J = 8.2$	128.6	C3'/C5'	C2'/C6', C4', C1
3'/5'	7.41 d, $J = 8.2$	129.4	C2'/C6'	C3'/C5', C1'
4'	-	145.2	-	-
7'	2.42 s	20.9	C4'	C3'/C5'
NH_2^+	8.92 br s	-	-	-

In the case of (\pm)-4'-methyl-*N*-benzylcathinone (4-MBC, **3d**) the ^1H NMR spectrum (obtained at 60 °C in d_6 -DMSO, Figure 29-a) showed the characteristic centrosymmetric AA'BB' spin system for an unsymmetrically *para*-disubstituted aromatic ring ($\delta^1\text{H} = 7.93$ ppm, AA'BB', 2H, d, $J = 8.4$ Hz), where the partner AA'BB' resonance (*circa.* $\delta^1\text{H} = 7.41$ ppm) appeared co-incident with the resonances associated with protons on the *N*-benzyl group ($\delta^1\text{H} = 7.41 - 7.45$ ppm, 5H, multiplet). Additionally, aromatic signals appeared at $\delta^1\text{H} = 7.55 - 7.57$ ppm (2H, m), a deshielded one-hydrogen quartet was present at $\delta^1\text{H} = 5.27$ ppm ($\text{CH}(\text{NH}_2^+\text{CH}_2\text{Ph})\text{CH}_3$, $J = 7.2$ Hz), together with a deshielded two-hydrogen doublet of doublets at $\delta^1\text{H} = 4.21$ ppm ($\text{CH}(\text{NH}_2^+\text{CH}_2\text{Ph})\text{CH}_3$, $J = 12.8, 7.2$ Hz) (characteristic of the non-equivalent hydrogens with additional geminal coupling, on the benzylmethylene carbon proximal to the chiral centre), a slightly deshielded

methyl singlet attributable to the methyl group attached to the aromatic ring (ArCH₃, $\delta^1\text{H} = 2.42$ ppm), a methyl doublet (CH(NH₂⁺ CH₂Ph) CH₃, $\delta^1\text{H} = 1.53$ ppm, $J = 7.2$ Hz) and finally a broad signal at $\delta^1\text{H} = 9.40$ ppm for the exchangeable ammonium salt protons, which is consistent with other reported cathinone derivatives (Table 9) [63].

Table 9. ¹H (400 MHz), ¹³C (100 MHz) NMR spectral data and ¹H-¹³C long-range correlations of (±)-4'-methyl-N-benzylcathinone.HBr (4-MBC, 3d) in *d*₆-DMSO. Chemical shifts (δ) in ppm; Coupling constants (J) in Hz.



Position	¹ H	¹³ C	² J	³ J
1	-	195.1	-	-
2	5.27 q, $J = 7.2$	57.0	C1, C3	NCH ₂ Ph
3	1.53 d, $J = 7.2$	15.7	C2	C1
4	4.21 dd, $J = 7.2, 12.8$	48.7	-	C2
5	-	131.5	-	-
6/10	7.56, m ^a	128.3	C7, C9	-
7/9	7.44, m ^b	129.8	C6, C10	-
8		128.8	-	-
1'	-	130.2	-	-
2'/6'	7.93 d, $J = 8.2$	128.6	C3'/C5'	C2'/C6', C4', C1
3'/5'	7.41 d, $J = 8.2^c$	129.4	C2'/C6'	C3'/C5', C1'
4'	-	145.2	-	-
7'	2.42 s	20.9	C4'	C3'/C5'
NH ₂ ⁺	9.40 br s	-	-	-

^a Expected multiplicity would be a 2H doublet of doublets (C6/C10).

^b Co-incident resonances. Expected multiplicity would be a 2H triplet (or doublet of doublets, C7/C9) and a 1H triplet (C8).

^c Expected coupling constant based upon the C2'/C6' measured value.

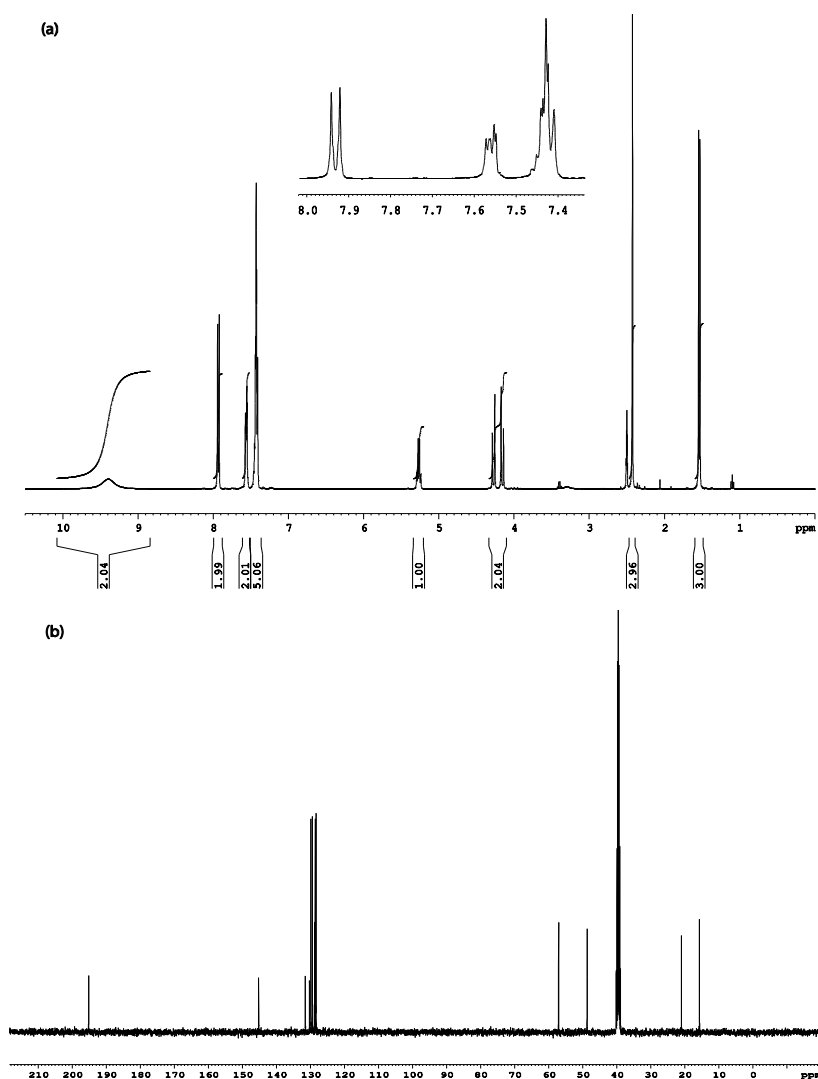


Figure 29: (a) ¹H NMR spectrum (400 MHz, *d*₆-DMSO, 60 °C) and (b) ¹³C NMR spectrum (100 MHz, *d*₆-DMSO, 60 °C) of (±)-4'-methyl-*N*-benzylcathinone.HBr (4-MBC, **3d)**

The ¹³C NMR spectrum (obtained at 60 °C in *d*₆-DMSO, Figure 29b) also supports that the synthesised reference sample of 4-MBC (**3d**) is predominantly pure with thirteen distinct carbon signals. Full spectral analysis using both 2D [¹H, ¹³C] HMQC and HMBC methods (Figures 30-31) allowed assignment of the carbon and hydrogen resonance. For 4-MBC (**3d**) the *N*-CH₂Ph resonance ($\delta^1\text{H} = 4.21$ ppm, C4) gave a ³*J* correlation to C2 ($\delta^1\text{H} = 5.27$ ppm) which in turn gave a ²*J* correlation to C1 and C3.

The resonances for the benzyl moiety should exhibit the characteristic doublet of doublets (2H, C6/C10), doublet of doublets (2H, C7/C9) and triplet (1H, C8) multiplicities. However, these resonances appear as two complex multiplets: $\delta^1\text{H} = 7.44$ (C7/C9 and C8 with 2J correlation to C6/C10) and 7.56 ppm (C6/C10 with 2J correlation to C7/C9) respectively. The complex splitting of the aromatic resonances observed in the aromatic region of the ^1H NMR spectrum is not uncommon in benzyl-substituted compounds and is ascribed to second-order splitting effects [120]. The resonance for C2 is in turn coupled to the methyl doublet (C3) and in the [^1H , ^{13}C] HMBC NMR spectrum the protons of the methyl resonance ($\delta^1\text{H} = 1.53$ ppm) are coupled to a deshielded carbon ($\delta^{13}\text{C} = 195.1$ ppm, C1) concluding the assignment of the 2-aminobenzyl-propan-1-one side chain. Further couplings in the [^1H , ^{13}C] HMBC NMR spectrum between H2'/H6' and C1 (3J) once again supports placement of the propan-1-one side chain at C1' on the second aromatic nucleus (between C6' and C2') and correlations between H2'/H6' and H3'/H5' confirmed the AA'BB' aromatic system. The methyl singlet at $\delta^1\text{H} = 2.42$ ppm (C7') exhibits a 3J [^1H , ^{13}C] HMBC correlation to C3'/C5' and a 2J correlation to C4' completing the assignment of all resonances for 4-MBC (**3d**) and is consistent with the data observed for structurally-related cathinones [63].

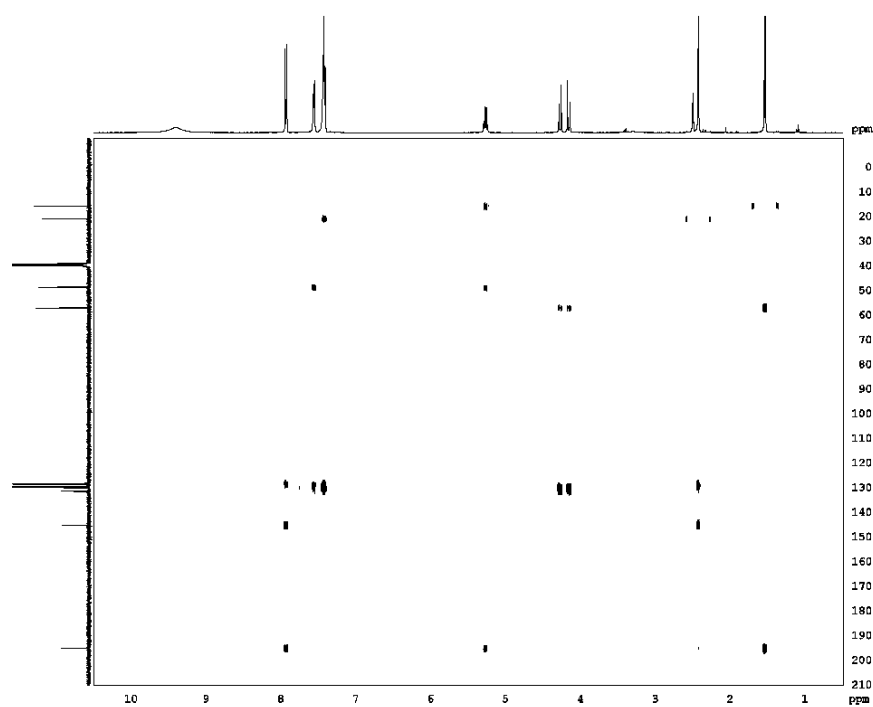


Figure 30: 2D [^1H , ^{13}C] HMBC NMR spectrum of (\pm)-4'-methyl-*N*-benzylcathinone hydrobromide (4-MBC, 3d).

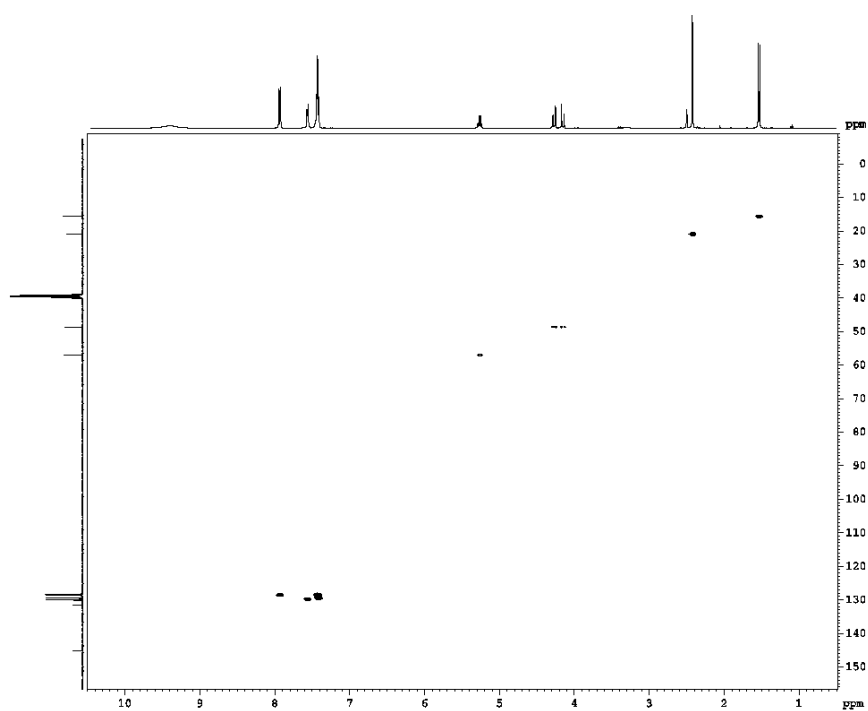


Figure 31: 2D [^1H , ^{13}C] HMQC NMR spectrum of (\pm)-4'-methyl-*N*-benzylcathinone hydrobromide (4-MBC, 3d).

The HRESIMS analysis of (\pm)-4'-methyl-*N*-ethylcathinone hydrobromide (4-MEC, **3c**) gave an $[M+H]^+$ peak at $m/z = 192.1381$ (calculated for $C_{12}H_{18}NO = 192.1383$) supporting the molecular formula of $C_{12}H_{17}NO$ and the identity of the sample as (\pm)-MEC. The mass spectrum which is in agreement with the data reported by both Brandt *et al.* [19] and Jankovics *et al.* [116] of 4-MEC (**3c**) is shown in Figure 31-a and exhibits an $[M+H]^+$ parent ion ($m/z = 192.1381$) of moderate abundance (34 %, $C_{12}H_{18}NO$), with the observed fragment ions (through collision induced decomposition) at $m/z = 174.1276$ (100 %, calculated for $C_{12}H_{16}N = 174.1277$), 159.1041 (30 %, calculated for $C_{11}H_{13}N = 159.1043$), 145.0885 (57 %, calculated for $C_{10}H_{11}N = 145.0886$), 131.0729 (16 %, calculated for $C_9H_9N = 131.0730$), 119.0855 (25 %, calculated for $C_9H_{11} = 119.0855$) and 91.0542 (6 %, calculated for $C_7H_7 = 91.0542$). The novel *N*-benzyl derivative (4-MBC, **3d**) was also analysed using HRESIMS and gave an $[M+H]^+$ peak at $m/z = 254.1537$ (calculated for $C_{17}H_{20}NO = 254.1539$) confirming the molecular formula of $C_{17}H_{19}NO$ and the identity of the sample as (\pm)-4'-methyl-*N*-benzylcathinone. The mass spectrum of 4-MBC (**3d**) is shown in Figure 32-b and also exhibits a moderately abundant $[M+H]^+$ parent ion ($m/z = 254.1537$, 34 %, $C_{17}H_{20}NO$), with the observed CID fragment ions at $m/z = 236.1433$ (10 %, calculated for $C_{17}H_{18}N = 236.1434$), 146.0964 (7 %, calculated for $C_{10}H_{12}N = 146.0964$), 119.0855 (3 %, calculated for $C_9H_{11} = 119.0855$) and 91.0542 (100 %, calculated for $C_7H_7 = 91.0542$). Fragment ions present in spectra show in below figure (Figure 32) can be explained by losses and rearrangements as shown in Scheme 5 and 6, fragment ions in both compounds occurring 18 Da below parent molecular ions suggest a loss of H_2O (neutral fragment) such as (4-MEC (**3c**); $m/z = 174.1276$) and (4-MBC (**3d**); $m/z = 236.1433$). The fragment pattern of conjugated indole consider as stable fragment and similar fragmentation pattern can be formed in both compounds (4-MEC (**3c**); $m/z = 145.0885$, $m/z = 131.0729$) and (4-MBC (**3d**); $m/z = 146.0964$), also the fragment ions can be rearranged into the seven membered ring to form (Tropylium ion) at $m/z = 91.0542$ in both compounds.

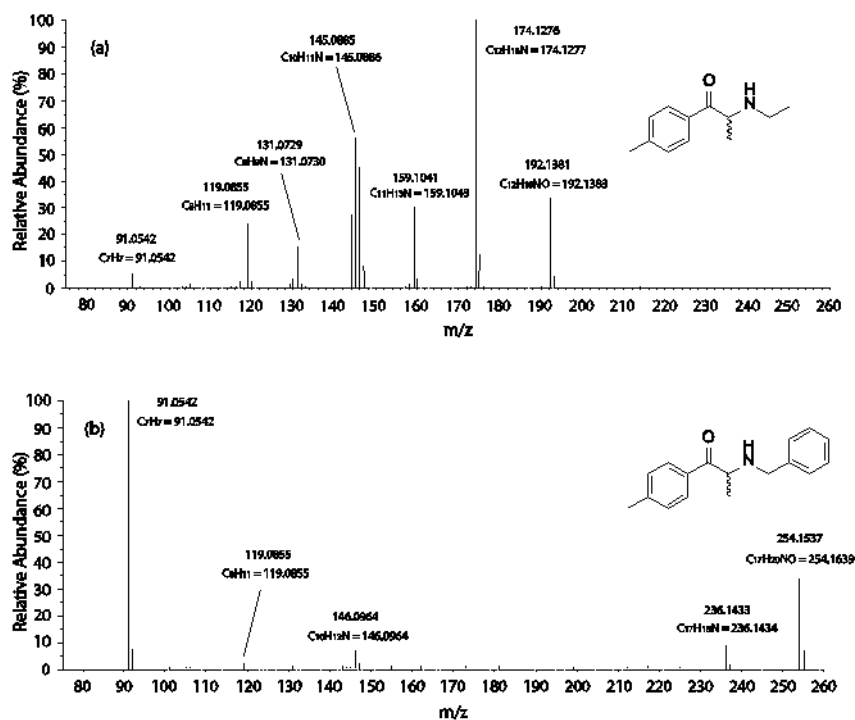
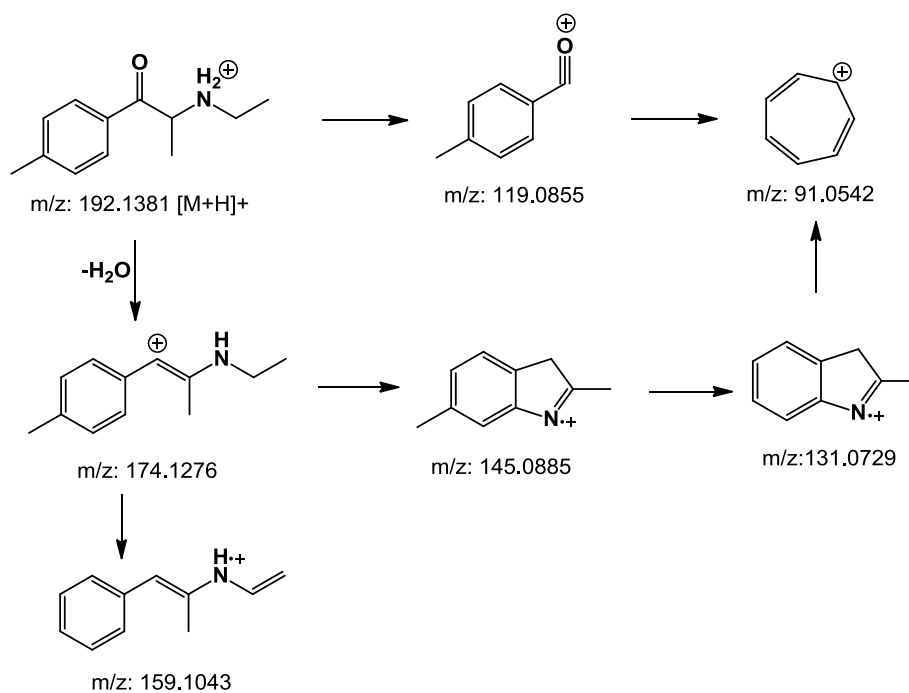
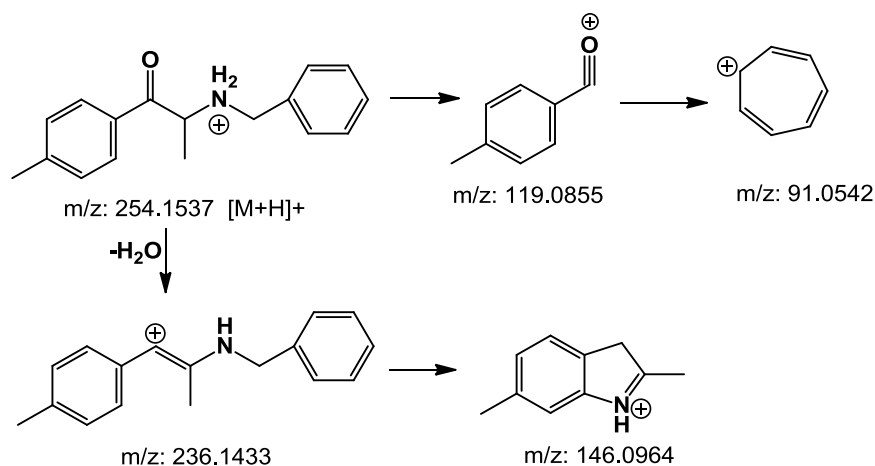


Figure 32. HRESIMS spectra of (a) (±)-4'-methyl-N-ethylcathinone.HBr (4-MEC, 3c) and (b) (±)-4'-methyl-N-benzylcathinone.HBr (4-MBC, 3d).



Scheme 5. Proposed fragmentation of 4'-methyl methyl-N-ethylcathinone.HBr (4-MEC, 3c) under ESI-MS conditions.



Scheme 6. Proposed fragmentation of 4'-methyl methyl-*N*-benzylcathinone.HBr (4-MBC, **3d) under ESI-MS conditions.**

The infrared spectra of (\pm)-4'-methyl-*N*-ethylcathinone (4-MEC, **3c**, Figure 33) and (\pm)-4'-methyl-*N*-benzylcathinone (4-MBC, **3d**, Figure 34) were collected on an attenuated total reflection infrared (ATR-FTIR) spectrometer. The spectra show strong C=O absorption bands at 1687.3 (4-MEC,**3c**) and 1683.9 (4-MBC,**3d**) cm^{-1} respectively. Additionally both samples exhibit broad C=C absorptions at 1605.4 (4-MEC,**3c**) and 1604.5 (4-MBC, **3d**) cm^{-1} , indicative of an aromatic nucleus, and 2735.4 (4-MEC, **3c**) and 2770.6 (4-MBC, **3d**) cm^{-1} due to the NH_2^+ stretch, which is consistent with the spectra previously obtained for (\pm)-mephedrone [63] and 4-MEC (**3c**) [116].

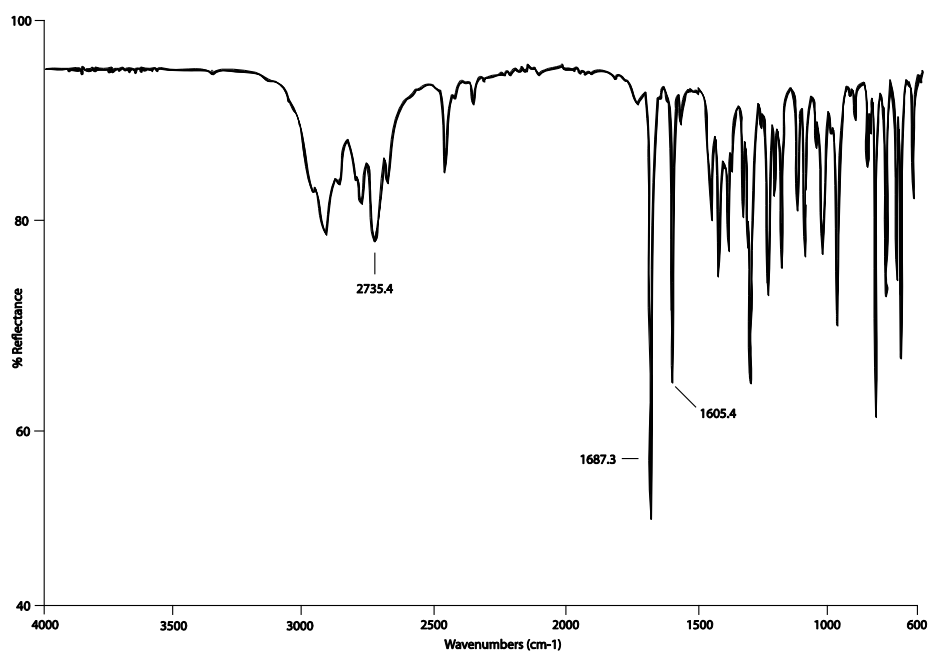


Figure 33: ATR-FTIR spectrum of (±)-4'-methyl-N-ethylcathinone.HBr (4-MEC, 3c)

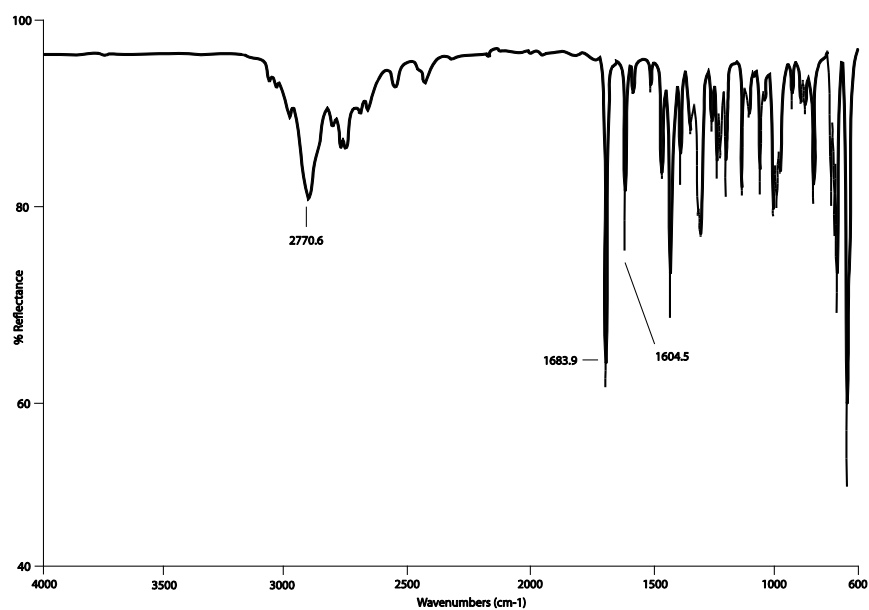


Figure 34. ATR-FTIR spectrum of (±)-4'-methyl-N-benzylcathinone.HBr (4-MBC, 3d).

The theoretical wavelength of maximum absorbance (as calculated from Scott's Rules) [121] of both derivatives was determined to be 256 nm. The ultraviolet

spectrum of (\pm)-4'-methyl-*N*-ethylcathinone (4-MEC; **3c**) obtained in absolute ethanol (Figure 35- a, denoted by —) is in good agreement with the theoretical value and shows λ_{max} at 260.0 nm ($A = 0.693$, $c = 1.02 \times 10^{-3} \text{ g } 100 \text{ mL}^{-1}$). Spectra exhibiting a slight bathochromic shift (*ca.* 4 nm) due to the solvent effect were obtained for 4-MEC (**3c**) in deionised water ($\lambda_{\text{max}} = 264.0 \text{ nm}$, $A = 0.621$, $c = 1.04 \times 10^{-3} \text{ g } 100 \text{ mL}^{-1}$) or 0.1 M aqueous hydrochloric acid ($\lambda_{\text{max}} = 264.0 \text{ nm}$, $A = 0.607$, $c = 1.04 \times 10^{-3} \text{ g } 100 \text{ mL}^{-1}$). In 0.1 M aqueous sodium hydroxide a hypsochromic shift (with a slight hyperchromic shift reduction in absorbance intensity) to 260.0 nm ($A = 0.555$, $c = 1.04 \times 10^{-3} \text{ g } 100 \text{ mL}^{-1}$) was observed in the spectrum of 4-MEC (**3c**) and may be due to a change in the ionisation of the sample. Similar ultraviolet spectra and wavelength maxima were obtained for the corresponding *N*-benzyl derivative (4-MBC; **3d**, Figure 35a – 35d, denoted by ----), though the UV absorbance intensity of 4-MBC (**3d**) was observed to be approximately 25 % lower than 4-MEC (**3c**) in each case. The UV data for both derivatives, which is consistent with that obtained for (\pm)-mephedrone (4-MMC,**3a**) [63], is summarised in Table 10.

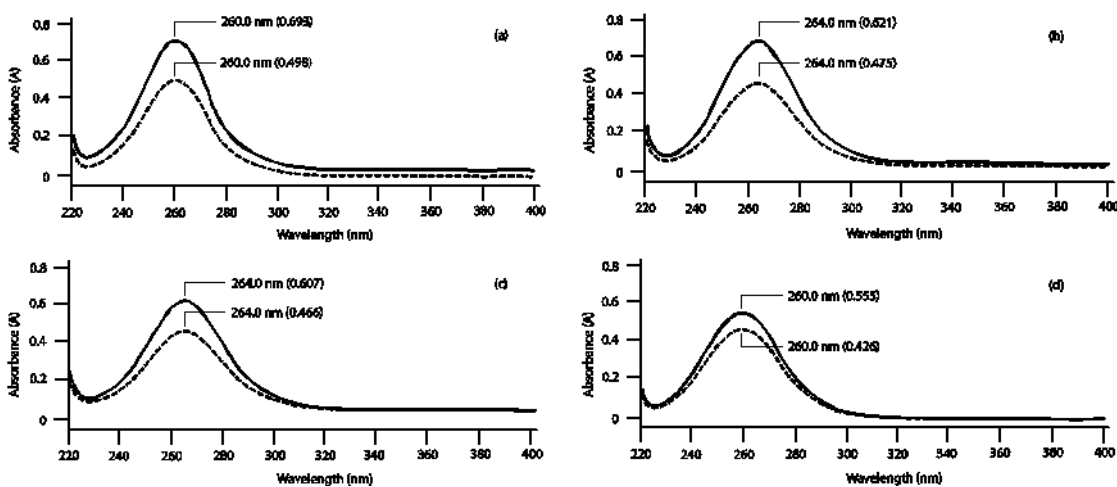


Figure 35. UV spectra of (\pm)-4'-methyl-*N*-ethylcathinone.HBr (**3c**, —) and (\pm)-4'-methyl-*N*-benzylcathinone.HBr (**3d**, ---) in (a) EtOH: 4-MEC (**3c**), $c = 1.02 \times 10^{-3} \text{ g } 100 \text{ mL}^{-1}$; 4-MBC (**3d**), $c = 1.04 \times 10^{-3} \text{ g } 100 \text{ mL}^{-1}$; (b) H₂O: 4-MEC (**3c**), $c = 1.04 \times 10^{-3} \text{ g } 100 \text{ mL}^{-1}$; 4-MBC(**3d**), $c = 1.06 \times 10^{-3} \text{ g } 100 \text{ mL}^{-1}$; (c) 0.1 M aqueous HCl: 4-MEC (**3c**), $c = 1.04 \times 10^{-3} \text{ g } 100 \text{ mL}^{-1}$; 4-MBC(**3d**), $c = 1.06 \times 10^{-3} \text{ g } 100 \text{ mL}^{-1}$ and (d) 0.1 M aqueous NaOH: 4-MEC (**3c**), $c = 1.04 \times 10^{-3} \text{ g } 100 \text{ mL}^{-1}$; 4-MBC(**3d**), $c = 1.06 \times 10^{-3} \text{ g } 100 \text{ mL}^{-1}$.

Table 10. Ultraviolet spectral data of (\pm)-4'-methyl-N-ethylcathinone.HBr (4-MEC) (3c**) and (\pm)-4'-methyl-N-benzylcathinone.HBr (4-MBC) (**3d**).**

Solvent	(\pm)-4'-methyl-N-ethylcathinone hydrobromide (4-MEC) (3c)				(\pm)-4'-methyl-N-benzylcathinone hydrobromide (4-MBC) (3d)			
	EtOH	H ₂ O	0.1 M HCl	0.1 M NaOH	EtOH	H ₂ O	0.1 M HCl	0.1 M NaOH
Concn. (g 100 mL ⁻¹)	1.02 x 10 ⁻³	1.04 x 10 ⁻³	1.04 x 10 ⁻³	1.04 x 10 ⁻³	1.04 x 10 ⁻³	1.06 x 10 ⁻³	1.06 x 10 ⁻³	1.06 x 10 ⁻³
λ_{max} (nm)	260.0	264.0	264.0	260.0	260.0	264.0	264.0	260.0
Absorbance (A)	0.693	0.621	0.607	0.555	0.498	0.475	0.466	0.426

2.3.3 The HPLC development/analysis work

Previous researchers have reported utilising HPLC and LC-MS techniques to determine (\pm)-mephedrone for quality control [63, 122, 123], toxicological [124-126] and bioanalytical [127, 128] screening purposes. However, no fully validated liquid chromatographic methods (or limits of detection and quantification) for the mephedrone derivatives 4-MEC (**3c**) and 4-MBC (**3d**), or for the analysis of NRG-2 products, have been published. The recently published, validated HPLC method [63] (which can detect (\pm)-mephedrone at levels of 0.08 $\mu\text{g mL}^{-1}$) was further developed and re-validated to screen for (\pm)-mephedrone (4-MEC, **3a**) and the two structurally-related derivatives: 4-MEC (**3c**) and 4-MBC (**3d**). The UV detection wavelength was changed and mobile phase composition was modified by increasing the percentage of organic modifier, to ensure both optimal detection of the analytes and a rapid analysis time.

In this thesis, the three samples of NRG-2 were found to contain three cathinone derivatives: 4-MMC (mephedrone, **3a**), 4-MEC (4-methyl-N-ethylcathinone, **3c**) and 4-MBC (4-methyl-N-benzylcathinone, **3d**), the structure of two of these compounds were elucidated.

The starting point was to develop a published HPLC into a method that could separate and identify cathinone derivatives with shorter retention times, the method development was carried out using an adaptation of the HPLC method reported by

Santali *et al.*[63] with the following modification: mobile phases composition initially modified by increasing the percentage of organic modifier to 60 % (methanol), the column temperature was not controlled and the UV detection wavelength was changed to 264 nm. With these conditions it was found that the peaks of 4-MMC (3a) ($t_R = 2.7$ min) and 4-MEC (3c) ($t_R = 2.8$ min) were very close and the resolution had to be increased by increasing the retention time (Figure 36).

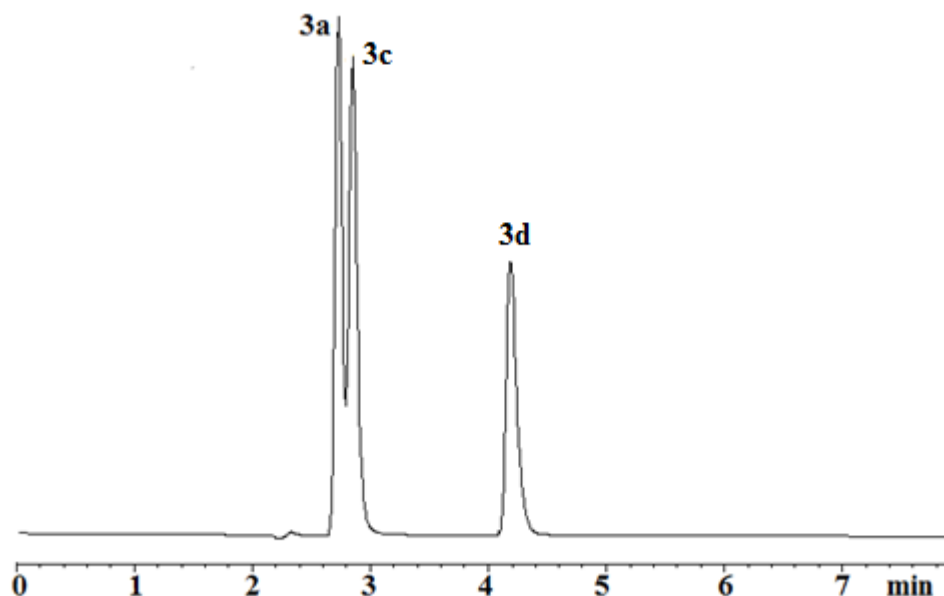


Figure 36 : Representative chromatograms of solutions containing: (\pm)-mephedrone.HBr (3a, $5 \mu\text{g mL}^{-1}$); (\pm)-4'-methyl-*N*-ethylcathinone.HBr (4-MEC) (3c, $5 \mu\text{g mL}^{-1}$); (\pm)-4'-methyl-*N*-benzylcathinone.HBr (4-MBC) (3d, $5 \mu\text{g mL}^{-1}$) obtained using ACE 3 C₁₈ column (150 mm x 4.6 mm i.d., particle size: 3 μm); mobile phase: methanol:10 mM ammonium formate (pH 3.5) (60:40); Detector wavelength: 264 nm.

It was therefore decided to lower the amount of organic modifier to 50%. Unfortunately, the analytes 4-MMC (3a) and 4-MEC (3c) eluted at 2.9 and 3.5 minutes respectively, but they gave poor peak shapes and resolution. In addition peak for 4-MBC (3d) exhibited tailing (Figure 37).

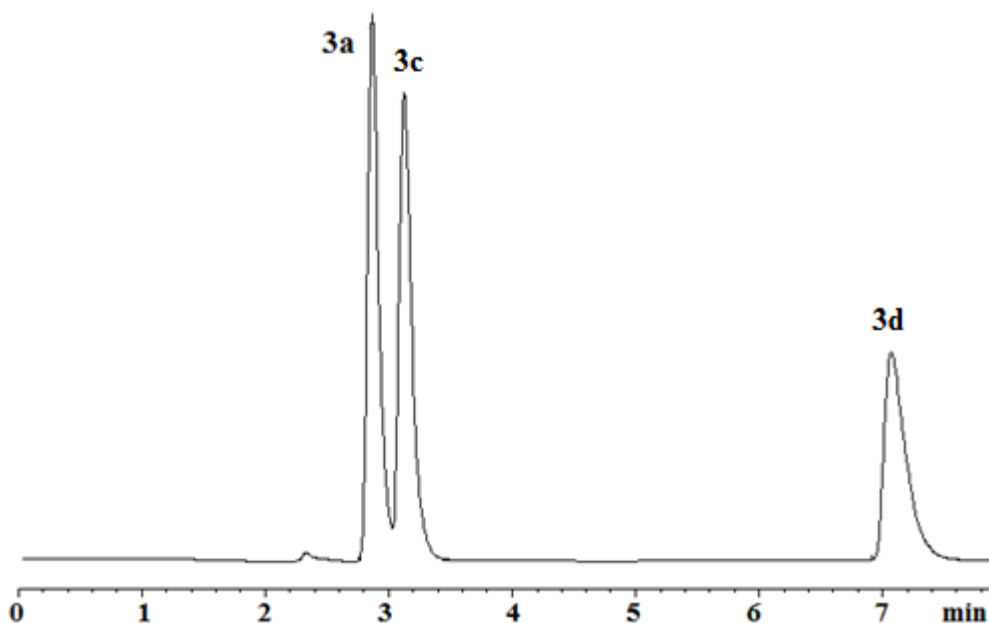


Figure 37: Representative chromatograms of solutions containing: (\pm)-mephedrone.HBr (4-MMC) (3a, $5 \mu\text{g mL}^{-1}$); (\pm)-4'-methyl-N-ethylcathinone.HBr(4-MEC) (3c, $5 \mu\text{g mL}^{-1}$); (\pm)-4'-methyl-N-benzylcathinone.HBr (4-MBC) (3d, $5 \mu\text{g mL}^{-1}$) obtained using ACE 3 C₁₈ column (150 mm x 4.6 mm i.d., particle size: 3 μm); mobile phase: methanol:10 mM ammonium formate (pH 3.5) (50:50); Detector wavelength: 264 nm.

Thus again the amount of organic modifier was lowered slightly to 46%. Encouragingly the analytes 4-MMC (3a), 4-MEC (3c) and 4-MBC (3d) eluted at 3.8, 4.2 and 11.6 minutes respectively (Figure 38-a, 38-c). This mobile phase composition produced chromatographic separation which made it suitable for use as an external standard method for the quantification of these cathinone derivatives.

Table 11. Summary of validation data for the quantification of (±)-mephedrone.HBr(3a), (±)-4'-methyl-N-ethylcathinone.HBr (4-MEC)(3c) and (±)-4'-methyl-N-benzylcathinone.HBr (4-MBC)(3d) obtained using ACE 3 C₁₈ column (150 mm x 4.6 mm i.d., particle size: 3 µm); mobile phase: methanol:10 mM ammonium formate (pH 3.5) (46:54); detector wavelength: 264 nm.

	4-MMC (3a)	4-MEC (3c)	4-MBC (3d)
t_R (min) ($t_0 = 2.2$ min ^a)	3.8	4.2	11.6
RRT ^b	1	1.11	3.03
Capacity factor (k')	0.73	0.91	4.23
Response factor (RRF) ^c	1	0.8	0.43
N (plates)	13,500 (90,000) ^f	14,450 (96,333) ^f	20,100 (134,000) ^f
H (m)	1.11×10^{-5}	1.04×10^{-5}	7.46×10^{-6}
Resolution (R_s)	-	-	-
Symmetry factor (A_s)	1.4	1.32	1.22
LOD ^d (µg mL ⁻¹)	0.03	0.03	0.05
LOQ ^e (µg mL ⁻¹)	0.09	0.08	0.14
Co-efficient of regression (r^2)	0.999 ^g	0.999 ^h	0.999 ⁱ
Precision (% RSD) (n = 6)			
10 µg mL ⁻¹	0.72	1.80	1.30
5 µg mL ⁻¹	0.23	0.50	0.88
2.5 µg mL ⁻¹	0.62	0.66	0.97
1 µg mL ⁻¹	0.21	0.12	0.30
0.5 µg mL ⁻¹	0.60	0.08	0.24

^a Determined from the retention time of uracil eluting from the column.

^b Relative retention time (with respect to (±)-mephedrone,4-MMC, **3a**).

^c Relative response factor (with respect to (±)-mephedrone,4-MMC, **3a**).

^d Limit of Detection (based on the standard deviation of the response and the slope).

^e Limit of Quantification (based on the standard deviation of the response and the slope).

^f N expressed in plates per metre.

^g $y = 50.933x - 1.2239$.

^h $y = 33.324x - 0.7367$.

ⁱ $y = 11.530x - 0.636$.

The three methcathinone derivatives eluted with a slight peak tailing ($A_s \sim 1.2 - 1.4$) being observed in each case. Calibration standards were prepared and demonstrated a linear response ($r^2 = 0.999$) over a $0.5 - 10 \mu\text{g mL}^{-1}$ range with good repeatability in each case (RSD = 0.08 – 1.80 %, $n = 6$). The limits of detection and quantification were determined to be 0.03 and 0.09 for 4-MMC (3a), 0.03 and 0.08 for 4-MEC (3c)

and 0.05 and 0.14 $\mu\text{g mL}^{-1}$ for 4-MBC (3d) respectively, which was more sensitive than the previously reported method. The validation parameters for the three analytes are summarised in Table 11. The method was further developed in order to screen for methcathinones (4-MMC (3a), 4-MEC (3c) and 4-MBC (3d)) in the presence of a number of common diluents. The diluents chosen for the study were caffeine, benzocaine (based upon the data reported by Brandt *et al.* on the analysis of “street” samples of NRG-2 [19]), sucrose, glucose, mannitol and lactose. The mobile phase composition utilised for the quantification of the pure substances was suitable to ensure a rapid analysis time (*ca.* 13 min) and baseline resolution between the analytes (Figure 37d). The validation parameters for the chromatographic method are summarised in Table 12. All five strongly UV-absorbing components (4-MMC (3a), 4-MEC (3c) and 4-MBC (3d), caffeine and benzocaine) demonstrated a linear response ($r^2 = 0.999 - 1$) over a 0.5 – 10 $\mu\text{g mL}^{-1}$ range with excellent repeatability (RSD = 0.03 – 1.90 %, $n = 6$) and limits of detection (0.02 $\mu\text{g mL}^{-1}$) and quantification (0.05 – 0.09 $\mu\text{g mL}^{-1}$) respectively. The UV-inactive analytes (sucrose, glucose, mannitol and lactose) were shown not to interfere with the five target analytes.

Table 12. Summary of validation data for the quantification of (±)-mephedrone.HBr (4-MMC) (3a), (±)-4'-methyl-N-ethylcathinone.HBr (4-MEC) (3c) and (±)-4'-methyl-N-benzylcathinone.HBr (4-MBC) (3d) in the presence of common adulterants using ACE 3 C₁₈ column (150 mm x 4.6 mm i.d., particle size: 3 µm); mobile phase: methanol:10 mM ammonium formate (pH 3.5) (46:54); detector wavelength: 264 nm.

	Caffeine	4-MMC(3a) ^{e,f}	4-MEC(3c)	Benzocaine	4-MBC(3d)
t_R (min) ($t_0 = 2.2$ min ^d)	3.2	3.8	4.2	8.5	11.6
RRT ^b	0.84	1	1.11	2.24	3.05
Capacity factor (k')	0.45	0.73	0.91	2.86	4.27
Response factor (RRF)	0.55	1	0.58	0.79	0.58
Resolution (R_s)	-	4.4	3.1	23.7	9.4
Symmetry factor (A_s)	0.97	0.99	0.99	0.98	0.88
LOD ^c (µg mL ⁻¹)	0.02	0.02	0.02	0.02	0.02
LOQ ^d (µg mL ⁻¹)	0.05	0.07	0.07	0.05	0.09
Co-efficient of regression (r^2)	1 ^g	0.999 ^h	0.999 ⁱ	1 ^j	0.999 ^k
Precision (% RSD) (n = 6)					
10 µg mL ⁻¹	0.21	0.10	0.19	0.14	0.46
5 µg mL ⁻¹	0.29	0.10	1.00	0.29	0.54
2.5 µg mL ⁻¹	1.54	1.17	0.07	0.52	0.03
1 µg mL ⁻¹	0.49	0.07	0.81	0.43	1.90
0.5 µg mL ⁻¹	0.74	0.03	1.76	0.75	1.65

^a Determined from the retention time of uracil eluting from the column.

^b Relative retention time.

^c Limit of Detection (based on the standard deviation of the response and the slope).

^d Limit of Quantification (based on the standard deviation of the response and the slope).

^e $N = 90,833$ plates per metre.

^f $H = 1.10 \times 10^{-5}$ m.

^g $y = 17.195x + 0.2407$.

^h $y = 56.714x - 1.2765$.

ⁱ $y = 21.91x - 0.7506$.

^j $y = 19.861x - 0.7602$.

^k $y = 36.834x - 0.6905$.

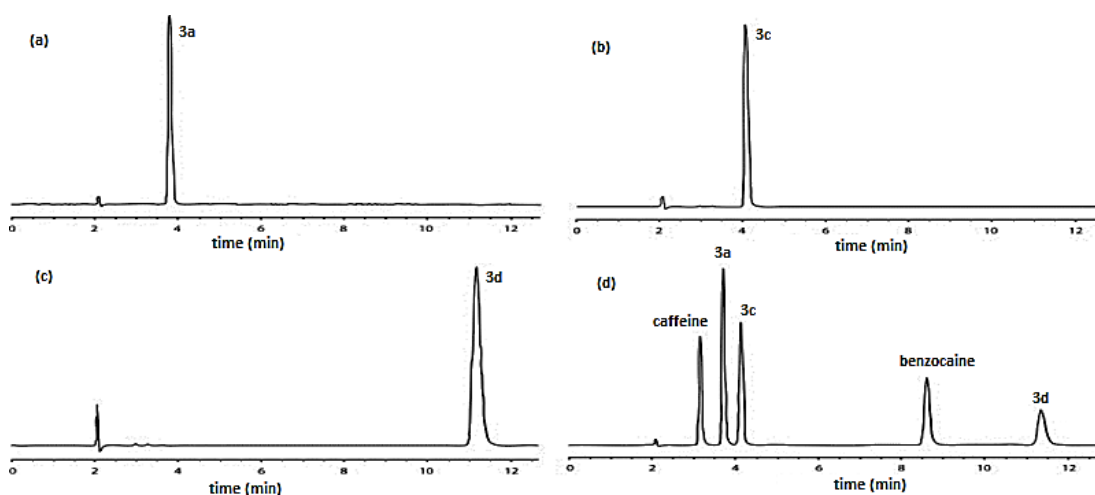


Figure 38. Representative chromatograms of solutions containing: (a) (±)-mephedrone.HBr (4-MMC) (3a, 5 $\mu\text{g mL}^{-1}$); (b) (±)-4'-methyl-N-ethylcathinone.HBr (4-MEC) (3c, 5 $\mu\text{g mL}^{-1}$); (c) (±)-4'-methyl-N-benzylcathinone.HBr (4-MBC) (3d, 5 $\mu\text{g mL}^{-1}$) and (d) caffeine (5 $\mu\text{g mL}^{-1}$); (±)-mephedrone.HBr (4-MMC) (3a, 5 $\mu\text{g mL}^{-1}$), (±)-4'-methyl-N-ethylcathinone.HBr (4-MEC) (3c, 5 $\mu\text{g mL}^{-1}$), benzocaine (5 $\mu\text{g mL}^{-1}$) and (±)-4'-methyl-N-benzylcathinone.HBr (4-MBC) (3d, 5 $\mu\text{g mL}^{-1}$) obtained using ACE 3 C_{18} column (150 mm x 4.6 mm i.d., particle size: 3 μm); mobile phase: methanol:10 mM ammonium formate (pH 3.5) (46:54); Detector wavelength: 264 nm; t_0 (2.2 min) was determined from the t_R of a solution of uracil.

Three NRG-2 samples obtained from Internet vendors were all purported to be >99 % pure and to contain 1 g of NRG-2. The samples were arbitrarily labelled NRG-2-A, NRG-2-B and NRG-2-C. Preliminary LC-MS analysis (Figure 39) indicated that two of the samples contained single components (NRG-2-A: $t_R = 13.41$ min, $m/z = 178.12$ $[\text{M}+\text{H}]^+$; NRG-2-B: $t_R = 14.32$ min, $m/z = 192.14$ $[\text{M}+\text{H}]^+$) and one contained two compounds (NRG-2-C: $t_R = 14.56$ min [major], $m/z = 192.14$ $[\text{M}+\text{H}]^+$; $t_R = 18.91$ min [minor], $m/z = 254.15$ $[\text{M}+\text{H}]^+$).

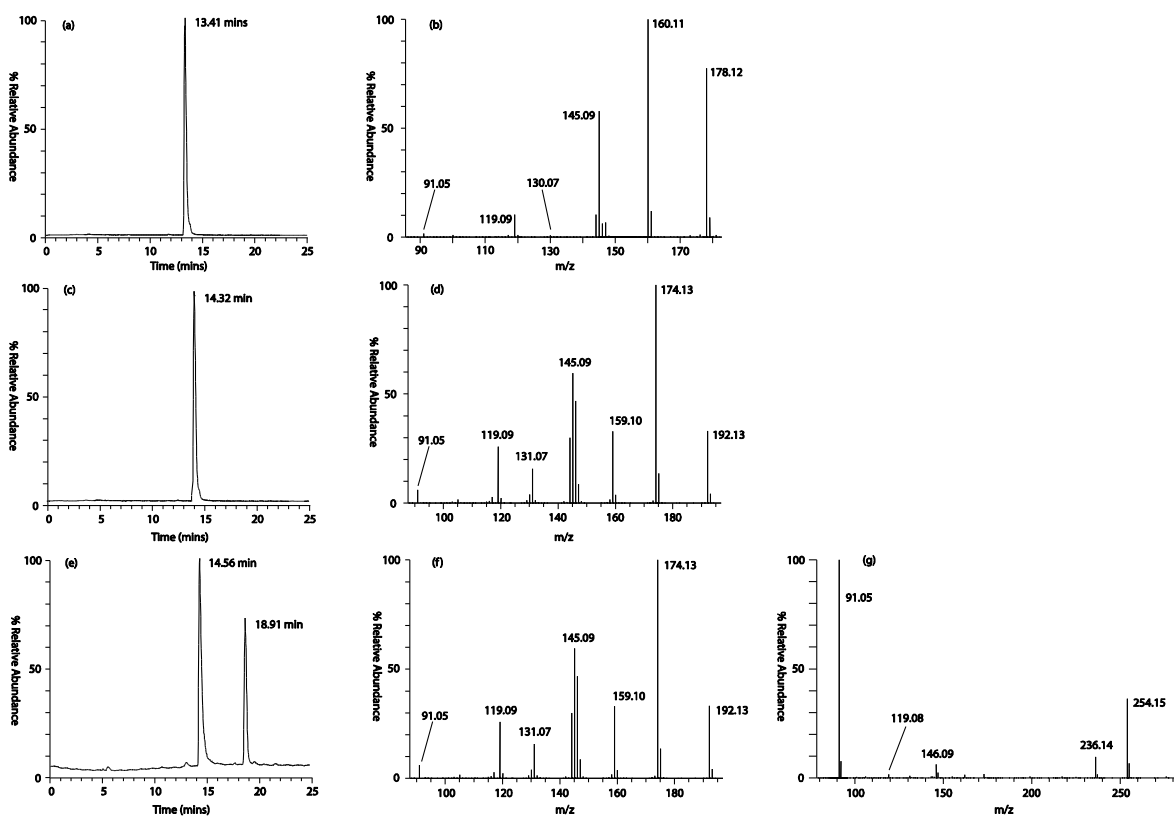


Figure 39. LC-MS analysis of three NRG-2 products obtained using ACE 3 C₁₈ column (150 mm x 4.6 mm i.d., particle size: 3 μm); mobile phase and gradient programme (see Section 2.2.6 for details): (a) LC chromatogram for NRG-2-A; (b) ESI mass spectrum (+ve ion mode) of peak ($t_R = 13.41$ min) corresponding to mephedrone (4-MMC)(3a, $[M+H]^+ = 178.12$); (c) LC chromatogram for NRG-2-B; (d) ESI mass spectrum (+ve ion mode) of peak ($t_R = 14.32$ min) corresponding to 4-MEC (3c, $[M+H]^+ = 192.14$); (e) LC chromatogram for NRG-2-C; (f) ESI mass spectrum (+ve ion mode) of peak ($t_R = 14.56$ min) corresponding to 4-MEC (3c, $[M+H]^+ = 192.14$); (g) ESI mass spectrum (+ve ion mode) of peak ($t_R = 18.91$ min) corresponding to 4-MBC (3d, $[M+H]^+ = 254.15$).

Additional ¹H NMR analysis (conducted at 60 °C in *d*₆-DMSO) of NRG-2-A gave a spectrum (Figure 40a) consistent with (±)-mephedrone (3a, 4-MMC)[63] thus confirming its identity². The second sample, NRG-2-B, also exhibited the classical

² The spectrum obtained was consistent with the previously reported data [57]. However, the signal corresponding to the ammonium salt protons at *circa.* $\delta^1H = 9.35$ ppm was too broad to be observed.

AA'BB' pattern typical of an unsymmetrical *para*-disubstituted aromatic ring together with a quartet at $\delta^1\text{H} = 5.21$ ppm (corresponding to the chiral C2-centre) and a deshielded singlet (*circa.* $\delta^1\text{H} = 2.4$ ppm) attributable to a methyl group attached to an aromatic ring. Taken together, these data are characteristic of a mephedrone-like structure [63](Figure 40b). In addition the ^1H NMR spectrum exhibited signals at $\delta^1\text{H} = 1.28$ ppm and 3.04 ppm, which are characteristic of an ethyl side chain, where the methylene group demonstrates additional geminal coupling to the chiral centre at C2. This data indicates that the second sample is likely to contain the previously reported (\pm)-4'-methyl-*N*-ethylcathinone (**3c**, 4-MEC) and is in agreement with the data previously reported by other researchers [19, 116] .

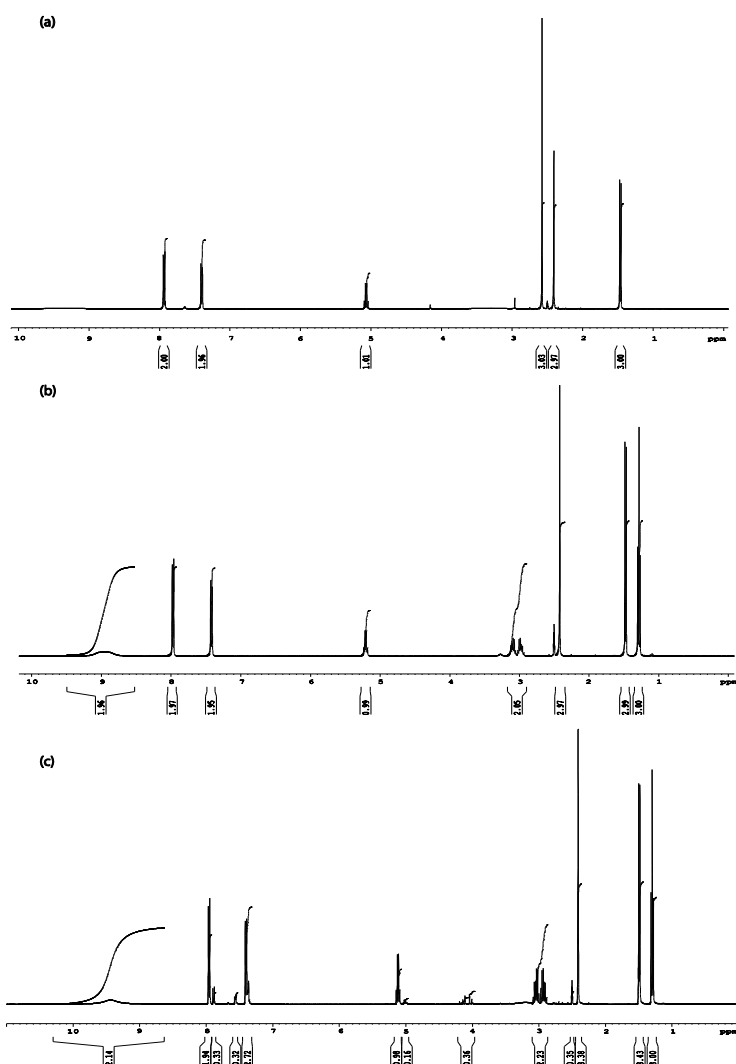


Figure 40. ^1H NMR spectra (400 MHz, d_6 -DMSO, 60 °C) of (a) NRG-2-A; (b) NRG-2-B and (c) NRG-2-C.

The LC-MS data for NRG-2-C shows that the sample contains two components (Figure 39). The major component ($t_R = 14.56$ min, $m/z = 192.14$ $[M+H]^+$) gives both a mass spectrum and characteristic signals in the 1H NMR spectrum (Figure 39c) that are both consistent with the data obtained for (\pm)-4'-methyl-*N*-ethylcathinone (**3c**, 4-MEC) thus confirming its identity and presence in the sample. The minor component ($t_R = 18.91$ min) gives a mass spectrum containing a molecular ion ($m/z = 254.15$ $[M+H]^+$) with a pattern of fragment ions, similar to 4-MMC(**3a**) and 4-MEC(**3c**), at $m/z = 236.14$, 146.09, 119.08 and 91.05 indicating a mephedrone-like structural motif and therefore two possible isomeric structures namely (\pm)-4'-methyl-*N*-benzylcathinone (**3d**, 4-MBC) or the (\pm)-4'-methyl-*N*-tolylcathinone derivative (**8**) (Scheme 4). The 1H NMR spectrum (Figure 39c) indicates that the minor component is a structurally-related mephedrone derivative due to the characteristic signals at $\delta^1H \sim 7.89$ ppm (AA'BB' system where the partner signal at $\delta^1H \sim 7.4$ ppm appears co-incident with other aromatic resonances), $\delta^1H \sim 2.40$ ppm (methyl group attached to an aromatic ring), $\delta^1H \sim 5.01$ ppm (corresponding to the proton attached to the chiral C2-centre) with additional aromatic signals (*circa.* $\delta^1H = 7.36 - 7.38$ and $7.55 - 7.57$ ppm) for a second aromatic ring. The presence of a doublet of doublets (*circa.* $\delta^1H = 4.08$ ppm), which is distinctive of an isolated methylene group exhibiting geminal coupling to the chiral centre at C2 (*cf.* 4-MEC), and the absence of an additional deshielded singlet (*circa.* $\delta^1H = 2.4$ ppm) attributable to a second aromatic methyl group, confirms that the structure of the minor component is likely to be (\pm)-4'-methyl-*N*-benzylcathinone (**3d**, 4-MBC) rather than the isomeric derivative (\pm)-4'-methyl-*N*-tolylcathinone (**8**).

The three “street” samples of NRG-2 were analysed using the HPLC validated adulterants method at a concentration of $10 \mu\text{g mL}^{-1}$. The results (Figure 41) confirm that two of the samples contained single components (NRG-2-A: $t_R = 3.8$ min, mephedrone, Figure 41a; NRG-2-B: $t_R = 4.2$ min, 4-MEC, Figure 41b), one contained two (NRG-2-C: $t_R = 4.2$ min [major, 4-MEC] and $t_R = 11.5$ min [minor, 4-MBC], Figure 41c) and all the samples were predominately pure with none of the common diluents reported by Brandt *et al.* [19] being present. This study indicates that this protocol can be considered suitable for the rapid analysis of these products.

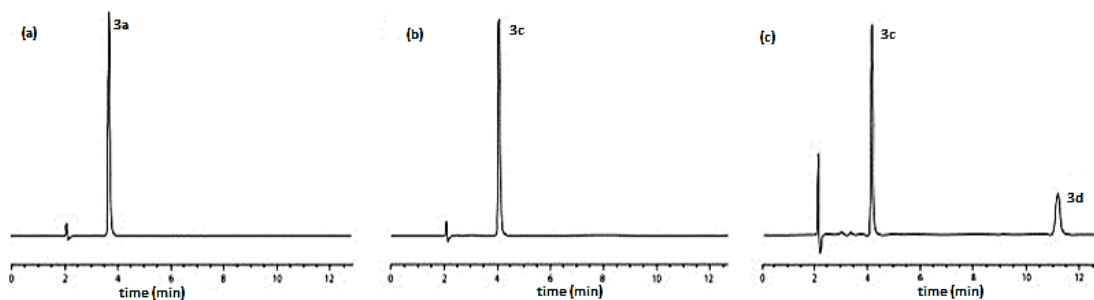


Figure 41. Representative chromatograms of solutions containing: (a) NRG-2-A ($10 \mu\text{g mL}^{-1}$); (b) NRG-2-B ($10 \mu\text{g mL}^{-1}$) and (c) NRG-2-C ($10 \mu\text{g mL}^{-1}$) obtained using ACE 3 C₁₈ column (150 mm x 4.6 mm i.d., particle size: 3 μm); mobile phase: methanol:10 mM ammonium formate (pH 3.5) (46:54); Detector wavelength: 264 nm; t_0 (2.2 min) was determined from the t_R of a solution of uracil.

2.3.4 Re-development and validation of a HPLC method for the separation and identification ten of NRG-2 samples containing Cathinone derivatives and potential adulterants.

The 4-FMC(4c) sample was injected and the peak eluted at 4.9 minutes; caffeine eluted at 5.2 minutes; 4-MMC (3a) was eluted at 6.6 minutes; 4-MEC (3c) was eluted at 7.2 minutes; MDPV(7c) was eluted at 8.4 minutes; benzocaine was eluted at 10.1 minutes; and 4-MBC (3d) was eluted at 10.8 minutes. The optimised method was carried out under gradient condition. Solvent A was aqueous ammonium formate buffer (10mM, pH 3.5 \pm 0.02), and solvent B was methanol; the flow rate was 0.8 mL min^{-1} , the gradient programme was as follows: 30% B (0 minute) to 60% at 7 minutes to 60% B at 12 minutes to 30% at 18 minutes, obtained using ACE 3 C₁₈ column (150 mm x 4.6 mm i.d., particle size: 3 μm). Detector wavelength: 264 nm.

2.3.4.1 Preparation of calibration series solutions for Analytes/adulterants

As a first separation attempt, seven substituted cathinones and adulterants were run individually on the same isocratic method which had been validated for the

separation of compounds which might be present in a street sample of NRG-2 as was discussed in the study by Brandt *et al.* [19].

Isocratic elution was carried out using a HPLC method with a detection wavelength of 264 nm, for the separation of five cathinone derivatives (4-MMC (3a), 4-MEC (3c), 4-MBC (3d), MDPV, 4-FMC) and 2 UV active adulterants (caffeine and benzocaine). The method used an ACE C₁₈ (150 x 4.6 mm i.d, 3 µm) column, employing a 10 mM ammonium formate (pH 3.5 ± 0.02) as mobile phase A; and methanol as mobile phase B (B: A ; 46:54). The chromatograms of individual runs showed co-elution for some compounds.

The first parameter to be changed was the pH of the mobile phase buffer which was increased 3.5 to 4.0. The mixture of seven compounds in this case was run and the only issue with the method was co-elution of peaks (a) and (b). The order of elution was determined by injection of pure reference standards (Figure 42).

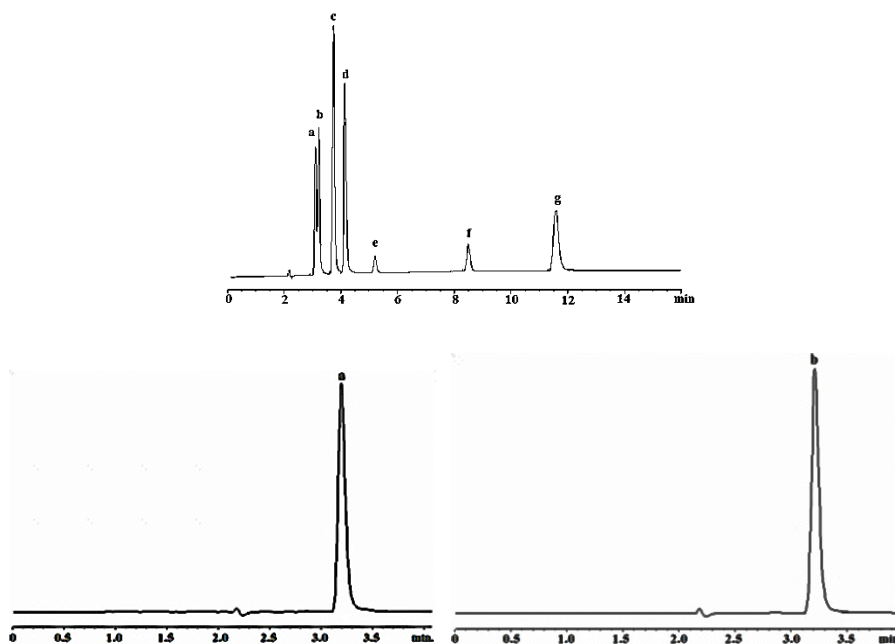


Figure 42. Representative chromatograms of solutions containing seven compounds obtained using ACE 3 C₁₈ column (150 mm x 4.6 mm i.d., particle size: 3 μ m); mobile phase: methanol: 10 mM ammonium formate (pH 4) (46:54); Detector wavelength: 264 nm. , the order of elution was determined by injection of pure reference standards : (t_{RS} ; 4-FMC(a;4c) 3.1 min, caffeine(b) 3.2 min ,4-MMC(c;3a) 3.7 min,4-MEC(d;3c) 4.1 min. ,MDPV(e;7c)5.2 min ,benzocaine(f) 8.5 min,4-MBC(g;3d)11.6 min.).

The chromatograms which were obtained for each of the seven compounds showed that peaks (a) and (b) were due to 4-FMC and caffeine respectively. The retention of these compounds did not change with pH. Thus this method succeeded in separating all the compounds in the mixture but still lacked complete separation of 4-FMC ($t_R = 3.1$ minutes) and caffeine ($t_R = 3.2$ minutes).

The HPLC method was been modified again in order to separate the mixture of seven compounds. The organic modifier was reduced to 39% using pH 3.5 with the aqueous component and then organic modifier was increased to 60 % using a pH 4.0 with the aqueous component. The results are shown in Figures 43 and 44 respectively. The separation was not improved since (a) and (b) still co-eluted with

39% organic modifier and several peaks co-eluted when 60% organic modifier was used.

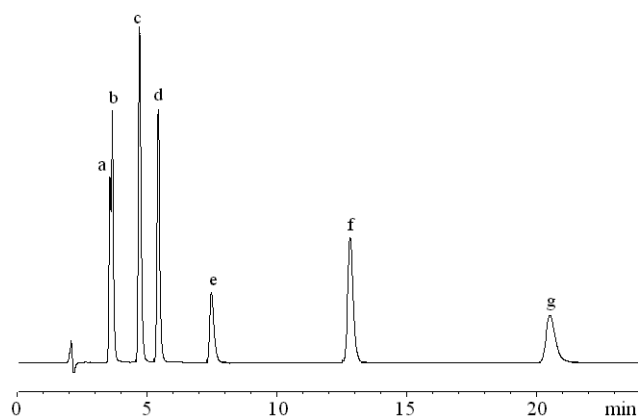


Figure 43 : Representative chromatograms of solutions containing seven compounds ($10 \mu\text{g mL}^{-1}$) obtained using ACE 3 C_{18} column (150 mm x 4.6 mm i.d., particle size: $3 \mu\text{m}$); mobile phase: methanol: 10 mM ammonium formate (pH 3.5) (39:61); Detector wavelength: 264 nm. (t_{RS} ; 4-FMC(a;4c) 3.6 min, caffeine (b) 3.7 min, 4-MMC(c;3a) 4.7 min, 4-MEC(d;3c) 5.4 min, MDPV(e;7c) 7.5 min, benzocaine(f) 12.8 min, 4-MBC(g;3d) 20.5 min.)

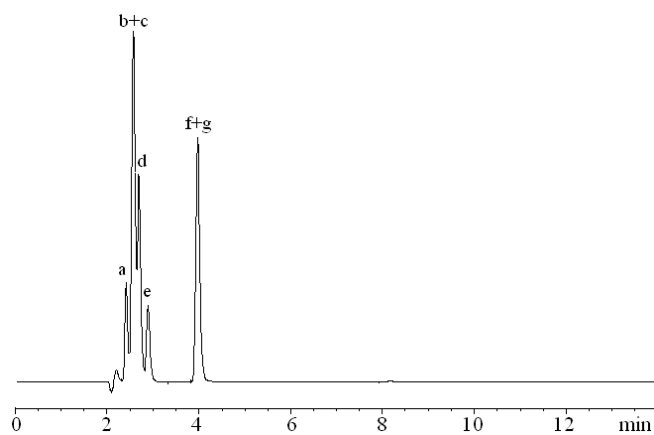


Figure 44 : Representative chromatograms of solutions containing seven compounds ($10 \mu\text{g mL}^{-1}$) obtained using ACE 3 C_{18} column (150 mm x 4.6 mm i.d., particle size: $3 \mu\text{m}$); mobile phase: methanol: 10 mM ammonium formate (pH 4) (60:40); Detector wavelength: 264 nm. (t_{RS} ; 4-FMC(a;4c) 2.4 min, caffeine (b) 2.6 min, 4-MMC(c;3a) 2.6 min, 4-MEC(d;3c) 2.7 min, MDPV(e;7c) 2.9 min, benzocaine(f) 4.0 min, 4-MBC(g;3d) 4.0 min.)

Thus variations in the isocratic method did not result in separation of all seven standards. It was thought that using a gradient method might improve the separation of the mixture of seven standards.

Thus the next parameter to be varied was the mobile phase composition in gradient mode, A gradient method starting with methanol-10mM ammonium formate (pH: 3.5) at 30:70 was used (Table 13). Starting with 30% B and avoiding starting with 0%B was essential for quick equilibration of the column between gradient runs [129].

The mixture of seven compounds was run with a gradient method (M1) as shown in Table 13. The chromatogram showed only six peaks and when individual compounds were run under the same conditions it was observed that there was no peak for 4-MBC (3d) after 18 minutes of run time. The same sample was run again with an extension in the run time with isocratic 30 % B, from 18 to 40 minutes. This resulted in the elution of a broad peak for 4-MBC (3d) at 28 minutes (Figure 45).

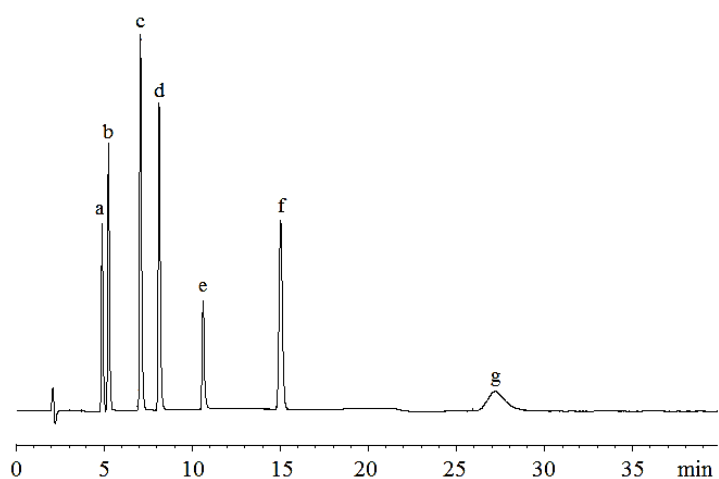


Figure 45. Gradient HPLC chromatogram of the mixture of 7 standard samples at eluting gradient condition [M1; 30% MeOH(0 min) → 40 % MeOH (7-15 min) → 30% MeOH (18 min) → ext. 30% MeOH (40 min)] obtained using ACE 3 C₁₈ column (150 mm x 4.6 mm i.d., particle size: 3 μm) , 10 mM ammonium formate (pH 3.5) ; Detector wavelength: 264 nm.

Table 13. Gradient program of methods (M1, M2 and M3) in the reverse phase HPLC analysis of NRG-2 compounds and adulterants using an external standard method.

Method	Flow rate (mL min ⁻¹)	Time(min)	%MeOH	% 10 Mm NH ₄ HCO ₂
M1	0.8	0	30	70
		7	40	60
		15	40	60
		18	30	70
M2	0.8	0	30	70
		4	46	54
		10	46	54
		20	30	70
M3	0.8	0	30	70
		7	60	40
		12	60	40
		18	30	70

Figure 46 shows the chromatogram obtained when running the mixture of seven compounds with method (M2: Table 13). It was able to separate all seven compounds with a ($t_R = 4.8$ min) and b ($t_R = 5.0$ min.) being only just resolved with a resolution value of 1.87. This method was optimized again by slightly changing the gradient programme to achieve the desired resolution in a shorter analysis time.

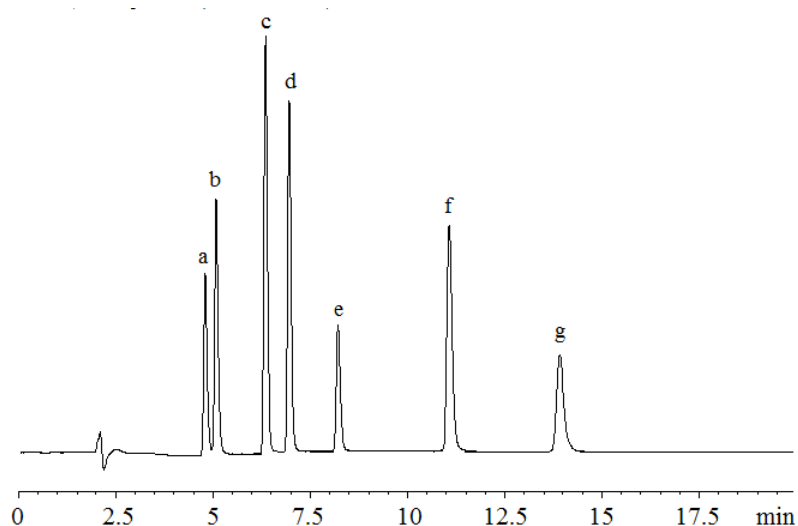


Figure 46. Gradient HPLC chromatogram of the mixture of 7 standard samples under gradient conditions (M2):30% MeOH (0 min) → 46 % MeOH (4-10 min) → 30% MeOH (20 min)] obtained using ACE 3 C₁₈ column (150 mm x 4.6 mm i.d., particle size: 3 μm), 10 mM ammonium formate (pH 3.5); Detector wavelength: 264 nm.

In gradient run shown in Figure 47, the modified gradient method (M3) improved the shape peak for all seven compounds as well as offering good resolution. However, in some cases with the calibration series chromatograms, particularly with a lower concentration of calibration, there were issues with chromatogram baseline which rose between 5 and 18 minutes and small system peaks were appeared in the chromatogram due to using gradient elution. The same system peaks were found in all fresh samples and the blank as well (Figure 47). This rise was due to methanol which has a background absorbance. Therefore, the peaks were not due to degradation and thus they should be neglected. Despite this issue, it was easy to get the integration of the analyte peaks exactly right.

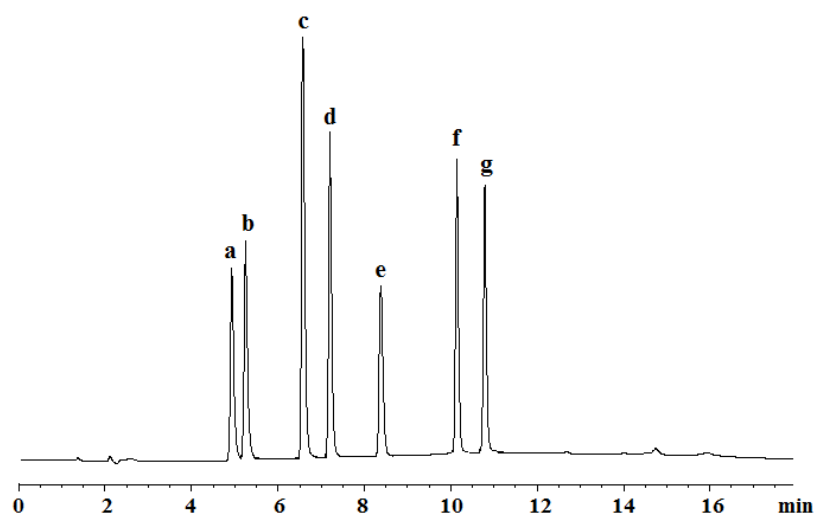


Figure 47. Gradient HPLC chromatogram of optimised separation of the mixture of seven standard samples with eluting gradient conditions M3: 30% MeOH (0 min) → 60 % MeOH (7 -12min) → 30% MeOH (18 min)] obtained using ACE 3 C₁₈ column (150 mm x 4.6 mm i.d., particle size: 3 μm), 10 mM ammonium formate (pH 3.5); Detector wavelength: 264 nm.

2.3.4.2 Validation M3 method of NRG-2

Both conditions M2 and M3 were sufficient to separate all the analytes, but the gradient method M3 was chosen due to since it produced a better resolution in a shorter analysis time. For quantification purposes, and since each analyte has a different UV absorbance value , the relative response factor for each analyte was calculated based on their peak areas obtained at 264 nm compared to 4-MMC (3a) as a reference.

Because this method was performed using a single wavelength UV absorbance detector at 264 nm as mentioned above, the response factor was calculated by injecting a mixture solution containing 10 μg mL⁻¹ of seven standard active compounds into the HPLC, and conditions when the calibration series of solutions were run, the data was collected as a peak area and then the equation which mentioned in Section (2.2.7) was used. Table 14 shows that the relative response factors for seven analytes were calculated using peak area of 4-MMC (3a) as a reference analyte.

The seven compounds eluted at 4.9 (4-FMC; 4c), 5.2 (caffeine), 6.6(4-MMC; 3a), 7.2(4-MEC; 3c), 8.4 (MDPV; 7c), 10.1 (Benzocaine), 10.8 (4-MBC; 3d) minutes respectively (Figure 46).

The optimised method (M3) was validated and the reproducibility was tested. This involved making up a fresh solution of calibration standards which contained seven of the cathinone compounds and their adulterants in HPLC grade water and then running the mixture six times on the HPLC system. The calibration standards demonstrated a linear response ($r^2 = 0.999 - 1.0$) over the range 0.5- 10 $\mu\text{g mL}^{-1}$ range for six of these compounds and over 2 - 40 $\mu\text{g mL}^{-1}$ for MDPV (7c). The mean, SD and RSD of each component could then be calculated and showed excellent reproducibility for all seven analytes (RSD = 0.01-0.80 %, n=6). The other validation parameters for the seven analytes are summarised in Table 14.

In addition, validation of this method provided verification of accuracy, precision, linearity and ruggedness. The limits of detection and limit of quantification for seven compounds were determined and are presented in Table 14.

Table 14 shows also some other validation parameters that were been calculated from the calibration series chromatograms included retention time, response factor, symmetry factor, and resolution.

Table 14 : Summary of validation data for the quantification of seven compounds, potentially present in ten NRG-2 samples, obtained using an ACE 3 C₁₈ column (150 mm x 4.6 mm i.d., particle size: 3 µm); gradient mobile phase elution as % B 30:60:60:30; detector wavelength: 264 nm.

	4-FMC (4c)	CAFFEINE	4-MMC (3a)	4-MEC (3c)	MDPV (7c)	BENZOCAI NE	4-MBC (3d)
<i>t_R</i> (min)	4.9	5.2	6.6	7.2	8.4	10.1	10.8
RRT ^a	0.74	0.79	1	1.09	1.30	1.53	1.64
Capacity factor(k')	1.09	1.18	1.77	2.05	2.59	3.36	3.68
Response factor(RRF) ^b	1.95	0.53	1	0.75	0.11	0.64	0.63
<i>N</i> (plates)	19,300 (128,666) ^e	22,800 (152,000) ^e	38,800 (258,666) ^e	45,400 (302,666) ^e	61,800 (412,000) ^e	102,200 (681,333) ^e	115,900 (772,666) ^e
<i>H</i> (m)	7.8 x 10 ⁻⁶	6.6 x 10 ⁻⁶	3.9 x 10 ⁻⁶	3.3 x 10 ⁻⁶	2.4 x 10 ⁻⁶	1.5 x 10 ⁻⁶	1.3 x 10 ⁻⁶
Symmetry factor (<i>A_s</i>)	1.05	0.76	1.21	0.38	1.71	1.57	1.30
Resolution <i>R_s</i>	-	2.18	9.87	4.61	8.90	13.26	5.18
LOD ^c (µg/mL)	0.12	0.04	0.048	0.029	0.12	0.25	0.13
LOQ ^d (µg/mL)	0.36	0.12	0.14	0.089	0.36	0.76	0.41
Co-efficient of regression (<i>r</i> ²)	0.9999 ^f	1 ^g	1 ^h	1 ⁱ	1 ^j	0.9995 ^k	0.9999 ^l
Precision (%RSD) (n=6)	0.489	0.799	0.282	0.420	-	0.663	0.440
0.5 µg/ml	0.356	0.130	0.0920	0.483	-	0.283	0.328
1.0 µg/ml	0.0812	0.107	0.0910	0.0973	-	0.110	0.0149
2.5 µg/ml	0.0891	0.0386	0.0824	0.0310	-	0.0399	0.0370
5.0 µg/ml	0.0467	0.0537	0.0446	0.0483	-	0.0140	0.0436
10 µg/ml							
Precision (%RSD) (n=6)	-	-	-	-	0.200	-	-
2.0 µg/ml	-	-	-	-	0.325	-	-
4.0 µg/ml	-	-	-	-	0.0753	-	-
10 µg/ml	-	-	-	-	0.0889	-	-
20 µg/ml	-	-	-	-	0.0258	-	-
40 µg/ml							

^a Relative retention time (with respect to (±)-mephedrone, 3a).

^b Relative response factor (with respect to (±)-mephedrone, 3a).

^c Limit of Detection (based on the standard deviation of the response and the slope).

^d Limit of Quantification (based on the standard deviation of the response and the slope).

^e *N* expressed in plates per metre.

$$^f y = 55.2 x - 1.0632$$

$$^g y = 16.265 x - 0.2148$$

$$^h y = 55.312 x - 0.1041$$

$$^i y = 30.548 x - 0.623$$

$$^j y = 0.6408 x$$

$$^k y = 24.056 x - 1.9077$$

$$^l y = 23.086x - 0.2623$$

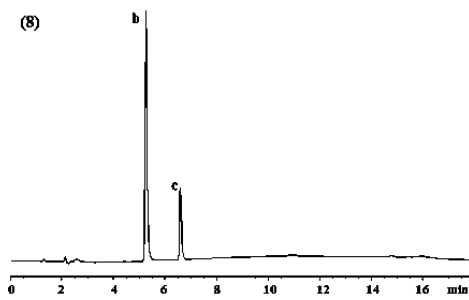
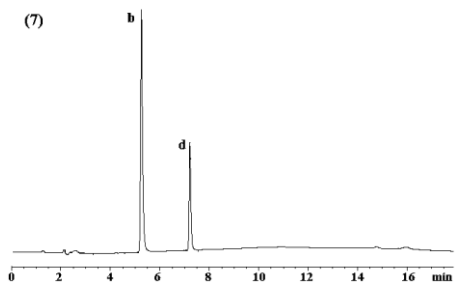
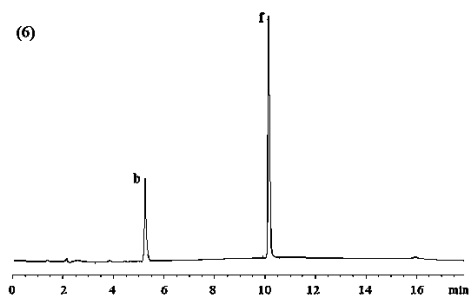
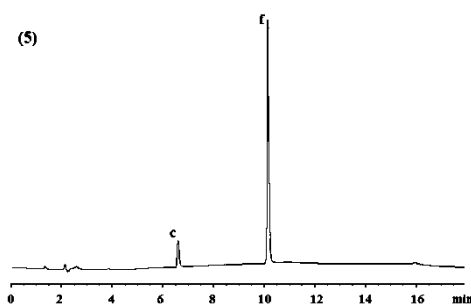
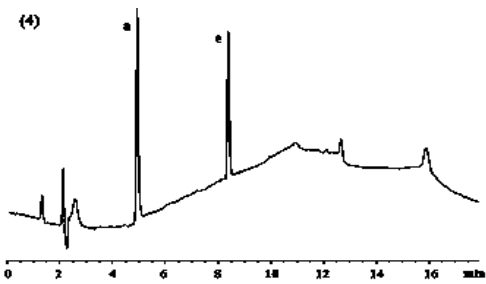
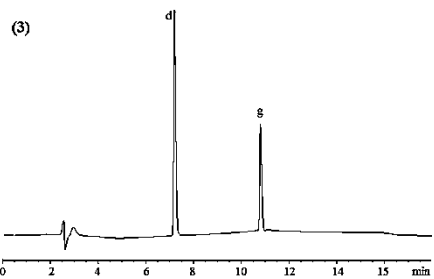
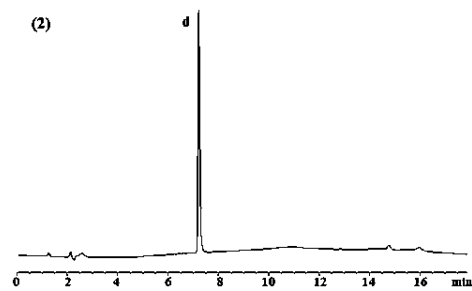
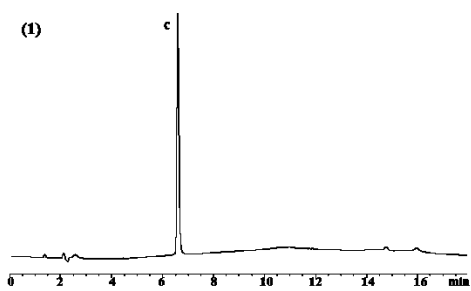
(-) this concentration was not used.

2.3.4.3 Application of a Quantitative HPLC method for the determination of cathinone derivatives in NRG-2 samples

Once the final method had been developed and validated, the ten NRG-2 products were run using the final method (M3) to separate and identify the cathinone compounds and adulterants in NRG-2 samples. Ten NRG-2 products were purchased online from different UK-Based websites. All of them were delivered as a white powders or crystals in plastic bags. The samples were dissolved in water and analysed by HPLC based on the HPLC method described above.

Representative chromatograms for the ten samples are shown in Figure 48. The active components in the ten samples were identified and are presented in Table 15. These data were consistent with the LC-MS data obtained in a previous study [130], thus our results confirming that the HPLC method was capable of identifying a range of cathinones and adulterants.

The content of the seven compounds in 10 mg of powder assayed from the street samples could be determined from the calibration data shown in Table 14.



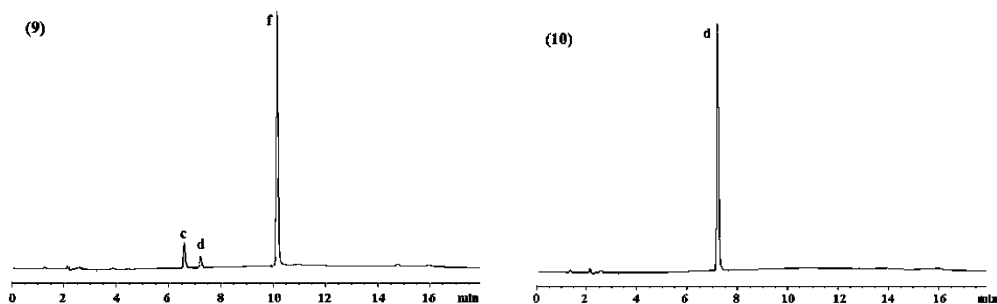


Figure 48. Representative chromatograms of solutions containing: (1) NRG-2-1 ($10 \mu\text{g mL}^{-1}$); (2) NRG-2-2 ($10 \mu\text{g mL}^{-1}$); (3) NRG-2-3 ($10 \mu\text{g mL}^{-1}$); (4) NRG-2-4 ($10 \mu\text{g mL}^{-1}$); (5) NRG-2-5 ($10 \mu\text{g mL}^{-1}$); (6) NRG-2-6 ($10 \mu\text{g mL}^{-1}$); (7) NRG-2-7 ($10 \mu\text{g mL}^{-1}$); (8) NRG-2-8 ($10 \mu\text{g mL}^{-1}$); (9) NRG-2-9 ($10 \mu\text{g mL}^{-1}$); (10) NRG-2-10 ($10 \mu\text{g mL}^{-1}$) obtained using gradient condition [30% methanol (0 min) \rightarrow 60 % methanol (7 -12min) \rightarrow 30% methanol (18 min)], and ACE 3 C_{18} column (150 mm x 4.6 mm i.d., particle size: 3 μm), 10 mM ammonium formate (pH 3.5); Detector wavelength: 264 nm. . the order of elution was determined by injection of pure reference standards : (a) 4-FMC ; (b)caffeine ; (c)4-MMC(3a);(d)4-MEC(3c);(e) MDPV ; (f) Benzocaine;(g)4-MBC(3d).

The data in Table 15 shows that the product composition varied significantly and nine NRG-2 samples contained of five different cathinone derivatives including mephedrone. Product No. 6 appeared to contain a mixture of caffeine and benzocaine, however, and cathinones could not be detected in this product.

Ten NRG-2 products were purchased from different web sources and numbered them as NRG2-1, NRG2-2, NRG2-3, NRG2-4, NRG2-5, NRG2-6, NRG2-7, NRG2-8, NRG2-9, and NRG2-10. Some NRG-2 products contained cathinone derivative alone or mixed with adulterants such as caffeine and benzocaine , and these findings supported the results were published previously by Brandt *et al.* [19]. Further identification and confirmation was made by Dr Sutcliffe and his student in Strathclyde University (SIPBS) using NMR spectroscopy which confirmed the substances below. Some of these products consisted of a few inactive compounds which are highly polar (sucrose, glucose, citric acid, taurine), and liquid chromatography was unable to identify them. Thus the identification of these

compounds was finally confirmed with diffusion measurements performed using 2D DOSY NMR experiments[130].

Table 15 : HPLC quantitation results of 10 NRG-2 products were purchased from the UK-based website

Sample No.	4-FMC (%w/w) (±RSD)	Caffeine (%w/w) (±RSD)	4-MMC (%w/w) (±RSD)	4-MEC (%w/w) (±RSD)	MDPV (%w/w) (±RSD)	Benzocaine (%w/w) (±RSD)	4-MBC (%w/w) (±RSD)
Sample1	-	-	40.32 (±0.072)	-	-	-	-
Sample2	-	-	-	63.66 (±0.030)	-	-	-
Sample3	-	-	-	11.33 (±0.26)	-	-	6.30 (±0.55)
Sample4	8.06 (±0.71)	-	-	-	14.51 (±0.12)	-	-
Sample5	-	-	6.95 (±0.013)	-	-	93.87 (±0.010)	-
Sample6	-	34.21 (±0.069)	-	-	-	68.77 (±0.055)	-
Sample7	-	76.03 (±0.054)	-	19.16 (±0.36)	-	-	-
Sample8	-	87.99 (±0.080)	11.15 (±0.073)	-	-	-	-
Sample9	-	-	6.04 (±0.31)	3.67 (±0.18)	-	79.59 (±0.031)	-
Sample10	-	-	-	86.06 (±0.098)	-	-	-

(-) =NOT DETECTED

2.4 Conclusions

A validated method for comprehensive analytical profiling and quantitative analysis of two new methcathinone-derivatives: 4-MEC (**3c**) and 4-MBC (**3d**) either in their pure form or in the presence of common excipients was developed. It is envisaged that the method presented will be valuable as a reference point for future analysis of these and related compounds as they emerge on the illicit drug market.

The HPLC method was further developed and validated to screen for ten NRG-2 products in the presence of number of adulterants. Ten samples were analysed in the similar fashion of standard method which was used with three methcathinone derivatives (4-MMC, 3a), (4-MEC, 3c) and (4-MBC, 3d) except that a gradient method was used rather than an isocratic method.

The data presented in section 2.4 indicates that the NRG-2 products which were available via internet websites appeared to contain a mixture of cathinone derivatives and /or some adulterants included 4-MMC (3a), 4-MEC (3c), 4-MBC (3d), MDPV, 4-FMC, caffeine and benzocaine. The optimised gradient method can be employed as an absolute qualification and quantification method for NRG-2 products. This method was developed and the adulterants chosen according to work done by Brandt *et al.* [19] which has shown that many legal highs (including NRG-2) contain a wide range of constituents which range from legal stimulants (caffeine), anaesthetics (benzocaine, procaine) and controlled substances (cathinones).

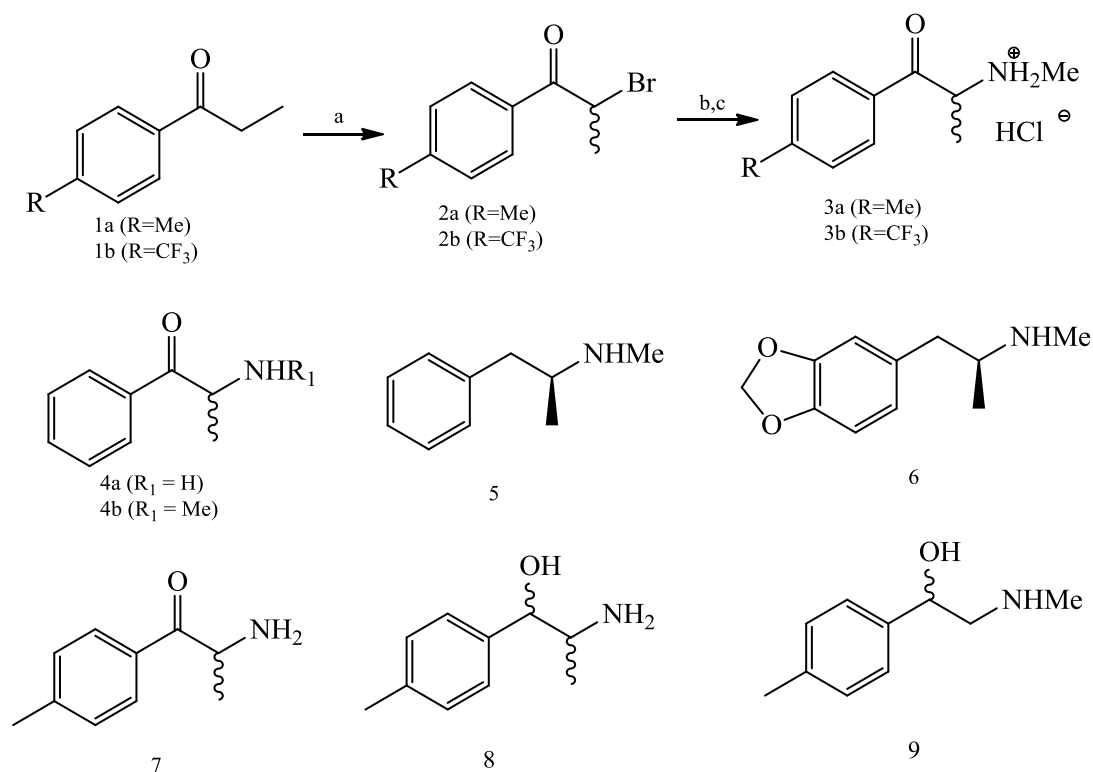
Chapter 3: Elucidation of the Phase I and Phase II metabolic pathways of (±)-4'-methylnmethcathinone (4-MMC), (±)-4'-(trifluoromethyl) methcathinone (4-TFMMC) and (±)-4'-methyl-N-ethylcathinone (4-MEC) in rat liver hepatocytes using LC-MS and GC-MS

3.1 Introduction

As previously discussed, “legal highs” may be bought through the internet at low cost and are sometimes pure compounds which display highly similar chemical structures to existing and illegal drugs of abuse within the phenethylamine class. (±)-4'-Methylnmethcathinone or (±)-mephedrone (3a, 4-MMC) [16, 63, 109] is a synthetic β -ketoamphetamine that is structurally similar to methcathinone (4b), related to cathinone (4a), a psychoactive compound found in Khat. (±)-Mephedrone has emerged in drug seizures as its use, as a “legal high” replacement for controlled stimulants including amphetamines such as methamphetamine (5) and MDMA (6; 1e), has increased (Scheme 7), a number of evolved cathinone-based “legal high” products (for example: NRG-1 and NRG-2) have become available in the United Kingdom [19, 131] and recent media reports indicate that the use of (±)-mephedrone (and derivatives thereof) has continued to rise despite the legislative change. The prevalence of these cathinone-derived “legal highs” has given rise to a number of legal, analytical and clinical challenges in the detection/identification of the substances themselves and within the context of treatment of individuals presenting at Accident and Emergency Units [111-114, 124, 125].

Cathinone derivatives, such as mephedrone (4-MMC, 3a) and 4-MEC (3c) are increasing worldwide. In the UK, where mephedrone and 4-MEC(3c) evolved NRG-2 product have been greatly drawing both mass media and Government attention, questions have been raised about the safety of prolonged use of these substances among young people, yet little information is available regarding pharmacokinetics and toxicity risks of this substances. Metabolic pathways for these substances were reported for 4-MMC (3a) in some studies, however, there has been little discussion

about phase II metabolism using indirect methods, and there is no reliable evidence that phase II metabolism occurred. Thus in this chapter, the identification of *in vitro* rat metabolites of 4-MMC (3a) and 4-MEC (3c) using direct analysis of *in vitro* metabolites was carried out to identify the major metabolic pathways of these substances. This could provide some support for understanding the pharmacokinetic behaviour and toxicity risks.



Scheme 7. Reagents and Conditions: (a) Br₂ / HBr (48 % in water) / CH₂Cl₂ / rt / 1h (2a, 99.6 %; 2b, 99.8%); (b) MeNH₂.HCl / NEt₃ / CH₂Cl₂ / rt / 24h; (c) HCl (4 M in 1, 4-dioxane) / EtOH / rt / 1h (3a, 51.7 % from 2a; 3b, 62.3 % from 2b).

Meyer *et al.* recently reported the Phase I metabolism of (±)-mephedrone and detection of the other cathinone derivatives in both rat and human urine using gas chromatography-mass spectrometry using electron-impact ionisation (GC-EI-MS) [66, 67]. Six major Phase I metabolites of (±)-mephedrone (4-MMC, 3a) were observed in both rat and human urine and these were shown to be products of simple

oxidative, reductive and *N*-dealkylation reactions. It was observed that, in both rat and human subjects, the drug underwent *N*-demethylation to give the primary amine normephedrone (7) that was further transformed by reduction of the beta-ketone moiety to form a mixture of two diastereomic 4'-methylnorephedrine derivatives (8). Direct reduction of (±)-mephedrone yielded 4'-methylephedrine (9) as a single diastereoisomer via a stereoselective enzymatic reduction due to steric hindrance of the *N*-methyl group. The authors did not detect any direct products arising from Phase II metabolism and this is believed to be due to the utilisation of an enzymatic hydrolysis step (glucuronidase and arylsulfatase) during the sample preparation and clean-up protocol [67] prior to analysis. However, they repeated their experiments without the use of enzymatic hydrolysis, assuming that the metabolites of mephedrone were transformed glucuronides/sulfates metabolites. They observed an increase in its phase I metabolites when the hydrolysis was applied. A recent report, by Meyer *et al.*, examining the metabolism of two new cathinone-derived recreational substances, 3-bromo- and 3-fluoromethcathinone (5c), in human liver microsomes has identified a number of Phase I metabolites using high resolution mass spectrometry. The study also detected the glucuronide-conjugated metabolites of both of these substances in samples of rat urine [132].

Although it is assumed that (±)-mephedrone should undergo further Phase II metabolism the detection/identification of any conjugated products from these pathways has yet to be reported. As knowledge of the ADME processes for biologically active molecules is a prerequisite for their toxicological risk assessment it is prudent to elucidate both the Phase I and II metabolic pathways for (±)-mephedrone – especially in light of its recent re-emergence on the recreational drug scene – this chapter seeks to address this deficiency by presenting the elucidation of both Phase I and Phase II metabolic events in rat hepatocyte preparations using LC-MS and LC-MS² methods. Additionally the chapter investigates bioisosterism at the primary site of metabolism in (±)-mephedrone (4-MMC, 3a) and the effect this structural modification has on the metabolic profile of this compound class by using (±)-4'-(trifluoromethyl)methcathinone hydrochloride (4-TFMMC, 3b), which has been recently described by Cozzi *et al.* [133], as the test compound.

Concentrations of (\pm)-mephedrone detected in the blood of human subjects which have been analysed as part of forensic toxicology investigations varies considerably. For example, analysis of two non-fatal cases of (\pm)-mephedrone abuse and toxicity has yielded blood values of $150 \mu\text{g L}^{-1}$ and $230 \mu\text{g L}^{-1}$. Because blood concentrations are not always reported in these cases, it is difficult to estimate the maximal blood concentration after oral administration, however, in the experiments reported in this study $100 \mu\text{M}$ (equivalent to $213.7 \mu\text{g L}^{-1}$) (\pm)-mephedrone was incubated with the hepatocytes to profile its metabolism. This reflects blood concentrations anticipated in persons abusing (\pm)-mephedrone without incurring fatal consequences [113, 125]. The ZICHILIC column offers major advantages for analysis of polar compounds by LC-MS compared to when a reverse phase column (RPC) is used. For example, in the case of analysing polar components RPC has shown low retention time and elution of compounds very near to the void volume. It also requires high water containing eluents which are not suitable for subsequent ESI-MS detection[134]; using Acetonitrile/water eluents with a buffer would be more suitable for an LC/MS technique.

Figure 49 shows the principal of HILIC column stationary phase, which involves water layer in its phase forming a sequent that is linked with column surface as a pseudo-stationary phase, theoretically the stationary phase coated by zwitter ion that can minimising ion exchange interaction with the analyte, also chain length of the column is optimised so that positive and negative charges on the column surface interact and cancel each other, however ion exchange interaction also possible to occurs. It shows that the high concentration of organic modifier used with HILIC columns can lead to strong interaction between the stationary phase and polar compounds, therefore compounds will be retained, but increasing the aqueous content of eluents will decrease the interaction between stationary phase and polar compounds [100, 135] and cause early elution. The polar analytes interact with the water layer associated with the polar stationary phase. The strength of this interaction depends on the functional groups present in the structure of the analyte molecule and is relative to mobile phase. Using mobile phases with high organic solvent content a favours ionisation under ESI ionisation conditions as well as other benefits to reduce

the diffusion related mass transfer terms in the van Deemter equation , thus increasing the column efficiency[92, 100].

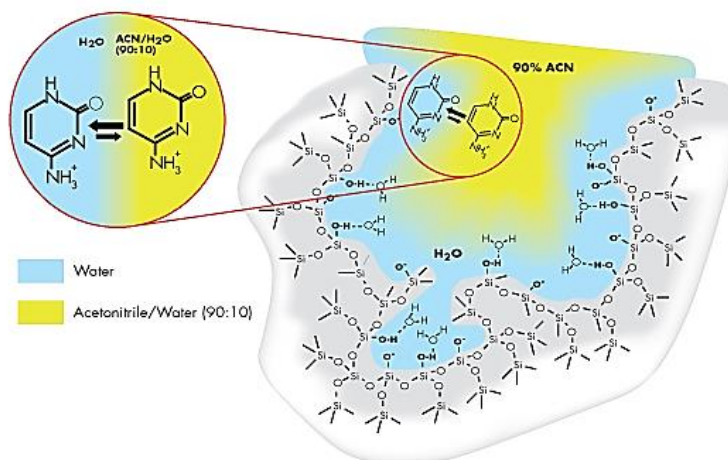


Figure 49. ZIC –HILIC column provides an ideal mechanism for the analysis of polar compounds [135]

3.2 Experimental

3.2.1 Chemicals and Materials

4-MMC (3a) and 4-TFMMC (3b) were synthesized in house in the SIBPS Laboratories at University of Strathclyde, UK. HPLC grade acetonitrile was obtained from Fisher Scientific, UK, and Formic acid (98%) was obtained from BDH, (DORSET, UK), water was obtained from in-house Milli-Q water purification station. Glycine-d₅ (98+ atom %D) was obtained from Sigma-Aldrich Co. Ltd, UK.

The round bottom flasks were rotated by attachment to a Buchi Rotavapor-R (Buchi Laboratory Technik AG.Switzerland).

All reagents for the synthesis were of commercial quality (obtained from Sigma–Aldrich, Gillingham, UK, Alfa-Aesar, Heysham, UK or Fisher Scientific, Loughborough, UK) and used without further purification. Solvents were dried, where necessary, using standard procedures. (±)-4'-Methyl-2-bromopropiophenone (2a); (±)-4'-(trifluoromethyl)-2-bromopropiophenone (2b) and (±)-4'-methylmethcathinone hydrochloride (3a, 4-MMC) were prepared using the methods

reported previously [63, 136]. ^1H and ^{13}C NMR spectra were acquired on both JEOL AS-400 (JEOL, Tokyo, Japan) and Bruker Avance 400 (Bruker, Karlsruhe, Germany) NMR spectrometers operating at a proton resonance frequency of 400 MHz. Infrared spectra were obtained in the range 4000-400 cm^{-1} using a ThermoScientific Nicolet iS10ATR-FTIR instrument (ThermoScientific, Rochester, USA). Mass spectra were recorded on a ThermoScientific LTQ Orbitrap mass spectrometer (ThermoScientific, Rochester, USA) using electrospray ionisation. Ultraviolet spectra were obtained using a Unicam 300 UV spectrophotometer (ThermoScientific, Rochester, USA). Thin-Layer Chromatography (TLC) was carried out on aluminium-backed SiO_2 plates (Merck, Darmstadt, Germany) and spots were visualised using ultra-violet light (254 nm). Microanalysis was carried out using a PerkinElmer 2400 Series II elemental analyser (PerkinElmer, San Jose, USA). Melting points were determined using differential scanning calorimetry (DSC; Netzsch STA449 C, Netzsch-Gerätebau, Wolverhampton, UK). Optical rotation values $[\alpha]_{\text{D}}^{22}$ ($10^{-1} \text{ deg cm}^2 \text{ g}^{-1}$) were performed on a Bellingham & Stanley ADP-220 polarimeter (Bellingham & Stanley, Tunbridge Wells, UK). Calculated Log P and pKa values were determined using Pipeline Pilot software, Vers. 7.5 (Accelrys, San Diego, USA).

For GC-MS experiment, all chemicals used were analytical grade, acetic anhydride and pyridine were purchased from Sigma- Aldrich, UK, methanol and formic acid were obtained from Fisher scientific, UK. Sample dryness was carried out by Techne system (Techne Sample Concentrator Model FSC400D) which was purchased from (Bibby Scientific Limited, Stone, Staffordshire, UK).

Solid phase extraction (SPE) cartridges, ISOLUTE, SCX-2, 200mg, 3mL (part no.: 532-0020-B) were purchased from Biotage (HERTFORD, UK).

3.2.2 Synthesis of (\pm)-4'-(trifluoromethyl) methcathinone hydrochloride (3b, 4-TFMMC) and (\pm)-4'-(methyl) methcathinone hydrochloride (3a, 4-MMC)

4-TFMMC (3b) compound was prepared using the previously reported method of synthesis 4-MMC (3a) [63] with the following modifications: To a suspension of

(±)-4'-trifluoromethyl-2-bromopropiophenone (2b, 5.60 g, 20 mmol) [136] and methylamine hydrochloride (1.35 g, 20 mmol) in dichloromethane (40 mL) was added triethylamine (5.58 mL, 40 mmol). The mixture was stirred at room temperature overnight and then acidified (pH ~ 1) with 6 M hydrochloric acid (50 mL). The aqueous layer was washed with dichloromethane (3 x 50 mL), basified (pH ~ 10) with 5 M sodium hydroxide (circa. 100 mL) and then re-extracted with dichloromethane (3 x 50 mL). The combined organic fractions were dried (MgSO₄) and concentrated *in vacuo* to give a viscous yellow oil. The oil was dissolved in ethanol (4 mL), treated with hydrogen chloride (4 M solution in 1, 4-dioxane, 6 mL) and stirred at room temperature for 1h. The mixture was diluted with diethyl ether (100 mL) and stirred until a pale yellow solid formed (circa. 30 min). The crude product was filtered, washed with diethyl ether and recrystallised from acetone to afford (±)-4'-(trifluoromethyl) methcathinone hydrochloride (1.66 g, 62.3 % from 2b)³ as a colourless powder. Mpt. (acetone) 226.78 °C; Rf [SiO₂, EtOAc:n-hexane (1:3)] = 0.10; [α]_D²² = 0 (c = 0.5 g 100 mL⁻¹ in MeOH); Found: C, 49.38; H, 4.91; N, 5.24. C₁₁H₁₃F₃ClNO requires C, 49.36; H, 4.90 and N, 5.23 %; UV (EtOH): λ max = 239.0 nm (A = 0.854, c = 2.0 x 10⁻³ g 100 mL⁻¹); IR (ATR-FTIR): 2701.1 (NH₂⁺), 1689.4 (C=O), 1328.5 cm⁻¹ (CF₃); ¹H NMR (400 MHz, 60 °C, *d*₆-DMSO) δ ¹H (ppm) = 9.73 (2H, br s, CH(NH₂⁺ CH₃)CH₃); 8.24 (2H, d, J = 8.0 Hz, AA'BB'), 7.95 (2H, d, J = 8.0 Hz, AA'BB'), 5.23 (1H, q, J = 7.2 Hz, CH(NH₂⁺ CH₃)CH₃), 2.62 (3H, s, CH(NH₂⁺ CH₃)CH₃) and 1.50 ppm (3H, d, J = 7.2 Hz, CH(NH₂⁺ CH₃)CH₃); ¹³C NMR (100 MHz, 60 °C, *d*₆-DMSO) δ ¹³C (ppm) = 195.6 (C=O, C1), 136.2 (ArC, C1'), 133.4 (q, J = 31.9 Hz, ArC, C4'), 129.4 (2 x ArCH, C2'/C6'), 125.7 (q, J = 3.5 Hz, 2 x ArCH, C3'/C5'), 123.3 (q, J = 271.4 Hz, ArCF₃, C7), 58.3 (CHCH₃, C2), 30.3 (NCH₃), and 14.6 ppm (CHCH₃, C3); ¹⁹F NMR (376 MHz, 60 °C, *d*₆-DMSO) δ ¹⁹F (ppm) = -61.92 (ArCF₃), LRMS (ESI+, 70 eV): m/z = 232 (41 %, [M+H]⁺), 214 (100), 199 (20), 173 (8) and 145 (16); HRMS (ESI+, 70 eV) calculated for [M+H] C₁₁H₁₃F₃NO: 232.0944, found: 232.0941.

³ All ¹H-NMR spectra were recorded at 60 °C to ensure that the signal for the protons situated on the chiral centre (C2, δ ¹H = circa. 5.2 ppm) which broadens and coalesces at ambient temperature was fully resolved. The chemical shifts of all signals were observed to be consistent at both ambient (25 °C) and high (60 °C) temperatures. For consistency the ¹³C-NMR spectra were obtained under analogous conditions. Samples were filtered prior to analysis.

3.2.3 Biotransformation of 4-MMC (3a), 4-TFMMC (3b) and 4-MEC (3c) in Sprague-Dawley rat hepatocytes

All animal procedures adhered to UK Home Office Guidelines and were carried out under Licence PPL/60/3685. Freshly isolated rat hepatocytes were prepared by collagenase perfusion of the livers of male Sprague-Dawley rats (body weight range: 200 – 250 g , University of Strathclyde) using a modification of the method by Moldeus *et al.*[137]. The cell viability was confirmed using a Trypan blue exclusion test. All incubations were carried out in triplicate. 4-MMC (3a, 100 μ M) or 4-TFMMC (3b, 100 μ M) and 4-MEC (3c, 100 μ M) were incubated in 50 mL round-bottomed flasks with a hepatocyte suspension (2×10^6 viable cells mL^{-1}) in Krebs-Henseleit (KH) buffer containing 12.5 mM HEPES (pH 7.4). The samples were incubated with constant rotation at 37°C under an atmosphere of oxygen: carbon dioxide (95:5) for 120 minutes. Control incubations of (i) rat hepatocytes (in the absence of 4-MMC (3a), 4-TFMMC (3b) or 4-MEC (3c)) and (ii) solutions of 4-MMC (3a), 4-TFMMC (3b) or 4-MEC (3c) dissolved in KH buffer (pH7.4) were also carried out (in triplicate) and analysed using an analogous protocol.

3.2.4 Instrumentation

3.2.4.1 *Exactive Orbitrap Mass spectrometer*

Sample can be introduced into the ESI source using various methods including direct injection or an Ultra- HPLC system. In this study samples were analysed using Exactive orbitrap spectrometer operated on –line with UltiMate[®] 3000 Standard LC systems (Dionex Corporation,USA) , combined with orbitrap mass spectrometer , which was obtained from (Thermofisher, Hemel Hempstead, UK) , equipped with an electrospray ionization (ESI) source system, and a data system (Xcalibur Version 2.0). The interface was adjusted to the following conditions: ion mode was positive and negative switch mode; spray voltage was 4.5 kV; capillary temperature was 250 °C; sheath gas flow rate (nitrogen) was 45; auxiliary gas flow rate (nitrogen) was 15 (units not specified by the manufacturer). The full-scan mass spectrum to obtain the protonated molecules $[\text{M} + \text{H}]^+$ of each metabolite was collected in the mass range from m/z 50 to 1200.

The LC conditions were as follows: The column fitted with ZIC-HILIC Column (5 μ m, 150 \times 4.6mm; SeQuant, Darmstadt, Germany) and guard column (HiChrom Limited, Reading, UK) were used for all analysis. The mobile phase consisted of Acetonitrile /water/formic acid, at a flow rate of 0.3 mL min⁻¹. The elution was carried out by binary gradient mode in which Solvent A was 0.1% v/v formic acid/water; and solvent B was 0.1% v/v formic acid/acetonitrile, with an injection volume of 10 μ L. The gradient programme was as follows: 20% A (0 min) to 50% A (at 12 min), to 50% A (at 26 min), to 80% A (at 28 min), to 80% A (at 36 min.), to 20% A (at 37 min) and finally to 20% A at 46 min.

Data processing was carried out using SIEVE Ver. 1.2.1 (ThermoFisher, Hemel Hempstead UK), ToxID Ver. 1.2.1 (ThermoFisher, Hemel Hempstead UK) and MetWorks Ver. 1.3 (ThermoFisher, Hemel Hempstead UK) software.

3.2.4.2 LTQ-Orbitrap Mass Spectrometer

LC-MS² spectra were obtained by using a Finnigan LTQ Orbitrap (Thermo-Fisher Corporation, Hemel Hempstead, UK) with the same source, control software and chromatographic conditions specified above. Furthermore, MS/MS spectra were obtained with positive ion ESI detection, the selected precursor ions were fragmented through CID with neutral gas (helium) molecules in the ion trap, which could provide characteristic fragment ions of each metabolite. The relative collision energy was set at 40 eV.

3.2.4.3 GC-MS instrument

All GC-MS analyses were carried out on a Thermo DSQ GC-MS system. An HP-5MS column was used (30m \times 0.25mm \times 0.25 μ m) with helium as the carrier gas. The Trace GC was coupled to the DSQ MS, which had electron ionisation energy of 70eV and operated in TIC mode with a scanning range of m/z 50-550. The MS source and quadrupole temperatures were 230 $^{\circ}$ C and 150 $^{\circ}$ C respectively. The parameters that were changed during development of the method were: injector

temperature, oven temperature programme, column flow rate, split ratio and injection volume.

The final optimised method has been titled 'mephedronesplit-40' and its conditions are as follows: GC oven temperature programme = 90°C 1minute, 8°C min⁻¹ 300°C 10minutes. Total run time = 37.25min. Injector temperature = 225°C. Split mode (1:40). Carrier gas = helium. Flow rate = 1mL min⁻¹. Injection volume = 3µL.

3.2.5 Solutions

3.2.5.1 Mobile phase preparation for HPLC

The mobile phase which consisted of (A) 0.1% formic acid in water and (B) 0.1% formic acid in acetonitrile was prepared as follows: mobile phase A was prepared by adding 1mL of formic acid to 1 litre of water, and mobile phase B by adding 1 mL of formic acid to 1 litre of acetonitrile.

3.2.5.2 Preparation of stock and sample for incubation

In this study, metabolism of 4-MMC.HCl (3a), 4-TFMMC.HCl (3b) and 4-MEC.HCl (3c) (MW of 4-MMC.HCl: 213.7; MW of 4-TFMMC.HCl: 267.7; MW of 4-MEC.HCl: 228.1) using rat hepatocytes was investigated by preparing a 100µM solution of 4-MMC (3a), 4-TFMMC (3b) and 4-MEC (3c) in 10 mL of incubation mixture in separate 10mL flasks and then incubating with the cells for 2 hours. To prepare 10 mM of stock solution of 4-MMC (3a), 21.37 mg of 4-MMC.HCl was transferred to a 10 mL volumetric flask, and dissolved in 10 mL of water. As a result, stock solutions of 10 mM of 4-MMC.HCl contained 2.13 mg mL⁻¹. At the same time, 26.8 mg of 4-TFMMC.HCl was transferred to a 10 mL volumetric flask, dissolved in water and made up to 10 mL to prepare 10 mM stock solution of 4-TFMMC (3b). 10mM sock solution of 4-MEC (3c) was prepared in a different experiment and it contained 2.28 mg mL⁻¹. From the stock solutions, working concentrations of each drug were prepared as follows: 0.1 mL of stock solution was transferred by

automatic pipette to a 50 mL round-bottomed flask, and made up to 10mL with hepatocyte suspension to produce a final solution of 100 μ M.

3.2.5.3 Sample preparation for LC/MS

Aliquots (0.5 mL) were removed, at 0, 30 and 120 minutes intervals, from the hepatocyte incubations with each drug, and quenched by addition of acetonitrile (1 mL). The samples were centrifuged (10^4 rpm, 15 minutes) and any remaining protein removed by further addition of acetonitrile (0.2 mL) and subsequent filtration through a Biotage Isolute® PPT+ protein precipitation plate (Biotage Limited, Sweden) [138].

The filtrate was collected and analyzed by either LC-MS or LC-MS². The efficiency of recovery from the hepatocyte matrix was determined to be 97.4 \pm 6.8% (for 4-MMC (**3a**), n = 5), 82.1 \pm 9.9% (for 4-TFMMC (**3b**), n = 5) and 88.9 \pm 7.0 % (for 4-MEC (**3c**), n=5) respectively.

3.2.6 Preparation of hepatocyte perfusion solutions

3.2.6.1 Materials

3.2.6.1.1 Stock Buffers

1. Hank's Buffer (10x)

Hank's buffer contains the materials (salts) below which were weighed accurately and transferred to a 1 litre volumetric flask, then dissolved with distilled water, made up to the mark and stored at 4°C until used.

NaCl	80.0 g
KCl	4.0 g
MgSO ₄ .7H ₂ O	2.0 g
Na ₂ HPO ₄ .2H ₂ O	0.6 g
KH ₂ PO ₄	0.6 g

2. Krebs-Henseleit Buffer (2x)

The chemicals listed below were measured accurately, and added in the order as shown below into a 2 litre brown bottle, then bubbled with 5% CO₂ and 95% O₂ for 10 minutes. At the same time, 9.71 g of NaHCO₃ was weighed accurately, transferred into a 1 litre volumetric flask, then dissolved with distilled water and made up to the mark. It was also bubbled for 10 minutes with 5% CO₂ and 95% O₂, after which it was added to the salts solution shown below and the final solution was stored at 4°C.

Distilled water	785mL
16.09% (w/v) NaCl	200mL
1.10% (w/v) KCl	150mL
0.22M KH ₂ PO ₄	25mL
2.74% (w/v) MgSO ₄ .7 H ₂ O	50mL
0.12 M CaCl ₂ .6 H ₂ O	100mL

3.2.6.1.2 Perfusion Buffers

1. Hank's I buffer

The chemicals below were weighed accurately and transferred into a 500 mL volumetric flask, 50 mL of Hank's (10x) buffer stock were added, the pH of this solution was adjusted to 7.4 using 5 M NaOH, and the volume was made up to 500 mL with distilled water.

NaHCO ₃	1.05g
N-[2-hydroxyethyl] piperazine-N'-[2-ethanesulphonic acid](Hepes)	1.50g
Bovine Serum Albumin (BSA) (fraction V)	3.33g
Ethylene glycol-bis-(β-amino-ethylether) N'N' tetraacetic acid (EGTA)	114mg

2. Hank's II buffer

The chemicals below were weighed accurately and transferred into a 500 mL volumetric flask, 50 mL of Hank's (x10) buffer stock were added, the pH of this solution was adjusted to 7.4 using 5 M NaOH, and the volume was made up to 500 mL with distilled water. This solution was also used as a Hank's Balanced Salt Solution (HBSS) for incubating the hepatocytes with the drug substrates.

NaHCO ₃	1.05g
N-[2-hydroxyethyl]piperazine-N'-[2-ethanesulphonic acid](Hepes)	1.50g
CaCl ₂ .2H ₂ O	147mg

3. Krebs-Albumin Buffer (KA)

The chemicals below were weighed accurately and transferred into a 500 mL volumetric flask, 250 mL of Krebs-Henseleit Buffer (2x) stock was added to the weighed substances, the pH of this solution was adjusted to 7.4 using 5 M NaOH, and made up to 500 mL with distilled water.

N-[2-hydroxyethyl]piperazine-N'-[2-ethanesulphonic acid](Hepes)	1.50g
BSA	5.0g

4. Krebs-Hepes Buffer (KH)

1.5 g of Hepes was weighed accurately and transferred into a 500 mL volumetric flask, 250 mL of Krebs-Henseleit Buffer (2x) stock was added to the weighed substance, the pH of this solution was adjusted to 7.4 using 5 M NaOH, and made up to 500 mL with distilled water.

All the perfusion buffers were filter sterilised using a 0.22 µm membrane vacuum filter /storage system (Corning[®] Vacuum Filter/Storage Bottle Systems), and then stored at 4°C.

3.2.6.1.3 Other Materials

1. A male Sprague-Dawley rats (200-250g).
2. The perfusion apparatus (described below).
3. Carbogen cylinder (95% O₂ / 5% CO₂).
4. Instruments and surgical supplies (such as small and large scissors, small and large forceps, cannula and artery clip to hold the cannula in place).
5. Sodium pentobarbital (60mg mL⁻¹) (stored at 4° C in the dark) [139].
6. Sodium Heparin (5000 IU mL⁻¹) (stored at 4° C) [139].

3.2.7 Isolation of hepatocytes

Hepatocytes were prepared by *in vitro* perfusion of the rat liver. During the perfusion period all the solutions were bubbled with 5% CO₂ and 95% O₂ at 37°C. The apparatus used in the perfusion technique consisted of a peristaltic pump, reservoir, a water bath, three 200 mL plastic beakers with lids and the apparatus was connected together by flexible polythene tubes (Figure 50).

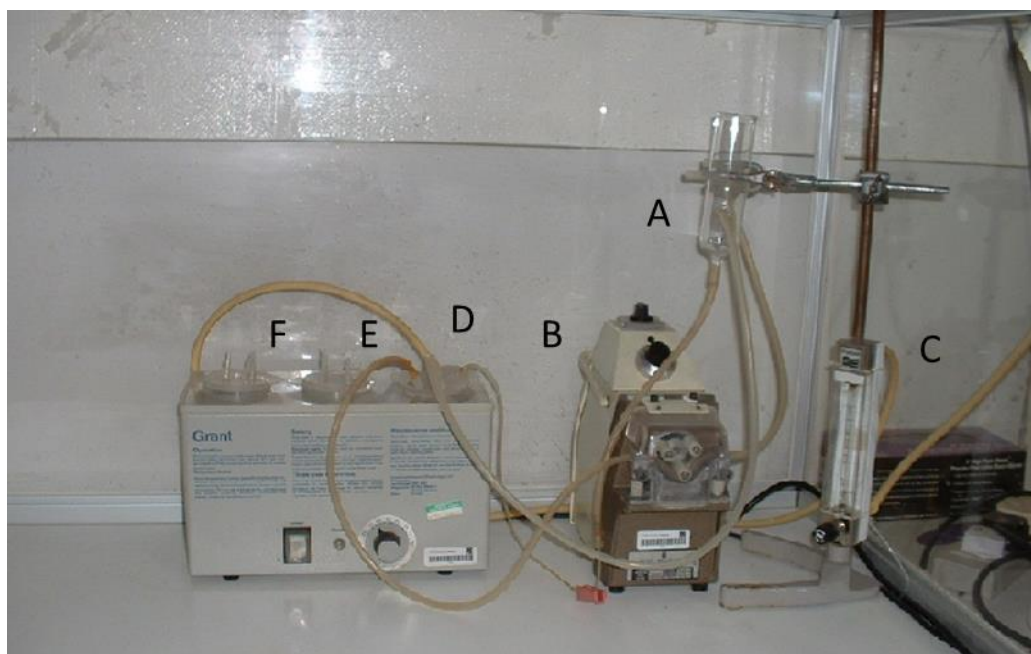


Figure 50. Apparatus used in perfusion technique: A reservoir; B pump; C gas regulator; D Ca²⁺ free perfusion solution; E collagenase solution; F BSA Containing dispersion buffer [140].

Male Sprague-Dawley rats (200-250g) were anaesthetised by an intraperitoneal injection of sodium pentobarbitone at a dose of 60 mg kg⁻¹ of body weight. The abdomen surface of the rat was wiped using ethanol 70 % (v/v), and the rat peritoneal cavity was opened a midtransversal incision (Figure 51).

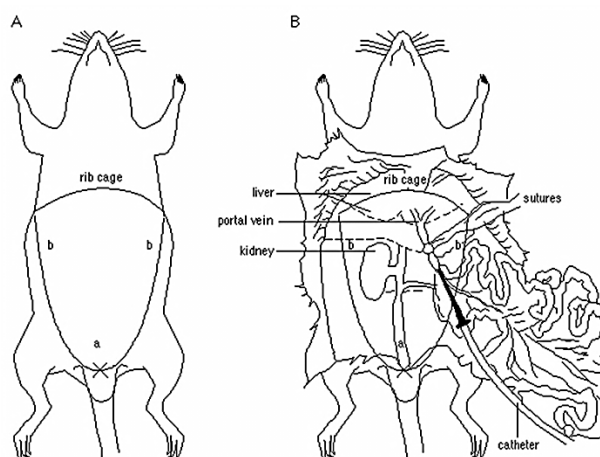


Figure 51. Diagram of surgical incisions to expose the abdominal cavity (A). Dissected view showing position of catheter in the portal vein (B) [77].

Heparin (0.1 mL, 1000 IU mL⁻¹) in sterile PBS was injected into the inferior vena cava. Then the hepatic portal vein was cannulated using stainless steel cannula with an internal diameter of 1.75 mm and exterior diameter of 2.5 mm. The cannula was held in place using a surgical bull dog clip. The perfusion was started using Hank's I and the liver was then dissected from the body, and then placed into a beaker containing Hank's I buffer, and recirculation occurred through the cannula. After circa 10 minutes in Hank's I, the liver was transferred into a beaker containing 150 mL of Hank's II buffer and 78 mg collagenase (250 Units mL⁻¹). Recirculation of the solution continued for circa 15-20 minutes or until the liver was soft and the cells in the liver sac had dissociated. The liver was then transferred into a Petri dish and the cannula was removed. The cells were then isolated using forceps into approximately 80 mL of Krebs Albumin buffer. The cell suspension was then filtered through a sterile cotton gauze mesh into a 100 mL bottle, to remove remaining connective tissue and clumps of cells. The cells were then allowed to settle under gravity. The supernatant was then removed while the precipitated cells were washed with 50 mL of Krebs Hepes buffer.

3.2.8 Viability and total live cell count

The cell viability and total live cell count was determined using a haemocytometer and the Trypan Blue Exclusion method. A 10 µL aliquot of the cell suspension was added to 990 µL of Trypan Blue (0.1 % w/v in PBS), the resultant was loaded onto the counting chambers of the haemocytometer on both side, and then examined under a Nikon Diaphot-TMD (Nippon Kogaku KK, Japan) light microscope, and cells in eighteen sections (volume=0.1 mm³) of haemocytometer chambers were counted. The percentage viability of cells was determined as following:

(No. of cell excluding Trypan Blue (Live)/total No. of cells) x100

The viable cell count was determined as following:

(No. of cells excluding Trypan Blue (Live)/18) x10⁴x100 (Dilution Factor)

Where 100 is initial dilution and 104 is the conversion factor to allow for the volume of the haemocytometer.

3.2.9 Incubation of 4-MMC (3a), 4-TFMMC (3b) and 4-MEC (3c) with freshly isolated rat hepatocytes

4-MMC (3a) , 4-TFMMC (3b) and 4-MEC (3c) (100 μM) separately were incubated with viable rat hepatocytes suspended with HBSS (2×10^6 cells mL^{-1}) for 2 hours at 37°C under an atmosphere of 95 % O_2 , and 5% CO_2 . Incubations were carried out in 50 mL round-bottomed flasks, using a rotary incubator in a water bath (incubation volume: 10 mL). The round bottom flasks were rotated (circa 30 rpm) by attachment to a Buchi Rotavapor-R (Buchi Laboratory Technik AG.Switzerland) using a four-way connector as shown in Figure 52.



Figure 52. Rotor incubator apparatus used for incubation of rat hepatocyte in suspension.

For all drugs incubations were carried out with three different hepatocyte preparations. The viability of hepatocyte cells was checked by the Trypan blue exclusion method. The reaction was started by the addition of 4-MMC (3a) or 4-TFMMC (3b) or 4-MEC (3c) (100 μ M) and then the reactions were terminated by the addition of acetonitrile (1mL). Control incubations with hepatocytes alone served as control and were incubated under identical conditions without added drugs, cell – free control flasks containing only drugs (each flask has 4-MMC (3a), 4-TFMMC (3b) and 4-MEC (3c) separately) with 10 mL of KH buffer were also incubated.

In these experiments five different incubation conditions were examined:

- Hepatocytes in KH buffer (Control).
- Hepatocytes + 4-MMC (3a) (100 μ M) in KH buffer (or 4-MEC (3c) (100 μ M)).
- Hepatocytes + 4-TFMMC (3b) (100 μ M) in KH buffer⁴.
- 4-MMC (3a) (100 μ M) in KH buffer (or 4-MEC (3c) (100 μ M)).
- 4-TFMMC (3b) (100 μ M) in KH buffer⁵.

After the 4-MMC (3a) and 4-TFMMC (3b) or 4-MEC (3c) are incubated in the presence of hepatocytes, five aliquots (0.5 mL) were taken from five incubation solutions (three incubation solutions in case of 4-MEC (3c)) at various incubation time point intervals (0, 30 and 120 minutes). These aliquots were placed into eppendorf tubes (1.5mL), the reaction was quenched by adding an aliquot of acetonitrile (1 mL). The samples of the incubated hepatocytes were stored at approximately - 80°C until analysis after extraction (Figure 53).

^{4,5} 4-TFMMC substrate was not incubated in the case of incubation experiments of 4-MEC were carried out.

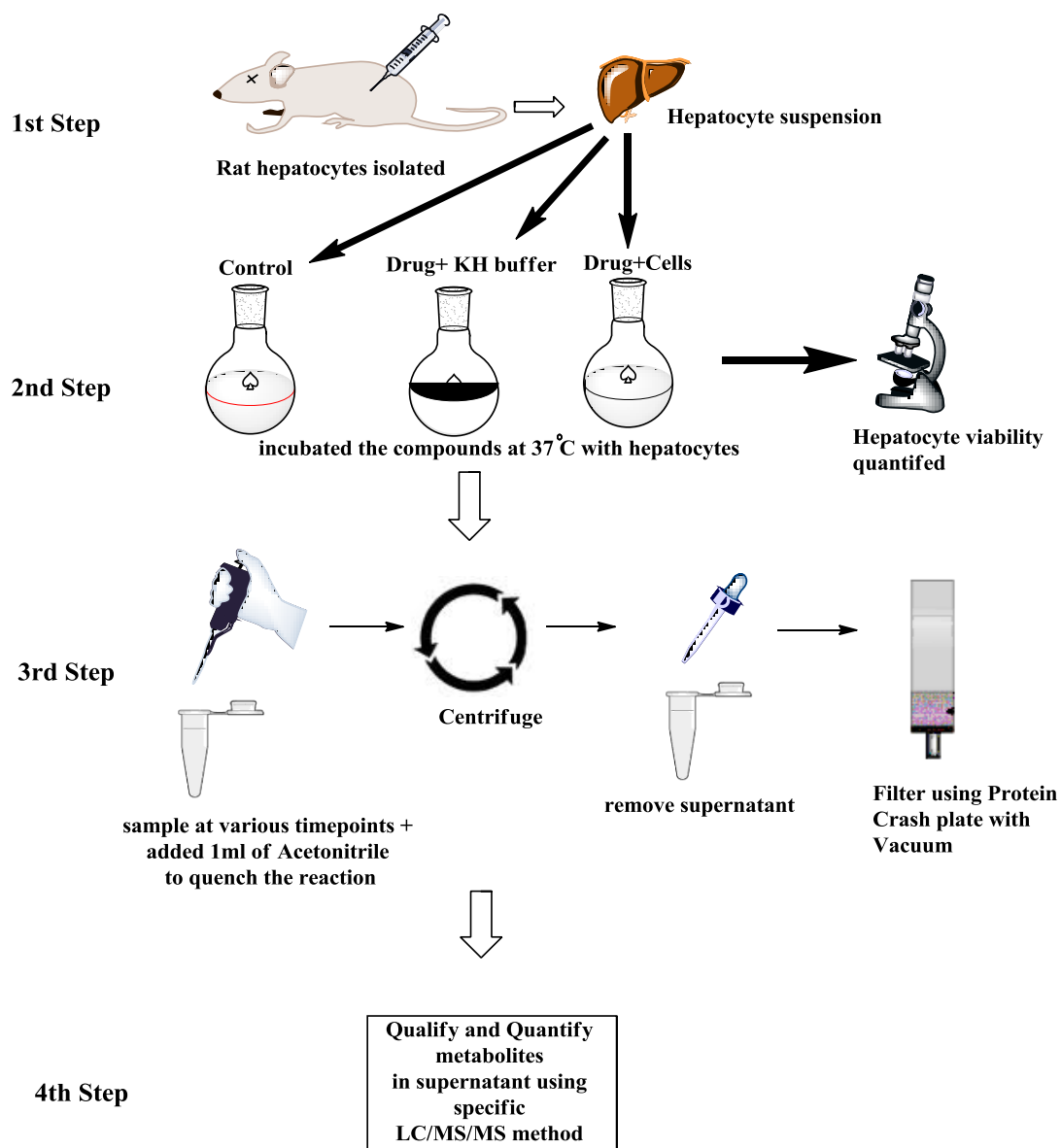


Figure 53. Schematic diagram illustrating isolation, incubation and extraction process of 4-MMC (3a), 4-TFMMC (3b) and 4-MEC (3c) incubated with rat hepatocytes.

3.2.10 Hepatocyte incubation samples extracted by using protein crash plates

The samples were thawed, and then centrifuged at high speed (10×10^3 rpm) using a mini centrifuge (Fisher Scientific Loughborough, England) for 15 minutes, the resultant supernatant was crashed using a protein crash method. The clear samples were collected and analysed by LC/MS and LC/MS², comparing the various incubation times to preincubation samples at time (Zero) and to the controls.

3.2.10.1 Protein Crash Method

The crash plates are attached to a vacuum manifold (Figure 54) and protein was crashed from the samples as following steps: The samples were thawed, then mixed with 0.2 mL acetonitrile and the two liquids are allowed to mix slowly while the protein precipitates. The acetonitrile was added first, and the reason for adding 0.2 mL of acetonitrile rather than using standard procedure (a 1: 4 ratio of sample + acetonitrile) was that the reaction of the incubation samples had already been stopped, and most of protein precipitated by the 1 mL amount of acetonitrile at the end of the incubation.

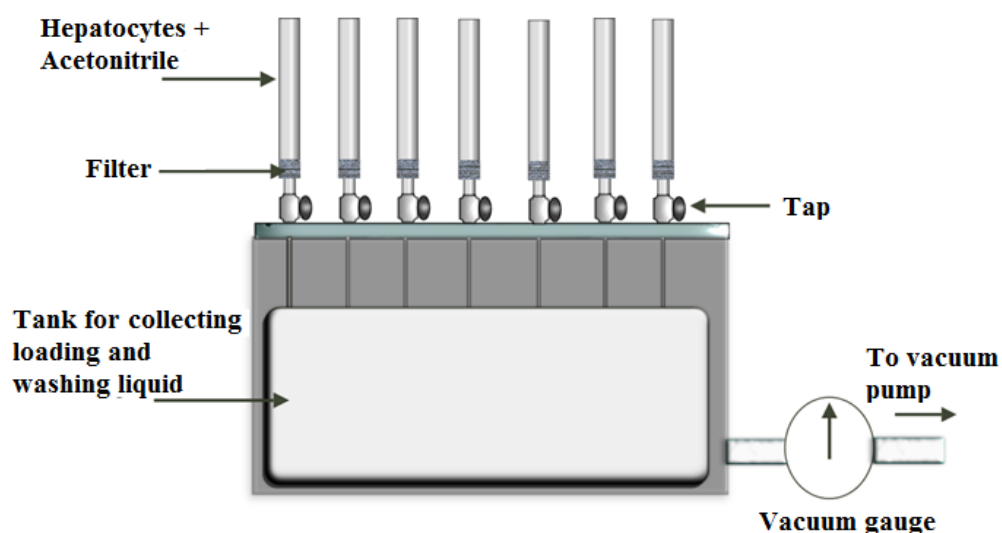


Figure 54 : Vacuum manifold which was used with the protein crash filter.

3.2.11 Effects of 4-MMC and 4-TFMCC on Hepatocyte Viability

In order to examine the effects of 4-MMC (3a) and 4-TFMCC (3b) on hepatocytes, the viability of cells was calculated using Trypan blue exclusion. An aliquot (50 μ L) of the incubation cells were added to 50 μ L of Trypan Blue (0.1% w/v). The hepatocytes were loaded onto a haemocytometer, and then 50 cells were counted from the centre section. The results were expressed as the percentage of live cells of the total 50 cells. The drugs had a minimal effect on cell viability over the course of the experiment (Table 16).

Table 16. Viability of hepatocytes (n=3) during the 2 hour treatment period with 100 μ M 4-MMC (3a) and 4-TFMCC (3b).

Time (minutes)	Viability (%) (\pm SD)		
	Control	4-MMC	4-TFMCC
0	82.7% (\pm 2.3)	80% (\pm 2)	79.3% (\pm 4.2)
30	78.7% (\pm 4.2)	72.7% (\pm 7.6)	76% (\pm 11.13)
120	72.7% (\pm 6.1)	70% (\pm 5.3)	74% (\pm 3.5)

3.2.12 Effects of 4-MEC on Hepatocyte Viability

The effect of 4-MEC (3c) on hepatocyte viability was carried out in a separate experiment using the same procedure as described above. Table 17 shows the minimal effect on hepatocytes during the incubation period with 100 μ M 4-MEC.

Table 17. Viability of hepatocytes (n=3) during the 2 hour treatment period with 100 μ M 4-MEC (3c).

Time (minutes)	Viability (%) (\pm SD)	
	Control	4-MEC
0	73.3% (\pm 6.1)	74.7% (\pm 11.5)
30	73.3% (\pm 10.1)	74.0 % (\pm 10.6)
120	70.0% (\pm 13.9)	64.7% (\pm 9.5)

3.2.13 GC-MS Procedure for Identification of 4-MMC (3a) Metabolites

Hepatocytes were incubated as described in section 3.2.8 and the sample preparation for GC-MS was carried out as following:

- Two tubes of 4mL of hepatocyte suspension after incubation with drug for 0, 30 and 120 minutes were thawed. Controls at the same time points were also taken.
- The samples were centrifuged at (10×10^3 rpm) for 20 minutes.
- The supernatant was transferred to a 4 mL vial and then blown to dryness under a stream of Nitrogen. The residues of samples were re-dissolved in 3mL of 0.1% Formic Acid, and filtered if necessary using a syringe filter.
- SCX column (3mL) was washed with 6 mL of 0.1% formic acid and then the sample loaded on slowly.
- The column was washed with 5 ml of methanol, and the washings discarded so all the drug related material will be retained. The sample was eluted with 5 mL of 1 M ammonia in methanol. Collected samples were immediately blown to dryness under a stream of Nitrogen and then dissolved each sample again in 200 μ L of 1:1; acetic anhydride: pyridine. The vials were then closed tightly and heated at 60 °C for 30 minutes.
- The mixture was blown to dryness under Nitrogen, and then the residue dissolved in 100 μ L of ethyl acetate.
- 3 μ L of final solution was injected into the GC-MS.

3.3 Results and Discussion

3.3.1 Synthesis of 4-MMC (3a), 4-TFMMC (3b)

Samples of (\pm)-4'-methylmethcathinone (3a, 4-MMC, (\pm)-mephedrone) and (\pm)-4'-(trifluoromethyl) methcathinone (3b, 4-TFMMC) were prepared as their corresponding hydrochloride salts. The synthesis of the two racemic target compounds was achieved using a modification of the previously reported method [63] from (\pm)-4'-methyl-2-bromopropiophenone (2a) and (\pm)-4'-(trifluoromethyl)-2-bromopropiophenone (2b) in 51.2% and 62.3% overall yield, respectively as stable, colourless to off-white powders after recrystallization from acetone (Scheme7). Although (\pm)-4'-(trifluoromethyl) methcathinone (3b, 4-TFMMC) has been recently disclosed by Cozzi *et al.* the analytical data reported is inconsistent with the proposed structure [133]. To ensure the authenticity of the material utilised in this study the synthesised sample of (3b, 4-TFMMC) was fully characterised (See Appendix 4) and the purity of both samples was confirmed by elemental analysis (>99.5% in both cases).

3.3.2 Using Multiple Mass Defect Filters for metabolite identification

In this study, Multiple Mass defect filtering (MMDF) in MetWorks software can capture Phase I metabolites from hydroxylation, *N*-dealkylation and oxidation by entering the elemental formula of the analyte in the analyte(s) dialog box. It can identify the metabolites even if the metabolism process has mass defects significantly different from the parent drug. Phase II metabolites can also be identified by applying the elemental formula of Phase I metabolites obtained as above described into the same dialog box.

Figure 55 shows the base peak chromatograms obtained from MetWorks following incubation of 4-MMC (3a) with hepatocytes and the output once MMDF has been applied to original data. The top chromatogram area (A) displays the base peak chromatogram of the raw data of 4-MMC (3a). Metworks is applied and each mass defect filter for a particular metabolite is added to the data in bottom chromatogram (B) automatically; all the data outside specified filters will be removed. The chromatogram result is accurate because it is based on exact mass and mass

deficiencies. Figures 55, 56 and 57 show an example of how the full chromatograms are changed after the single MMDF. The original chromatogram is on the top, and there are still a lot of background peaks in chromatogram (A). After MMDFs were applied, only peaks of Phase I metabolites remain in the chromatogram while almost of all the background peaks are gone. Metabolites at very low abundances can be easily identified.

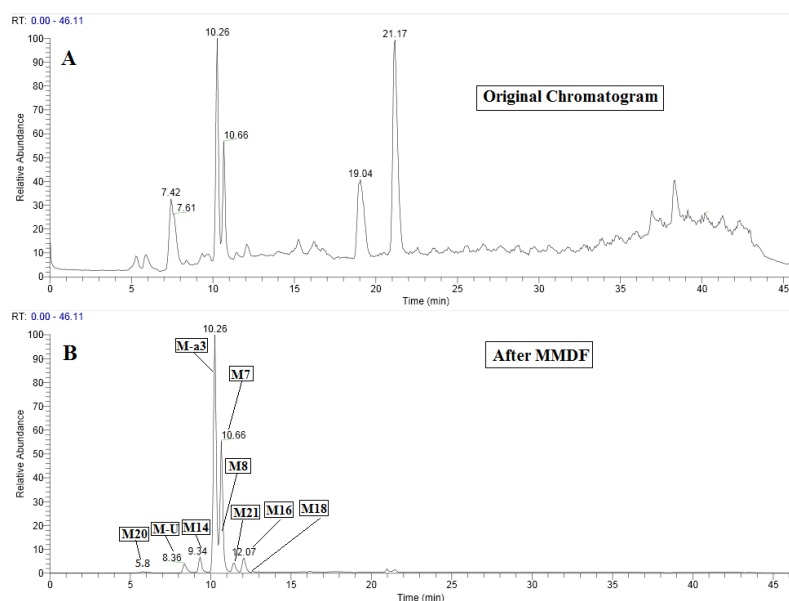


Figure 55. Application of Network software for the identification of 4-MMC (3a) metabolites in rat Hepatocytes; Base Peak chromatograms before and after MMDF processing.

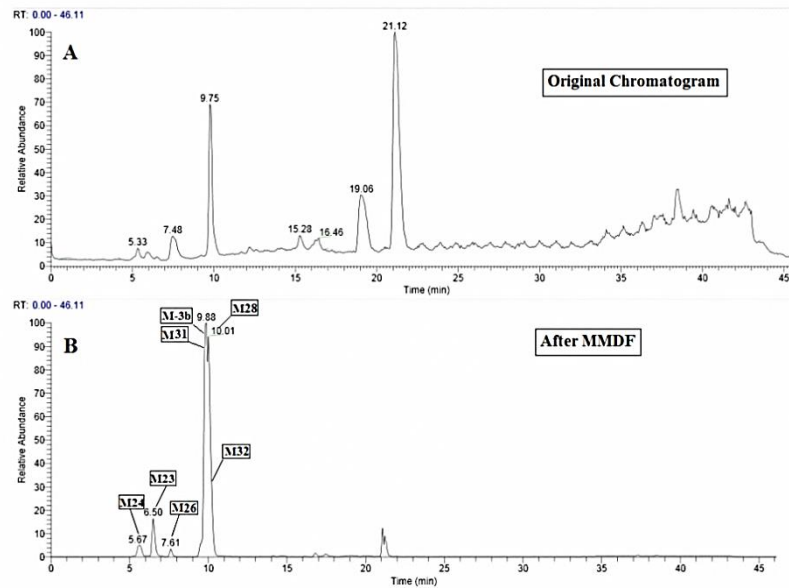


Figure 56. Application of Metwork software for the identification of 4-TFMMC(3b) metabolites in rat Hepatocytes; Base Peak chromatograms before and after MMDF processing.

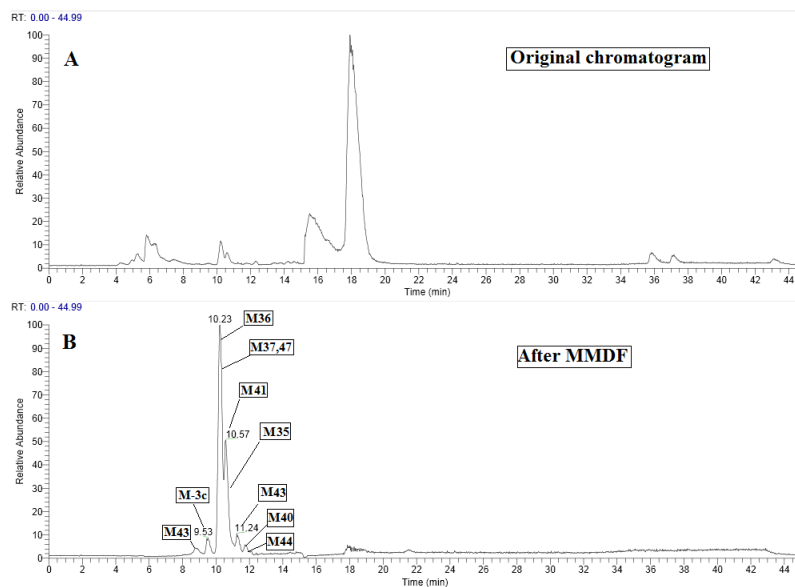


Figure 57. Application of Metwork software for the identification of 4-MEC (3c) metabolites in rat Hepatocytes; Base Peak chromatograms before and after MMDF processing.

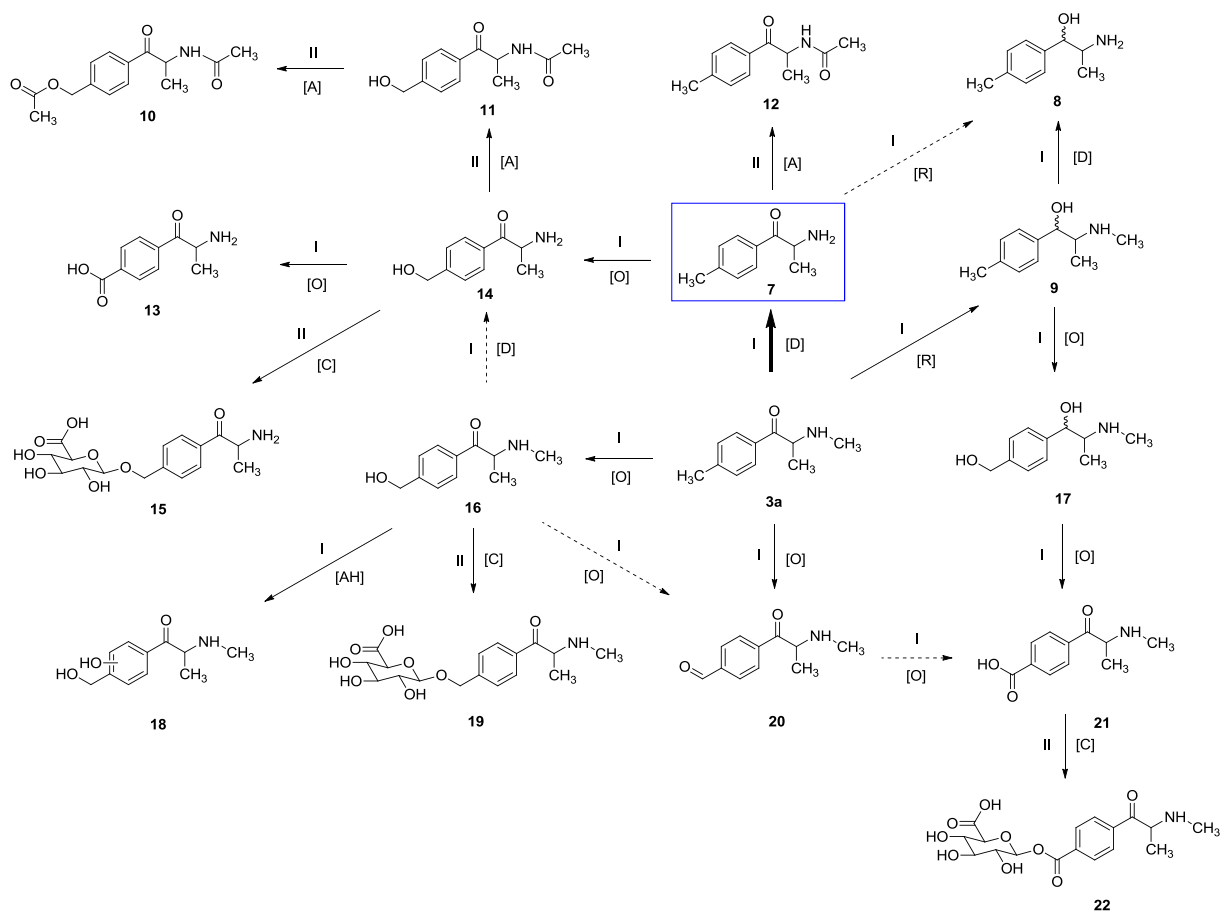
3.3.3 Biotransformation of 4-MMC (3a) in Sprague-Dawley rat hepatocytes

The zwitterionic ZIC[®]-HILIC stationary phase was found to be satisfactory for achieving the separation of 4-MMC (3a) and its metabolites since a standard C₁₈ stationary phase was unable to produce a strong retention of highly polar glucuronidated or oxidised metabolites such as (19) and (21) respectively. It was found that rat hepatocytes catalysed both Phase I and Phase II metabolism of 4-MMC (3a) and overall seventeen metabolites were putatively identified (Table 18, Scheme 8).

The positive ion LC/MS spectrum of mephedrone (3a,4-MMC) showed a protonated molecule $[M + H]^+$ at m/z 249.123 and the formula structure predicted using Xcaliber indicated that it could be the glycine conjugated metabolite (20, m/z =192.10) of 4-MMC(3a) with a chemical shift at m/z =57 Da. However it was difficult to understand at which functional group the conjugation had occurred, because the (-COOH) which is a specific reaction site for glycine conjugation was absent in molecules of this metabolite (see Table 7). Thus same procedure which has been reported in this chapter was used to confirm this metabolite by spiking a 0.1 mL of glycine-d₅ into the incubation suspension (0.1 mL of 2 mg mL⁻¹ of glycine-d₅ stock solution) at the beginning of incubation time, which can react with metabolite (20) to form glycine-d₅ conjugate products. The effect of 4-MMC (3a) and glycine-d₅ on the hepatocytes had little effect on cell viability over the course of the experiment. The LCHRMS could not detect the glycine-d₅-conjugated metabolite of 4-MMC (3a) in treated hepatocyte samples with glycine-d₅, which provided strong evidence for the absence of this metabolic pathway in 4-MMC (3a).

Table 18. LC-MS Exactive Orbitrap data for metabolites of 4-MMC (3a) incubated with Sprague-Dawley rat liver hepatocytes (120 min). See Scheme 8 for proposed metabolite structures. Key: gluc = glucuronic acid-H₂O; U = unidentified metabolite (t_R = 8.3 min; m/z = 194.1175); ND = Not Detected. The mass errors of the detected metabolites were within ± 1-1.5 ppm of their assigned elemental composition.

Met.	t _R (min)	m/z	Formula (ppm)	Base Peak (MS ²)	Major Fragment Ions
12	5.7	206.1175	C ₁₂ H ₁₆ NO ₂ (-0.22)	164 (-CH ₂ CO)	147 (48)
10	5.7	264.1227	C ₁₄ H ₁₈ NO ₄ (-1.2)	126	146(50), 164(45)
20	5.8	192.1019	C ₁₁ H ₁₄ NO ₂ (0.44)	119	164 (33,-CO), 105 (35),
19	6.1	370.1495	C ₁₇ H ₂₄ NO ₈ (-0.44)	194 (-gluc)	
15	6.5	356.1337	C ₁₆ H ₂₂ NO ₈ (-0.74)	338 (-H ₂ O)	180 (34, -gluc).
U	8.3	194.1175	C ₁₁ H ₁₆ NO ₂ (-0.39)	ND	
14	9.3	180.1018	C ₁₀ H ₁₄ NO ₂ (0.05)	132 (-CH ₂ OH) (-NH ₃)	144 (44)
3a	10.3	178.1226	C ₁₁ H ₁₆ NO (-0.23)	160 (-H ₂ O)	
9	10.5	180.1383	C ₁₁ H ₁₈ NO (-0.36)	162 (-H ₂ O)	160 (30)
7	10.7	164.1069	C ₁₀ H ₁₄ NO (-0.61)	146 (-H ₂ O)	
11	10.9	222.1124	C ₁₂ H ₁₆ NO ₃ (-0.54)	160	186 (41)
8	11.0	166.1226	C ₁₀ H ₁₆ NO (0.18)	120	
21	11.5	208.0967	C ₁₁ H ₁₄ NO ₃ (-0.43)	146 (-COO)	190 (78), 172 (34)
16	12.1	194.1175	C ₁₁ H ₁₆ NO ₂ (-0.23)	146 (-H ₂ O) (-CH ₂ OH)	158 (53)
18	12.2	210.1124	C ₁₁ H ₁₆ NO ₃ (-0.43)	135	
13	12.3	194.0812	C ₁₀ H ₁₂ NO ₃ (0.41)	146	158 (52-2x H ₂ O)
17	13.0	196.1331	C ₁₁ H ₁₈ NO ₂ (-0.078)	178 (-H ₂ O)	139 (53)
22	15.0	384.1289	C ₁₇ H ₂₂ NO ₉ (-0.15)	172 (190-H ₂ O)	190 (37, -glucuronic acid)



Scheme 8. Proposed scheme for the Phase I and II metabolism of (±)-mephedrone (4-MMC, 3a) in Sprague-Dawley rat liver hepatocytes. Metabolite numbers correspond to the metabolite data presented in Table 18. Key: [A] = acetylation; [R] = reduction; [D] = demethylation; [O] = oxidation; [C] = conjugation; [AH] = aromatic hydroxylation (The blue rectangle highlights the most abundance metabolite).

The elemental compositions and retention times of the metabolites are listed in Table 18. The mass error (when compared to their theoretical masses) of all the detected metabolites was within ± 1 -1.5 ppm of their assigned elemental composition. MS² spectra were obtained for the more predominant metabolites and this added further support to some of the assigned identities (Table 18), however, useful fragments were not obtained for all the metabolites. The most abundant metabolites after 30 minutes incubation were normephedrone (7, $t_R = 10.7$ min; $m/z = 164.1069$), 4'-(hydroxymethyl) methcathinone (16, $t_R = 12.1$ min; $m/z = 194.1175$) and 4'-(carboxy) methcathinone (21, $t_R = 11.5$ min; $m/z = 208.0967$) (Scheme 8). With the exception of *p*-(hydroxymethyl)methcathinone (16), the levels of these metabolites increased further between 30 and 120 minutes of incubation with a corresponding decrease in the level of unmetabolised drug (3a, $t_R = 10.3$ min). In contrast, the level of (16) decreased between 30 and 120 minutes and there was a corresponding increase in the levels of its corresponding glucuronide (19, $t_R = 6.1$ min; $m/z = 370.1495$). The glucuronide (15, $t_R = 6.5$ min; $m/z = 356.1337$) of 4'-(hydroxymethyl) cathinone (14) could also be clearly observed after 120 minute of incubation. Glucuronide formation is an important step in the elimination of many important endogenous substances from the body. Meyer *et al.*[67] obtained indirect evidence, using GC-MS as the method of analysis, for the presence of glucuronide or sulfate metabolites of 4-MMC (3a) in urine following enzymatic hydrolysis which caused an increase in the levels of the hydroxylated metabolites. In addition to the major metabolites observed in the current work, there were many minor metabolites including an acylglucuronide (22, $t_R = 15.0$ min; $m/z = 384.1289$) and three acetyl metabolites (10, $t_R = 5.7$ min; $m/z = 264.1227$), (11, $t_R = 10.9$ min; $m/z = 222.1124$) and (12, $t_R = 5.7$ min; $m/z = 206.1175$). In some cases chromatographic information can be used to differentiate isomeric possibilities, thus metabolite (11) is believed to result from acetylation on the hydroxyl group rather than the nitrogen since it runs much later ($t_R = 10.9$ min) on the ZIC[®]-HILIC column than metabolites (10) and (12) ($t_R = 5.7$ min)[141]. The proposed biotransformation of 4-MMC (3a) observed following its incubation with Sprague-Dawley rat hepatocytes is summarised in Scheme 8. It should be noted that different combinations of the proposed routes may be possible and the scheme shown illustrates only one of these. The ultimate goal of

Phase II metabolism is to increase water solubility of the resulting metabolites, therefore it is unlikely that following conjugation (particularly with glucuronic acid) that a further step of Phase I metabolism would occur in this case. The dynamic range of the instrument was sufficient to show both major and minor metabolites, as illustrated in Figure 57, showing that the extracted ion traces of the minor metabolites (10, 11, 15, 19 and 22) of (\pm)-mephedrone (3a ,4-MMC) , which, although of low abundance, can be observed quite clearly.

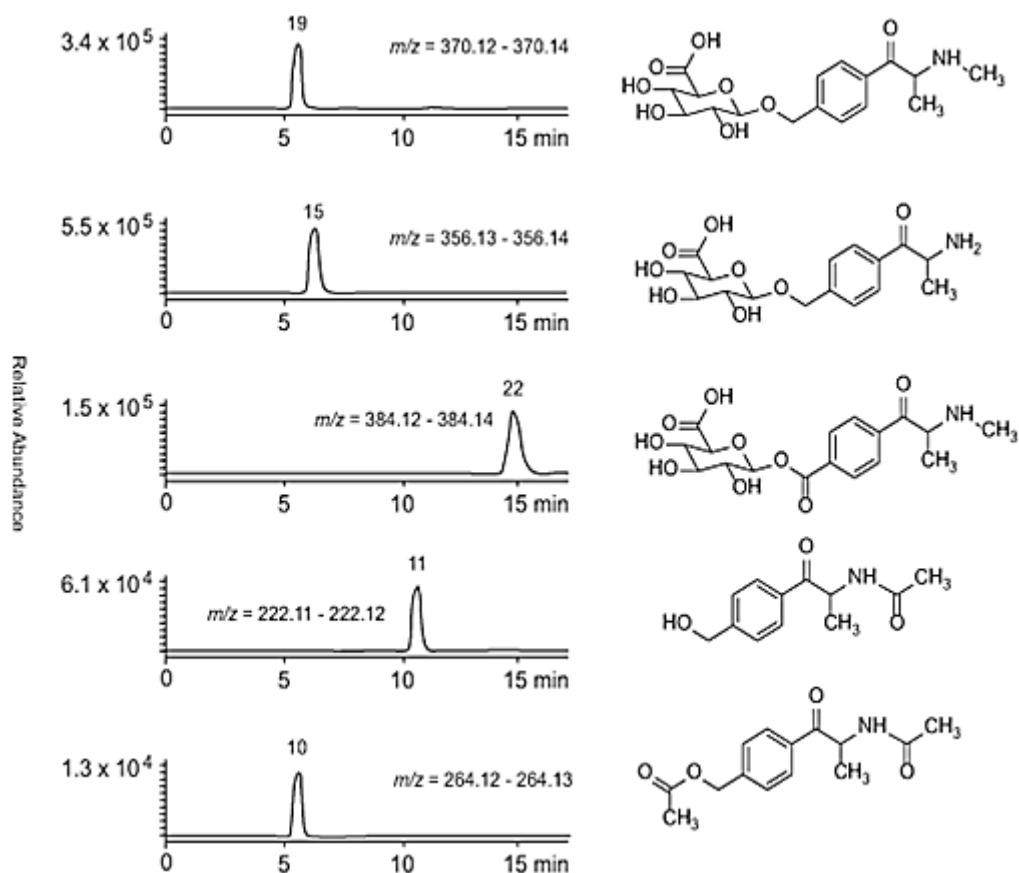


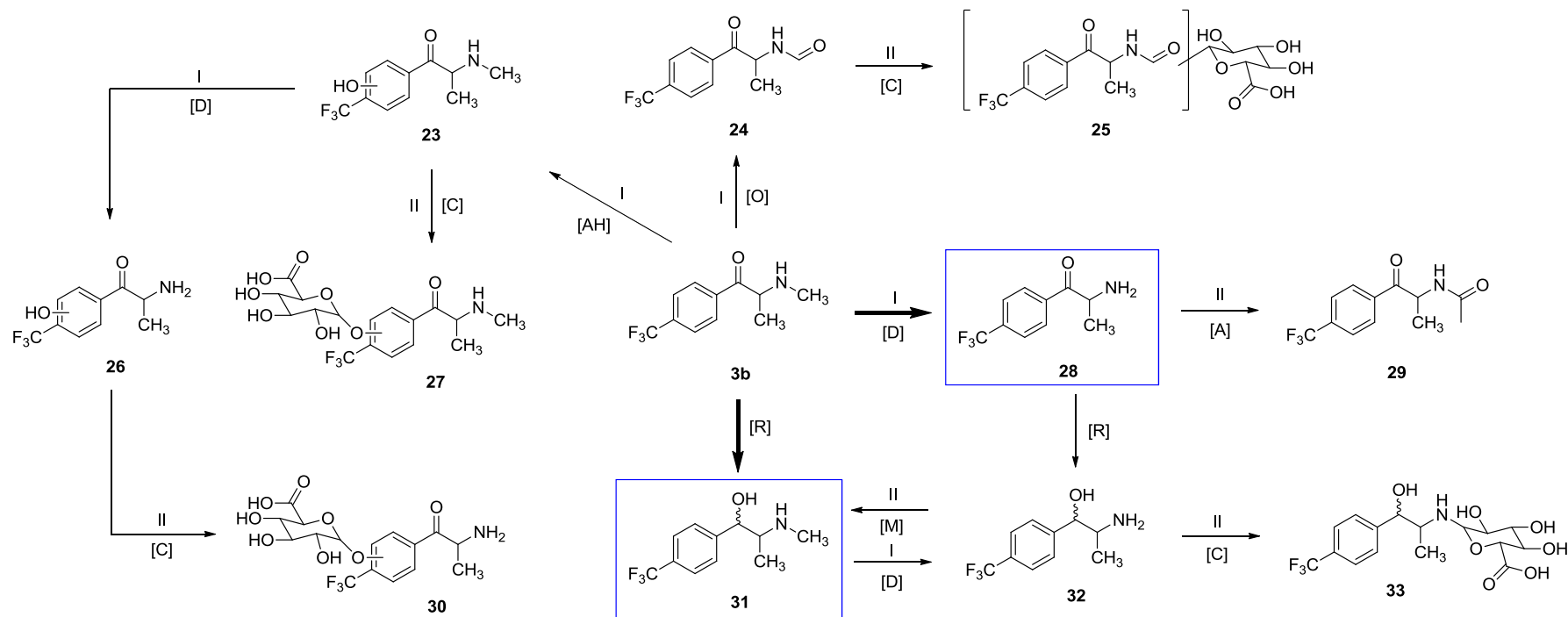
Figure 58. Extracted ion chromatograms of the minor metabolites (10, 11, 15, 19 and 22) of (\pm)-mephedrone (4-MMC, 3a) formed after incubation with Sprague-Dawley rat liver hepatocytes.

3.3.4 Biotransformation of 4-TFMMC (3b) in Sprague-Dawley rat hepatocytes

(±)-4'-(trifluoromethyl) methcathinone (3b, 4-TFMMC) was metabolised more slowly than (±)-4'-methylmethcathinone (3a, 4-MMC) and eleven metabolites were putatively identified (Table 19, Scheme 9). The mass error (when compared to their theoretical masses) of all the detected metabolites were again within ± 1-1.5 ppm of their assigned elemental composition.

Table 19. LC-MS Exactive Orbitrap data for metabolites of 4-TFMMC (3b) incubated with Sprague-Dawley rat liver hepatocytes (120 min). See Scheme 9 for proposed metabolite structures. Key: gluc = glucuronic acid-H₂O. The mass errors of the detected metabolites were within ± 1-1.5 ppm of their assigned elemental composition.

Met	t _R (min)	m/z	Formula (ppm)	Base Peak (MS ²)	Major Fragment Ions
29	5.5	260.0891	C ₁₂ H ₁₃ F ₃ NO ₂ (-0.69)	218 (-CH ₂ CO)	173 (47)
24	5.6	246.0735	C ₁₁ H ₁₁ F ₃ NO ₂ (-0.61)	173 (-C ₃ H ₇ NO)	159 (74)
27	5.9	424.1212	C ₁₇ H ₂₁ F ₃ NO ₈ (-0.44)	248 (-gluc)	
30	6.1	410.1055	C ₁₆ H ₁₉ F ₃ NO ₈ (-0.48)	234 (-gluc)	270 (73), 216 (80)
25	6.1	422.1055	C ₁₇ H ₁₉ F ₃ NO ₈ (-0.61)	228 (-glucuronic acid)	159 (39)
23	6.6	248.0890	C ₁₁ H ₁₃ F ₃ NO ₂ (-1.0)	173 (-C ₃ H ₇ NO-H ₂)	
26	7.7	234.0735	C ₁₀ H ₁₁ F ₃ NO ₂ (-0.72)	216 (-H ₂ O)	188(14)
3b	9.8	232.0941	C ₁₁ H ₁₃ F ₃ NO (-1.2)	201 (-NH ₂ CH ₃)	194 (97), 145 (65)
31	10.0	234.1098	C ₁₁ H ₁₅ F ₃ NO (-1.1)	201 (-H ₂ O) (-CH ₃)	214 (47), 196 (54).
28	10.1	218.0786	C ₁₀ H ₁₁ F ₃ NO (-0.30)	173 (-C ₂ H ₇ N)	
32	10.2	220.0943	C ₁₀ H ₁₃ F ₃ NO (-0.48)	175 (-C ₂ H ₇ N)	173 (65)
33	11.3	396.1263	C ₁₆ H ₂₁ F ₃ NO ₇ (-0.54)	202 (-glucuronic acid)	360 (66), 220 (60)



Scheme 9. Proposed scheme for the Phase I and II metabolism of (±)-4'-(trifluoromethyl) methcathinone (4-TFMMC, 3b) in Sprague-Dawley rat liver hepatocytes. Metabolite numbers correspond to the metabolite data presented in Table 19. Key: [A] = acetylation; [R] = reduction; [D] = demethylation; [O] = oxidation; [C] = conjugation; [AH] = aromatic hydroxylation; [M] = methylation (The blue rectangle highlights the most abundance metabolites).

The major metabolites were 4'-(trifluoromethyl) cathinone (28, $t_R = 10.1$ min; $m/z = 218.0786$), (\pm)-4'-(trifluoromethyl) ephedrine (31, $t_R = 10.0$ min; $m/z = 234.109$) and (\pm)-4'-(trifluoromethyl) norephedrine (32, $t_R = 10.2$ min; $m/z = 220.0943$). The modification of the 4'-methyl- to the corresponding isosteric 4'-trifluoromethyl-group in 4TFMMC (3b) blocks the possibility of formation of the 4'-hydroxymethyl- and 4'-carboxy-metabolites which are formed from 4-MMC (3a) and this may be responsible, to a large extent, for slowing down the overall metabolism. Hydroxylated metabolites were less abundant in 4-TFMMC (3b) metabolism but, despite this, small amounts of glucuronidation could be detected. The lower levels of hydroxylation and subsequent glucuronidation contribute to making the *in vitro* pharmacokinetics of the 4'-trifluoromethyl analogue of (\pm)-mephedrone in rat hepatocytes very different from those of the parent drug 4-MMC (3a). Again the extracted ion traces confirm the ability of the instrument to clearly detect the low abundance metabolites (27, 29, 30 and 33) of 4-TFMMC (3b) (Figure 58).

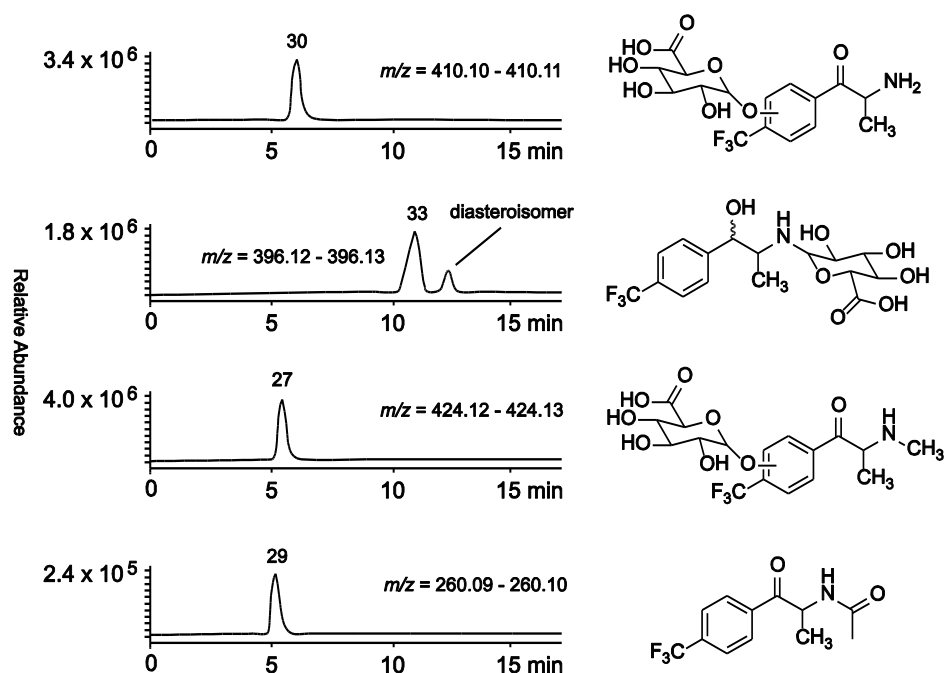


Figure 59. Extracted ion chromatograms of the minor metabolites (27, 29, 30 and 33) of (\pm)-4'-(trifluoromethyl) methcathinone (4-TFMMC, 3b) formed after incubation with Sprague-Dawley rat liver hepatocytes.

3.3.5 Biotransformation of 4-MEC (3c) in Sprague-Dawley rat hepatocytes

(±)-4'-methylethcathinone (3c,4-MEC) undergoes Phase I and II metabolism. Although, the metabolic pathways and patterns of 4-MEC (3c) observed in Sprague-Dawley rat liver hepatocytes were similar to that seen in 4-MMC (3a), it was metabolised significantly faster than (±)-4'-methylethcathinone (3a, 4-MMC). As same as the hepatocyte metabolism of 4-MMC (3a) and 4-TFMMC (3b), the hepatocyte metabolism of 4-MEC (3c) have not been previously reported. Based on present data, the elemental composition and retention times of the metabolites are listed in Table 20, and the proposed principal metabolic pathways for 4-MEC (3c) illustrated in Scheme 10. The structures of most 4-MEC metabolites were investigated using the LTQ Orbitrap mass spectrometer and the fragmentation pattern is illustrated in Table 20, and the proposed of some fragment structures are presented in appendix (1). In addition, Figure 60 shows the extracted ion chromatogram of 4-MEC (3c) control (3c, m/z 192.1383) (0 and 120 minute of incubation in cell-free KH buffer under the same conditions as used for incubations with hepatocytes). Figure 60 illustrates that 4-MEC (3c) has the same area at the beginning of the control incubation (0 minute) as at the end of the incubation time (120 minute). This is evidence that the drug is not affected by the environment during the incubation. The drug completely disappeared in the sample which was incubated with hepatocytes, and this must be due entirely to metabolism.

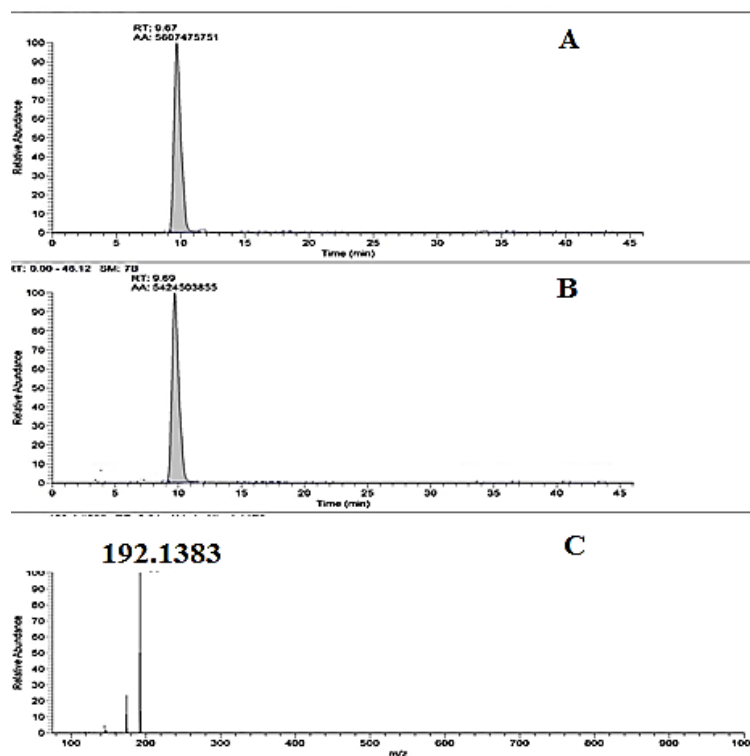


Figure 60. Representative chromatogram obtained using Exactive LC/MS with sample of 4-MEC(3c) incubated in KH buffer ,from (A) 0 min to (B) 120 min, and (c) MS spectrum of 4-MEC(3c).

Incubation of 4-MEC (3c) with fresh Sprague-Dawley rat liver hepatocytes showed that the drug was rapidly metabolised, and was almost completely metabolised after 120 minute of incubation time. The major metabolites were (37 and 47, $m/z = 222.1125$) which have the same accurate mass. Figure 61 shows that the major metabolite after 30 minutes incubation was detected as a peak which could be due to either the Phase I metabolite of 4-carboxy-MEC (37) of the Phase II metabolite of acetylated 4-MEC (47). Therefore, these two metabolites cannot be differentiated by mass spectrometry as they have the same mass and would need to be separated chromatographically. Sufficient separation of the metabolites from these peaks is not always possible, interference between these two metabolites is shown in Figure 61: the chromatogram (61- a) at 30 minute incubation time, and (61- b) at 120minute incubation time, and ESI spectra (61- c) of the two predicted metabolic pathways (37, 47) which have the same exact m/z 222.1125. Both of the metabolites are

identified by accurate mass which detected two oxygen atoms in the formula more than 4-MEC itself. Thus, it is assumed that two metabolic pathways are present, and the resulting metabolites occurred and were also identified in previous work of mephedrone [68]. Thus, the above pathways can be predicted to occur with 4-MEC (3c) because it has the same aromatic moiety as mephedrone, in addition, the proposed pathways show in scheme 10 for all metabolites of 4-MEC (3c) indicate that metabolites (37, $m/z=222.1125$) and (47, $m/z=222.1125$) should be consistent in these metabolism reactions, metabolite (37, $m/z=222.1125$) could be transformed to metabolite (44, $m/z=194.0813$) or metabolite (45, $m/z=398.1445$) which could not be formed without passing through metabolite (37, $m/z=222.1125$), also the scheme shows that metabolite (47, $m/z=222.1125$) which has the same m/z was transformed to metabolite (50, $m/z=264.1230$).

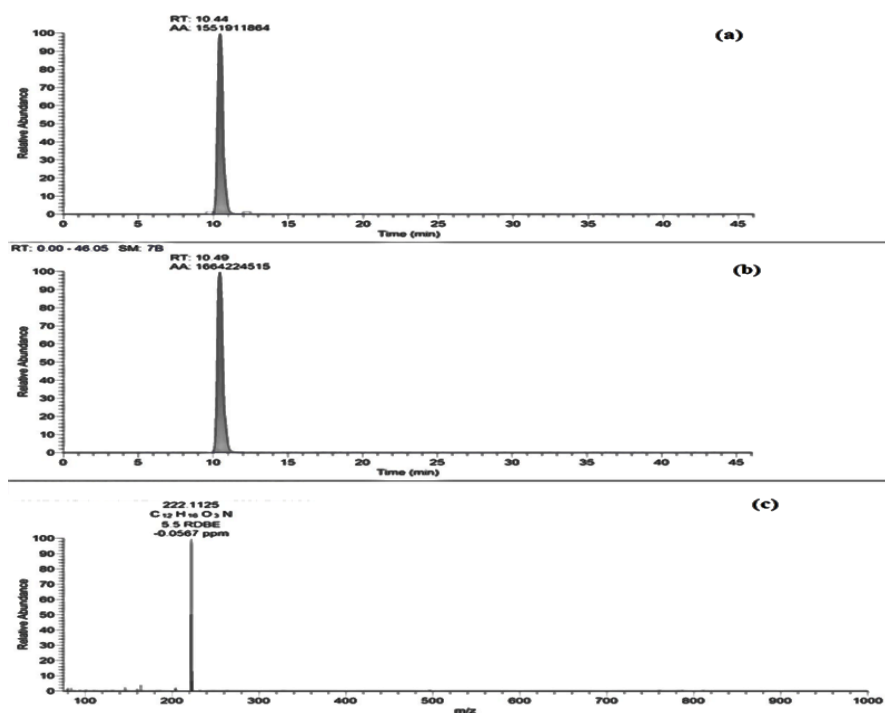


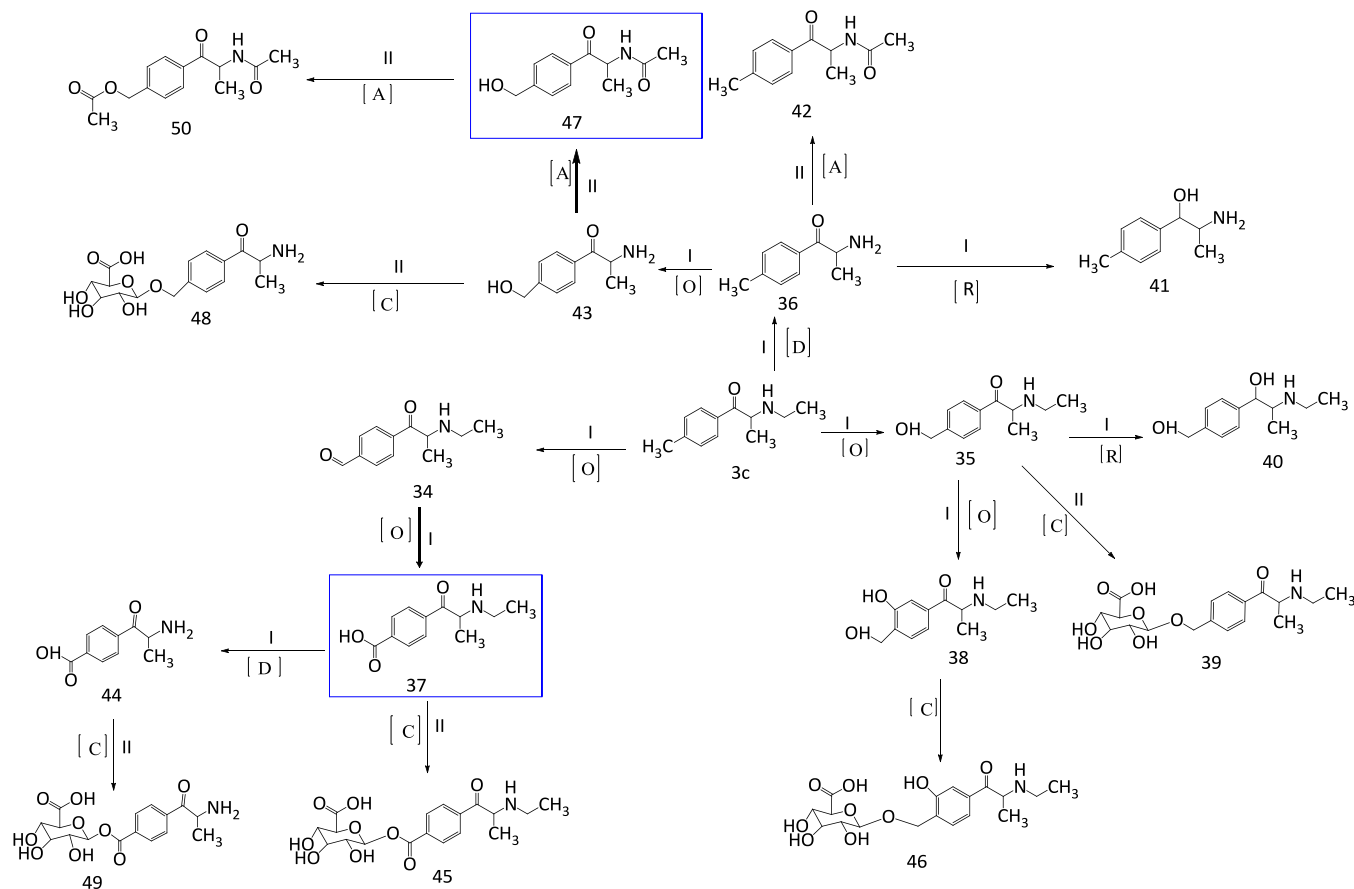
Figure 61. LC-MS analysis of the main 4-MEC metabolite; (a) selected ion chromatogram showing m/z 222.1125 at 30 min incubation, and (b) after two hours incubation period (c) positive product ion spectrum of m/z 222.1125.

Hydroxytolyl-MEC (35, $m/z= 208.1332$) was formed with high abundance after 30 minutes , but could not be detected clearly after 120 minutes because it transformed further to several Phase I metabolites including (38, $m/z= 224$;40, $m/z= 210.1489$) as well as to Phase II metabolites including glucuronide metabolites (39, $m/z = 384.1652$; 46, $m/z= 400.1601$).

In addition, desethyl-MEC (36, $m/z = 164.1070$) is decreased further between 30 and 120 minutes of incubation due to transformation through further metabolic pathways including an oxidation metabolite (43, $m/z = 180.1019$), a reduction metabolite (41, $m/z = 166.1227$), and *N*- acetylation metabolite (42, $m/z= 206.1176$).

Table 20 : LC-MS Exactive Orbitrap data for metabolites of 4-MEC (3c) incubated with Sprague-Dawley rat liver hepatocytes (120 min). See Scheme 10 for proposed metabolite structures. Key: gluc = glucuronic acid-H₂O. The mass errors of the detected metabolites were within $\pm 1-1.5$ ppm of their assigned elemental composition.

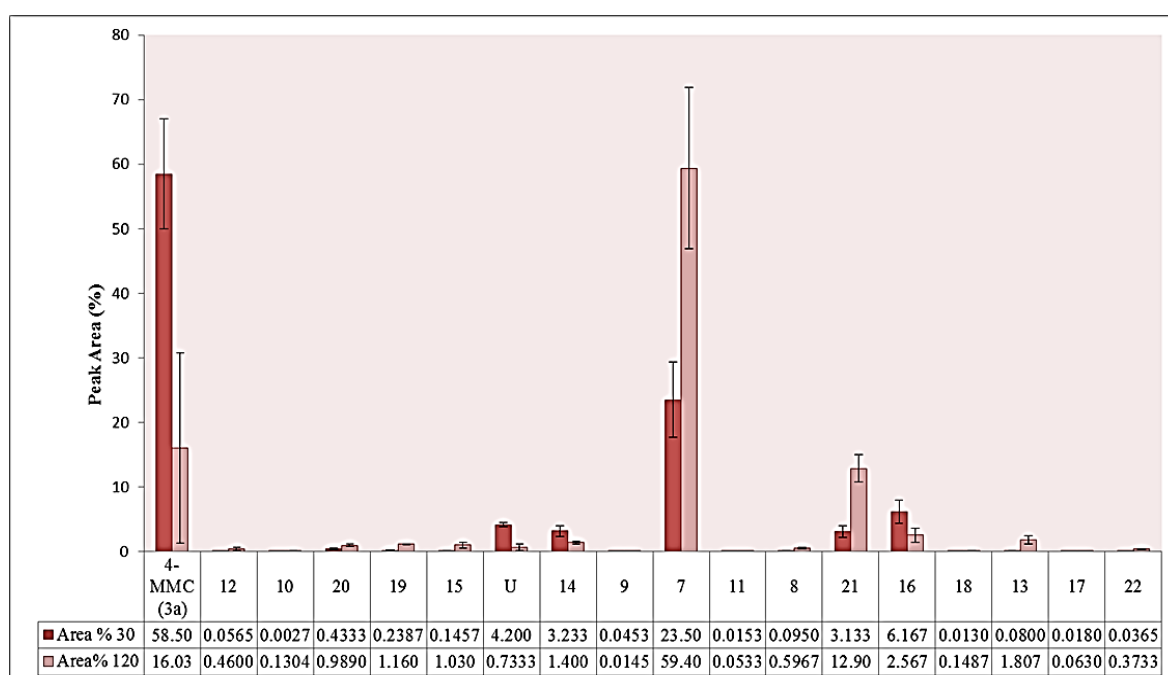
Met.	R _t (min)	m/z	Formula (ppm)	Base Peak(MS ²)	Major fragment Ions (%)
50	5.9	264.1230	C ₁₄ H ₁₈ NO ₄ (0.047)	246(-H ₂ O)	164(13),146(2.5)
34	6.2	206.1176	C ₁₂ H ₁₆ NO ₂ (0.29)	178	160(13),147(88), 117(23)
48	6.7	356.1339	C ₁₆ H ₂₂ NO ₈ (-0.32)	180 (-gluc)	162(46.6),144(10),119(12)
43	8.8	180.1019	C ₁₀ H ₁₄ NO ₂ (0.22)	144(-2H ₂ O)	147(13),132(4),134(47),162(3.7)
3c	9.6	192.1383	C ₁₂ H ₁₈ NO (-0.16)	174 (-H ₂ O)	147(4.6)
36	10.3	164.1070	C ₁₀ H ₁₄ NO (0.21)	119	131(14), 146(1.09)
37, 47	10.4	222.1125	C ₁₂ H ₁₆ NO ₃ (-0.057)	160	185(42),132(23),131(4)
41	10.6	166.1227	C ₁₀ H ₁₆ NO (0.24)	120	131(6)
35	10.8	208.1332	C ₁₂ H ₁₈ NO ₂ (-0.055)	160	133(6),172(50),190(13)
38	10.9	224.1281	C ₁₂ H ₁₈ NO ₃ (-0.30)	178	206(8)
42	10.9	206.1176	C ₁₂ H ₁₆ NO ₂ (0.44)		
40	11.5	210.1489	C ₁₂ H ₂₀ NO ₂ (0.19)	162	161(16),160(36),172(19.7),174(25)
44	11.8	194.0813	C ₁₀ H ₁₂ NO ₃ (0.67)	132	133(76), 158(95)
39	13.7	384.1652	C ₁₈ H ₂₆ NO ₈ (-0.26)	208 (-gluc)	190(3),172(25),160(17)
45	13.8	398.1445	C ₁₈ H ₂₄ NO ₉ (-0.14)	380 (-H ₂ O)	222(20),204(24),186(58),160(7)
46	14.4	400.1601	C ₁₈ H ₂₅ NO ₉ (-0.11)	364 (-H ₂ O)	224(18),206(96),188(20),133(10)
49	15.5	370.1132	C ₁₆ H ₁₉ NO ₉ (-0.098)	352(-H ₂ O)	194(13),176(11),158(19.6)



Scheme 10. Proposed scheme for the Phase I and II metabolism of (±)-4'-methyl-N-ethylcathinone (4-MEC, 3c) in Sprague-Dawley rat liver hepatocytes. Metabolite numbers correspond to the metabolite data presented in Table 21. Key: [A] = acetylation; [R] = reduction; [D] = desethylation; [O] = oxidation; [C] = conjugation; [AH] = aromatic hydroxylation (The blue rectangle highlights the most abundance metabolites).

3.3.6 Metabolic profiling of 4-MMC (3a) and 4-TFMMC (3b)

Drugs are eliminated from the body by excretion and by transformation to metabolites. These processes occur simultaneously, but the extent to which of these processes predominate varies from one drug to another. As the amount of drug in a system depends on both its rates of absorption and elimination the amount of a specific metabolite present also depends on its rate of formation and elimination. The metabolic profiles of (\pm)-4'-methylmethcathinone (4-MMC, 3a, pKa = 8.69; Log P = 1.96) and (\pm)-4'-(trifluoromethyl) methcathinone (4-TFMMC, 3b, pKa = 7.63; Log P = 2.47) were determined using three separate incubations of the drugs with isolated rat hepatocytes (Figures 62 and 63).

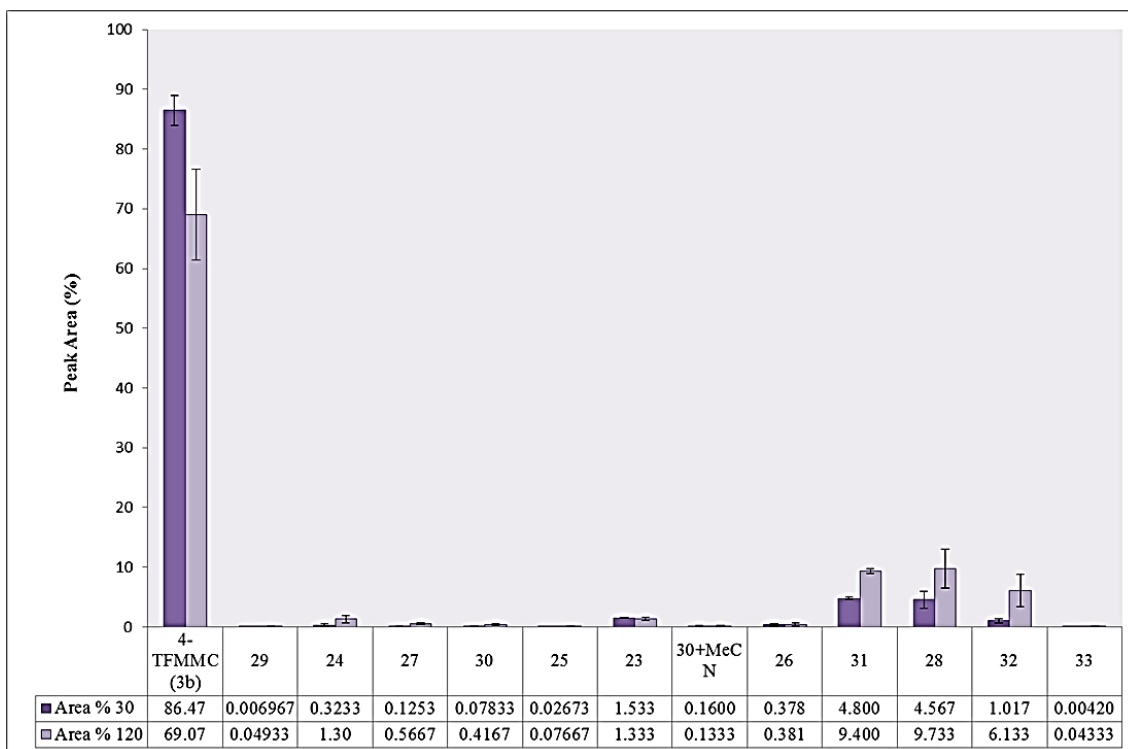


■ Amount of metabolites of 4-MMC (3a) formed after 30 min incubation.

■ Amount of metabolites of 4-MMC (3a) formed after 120 min incubation.

Peak Area (%) = (Peak area of metabolite / sum the Peak areas of all observed compounds) x 100.

Figure 62 : Relative amounts of metabolites of (\pm)-mephedrone (4-MMC, 3a) formed after incubation with Sprague-Dawley rat liver hepatocytes (n = 3); \pm SEM% area for 4-MMC (3a) = 58.5 \pm 8.6% (30 min) and 16 \pm 15% (120 min); U = unidentified metabolite (t_R = 8.3 min; m/z = 194.1175) (The number on the x-axis refer to the metabolite numbers on Table 18 and Scheme 8).



■ Amount of metabolites of 4-TFMMC (3b) formed after 30 min incubation.

■ Amount of metabolites of 4-TFMMC (3b) formed after 120 min incubation.

Peak Area (%) = (Peak area of metabolite / sum the Peak areas of all observed compounds) x 100.

Figure 63. Relative amounts of metabolites of (\pm)-4'-(trifluoromethyl) methcathinone (4-TFMMC, 3b) formed after incubation with Sprague-Dawley rat liver hepatocytes (n = 3); \pm SEM% area for 4-TFMMC (3b) = $86.5 \pm 2.5\%$ (30 min) and $69 \pm 7.6\%$ (120 min) (The number on the x-axis refer to the metabolite numbers on Table 19 and Scheme 9).

The relative levels of the detected metabolites of 4-MMC (3a) indicates that from the eleven metabolites identified in freshly isolated cells, only normephedrone (7, $m/z = 164.1069$) was formed in large amounts⁶. In addition, the formation of metabolite 4'-(carboxy) methcathinone (21, $m/z = 208.0967$) increased after two hours

⁶ The detector response(s) for the analytes (3a) and (3b) and their corresponding metabolites was assumed to be equivalent in this study.

incubation period by approximately 10%, however, the levels of 4'-(hydroxymethyl) methcathinone (16, $m/z = 194.1175$) and 4'-methylephedrine (9, $m/z = 180.1019$) began to decrease after 30 minutes (Figure 61). In the case of 4-TFMMC (3b) the histogram indicates that the major metabolites of (\pm)-4'-(trifluoromethyl) methcathinone were: 4'-(trifluoromethyl) cathinone (28, $m/z = 218.0786$), (\pm)-4'-(trifluoromethyl) ephedrine (31, $m/z = 234.109$) and (\pm)-4'-(trifluoromethyl) norephedrine (32, $m/z = 220.0943$) (Figure 62)⁷. The amount of (\pm)-4'-(trifluoromethyl) norephedrine (32) increased slowly throughout the two hour incubation period. The majority of Phase II metabolites identified in both 4-MMC (3a) and 4-TFMMC (3b) were found at very low levels at 30 minute as well as after 120 minute. A plot of the decrease in concentration (mean \log_{10} % peak area, $n = 3$) of (3a) and (3b) over the two hour incubation period was used to determine pharmacokinetic parameters for the two drugs (Figure 64).

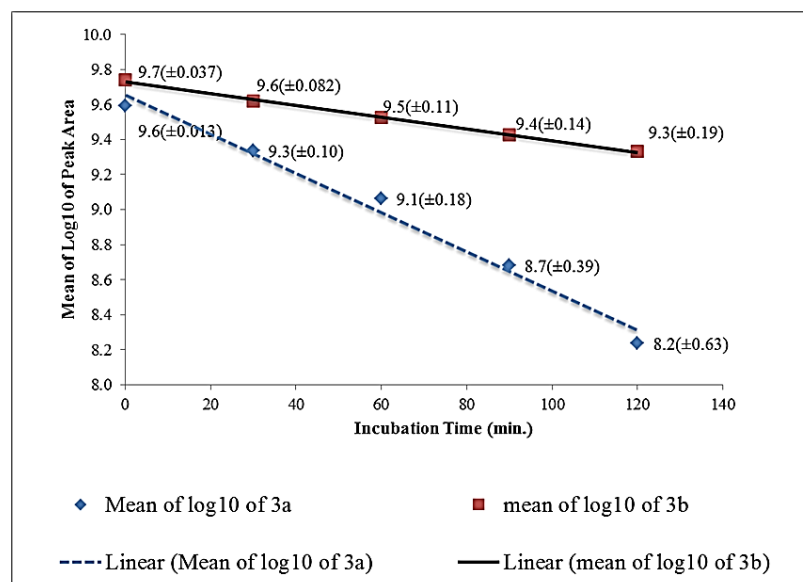


Figure 64. Plot of the rate of decrease (mean Log_{10} % peak area $\pm\text{SD}$) of (\pm)-mephedrone (4-MMC, 3a, ---, $y = -0.0112x + 9.6544$; $r^2 = 0.9848$) and (\pm)-4'-(trifluoromethyl) methcathinone (4-TFMMC, 3b, —, $y = -0.0034x + 9.7293$; $r^2 = 0.9974$) concentrations during incubation with Sprague-Dawley rat liver hepatocytes ($n = 3$).

⁷The detector response(s) for the analytes (3a) and (3b) and their corresponding metabolites was assumed to be equivalent in this study.

The present study was designed to estimate the half-lives of parent drugs based on plots of peak area rather than absolute concentrations, since the detector response of the analytes was assumed to be equivalent over the incubation period, and the decrease of concentration of 4-MMC (3a) and 4-TFMMC (3b) was determined by measuring their peak areas changes during the time.

The linear plot indicates, that for both 4-MMC (3a) and 4-TFMMC (3b), the rate of metabolism of both substances is directly proportional to the concentration of the drug within the system, and that a constant fraction of (\pm)-mephedrone (3a, 4-MMC) or (\pm)-4'-(trifluoromethyl) methcathinone (3b,4-TFMMC) is metabolised per unit time (i.e. first-order kinetics) [80].

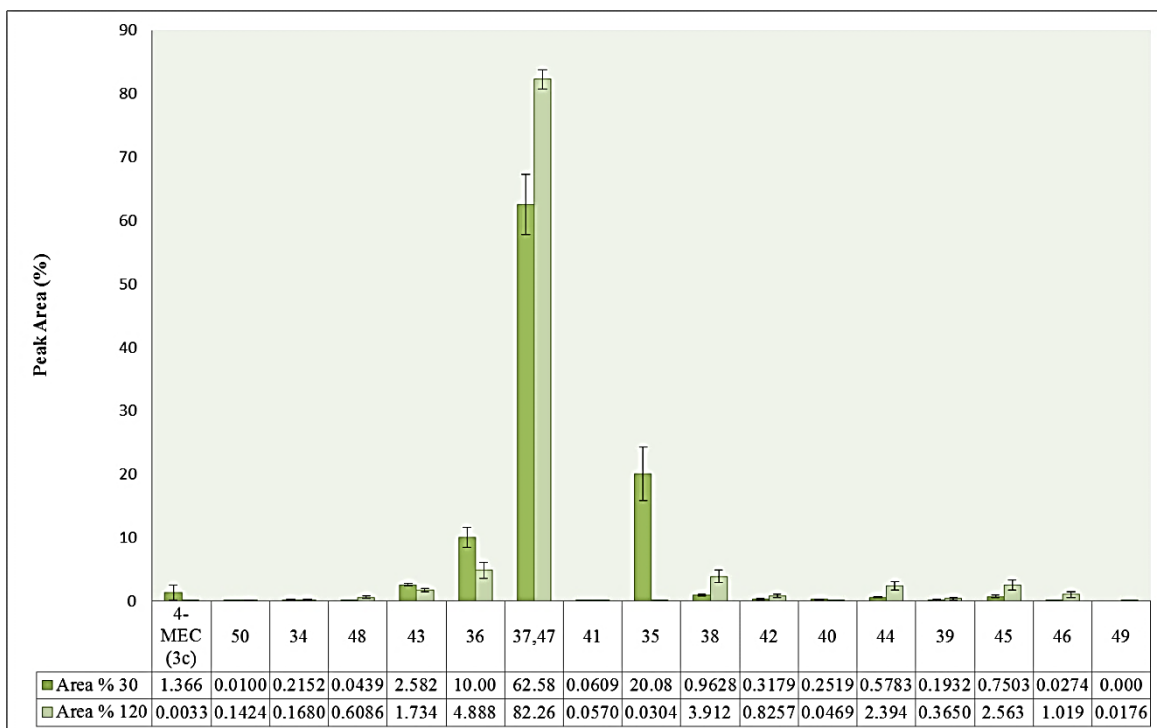
The metabolic rate constant (k_{met}), which is a composite of all the routes of metabolism, was estimated for each compound from the slope of the plots and determined to be: $1.12 \times 10^{-2} \text{ min}^{-1}$ (4-MMC, 3a, $n = 3$, ---) and $3.4 \times 10^{-3} \text{ min}^{-1}$ (4-TFMMC, 3b, $n = 3$, —) respectively (Figure 63).

The half-life ($t_{1/2}$) of the two illicit drugs in rat liver hepatocytes was calculated, using the expression: $t_{1/2} = 0.693/k_{met}$, to be: 61.9 minutes (3a, $n = 3$) and 203.8 minutes (3b, $n = 3$) respectively. The data indicate that (\pm)-4'-(trifluoromethyl) methcathinone (3b, 4-TFMMC) has a significantly longer (circa. 3x greater) half-life than (\pm)-4'-methylmethcathinone (3a, 4-MMC). It is apparent that substitution of the 4'-methyl- group (in 4-MMC (3a)) with a more lipophilic isosteric 4'-trifluoromethyl- moiety ($\text{Log P (3a)} = 1.96$ vs. $\text{Log P (3b)} = 2.47$) has a noteworthy effect on blocking the major metabolic pathway for these cathinone-derived “legal highs” and decreasing overall metabolic rate. This observation may have important implications in terms of the duration of the effects and the medical toxicology of related cathinone-derived substances within the body.

3.3.7 Metabolic profiling of 4-MEC (3c)

Figure 65 shows that 4-MEC (3c) undergoes combined Phase I and II reactions. The 4- carboxyl –MEC (37, $m/z = 222.1125$) or *N*-acetylation of desethylhydroxytolyl-MEC (47, $m/z = 222.1125$) were formed with high abundance after 30 minutes and then increased after two hour incubation period by approximately 20%, while metabolite (35, $m/z = 208.1332$) was significantly decreased (approximately 20 %) after two hours incubation period due to further metabolism via several routes resulting in a variety of Phase I and II metabolites.

The major Phase II metabolic steps were glucuronidation, which can occur at position 4 of aromatic ring; most of glucuronidation occurs following hydroxylation of the tolyl moiety in the aromatic ring. The glucuronide metabolites could be observed clearly after 120 minutes, and the most abundant glucuronide was metabolite (45, $m/z = 398.1445$) after two hours of incubation, which results from conjugation of the 4-carboxy moiety of metabolite (37, $m/z = 222.1125$).



- Amount of metabolites of 4-MEC (3c) formed after 30 min incubation.
- Amount of metabolites of 4-MEC (3c) formed after 120 min incubation.

Peak Area (%) = (Peak area of metabolite / sum the Peak areas of all observed compounds) x 100.

Figure 65. Relative amounts of metabolites of (\pm)-4'-methyl-N-ethylcathinone (4-MEC, 3c) formed after incubation with Sprague-Dawley rat liver hepatocytes (n = 3); \pm SEM% area for 4-MEC (3c) = $1.4 \pm 1.2\%$ (30 min) and $0.0033 \pm 0.0033\%$ (120 min) (The number on the x-axis refer to the metabolite numbers on Table 20 and Scheme 10).

The linear plot indicates that for 4-MEC (3c), the rate of transformation of the drug is directly proportional to concentration. This experiment was carried out with a 60 minutes incubation instead of 120 minutes, because 4-MEC (3c) was rapidly metabolised with rat hepatocytes.

The metabolic rate constant (K_{met}) was estimated for 4-MEC (3c) from the slope of the plot and determined to be $8.31 \times 10^{-2} \text{ min}^{-1}$ (3c, n=3, ___). The half -life ($t_{1/2}$) of the 4-MEC (3c) in rat hepatocytes was calculated using expression: $t_{1/2}=0.693/ K_{met}$,

to be 8.3 minutes (3c, n=3), and it has significantly shorter half-life than mephdrone (Figure 66).

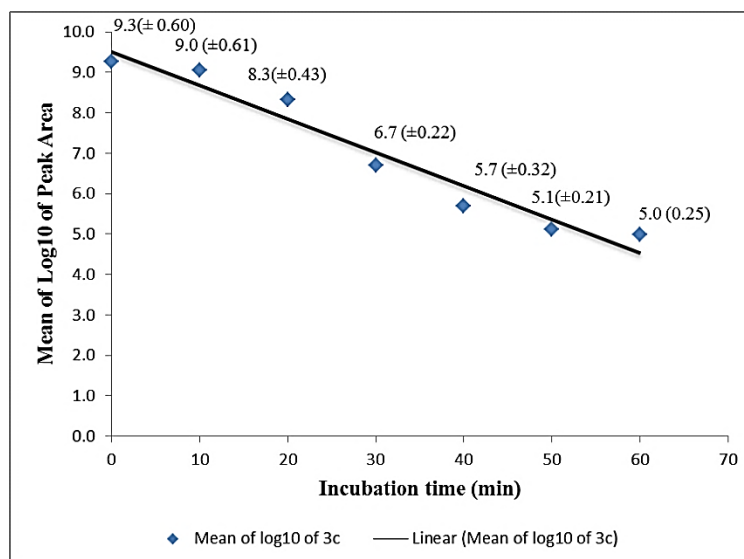


Figure 66 : Plot of the rate of decrease (mean Log₁₀ % peak area ±SD) of (±)-4'-methyl-N-ethylcathinone concentration (3c, 4-MEC) (4-MEC, 3c, __, $y = 0.0831x + 9.5159$; $r^2 = 0.9494$) during incubation with Sprague-Dawley rat liver hepatocytes (n = 3).

3.3.8 LC/MSⁿ

Mass spectrometry is the technique of choice for structure elucidation of drug metabolites, MS² fragmentation of Phase I and II metabolites were obtained on an Orbitrap LTQ instrument and major fragment ions of 4-MMC(3a), 4-TFMMC (3b), 4-MEC(3c) metabolites are presented in Tables (18,19 and 20).

A complex mixture of metabolites was formed following the incubation of all of the above drugs (4-MMC (3a), 4-TFMMC (3b), and 4-MEC (3c)) with rat hepatocytes, and the following Figures show the MS² for some proposed metabolites. For example, Figure 67 shows that the mass spectra for the hydroxylated metabolites of both 4-MMC (16, $m/z = 194.1175$) and 4-TFMMC (3b) (23, $m/z = 248.0890$) in the aromatic ring. It is not possible to determine which position in the ring the hydroxylation has occurred by using the ESI mass spectrum. The base peak of major fragment ion at m/z 146 [(-CH₂OH) (-H₂O)] and m/z 173[(-C₃H₇N) (-H₂O)] for 4-

MMC and 4-TFMMC(3b) respectively does not provide any additional information as to which position of the ring the hydroxylation occurs, EI-MS was used in GC-MS (section 3.4) in order to produce alternative fragmentation from which it might be possible to tell from the mass spectra in which position the hydroxylation occurs. The fragments at m/z 146 and 158 produced from metabolite 16 are both difficult to explain.

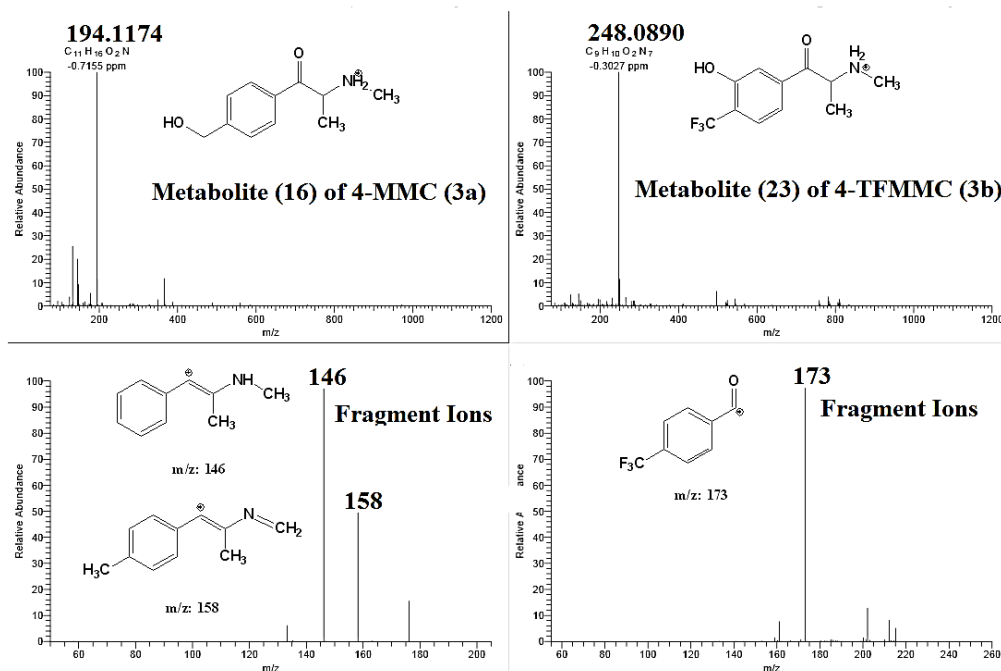


Figure 67. MS² fragmentation obtained on LTQ Orbitrap of hydroxylated mephedrone and hydroxylated 4-TFMMC.

The fragments of the most glucuronide metabolites were shifted to 176 mass units below the glucuronide metabolites of 4-MMC (3a), 4-TFMMC (3b), and 4-MEC (3c) due to neutral loss of the glucuronic acid-H₂O. Loss 42 Da (ketene) from acetylated metabolite 29 (m/z =260.0891) can be observed resulting in a fragment ion at m/z =218.

Loss of neutral fragments such as CO₂ and H₂O does not provide any additional information. In some cases for metabolites 4-TFMMC (3b), a further fragment ion

occurring 20 Da below molecular ion suggests strongly a loss of a HF. For example metabolite 31 ($m/z = 234.1098$) and its fragment ion ($m/z=214$) (See Figure 68).

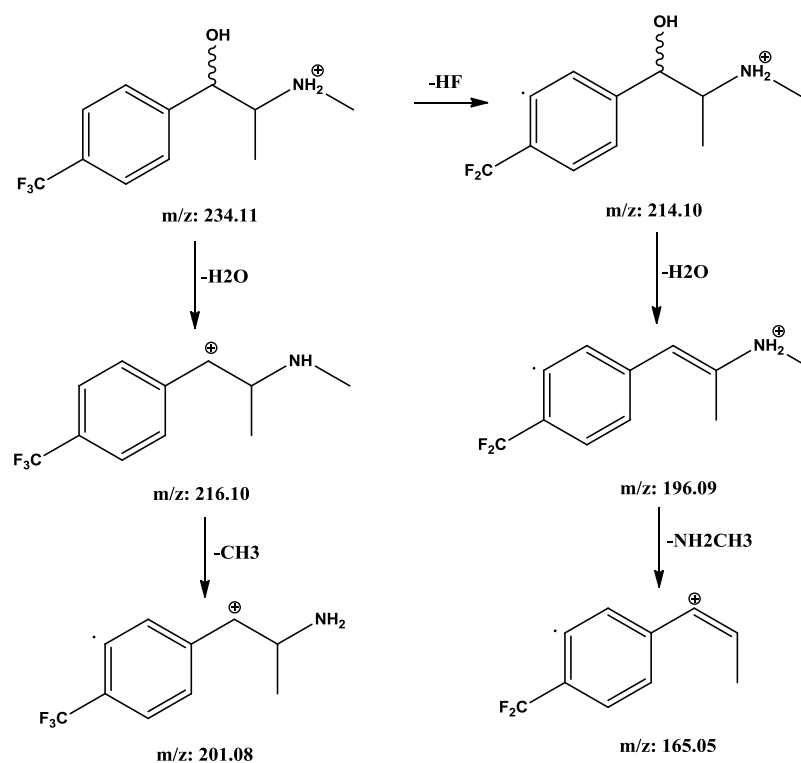


Figure 68. Scheme for the proposed fragmentation of metabolite 31

The fragments of a conjugated indole play an important role in stabilizing the fragmentation in gas phase [68] which was reported in previous metabolism studies of mephedrone investigated by Pedersen *et al.*, as well as found while investigated mephedrone fragmentation in our study. For example, the MS^2 spectra of fragmentation of 4-MMC (3a) metabolites (13, $m/z = 194.0812$) (14, $m/z = 180.1018$) and (16, $m/z = 194.1175$) showed that fragmentation pattern can be formed a conjugated indole fragment. In addition MS^2 spectrum of fragmentation of 4-MEC (3c) metabolites such as 48 ($m/z = 356.1339$), 43 ($m/z = 180.1019$) and 36 ($m/z = 164.1070$) showed a similar fragmentation pattern to that which was observed with 4-MMC (3a). However, metabolite 35 ($m/z = 208.1332$) was only detected in 4-MEC (3c) and its ethyl indole fragments at m/z 160.11 (See Appendix 1).

3.4 Structural elucidation of Hydroxylated metabolite of mephedrone by gas chromatography–mass spectrometry

The position of hydroxylation of aromatic cannot be detected exactly by HRESIMS technique, as described above, while using EI technique more helpful to determine the position of aromatic hydroxylation and GC-EI-MS with derivatization could provide useful structural elucidation of this type of metabolite.

3.4.1 GC-MS identification of metabolites

The major metabolites of mephedrone formed following incubation with rat hepatocytes were separated by GC and characterised by EI-MS after extraction and derivatisation via acetylation. Mephedrone (3a, 4-MMC) and its major metabolites were easily derivatised by acetylation. Derivatisation provides an increase in the molecular weight of the original metabolites. For example, addition of acetate to 4-MMC (3a) (MW=177), leads to a derivative with MW=219 with changed polarity and volatility properties.

Figure 69 shows the EI mass spectra of mephedrone (3a, 4-MMC) and two major metabolites with the proposed structures of acetylated metabolites. Cleavage shown in Figures (69-a and 69-b) leads to an ion at m/z 119 which is observed with high abundance in mephedrone (3a, m/z = 219) and metabolite 7 (m/z = 205) respectively. This fragment arises from alpha homolytic cleavage next the ketone group in the side chain of 4-MMC (3a) and its metabolite. Cleavage between the carbonyl and the benzene ring results in the formation of the tropylium ion at m/z 91 [142].

The fragmentation pattern is not exactly the same for all 4-MMC metabolites and this could be useful to differentiate between the different metabolites by specific fragments. For instance, the position of hydroxylation of the tolyl moiety in metabolite 16 (m/z = 277) was assumed, because this metabolite has a different retention time to mephedrone even though it produced the same predominant fragments at m/z 100 and m/z 58. The electron impact spectrum does not locate the hydroxyl group since all the fragments formed would be the same if the hydroxyl

were on the tolyl group or within the ring (Figure 69-c). The fragment at m/z 135 is characteristic of a hydroxyl group either attached to the ring or on the tolyl group. The fragment at m/z 100 indicates the hydroxyl group is not in the side chain.

Screening the low intensity of the other mephedrone metabolites that were detected in LC-HRMS was not successful due to the lower sensitivity of the GC-MS apparatus. The GC-MS procedure allowed characterisation of only high concentrations of metabolites in the matrix.

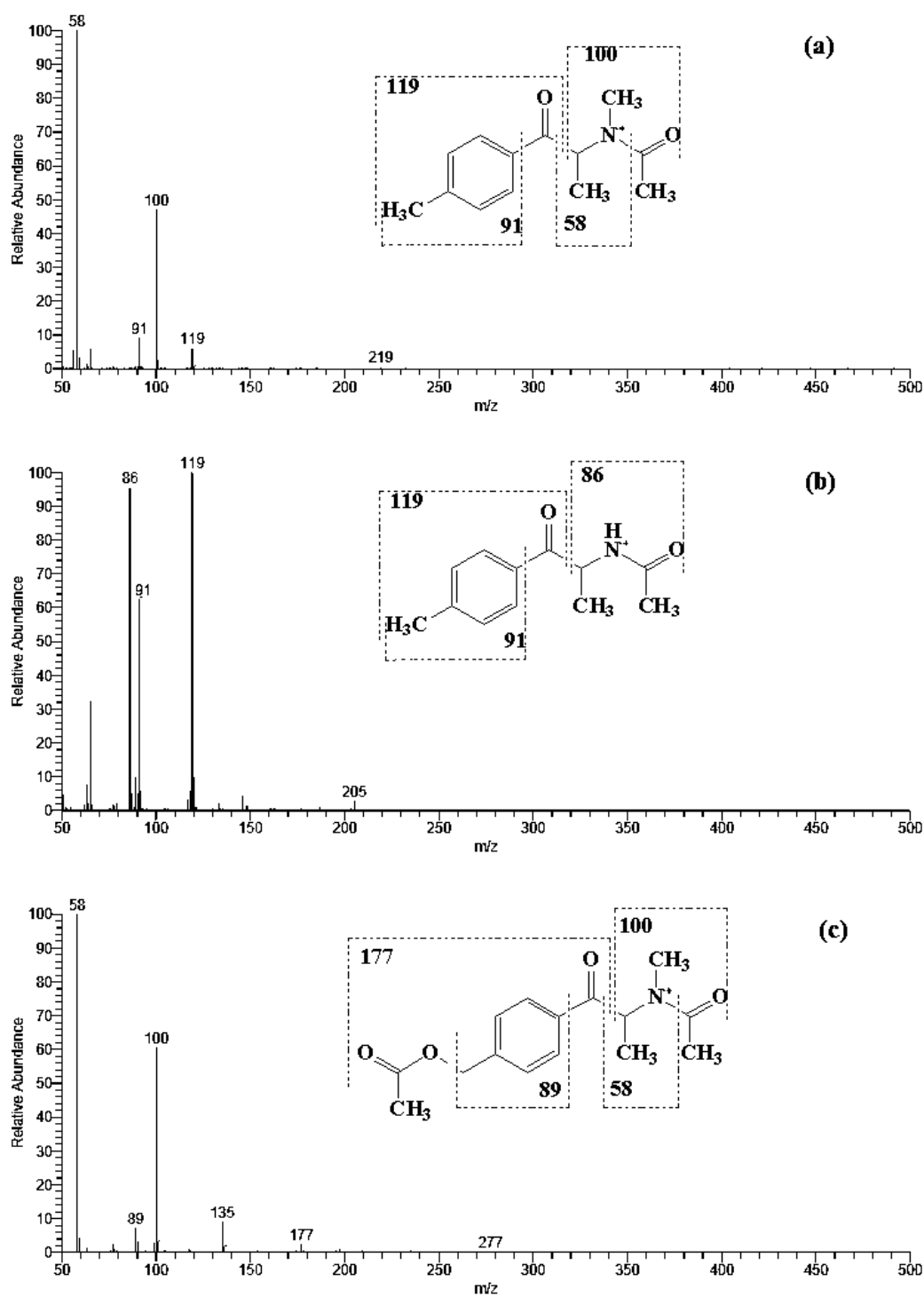


Figure 69. EI mass spectra, structure and predominant fragmentation patterns of (a) 4-MMC (3a) (b) metabolite (7, m/z=164.1069) (c) metabolite (16, m/z=194.1175).

3.5 Conclusions

Cathinone-derived “legal highs”, such as 4-MMC (3a), 4-TFMMC (3b), and 4-MEC (3c) are extensively biotransformed by rat hepatocytes via Phase I and II metabolic processes. The data presented both confirm and expand upon previously reported observations through the identification of glucuronidated Phase II metabolites, however, no evidence of the formation of sulfated metabolites were detected in the current study. The drug concentration (100 μ M) utilised in the incubations may explain this observation, as sulfation processes (which are capacity limited reactions) become easily saturated at high concentrations thus favouring glucuronidation [81]. However, it is believed that at these drug concentrations, even small traces of any sulfated metabolites which may have formed should have been detectable. The bioisosteric derivative, 4-TFMMC (3b), shows significant differences in its metabolism compared to 4-MMC (3a) and indicates an alternative biotransformational pathway. The key pharmacokinetic parameters for both drugs reported herein may be of significance to medical toxicologists and used to predict both the *in vivo* metabolism and the likely pharmacokinetic effects of chemical/structural modifications within this class of controlled substances.

The LC-MS and LC-MS² assays presented here for detection and semi-quantification of metabolism of cathinone derivatives in rat hepatocytes are the first analyte procedures for Phase II metabolic pathway identification. As expected the Orbitrap MS is more selective and sensitive than quadrupole which is used in GC-MS analysis. Both systems can be used for detection and quantification of cathinone derivatives, but to identify low concentration metabolites, the Orbitrap MS was needed due to its higher sensitivity and resolution.

GC-EI-MS approach was very useful to confirm hydroxylation at the aromatic ring end of 4-MMC (3a). It was also useful to confirm the formation of normephedrone which is considered as the major metabolite in rat hepatocytes.

All the presented procedures have also proved to be applicable for identifying the metabolic pathways of all cathinone drug classes in the other biological samples [68, 132, 143]. In addition, using the mephedrone incubation and analysis procedures with 4-MEC (3c) which has different functional group *N*-Ethyl instead of *N*-methyl

in 4-MMC, it was shown that metabolic transformation was faster due to the presence of the ethyl moiety. The major metabolite was due to the oxidation of the tolyl moiety. The half-life of 4-MEC (3c) was shorter than the other cathinone derivatives that have been studied.

Chapter 4: Metabolism of mephedrone and 4-TFMMC using cryopreserved human hepatocytes and analysed by LC-MS and LC-MS²

4.1 Introduction

Cryopreserved hepatocytes are a powerful tool for *in vitro* metabolic profiling of drugs. Human donor livers are only sometimes available, and cell cryopreservation technology has helped to solve this limitation of human hepatocytes availability. It provides a solution to many problems related to storage and distribution of freshly isolated human hepatocytes allowing conservation of viability as well as Phase I and Phase II metabolic activities. Cryopreserved freshly isolated cells can be processed easily by several protocols in which hepatocytes are suspended in a cryopreservation medium. The most common cryopreservation solutions are dimethyl sulfoxide (DMSO), propylene glycol, acetamide or polyethylene glycol. Cells are usually placed in a programmable freezer. Their viability of hepatocytes upon thawing decreases and may be below 55-65% but can be improved by using Percoll density gradient centrifugation to remove dead cells [144]. The major problem when using cryopreserved hepatocytes in drug metabolism studies is that cells should remain viable after thawing and incubation at 37 °C in suspension. Comparing rat and human hepatocytes it was found that the viability of post-cryopreservation human cells was higher than post-cryopreservation rat cells when both were incubated at 37 °C in suspension. Coundouris *et al.* found that human hepatocytes survive the process of cryopreservation better than rat liver cells under the same preservation conditions [145]. Maintenance of the cell viability as well as the level of cytochrome P450 are essential to provide the quality of cryopreserved hepatocytes required to perform metabolism studies[146]. Li *et al.* reported that cryopreserved human hepatocytes had equivalent enzyme activities to freshly isolated human hepatocytes for CYP1A2, CYP 2A6, CYP 2C9, CYP 2C19, CYP 2D6, CYP 3A4 and also UDP-glucuronosyltransferases (UGTs) and sulfotransferases (SULTs) [147]. In addition, Pedersen *et al.* reported that the cytochrome P450 2D6 (CYP2D6) gene is the major enzyme responsible for metabolising mephedrone during *in vitro* Phase I metabolism

[68]. Although, CYP2D6 is reported to be a low abundance hepatic P450, it is the one of the most important enzymes for the metabolism of clinically used drugs and about 20-25% of these are metabolised at least in part by this enzyme. Polymorphism of the enzyme results in poor (PM), intermediate (IM) efficient or ultra-rapid metabolisers (UMs) of CYP2D6 drugs [148].

Polymorphism of CYP2D6 can affect the Pharmacokinetics of about 50% of clinically used drugs and it is observed at ordinary doses that many drugs suffer from unexpected adverse reactions or lack of therapeutic effects. It has been suggested that metabolic defects are caused by a deficiency of CYP2D6. Therefore, individual lacking functional CYP2D6 genes may metabolise selected CYP2D6 substrates at a lower rate [148]. Consequently, decreased rate of biotransformation of drugs through metabolic pathways may increase the possibility of toxicity.

Many of therapeutic classes are known to be metabolised by CYP2D6 which is involved in several pathways such as: *O*-demethylation of codeine (Analgesic class) encainide (antiarrhythmics) and methoxyamphetamine (recreational drugs); aromatic hydroxylation which occurs in drugs such as aprindine (antiarrhythmics class) desipramine (tricyclic antidepressants) tamoxifen (antiestrogen) and aliphatic hydroxylation which occurs in drugs such as perhexiline (calcium antagonist), metoprolol (beta adrenergic blocking agents) and sparteine (antiarrhythmics), some studies demonstrated that potential of CYP2D6 genotype to predict the risk of side effects and treatment outcome [149]. Spina and co-workers reported that thirty-one patients who were treated with oral desipramine and found after three weeks treatments at dosage of 100 mg per day that two patients with CYP2D6 poor metabolizer phenotype developed the highest plasma concentrations of desipramine (tricyclic antidepressant) and complained of severe side-effects [150]. This confirms presence of a genotype that affects the metabolism of drugs that are metabolised by CYP2D6.

Wuttke and co-workers studied the relation between the CYP2D6 genotype and the occurrence of metoprolol associated side effects among twenty-four patients. The data showed that subjects deficient in CYP2D6 had a 5-fold higher risk of developing of adverse effects during metoprolol treatment than patients who were

not poor metabolisers. Since risk of adverse effects of metoprolol is unknown, the clinical relevance of the CYP2D6 genotype for metoprolol therapy was determined with a combination of allele-specific polymerase chain reaction (PCR analysis) followed by polymerase chain reaction-restriction fragment length polymorphism (RFLP), allelic discrimination assays, and long-range PCR. This study demonstrated that patients who had adverse effects associated with metoprolol therapy and were phenotyped and genotyped as CYP2D6 deficient might be prone to having adverse effects with other drugs dependent on CYP2D6 for their metabolism[151].

Rau *et al.* showed that concentrations of metoprolol in plasma, which were assessed by HPLC, were 4.1-fold higher in poor metabolisers compared with normal metabolisers during long-term administration of metoprolol [152].

De la Torre and co-workers studied the impact of CYP2D6 polymorphisms on the pharmacokinetics of MDMA (ecstasy) in the ten healthy volunteers. MDMA (100 mg or placebo) was administered in two separate doses separated by an interval of 24 h. All volunteers were extensive metabolisers except for one who was found to possess the CYP2D6 *4/*4 genotype and was classified as poor metabolizer. It was found that MDMA and metabolite pharmacokinetics varied according to the CYP2D6 genotype and this could result in the emergence of acute or long-term toxicity associated with high plasma concentrations [153].

In the Chapter the Orbitrap based LC-MS was used for identifying metabolites in rat hepatocyte incubations and showed successful detection and structural elucidation of many mephedrone metabolites in rat hepatocytes[154].

The goal in this chapter was to apply the same method to profiling metabolites of mephedrone *in vitro* following incubation with human hepatocytes. This required the development of a new incubation procedure for the human cells.

4.2 Chemicals and Materials

4.2.1 Chemicals

All chemicals used in this chapter, were described in chapter 3 section 3.2.1.

4.2.2 Incubation materials

- Cryopreserved suspensions of human hepatocytes were obtained from (CellzDirect, USA, via Life Technologies), and this study was carried out using hepatocytes obtained from two different donors (in duplicate). Table 21 shows the personal and medical details of the two donors from whom the liver samples were obtained.

Table 21 Personal and medical details of donors from whom hepatocytes were obtained (Information supplied by Life Technologies).

Sample ID	Sex	Race	Donor Age (years)	Drug Treatment	Drug Use	Alcohol Use	Smoking	Cause of Death
HU4215	Male	Caucasian	39	Non Reported	No	Yes	Yes	Head Blunt Trauma injury
HU4226	Male	Caucasian	46	Creatine	Yes	No	No	Blunt Trauma

- Thawing Medium: Cryopreserved Hepatocytes Recovery Medium (CHRM[®]) (50 mL) (Lot: PLN00268) (APS Cat: 70001) (Invitrogen Life Technologies, Cat.: CM7000).
- Incubation Medium: Williams' Medium E (500mL) (Lot: 988827) (Cat. No. : A12176), Cocktail B (Lot: 1079913) (Cat No.:A13448) (Invitrogen Life Technologies).
- 24 well suspension culture plates were purchased from Greiner Bio-one (Lot; E10060ME).

Orbital Incubator S150 (Stuart Scientific, UK) was used for cell incubation, and set at 37 °C.

4.2.3 Analytical materials and Equipment

The samples were analysed using LC/MS (Exactive Orbitrap) and LC/MS² (Finnigan LTQ Orbitrap mass spectrometer) and the experimental conditions for these instruments were described in chapter 3 sections 3.2.2 and 3.2.3, the mobile phase was prepared as described in Chapter 3 section 3.2.3.1.

4.3 Preparation of drug stock solutions

4.3.1 Stock solutions

100 mM of 4-MMC (3a) and 4-TFMMC (3b) were separately made up in HPLC grade water as stock solutions (1). Second stock solutions (2) were prepared by transferring 10 µL of stock solutions(1) (100 mM) into tubes, then making them up to 5mL with incubation medium in order to prepare substrates at 200µM (2 x final concentration).

4.4 Method and incubation protocol

4.4.1 Thawing and plating protocol

- A Class II safety cabinet was used to carry out all the incubation stages.
- Cryopreservation medium (CHRM) was aliquoted into 50 mL tubes, and placed in a water bath to warm at 37 °C.
- 2 x 50 mL tubes of complete incubation medium (Williams' E Medium and Cocktail B) were prepared and warmed for 15-20 minutes at 37 °C.
- A vial of cryopreserved hepatocytes was transferred to cell laboratory from the storage unit in the liquid nitrogen store. The pressure in the vial was released as soon as possible, and the vial immersed in a 37 °C water bath. The vial was monitored while it thawed; it took less than two minutes. The

contents were poured into 50 mL warmed thawing medium (CHRM) as soon as possible, and the vial rinsed using pipette to ensure all cells removed. The tube was gently inverted at least twice to ensure a homogenous mixture.

- The mixture (thawed medium with cells) was centrifuged at 100 g for 10 minutes, then the tube was removed from the centrifuge being careful not to disturb the pellet in the bottom of conical tube, and the supernatant poured off completely.
- The cell pellet in the bottom of conical tube was gently resuspended by adding approximately 1-2 mL of warmed Williams' E medium. Then additional medium was added to give 2-6 mL.
- Using a sterile pipette the volume was recorded. In this study the volumes were 4.5 and 3.85 mL of the first and second batch of cells respectively.

4.4.2 Viability of hepatocytes using Trypan Blue exclusion

150 μ L of Williams' E medium were mixed with 50 μ L of Trypan Blue and 50 μ L of re-suspended hepatocytes in 1.5mL Eppendorf tubes in order to make a solution which was used for counting the cells. Before the hepatocyte suspension was added into the tube, the tube of hepatocyte suspension was gently inverted several times to ensure that a homogeneous cell suspension was obtained that would lead to an accurate cell count. 10 μ L of the mixture was loaded into the haemocytometer, the capillary action pulling the suspension into the haemocytometer chamber.

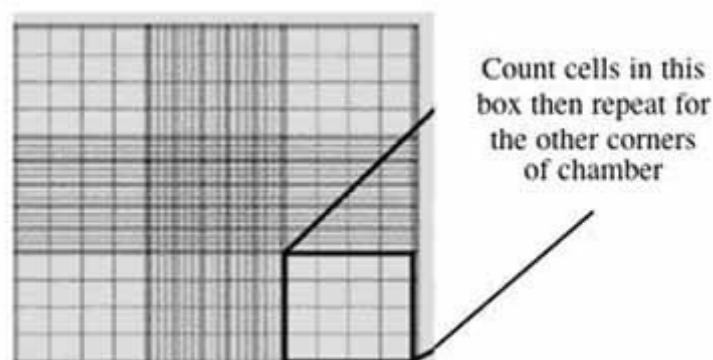


Figure 70. Counting hepatocytes using a Haemocytometer.

The haemocytometer chambers were examined under a Nikon Diaphot-TMD (Nippon Kogaku KK, Japan) light microscope, and immediately the cells were counted in 18 of the 0.1 mm^3 sections. The viable hepatocytes (clear colour) and dead hepatocytes (blue colour) were counted in the quadrants in each chamber of the haemocytometer (Figure 69). After performing the calculation to determine the total number of viable cells, Williams' E medium was used to dilute the hepatocytes to the desired final cell concentration.

4.4.3 The viability calculation

The viability of the cells in suspension could be determined by counting the total number of live and dead cells that fell within the eighteen quadrants and then calculating the percentage of those that were alive. The initial viability was 87.15% (± 0.07 ; $n=2$) in HU4215 cell samples and 90.2% (± 1.56 ; $n=2$) in HU4226 cell samples.

The suspensions were diluted to reach a concentration of approximately 10^6 cells mL^{-1} with 37°C Williams' E medium.

4.4.4 Incubation protocol

Eppendorf tubes were labelled for sampling from incubations with both drugs. The plates were arranged as shown in Figure 70. Two 24 well plates were used, consulting the template of the 24 well plates to see which substrate goes into which well (Figure 70). 0.25 mL of the substrate stock solutions (200 μM) were prepared as described in section 4.3.1 and added to the wells of the first 24 well plate, carefully noting which substrate went into which well. Twelve wells were then made up to 0.50 mL with incubation medium (Williams' E Medium to serve as blanks (no cells)) and 0.25 mL of cell suspension (10^6 cell mL^{-1}) was added to the other 12 wells. Six wells, of the second 24 well plate considered as control wells with no drugs, were filled with 0.25 mL of incubation medium (Williams' E Medium) and then were then made up to 0.50 mL with cell suspension (10^6 cell mL^{-1}). The concentration of cells in the incubations was 0.5×10^6 cell mL^{-1} .

	1	2	3	4	5	6
A [3a]	NC 0/30 min	NC 0/30 min	NC 60/90 min	NC 60/90 min	NC 120 min	NC 120 min
B [3a]	DC 0/30 min	DC 0/30 min	DC 60/90 min	DC 60/90 min	DC 120 min	DC 120 min
C [3b]	NC 0/30 min	NC 0/30 min	NC 60/90 min	NC 60/90 min	NC 120 min	NC 120 min
D [3b]	DC 0/30 min	DC 0/30 min	DC 60/90 min	DC 60/90 min	DC 120 min	DC 120 min

	1	2	3	4	5	6
A	CON 0/30 min	CON 0/30 min	CON 60/90 min	CON 60/90 min	CON 120 min	CON 120 min
B	X	X	X	X	X	X
C	X	X	X	X	X	X
D	X	X	X	X	X	X

Figure 71. The layout of 24-well plates: NC= No cell; DC=Drug with cell; CON=control (no drug); X= unfilled well.

Cells were incubated on a shaking table at 120 rpm, in an incubator at 37°C with an atmosphere of air / 5% CO₂ in the clean room. Each drug incubation was sampled in duplicate at 0, 30, 60, 90 and 120 minute time points. As described above, each well contained 0.5 mL of suspension, consequently, from each time point 10 µL was taken from the incubation into an Eppendorf tube for a quick check on viability using Trypan Blue. Aliquots (0.20 mL) of incubation suspension were then removed from individual wells and placed in Eppendorf tubes labelled for the appropriate time points, and the reaction was quenched by adding 0.70 mL of acetonitrile. Thus, each

well was used to take 2 time points, and samples were then frozen at - 80 °C until analysis.

4.4.5 Effects of 4-MMC (3a) and 4-TFMMC (3b) on viability of cryopreserved human hepatocytes

To examine the toxic effects of 4-MMC (3a) and 4-TFMMC (3b), samples were taken at regular time intervals (0, 30, 120 minutes). The viability of cryopreserved hepatocytes was measured using Trypan Blue exclusion and Table 22 shows the results expressed as the percentage of live cells. An aliquot (10 μ L) of the cell suspension was added to (10 μ L) of Trypan Blue (0.1%w/v), the mixture was loaded onto a haemocytometer and the cells counted under the microscope as described previously in section 3.2.9. It was found that the metabolism of 4-MMC (3a) and 4-TFMMC (3b) had no significant effect on the viability of hepatocytes over the duration of the 2h incubation at concentration of 100 μ M (See Table 22).

Table 22. Count viability of cryopreserved hepatocytes during the 2 hour incubation (n=4).

Time (minutes)	Viability (%) (\pm SD)		
	Control	4-MMC(3a)	4-TFMMC(3b)
0	79.5% (\pm 12.1)	79.3% (\pm 7.5)	83.3% (\pm 10.4)
30	75% (\pm 8.4)	79.3% (\pm 5.9)	76.3% (\pm 7.4)
120	71% (\pm 6.8)	68.5% (\pm 8.4)	74.3% (\pm 3.9)

4.4.6 Sample preparation for LC-MS

The samples were thawed at room temperature and centrifuged (10^4 rpm, 15 minutes), and any remaining protein was removed by further addition of acetonitrile (0.1 mL) and subsequent filtration through a Biotage Isolute® PPT+ protein precipitation plate (Biotage Limited, Sweden) [138], as described in Chapter 3, section 3.2.9.

The filtrate was collected and analyzed by either LC-MS or LC-MS². The efficiency of recovery was expressed as a percentage and computed as:

$$\frac{\text{Average area of drug with hepatocytes after filtration (time 0)}}{\text{average area of drug with incubation medium after filtration (time 0)}} \times 100$$

The efficiency of recovery from hepatocyte matrix was determined to be $104.5 \pm 3.8\%$ (for 4-MMC (**3a**), $n = 4$, \pm SD), $100.7 \pm 3.9\%$ (for 4-TFMMC (**3b**), $n = 4$, \pm SD) respectively.

4.5 Results and discussion

4.5.1 Effects of cryopreservation of human hepatocytes on drug-metabolizing enzymes

Table 23 shows the activities of a range of Phase I and Phase II reactions measured in the hepatocytes isolated from the two donors, demonstrating that they are competent for the CYP-catalysed reactions, and for the conjugation pathways which were shown in Chapter 3 take part in the metabolism of the mephedrone analogs being investigated.

Table 23. Profile activities of range of Phase I and Phase II reactions measured in hepatocytes isolated from two donors (Data obtained by Life Technologies).

Lot No.	HU4215	HU4226
Medium Method	WEM ^a	WEM
Enzymes	Metabolic activities*	
7-HCG ^b	844.00	401.00
7-HCS ^c	65.80	38.00
CYP1A2	146.00	54.90
CYP2B6	233.00	20.80
CYP2C8	2.97	1.39
CYP2C9	72.50	58.80
CYP2C19	170.00	39.50
CYP2D6	21.10	8.64
CYP2E1	74.00	81.20
CYP3A4 - TEST	1,580.00	613.00
CYP3A4/5 - MDZ	634.00	160.00
FMO	114.00	311.00

^a Williams' E medium.

^b Glucuronidation of hydroxycoumarin.

^c Sulphation of hydroxycoumarin.

*Metabolic activities are determined by HPLC or LC-MS² analysis and recorded as pmol /10⁶ cells/min.

In drug metabolism, the chemical modifications provided by different enzymes can be classified in terms of Phase I and Phase II metabolism. The cytochrome P450

(CYP) family are the most important Phase I metabolic enzymes which are found in liver cells, and there are at least 33 different CYP 450 enzymes classified into four main families from CYP 1 to CYP 4. Within each family there are several subfamilies which are designated by numbers and letters, for example CYP2C19 is enzyme 19 in subfamily C and main family 2. Phase I reactions of most current drugs are catalysed by five CYP enzymes CYP3A, CYP2D6, CYP2C9, CYP1A2, and CYP2E1 [79].

In our study, drug metabolizing enzymes were analysed in Life Technologies laboratory for activities and expression in cryopreserved human hepatocytes. This work was carried out in Drug discovery ADME/Tox Division of Life Technologies, Durham NC USA, by Dr. Jonathan P. Jackson. The expression of 13 CYP isoform enzymes was determined in the human hepatocytes which were obtained from the two donors (HU4215 and HU4226) after cryopreservation. Table 24 shows the genotypes determined for both donors. The analysis was performed in duplicate and each assay included a template control.

Table 24: Expression of 13 CYP enzymes determined in the donor hepatocytes used in this study (Data obtained by Life Technologies).

CYP enzyme	Genotype of HU4215	Genotype of HU4226
CYP2C19*2	WT/WT	WT/WT
CYP2C19*3	WT/WT	WT/WT
CYP2C19*6	WT/WT	WT/WT
CYP2C9*2	WT/WT	WT/WT
CYP2C9*3	WT/WT	WT/*3
CYP2C9*6	WT/WT	WT/WT
CYP2D6*3	WT/WT	WT/WT
CYP2D6*4	WT/*4	WT/*4
CYP2D6*6	WT/WT	WT/WT
CYP2D6*9	WT/WT	WT/WT
CYP3A5*3	*3/*3	*3/*3
CYP3A5*6	WT/WT	WT/WT
CYP3A5*8	WT/WT	WT/WT

*WT: Wild type

Pedersen and co-workers showed that the activity of CYP2D6 contributed to the microsomal metabolism of mephedrone [68].

Both donors used in the current study were heterozygous for the CYP2D6*4 allele. This allele synthesizes an enzyme devoid of activity (defective splice site), however, since these individuals were heterozygous their hepatocytes should have intermediate CYP2D6 activity (between a poor and effective metabolizer). Currently more than 46 different major polymorphic CYP2D6 alleles are known [148], but in the current study only 4 different CYP2D6 SNPs were tested for. Thus it is possible that the other alleles are affected by a different SNP which was not tested. The other

possible CYP2D6 defective alleles are CYP2D6*2, CYP2D6*10, CYP2D6*17, CYP2D6*41.

The activities of CYP2D6 (measured by the de-methylation of dextromethorphan) expressed as pmol/min per million cells for HU4215 and HU4226 were determined to be 21.1 and 8.64, respectively. Comparing CYP2D6 activity of these two donors to that of 196 other donors it appears that HU4215 and HU4226 fall at the median value and below. This comparison supports our genotyping data showing that the donors should have an intermediate CYP2D6 enzyme activity phenotype based upon the heterozygous genotype, and the activities are a little lower than expected.

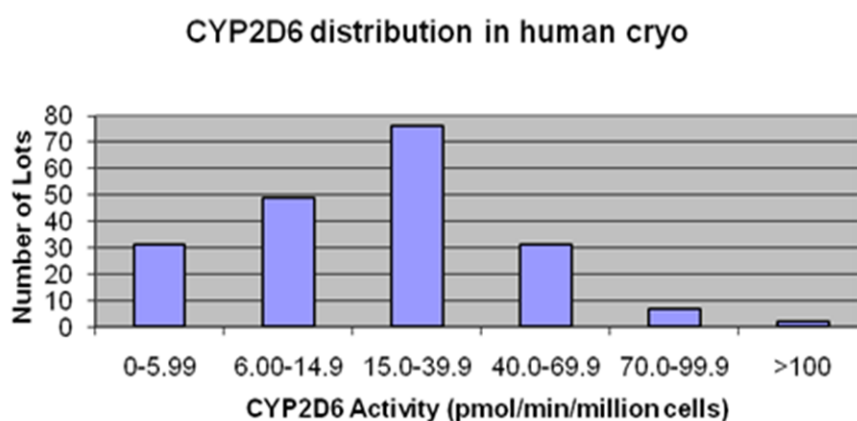


Figure 72 : CYP2D6 distribution in human cryopreserved hepatocytes of 196 donors (Data obtained by Dr. Jonathan P. Jackson, Drug discovery ADME/Tox Division of Life Technologies, Durham NC USA).

In the distribution of the 196 donors compared to HU4215 and HU4226 show in Figure 71, the median of the population was 19.6, average was 24.7, and the data ranged from 0.2 to 118 pmol/min/ 10^6 cells.

Additionally, both donors were homozygous null for CYP3A5*3 activity and HU4226 was heterozygous CYP2C9*3 individual. The CYP2C9*3 allele produces a defective enzyme with reduced activity, but CYP2C9*3 is not devoid of activity.

4.5.2 Biotransformation of 4-MMC (3a) and 4-TFMMC (3b) in Cryopreserved human hepatocytes

After 4-MMC (3a) and 4-TFMMC (3b) were incubated with human hepatocytes, samples were taken at various time points and compared to pre-incubated samples (time zero). Metabolites to be identified were present in the incubated samples at both 30 minutes and after 120 minutes. However, some of the metabolites previously identified in the rat hepatocyte incubations were not present in incubations with human hepatocytes, particularly some of the Phase II metabolites. The metabolism rate was slower in human hepatocytes than rat hepatocytes, and most of the metabolites were observed with lower abundance in human cells than in rat hepatocytes.

Figure 72 (A, B) and (E, F) shows selected ion chromatograms at 178.122 Da and 232.094 Da of 4-MMC (3a) and 4-TFMMC (3b) respectively. The chromatograms (A, E) represent [M+1] peaks at 30 minutes, while (B, F) show chromatograms for peaks after 120 minutes of incubation with human hepatocytes. Peaks areas for the selected ion chromatograms indicated only a small change in the levels of parent drugs during the incubation. This is also reflected in the ESI spectra in Figure 72 (C, D) and (G, H) which show only a small difference in the relative intensity of the molecular ion peak between the 30minute and 120minute of incubation periods.

LC-MS² experiments were conducted to support metabolite structural elucidation, and the proposed fragments of some 4-MMC (3a) and 4-TFMMC (3b) are presented in appendix (1).

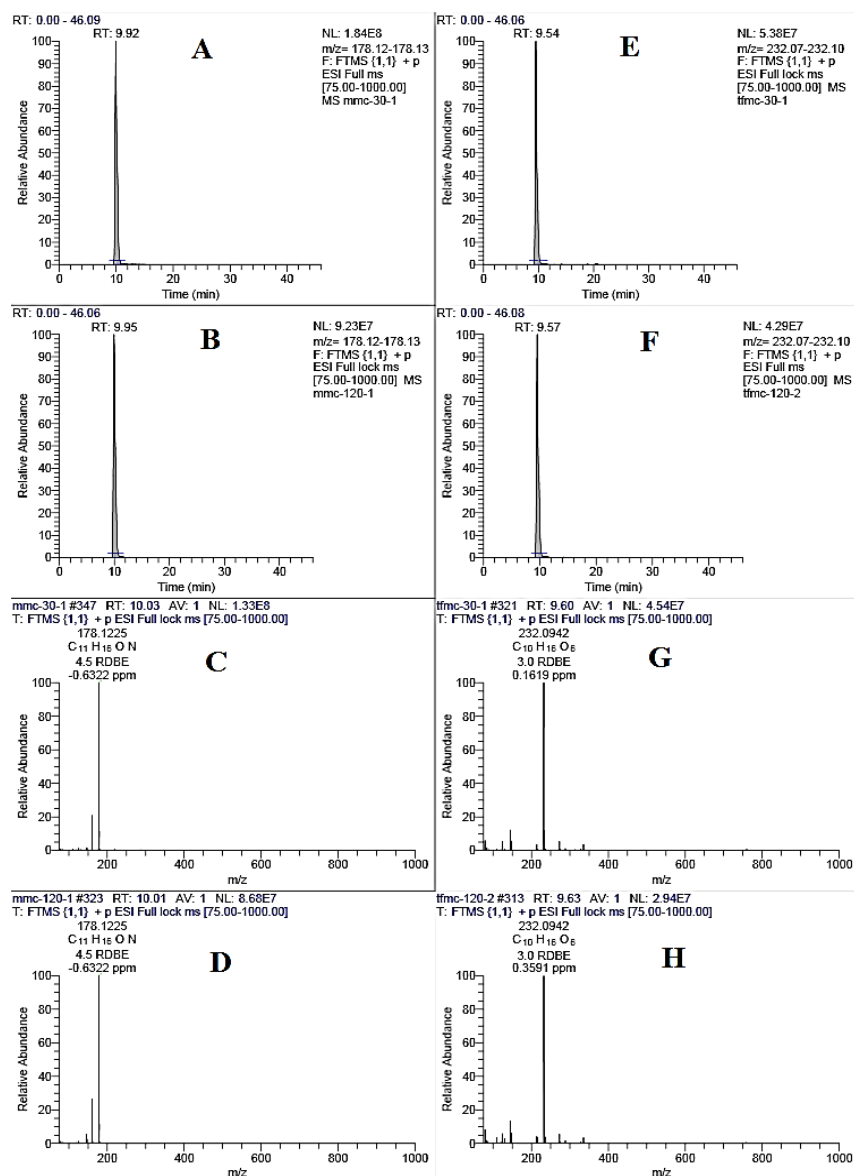


Figure 73. Selected ion chromatograms from LC-MS analysis and mass spectra of 4-MMC (3a) and 4-TFMMC (3b). (A) and (B) selected ion chromatograms illustrate the M^+ ion at $m/z = 178$, at 30 and 120 minutes respectively; (E) and (F) selected ion chromatograms illustrate the M^+ ion at $m/z = 232$, at 30 and 120 minutes respectively; (C) and (D) the mass spectra of the 178 M^+ ion identify the 3a compound, at 30 and 120 minutes respectively ; (G) and (H) the mass spectra of the 232 M^+ ion identify the 3b compound, at 30 and 120 minutes respectively.

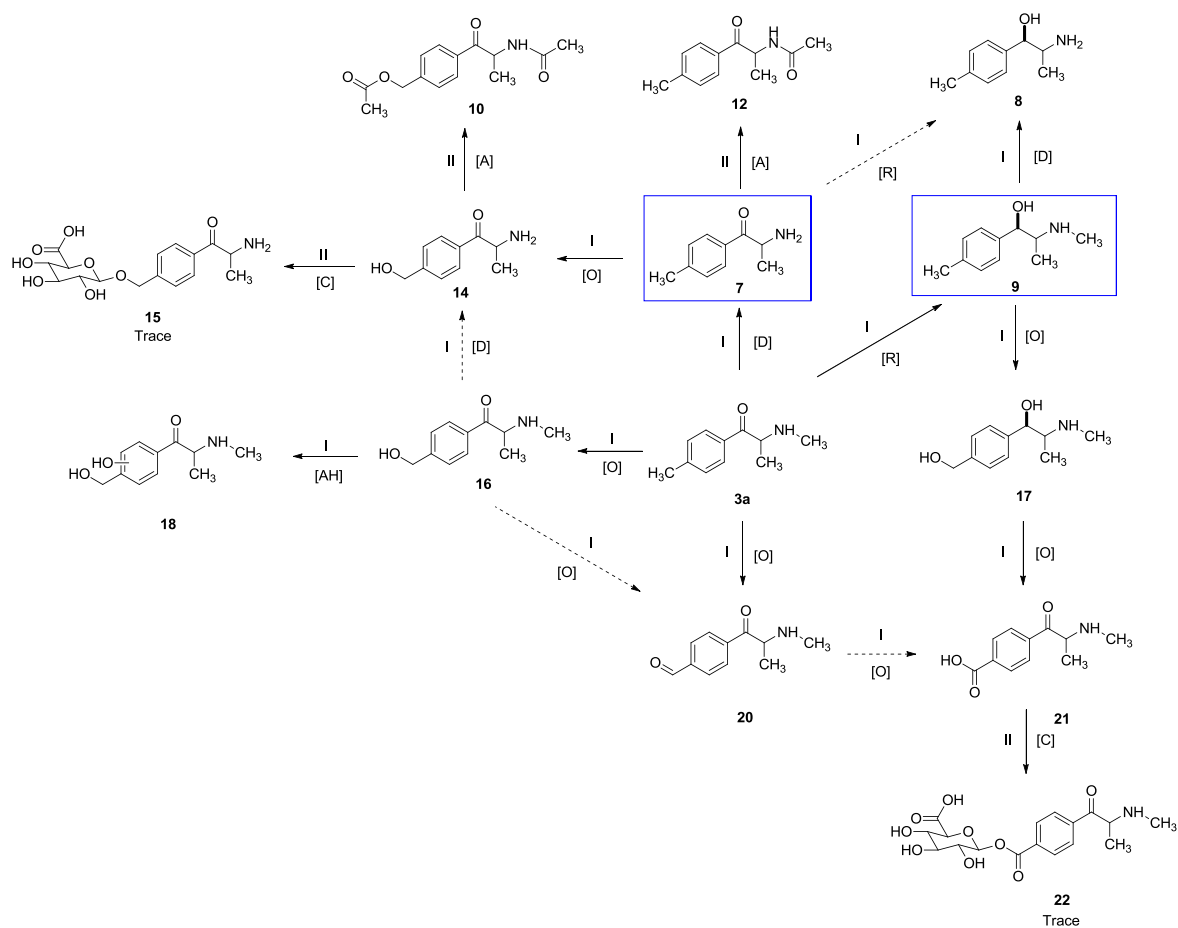
Table 25 lists some of Phase I metabolites of mephedrone (4-MMC, 3a), with a few Phase II metabolites such as glucuronide and acetylated metabolites, which were observed at the end of the 120 minute incubation period with trace abundance. The parent drug and its metabolites are shown in Table 25. The fragmentation patterns achieved using LTQ Orbitrap method were as previously reported (Chapter 3, section 3.2.2.2).

All the metabolic pathways of 4-MMC (3a) shown in scheme 11 were identified previously in our laboratory with the use of freshly prepared rat hepatocytes. Therefore, when comparing the metabolic profile either from rat or human hepatocytes, the same pathways of metabolism was observed, but with differences in the abundance of most of the metabolites. The rate of metabolism was much higher in rat than human hepatocytes. Also some metabolites were absent in human hepatocyte incubations which will be discussed later.

In this study, the major metabolites of 4-MMC (3a) were normephedrone (7, $t_R = 10.4$ min, $m/z = 164.1070$), 4-hydroxy-methylmethcathinone (16, $t_R = 8.3$ min, $m/z = 194.1175$). Also an unidentified metabolite (U, $m/z = 194.1176$) was observed as a major metabolite, and it may be the result of hydroxylation of mephedrone on the aromatic ring rather than hydroxylation of 4-methyl group as in metabolite 16. Metabolite U differs from metabolite 16 in that metabolite U has a different chromatographic behaviour.

Table 25 : LC-MS Exactive Orbitrap data for biotransformation of 4-MMC (3a) incubated with human hepatocytes (120 min). See Scheme 11 for proposed metabolite structures. Key: gluc = glucuronic acid-H₂O; U = unidentified metabolite (t_R = 8.3 min; m/z = 194.1176); ND = Not Detected. The mass errors of the detected metabolites were within ± 1- 2 ppm of their assigned elemental composition.

Met.	Rt (min)	m/z	Formula (ppm)	MS ² Base Peak	Other Ions (%)
12	6.0	206.1176	C ₁₂ H ₁₆ NO ₂ (0.044)	160	120(9)
20	6.0	192.1019	C ₁₁ H ₁₄ NO ₂ (-0.037)	164	146(9),119(4)
10	6.1	264.1228	C ₁₄ H ₁₈ NO ₄ (-0.53)	ND	
15	7.0	356.1335	C ₁₆ H ₂₂ NO ₈ (-1.3)	ND	
U	8.3	194.1176	C ₁₁ H ₁₆ NO ₂ (-0.0081)	ND	
14	9.0	180.1019	C ₁₀ H ₁₄ NO ₂ (0.12)	162	144(2)
18	9.4	210.1125	C ₁₁ H ₁₆ NO ₃ (-0.060)	135	192(17), 174(4.7), 162(13.6)
3a	9.9	178.1225	C ₁₁ H ₁₆ NO (-0.63)	160	147(3)
9	10.2	180.1382	C ₁₁ H ₁₈ NO (-0.68)	162	160(10)
7	10.4	164.107	C ₁₀ H ₁₄ NO (0.024)	146	147(16)
8	10.6	166.1226	C ₁₀ H ₁₆ NO (-0.13)	148	120(48)
21	11.1	208.0968	C ₁₁ H ₁₄ NO ₃ (-0.16)	146	190(71),172(34)
16	11.5	194.1175	C ₁₁ H ₁₆ NO ₂ (0.17)	146	176(12),158(51),133(5)
17	12.5	196.1332	C ₁₁ H ₁₈ NO ₂ (0.098)	138	178(92), 148(2)
22	14.4	384.1288	C ₁₇ H ₂₂ NO ₉ (-0.12)	ND	



Scheme 11. Proposed scheme for the Phase I and II metabolism of (±)-mephedrone (4-MMC, 3a) in cryopreserved human hepatocytes. Metabolite numbers correspond to the metabolite data presented in Table 25. Key: [A] = acetylation; [R] = reduction; [D] = demethylation; [O] = oxidation; [C] = conjugation; [AH] = aromatic hydroxylation (The blue rectangle highlights the most abundance metabolites).

The proposed biotransformation of 4-TFMMC (3b) detected after incubation of human hepatocyte is summarised in scheme 12, and supporting data obtained from some predominant metabolites obtained by using the LTQ Orbitrap in MS² mode are shown as proposed fragment structures in Table 26 . hydroxy (trifluoromethyl) methcathinone (23 ,t_R = 6.6 min, m/z = 248.0891), (±)-4'- (trifluoromethyl) ephedrine (31, t_R = 9.7 min, m/z = 234.1098) , and 4'-(trifluoromethyl) cathinone (28, t_R = 9.8 min, m/z = 218.0787) were identified as major Phase I metabolites. Further steps of Phase I metabolism are shown in Scheme 12 and some conjugated Phase II metabolism occurs producing a trace amount of *O*-glucuronidation (30, t_R = 6.3,m/z = 410.1059) and *N*-acetylation (29,t_R = 5.7 ,m/z = 260.0892) metabolites. The dynamic range of the HRMS was sufficient to detect them.

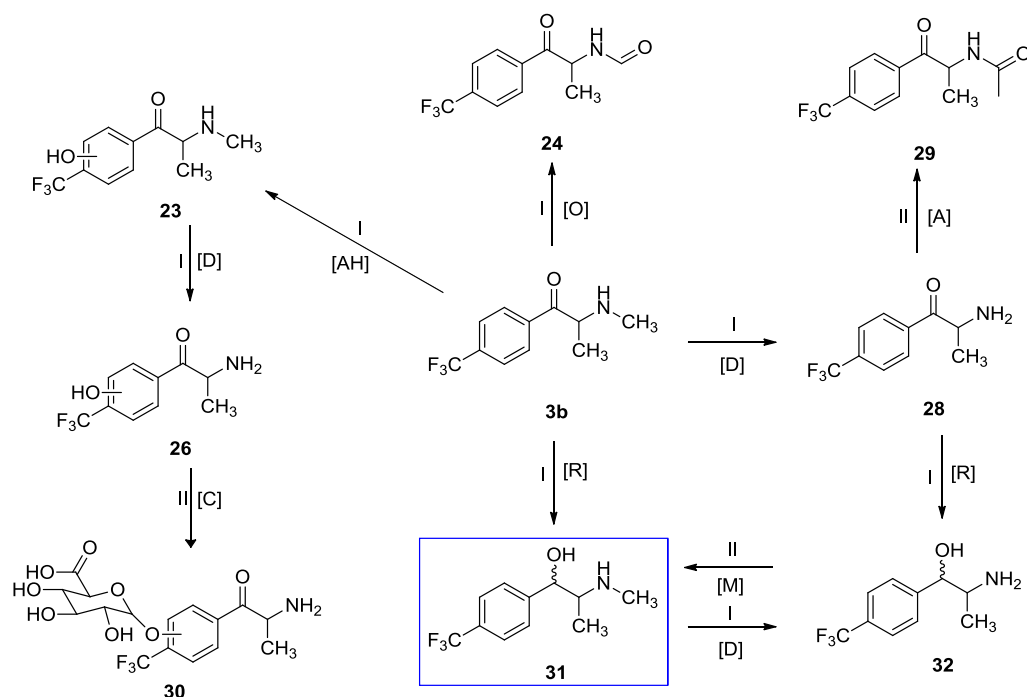
As mentioned in chapter 3, the aromatic hydroxylation metabolite of 4-TFMMC(3b) can be occur in the ring instead of the tolyl moiety which is blocked in this compound by CF₃ , and the aromatic ring itself becomes a site of metabolism, and substitutes the hydrogen atom in the ring within an electrophilic substituent.

MS/MS fragments shown specific neutral loss occurring in ESI-MS for certain chemical moieties in 4-MMC(3a) and 4-TFMMC(3b). For example, a water loss (-18 Da) can be commonly observed for keto moiety and alcohol moiety in the most metabolites. A neutral loss of CO (-28Da) can be observed from aldehyde moiety of metabolite such as (20, m/z=192.10) and (24, m/z=246.07), which cannot be observed in other metabolites, Tables 25 and 26 summarize some MS/MS ions for some metabolites.

Table 26. LC-MS Exactive Orbitrap data for biotransformation of 4-TFMCC (3b) incubated with human hepatocytes (120 min). See Scheme 12 for proposed metabolite structures. The mass errors of the detected metabolites were within ± 0.05 -1.0 ppm of their assigned elemental composition.

Met.	Rt (min)	m/z	Formula (ppm)	MS ² Base Peak	Other Ions
29	5.7	260.0892	C ₁₂ H ₁₃ F ₃ NO ₂ (-0.22)	216	218(27)
24	5.8	246.0736	C ₁₁ H ₁₁ F ₃ NO ₂ (-0.19)	218	173(17),200(29)
30	6.3	410.1059	C ₁₆ H ₁₉ F ₃ NO ₈ (0.41)	ND	
23	6.6	248.0891	C ₁₁ H ₁₃ F ₃ NO ₂ (-0.84)	173	230(45), 202(7),212(6)
26	7.5	234.0736	C ₁₀ H ₁₁ F ₃ NO ₂ (-0.26)	ND	
3b	9.7	232.0942	C ₁₁ H ₁₃ F ₃ NO (-0.79)	214	
31	9.7	234.1098	C ₁₁ H ₁₅ F ₃ NO (-0.82)	201	216(15),214(2), 196(7),165(23)
28	9.8	218.0787	C ₁₀ H ₁₁ F ₃ NO (0.047)	200	201(60),173(2.3)
32	9.8	220.0944	C ₁₀ H ₁₃ F ₃ NO (0.28)	202	
*ACN-28	9.8	259.1051	C ₁₂ H ₁₄ F ₃ N ₂ O (-0.78)	ND	

*ACN-28 = Adducts of Acetonitrile of metabolite (28)

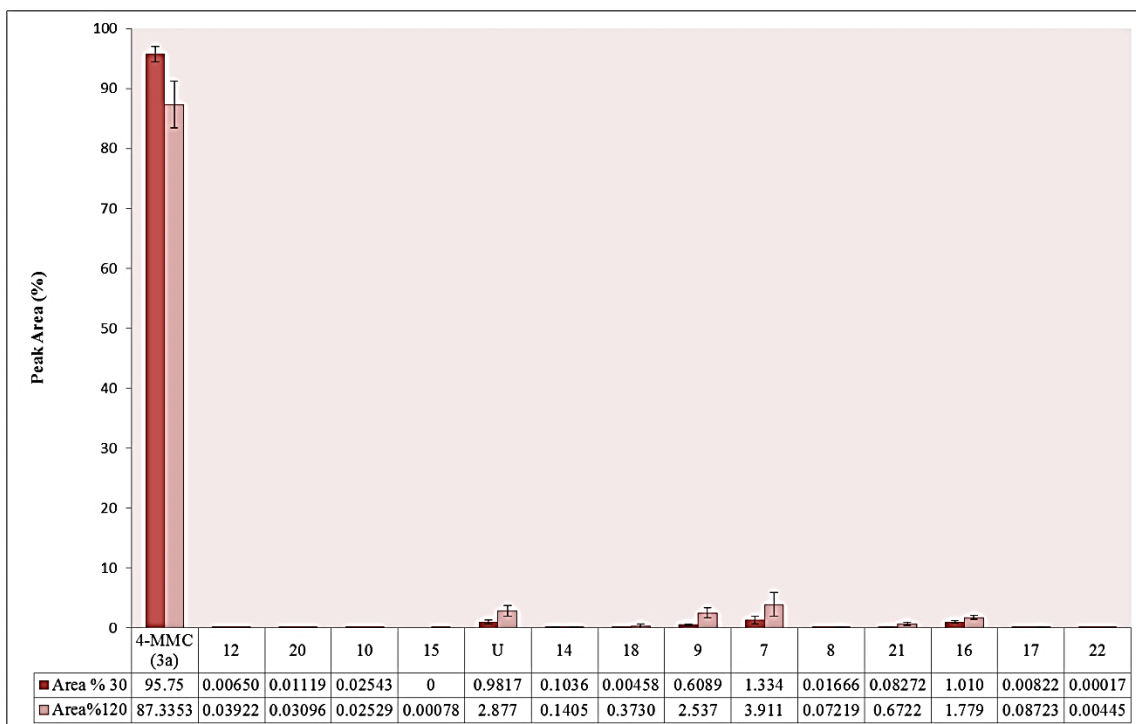


Scheme 12. Proposed scheme for the Phase I and II metabolism of (±)-4'-(trifluoromethyl) methcathinone (4-TFMMC, 3b) in cryopreserved human hepatocytes. Metabolite numbers correspond to the metabolite data presented in Table 26. Key: [A] = acetylation; [R] = reduction; [D] = demethylation; [O] = oxidation; [C] = conjugation; [AH] = aromatic hydroxylation; [M] = methylation (The blue rectangle highlights a most abundance metabolite).

4.5.3 Metabolic profiling of 4-MMC (3a) and 4-TFMMC (3b) in cryopreserved human hepatocytes.

The metabolic profiles of 4-MMC (3a) and 4-TFMMC (3b) were examined in cryopreserved human hepatocytes from the two donors. The Figures 73-74 show that 4-TFMMC(3b) was more extensively metabolised than 4-MMC(3a), however, the rate of Phase I and II metabolism was slow for both drugs, and the most abundant chemical detected in the incubations was the parent drugs themselves. The histogram (Figure 73) of 4-MMC (3a) indicates that normephedrone (7, m/z =164.1069) was formed in larger amounts than the other metabolites detected, and it increased after two hours incubation period by approximately 3%. The hydroxylated metabolites (U, m/z =194.1175) (9, m/z =180.1383) were also increased over the two hour incubation

period by approximately 2%. The major compound detected was mephedrone itself. Very low levels of glucuronidation and acetylation biotransformation could also be observed. There were two trace amounts of glucuronide metabolites that could be detected in one hepatocyte sample (donor HU4215), and these were not present in HU4226 incubation. A possible explanation for this might be that it was probably due to differences in enzyme activities between these two donors. Also, the results of this study indicate that incubation of samples from donor (HU4215) produce higher abundance of Phase I metabolites than the donor (HU4226). Particularly, the results found that donor (HU4215) produced relatively higher abundance of hydroxylated and dealkylated metabolites such as (7, 16, U) in comparison with donor HU4226 and this may account for the production of more Phase II metabolites such as glucuronides.



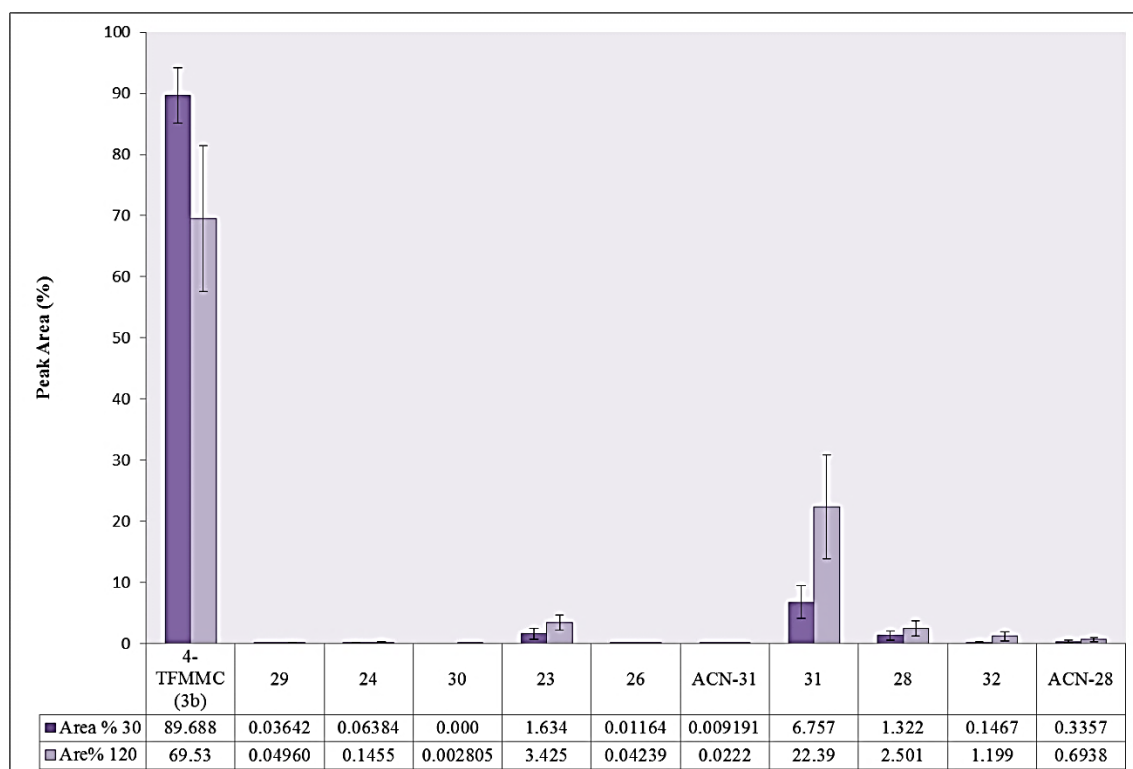
- Amount of metabolites of 4-MMC (3a) formed after 30 min incubation
- Amount of metabolites of 4-MMC (3a) formed after 120 min incubation.

Peak Area (%) = (Peak area of metabolite / sum the Peak areas of all observed compounds) x 100

Figure 74. Relative amounts of metabolites of (\pm)-mephedrone (4-MMC, 3a) formed after incubation with human hepatocytes (n = 4); \pm SEM% area for 4-MMC (3a) = $95.8 \pm 1.3\%$ (30 min) and $87.3 \pm 3.9\%$ (120 min); U = unidentified metabolite ($t_R = 8.3$ min; $m/z = 194.1180$) (The number on the x-axis refer to the metabolite numbers on Table 25 and Scheme 11).

The histogram shown in Figure 74 indicates that the major metabolite of 4-TFMMC (3b) was 4-(trifluoromethyl) ephedrine (31, $m/z=234.10$) that significantly increased after two hours incubation period by approximately 22 %. Two other metabolites were formed in moderate amounts and these were 23 ($m/z= 248.0891$) and 28 ($m/z=218.0787$). Comparing the two donors, it was found that donor HU4215 tended to produce more abundant metabolites levels than donor HU4226, particularly hydroxylated metabolites 31 ($m/z=234.1098$) 23 ($m/z= 248.0891$) and the demethylated metabolite 28 ($m/z=218.0787$). The Phase II metabolites of 4-TFMMC (3b) included a very low level of glucuronidated metabolite 30 ($m/z=410.1059$)

which was observed after two hours incubation period as well as an acetylated metabolite 29 ($m/z = 260.0892$) which was found at a very low levels after 30 and 120 minutes incubations.



■ Amount of metabolites of 4-TFMMC (3b) formed after 30 min incubation.

■ Amount of metabolites of 4-TFMMC (3b) formed after 120 min incubation.

Peak Area (%) = (Peak area of metabolite / sum the Peak areas of all observed compounds) x 100.

Figure 75. Relative amounts of metabolites of (\pm)-4'-(trifluoromethyl) methcathinone (4-TFMMC, 3b) formed after incubation with human hepatocytes (n = 4); \pm SEM% area for 4-TFMMC (3b) = $89.7 \pm 4.5\%$ (30 min) and $69.5 \pm 11.9\%$ (120 min) (The number on the x-axis refer to the metabolite numbers on Table 26 and Scheme 12).

Aliquots were taken from the incubation for measuring half-life of 4-MMC (3a) and 4-TFMMC (3b) at 0, 30, 60, 90, 120 minutes. The linear plots gave the slopes of 4-MMC (3a) and 4-TFMMC (3b) which were determined to be 1.0×10^{-3} and 3.2×10^{-3} , and were used to estimate the metabolic rate constants (k_{met}).

As discussed in chapter 3 and shown in Table 27 , the half-life calculation was conducted using the expression: $t_{1/2} = 0.693/k_{met}$, and the half-lives ($t_{1/2}$) of 4-MMC (3a) and 4-TFMMC (3b) in rat liver hepatocytes were calculated and were found to be: 61.9 min (4-MMC, 3a, n = 3) and 203.8 min (4-TFMMC, 3b, n = 3) respectively [154]. In human hepatocytes the half –life of both drugs was higher than in rat cells and that might be expected due to the difference between the species metabolism rates. Figure 75 shows that 4-TFMMC (3b) was found to have a shorter half-life than 4-MMC (3a); 693.0 minutes and 216.6 minutes for 4-MMC (3a) and 4-TFMMC (3b), respectively.

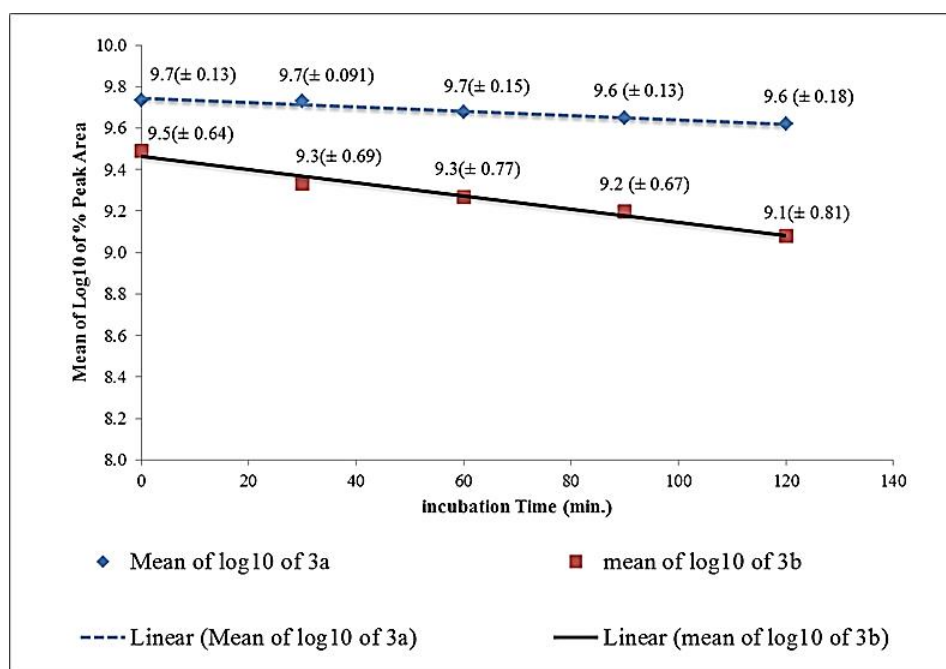


Figure 76. Plot of the rate of decrease (mean Log₁₀ % peak area ±SD) of (±)-mephedrone (4-MMC, 3a, ---, $y = -0.001x + 9.7443$; $r^2 = 0.9656$) and (±)-4-(trifluoromethyl) methcathinone (4-TFMMC, 3b, —, $y = -0.0032x + 9.4655$; $r^2 = 0.9738$) concentrations during incubation with cryopreserved human hepatocytes (n = 4).

Thus, half-lives of 4-MMC (3a) with human hepatocytes incubation and 4-TFMMC (3b) with human and rat incubation were calculated as estimation half-life since they were acquired outside of linear phase of incubation time.

Table 27. Comparison the K_{met} and half-life for both 4-MMC and 4-TFMCC with human and rat hepatocytes.

	Human cells (2=n)	Rat cells (n=3)
4-MMC (3a)		
K_{met} (min^{-1})	1.0×10^{-3}	1.12×10^{-2}
$t_{1/2}$ (minute)	693	61.9
% of unmetabolised drug at 120 minutes (\pm SEM %)	$87.3 \pm 3.9\%$	$16 \pm 15\%$
4-TFMCC (3b)		
K_{met} (min^{-1})	3.2×10^{-3}	3.4×10^{-3}
$t_{1/2}$	216.6	203.8
% of unmetabolised drug at 120 minutes (\pm SEM %)	$69.5 \pm 11.9\%$	$69 \pm 7.6\%$

4.5.4 Comparison of major Phase I and Phase II metabolism reactions in Rat and Cryopreserved Human Hepatocytes

Species differences in the metabolism of drugs are well documented. For example, studies utilising hepatocytes isolated from Wistar rat, Cynomolgus monkey, beagle dog and man incubated in culture for 180 minutes with diazepam, show that the profiles of metabolism of diazepam are quite different between species as well as the differences in the rate of metabolite formation [155].

In the present study, fourteen metabolite peaks of 4-MMC (3a) in cryopreserved human hepatocytes were detected, and are listed in the Table 25 according to their order of retention time. In comparison to the rat hepatocyte incubations previously reported, metabolites 19 ($m/z = 370.1495$) and 11 ($m/z = 222.1124$) were not detected in human cells. Nine metabolite peaks of 4-TFMCC in human hepatocytes were detected (Table 27) and in comparison with the rat hepatocytes, the human cells did not form metabolites 27 ($m/z = 424.1212$) and 33 ($m/z = 396.1263$) and 25 ($m/z = 422.1055$).

As reported in Chapter 3 after incubation with rat hepatocytes about 50% of 4-MMC(3a) was metabolised up to 120 minutes[154]. It was more rapidly metabolised

than in human hepatocytes even though the Phase II metabolites were low in both rat and human hepatocytes. Comparing the two results, it can be seen that very low metabolic reaction rate of human hepatocytes leads to the absence of some of Phase II metabolites.

4-MMC (3a) and 4-TFMMC (3b) were incubated with human hepatocytes on the same 24 well plate and both were exposed to the same conditions, but 4-TFMMC (3b) was more extensively metabolised than 4-MMC (3a). The human metabolic reaction of 4-TFMMC was accelerated by reduction of the keto moiety of 4-TFMMC which only occurred at a low levels with 4-MMC. In contrast with rat hepatocytes, 4-MMC is more rapidly metabolised than 4-TFMMC.

The increased rate of reduction of the keto moiety in 4-TFMMC (3b) in comparison with 4-MMC (3a) might be related to the electron withdrawing effect of the trifluoromethyl group which render the keto moiety more susceptible to nucleophilic attack.

In summary, we have shown similar metabolic pathways in rat and human hepatocytes. The known metabolic pathways for 4-MMC (3a) and 4-TFMMC (3b) were confirmed in this study. The investigation of rat and human hepatocytes showed formation of almost the same Phase I and II metabolites of 4-MMC (3a) and 4-TFMMC (3b), but with slower metabolism in human cells. Phase II reactions in human cells were lower than in rat and sometimes could not be detected. LC-MS cannot distinguish between endogenous compounds and metabolites which have the same m/z , such as the mass spectrum of m/z 222.1124 shown in Figure 77-D that may be belonged to metabolite 11 which can be observed in MS spectrum, but its peak could not be observed in Figure 77-B at 30minute and Figure 77-C at 120 minute, due to small intensity of this metabolite.

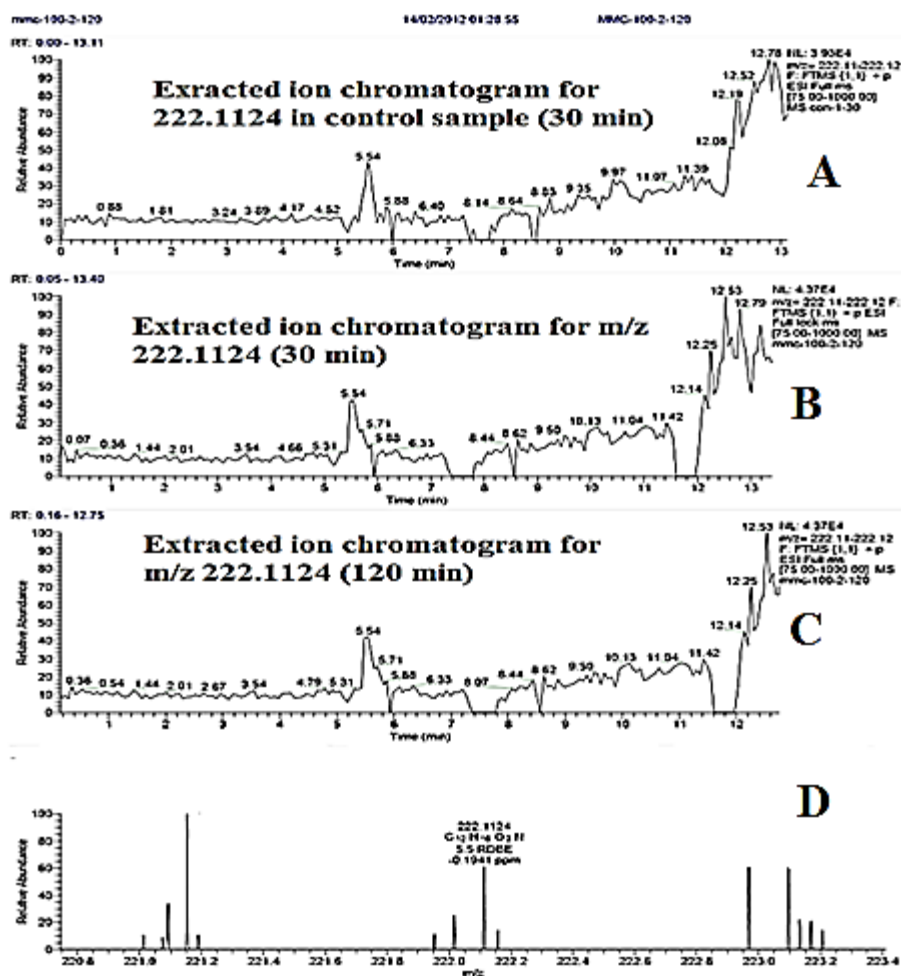


Figure 77. Extracted ion chromatograms of m/z 222.1224 of (A) control, and the human hepatocytes incubation with 4-MMC in (B) 30 minute (C) 120 minute and, note that peak at 5.54 minute is also seen in the control incubation and therefore is due to endogenous metabolite.

Comparing Phase I metabolites between rat and human hepatocytes it was found that demethylation of 4-MMC (3a) (7, $m/z=$ 164.107) and 4-TFMMC (3b) (28, $m/z=$ 218.0787) were more extensive in rat than human hepatocytes. In contrast, the reduction of the keto moiety of both 4-MMC (3a) (9, $m/z =$ 180.1382) and 4-TFMMC (3b) (31, $m/z =$ 234.1098) was greater in human hepatocytes than rat hepatocytes after a two hour incubation period. Glucuronidation of 4-MMC (3a) and 4-TFMMC (3b) with rat and human hepatocytes can be observed yielding *O*-

glucuronide metabolites in aromatic ring in both. In rat hepatocytes and additional glucuronide metabolite was formed in comparison with human hepatocytes. The *N*-glucuronide metabolite of 4-MMC (3a) (33, $m/z= 396.1263$) was present in rat hepatocytes and absent in human.

Although, some glucuronides were yielded in both drugs during incubation with rat and human hepatocytes, rat hepatocytes yielded greater amounts of glucuronides of 4-MMC(3a) (15, $m/z= 356.1337$), (22, $m/z= 384.1289$) and 4-TFMMC(3b) (30, $m/z= 410.1059$) than human hepatocytes.

4.6 Conclusions

Determination of the metabolism profile of mephedrone (3a, 4-MMC) and analogue of mephedrone (3b, 4-TFMMC) using human hepatocytes was very useful. The results showed that the biotransformation rates of 4-MMC (3a) and 4-TFMMC (3b) in human cells were always lower than those found previously in rat hepatocytes and presented in chapter 3. The rate of metabolism showed some differences between species. Also the analyses of cryopreserved human hepatocyte enzymes in this chapter can provide a background for assessing 4-MMC (3a) and 4-TFMMC (3b) metabolism reactions in human hepatocytes.

Although a site for metabolism of 4-TFMMC (3b) is blocked on the aromatic ring by modification with CF_3 , cryopreserved human hepatocytes metabolised 4-TFMMC (3b) faster than 4-MMC (3a). The rate of metabolism of 3b was accelerated by reduction of the keto moiety and formed dihydro-4-TFMMC (31, $t_R=9.7$ min, $m/z = 234.1098$), while the reduction of keto moiety in 4-MMC (3a) forms dihydromephedrone (9, $t_R=10.2$ min, $m/z = 180.1382$) with lower abundance compared with demethylation (7, $m/z = 164.1070$), which can be considered as the dominant 4-MMC (3a) metabolism pathway in human hepatocytes. 4-TFMMC in which the methyl moiety was replaced with CF_3 (4-trifluoromethyl moiety) thus blocking metabolism at this site and thus had a longer half-life than 4-MMC (3a) in rat hepatocytes. Surprisingly in human hepatocytes 4-TFMMC (3b) has shorter half-life than 4-MMC (3a) but this might be attributed to effects of the CF_3 , which is para to the ketone group, activating the keto group so that it is more susceptible to reduction.

Measurable quantities of Phase II metabolic pathways of 4-MMC (3a) and 4-TFMMC (3b) within rat hepatocyte were identified in our laboratory, while human production of these metabolites was not detected except as trace amounts of some Phase II conjugates, with lower acetates and glucuronide formation and also a large variation between the two different donors.

In this thesis, the findings indicate that although incubation of both rat and human hepatocytes with cathionines was performed using different protocols, they were able to give a comparable estimation between the metabolism observed by rat hepatocyte

and human hepatocytes for the major metabolic pathways of 4-MMC (3a) and 4-TFMMC (3b). Both incubations were performed with the same drug concentration, and the incubation time. Results of incubations 4-MMC (3a) and 4-TFMMC (3b) with human and rat hepatocytes indicate that these systems were able to give an estimated comparison of metabolic pathways between the two species by determining the amount of metabolites formed by them.

Chapter 5: Summary and suggestions for Future work

5.1 Summary

The findings of the thesis are summarised below chapter by chapter.

Chapter 2

- The cathinone constituents in NRG-2 products on the UK market were identified by producing a fully validated HPLC method. Law enforcement agencies require robust analytical methods to identify and quantify existing and new “legal highs” either in their pure form or adulterated samples.
- Characterization of three NRG-2 products was carried out by using NMR, HPLC, AT-IR, and LC-MS methods. In the current studies, two mephedrone derivatives and mephedrone itself were detected in three of the NRG-2 samples which were purchased online from UK-based websites. Reference samples of the two mephedrone derivatives (4-MEC,3c) and (4-MBC,3d) were synthesised as hydrobromide salts (racemic compounds) using previous methods reported by Sutcliffe *et al.* for mephedrone[63]. The full structural elucidation of these compounds was reported , NMR data were obtained at 60 °C in *d*₆-DMSO, and full spectral analysis using 2D HMQC and HMBC methods allowed clear assignment of all carbon and hydrogen resonances. The HRESIMS analysis of 4-MEC(3c) and 4-MBC(3d) using LC-MS Orbitrap gave [M+H]⁺ peak at *m/z* = 192.1381 and *m/z* = 254.1537 respectively, in which confirmed the molecular formula of 4-MEC(3c) (C₁₂H₁₈NO) and of 4-MBC(3d) (C₁₇H₂₀NO) that were consistent with Brandt *et al.* [19] and Jankovics *et al.*[116], with observed the CID fragment ions for both compounds. Also , the infrared spectra of 4-MEC (3c) and 4-MBC (3d) were collected on an ATR-FTIR spectrometer ; the spectra were consistent with the spectra which were previously obtained for mephedrone(3a,4-MMC) [63] and 4-MEC(3c) [116].

- The validated HPLC method [63] for mephedrone that had been published, was not fully validated for analysis of other mephedrone derivatives. This method was further validated to screen mephedrone and the two mephedrone derivatives that were detected in the three NRG-2 samples.
- The LC-MS data of the three NRG-2 products showed that samples contains mephedrone and two compounds; the major compound was 4-MEC (3c) and the minor compound was 4-MBC (3d), they gave both characteristic mass spectra and characteristic signals in NMR spectra that were consistent with the data obtained for reference samples of 4-MEC (3c) and 4-MBC (3d).
- The HPLC method was revalidated again to screen ten NRG-2 street samples which were purchased online from different UK-based websites. Mephedrone (3a, 4-MMC), 4-MEC (3c), 4-MBC (3d), 4-FMC and MDPV were detected in some of these samples. The data presented revealed that 90% of the NRG-2 samples examined here were found to contain a mixture of cathinone substances which have been banned under the Misuse of Drugs Act 1971. It was found that nine of ten samples contained five different cathinone derivatives in presence of the common adulterants benzocaine and caffeine.

In Chapter 3

- 4-MMC (3a), 4-TFMMC (3b) and 4-MEC (3c) were synthesized in house. The metabolism of them was studied in freshly isolated rat hepatocytes. Structural elucidation for the metabolites was carried out by LC-MS² using HILIC column with an LTQ-Orbitrap mass spectrometer. Phase I and II metabolites were detected for 4-MMC (3a), 4-TFMMC (3b) and 4-MEC (3c) incubated with hepatocytes with a range of metabolites including several glucuronides being detected. The results were partly consistent with Meyer *et al.*, who only described the Phase I metabolism of mephedrone and other cathinone derivatives using GC-MS techniques.

- The study compared both Phase I and II metabolism of mephedrone and its analogues, as well as demonstrated the ability of the Orbitrap LC-MS instrument to clearly detect low abundance of metabolites due to the dynamic range of the instrument that was sufficient to show both major and minor metabolites. The ZIC-HILIC column was found to be more satisfactory for the separation of the mephedrone and its metabolites since in comparison a C₁₈ column produced retention of polar hydroxylated metabolites and glucuronides of mephedrone. For 4-MMC (3a) and seventeen metabolites were putatively identified in the rat hepatocytes. 4-TFMMC (3b) was metabolised more slowly than mephedrone and eleven metabolites were putatively identified.
- Analysis of 4-MMC (3a) and 4-TFMMC (3b), following their incubation with rat hepatocytes suspension, by LC-MS was able to identify the metabolites of 4-MMC (3a) and 4-TFMMC (3b). The major metabolism pathways for 4-MMC (3a) which were observed after 30 minutes incubation were demethylation (normephedrone, 7) and oxidation of the tolyl moiety (4'-(hydroxymethyl)methcathinone, 16 and 4'-(carboxy)methcathinone, 21). The minor pathways were observed was conjugation with glucuronic acid. Glucuronidation was clearly observed after 120 minutes as well as acetylation (Phase II). The major metabolic pathways of 4-TFMMC (3b) were found to be demethylation (4'-(trifluoromethyl) cathinone, 28), and reduction of the ketone group ((±)-4'-(trifluoromethyl) ephedrine, 31) and ((±)-4'-(trifluoromethyl) norephedrine, 32). The modification of the 4'-methyl- to the corresponding isosteric 4'-trifluoromethyl- group in (3b) blocks the possibility oxidation of the tolyl group which occurs in (3a) and this may be responsible, to a large extent, for slowing down the overall metabolism. However, small amounts of glucuronidation metabolism could also be detected. The lower levels of hydroxylation and subsequent glucuronidation contribute to making the *in vitro* pharmacokinetics of the 4'-trifluoromethyl analogue of (±)-mephedrone in hepatocytes very different from those of the parent drug (3a). We found the rat hepatocytes also catalysed both Phase I and II metabolism pathways of 4-MEC (3c) and overall eighteen metabolites

were putatively identified. 4-MEC (3c) was metabolised more rapidly than mephedrone and the major metabolic pathways were as oxidation (metabolite 37) or acetylation (metabolite 47). Desethylation could also be detected as well as reduction (metabolite 41). Also the Phase II metabolism was observed as a glucuronic acid conjugation (metabolite 39 and 46) and showed the highest level of glucuronide formation at 120 minute and also *N*-acetylation (metabolite 42).

The half-lives ($t_{1/2}$) of 4-MMC (3a), 4-TFMMC (3b) and 4-MEC (3c) were calculated using expression: $t_{1/2} = 0.693/k_{met}$ to be: 61.9, 203.8 and 8.3 minutes respectively. The metabolic rate constants (k_{met}) were estimated for each compound from the slope of the plots of the rate of decrease for each compound.

Chapter 4

- Phase I and II metabolism of mephedrone (4-MMC, 3a) and 4-TFMMC (3b) were determined *in vitro* through incubation in cryopreserved human hepatocytes. The results were compared to those were previously found in rat hepatocytes in order to identify the differences in metabolism between the species. Following 2 h of incubation of 3a and 3b with cryopreserved human cells metabolism was found to be slower than in rat hepatocytes. The reduction of the keto moiety of both 4-MMC (3a) and 4-TFMMC (3b) resulting metabolites 9 and 31 was found to be greater in human hepatocytes than rat hepatocytes. In contrast, the demethylation of 4-MMC (3a) (metabolite 7) and 4-TFMMC (3b) (metabolite 28) was more extensive in rat than human hepatocytes after a two hour incubation period. Glucuronidation and acetylation pathways could also be observed in human hepatocytes in trace amounts due to the slow rate for producing Phase I metabolism. This result supports the idea that conjugation with glucuronic acid and acetylation are the main Phase II metabolic pathways in these compounds. In addition, no sulphate products were observed after incubation with both rat and human hepatocytes. The $t_{1/2}$ values were also calculated for each compound and a significant increase in $t_{1/2}$ was found in human hepatocytes (693.0 minutes for

4MMC (3a) and 216.6 for 4-TFMMC (3b)) in comparison with rat hepatocytes.

- Cathinone derivatives metabolism was measured in hepatocytes isolated from the two adult male donors (HU4215, HU4226). Selected metabolizing enzymes within the hepatocytes were characterised by Life Technologies laboratories for activity and expression. The expression of 13 CYP isoform enzymes, including CYP2D6, was determined in human hepatocytes which were obtained from the two donors.

5.2 Future work

After completing the work described in this thesis, future work was planned for cathinone derivative substances and legal highs includes:

- Analysis of additional street-samples.
- Metabolism studies of the other cathinones derivatives which were detected in our studies such as 4-MBC (3d) that found in NRG-2.
- Biological samples obtained from patients could be also used to examine the metabolic pathways of cathinone derivatives *in vivo* and compared to these results obtained from the experiments rat and cryopreserved human hepatocytes.
- Also synthesis of reference standards of proposed metabolites would be carried out to confirm the identity of putative metabolites that were observed.
- Additional human liver samples would be incubated with the drugs to characterise more fully the extent and nature of CYP2D6 involvement in the metabolism. Incidence of serious side effects from mephadrone could be related to the genetic polymorphism of CYP2D6 activity. Inhibitors such as quinidine could be used to find out whether or not this isoform is the main isoenzyme responsible for metabolism.
- Metabolomic studies (Identification and quantification of all metabolites in a biological system) [156] could be carried out with rat hepatocytes, cryopreserved human hepatocytes as well as human volunteers; this may explain the toxicity that is found with users who consumed cathinone products. Studying of organism's behaviour in terms of metabolic changes is possible through metabolomics, and various metabolic pathways can help researcher to predict the toxic effects and effectiveness of cathinone derivatives.

5.3 Final comments

The legal high compounds that are used as recreational drugs are rapidly modified, and available scientific literature is not yet sufficient to acquire technical knowledge and understanding of the nature and effects of these newly designed compounds. Thus it becomes very difficult, if not impossible, for health professionals and doctors to make accurate assessments of possible drug-related medical effects.

Mephedrone is one of the more common of legal high substances and it is available to purchase online as “plant feeder, not for human consumption” as well as being sold under a number of different brand names. It is desirable as it elicits euphoria, sociability, stimulation, sexual arousal and appreciation, but a lack of information about long-term side effects and toxicity despite it found on social networking sites, such as Facebook, Twitter and You Tube, means that mephedrone is associated with a number of negative side effects, including hallucinations, vasoconstriction, and possible psychosis. This project has demonstrated the information that can be shared to build up a reasonably accurate understanding of the characteristics of these recreational compounds. Also this project provides vital information on metabolism for many health professionals to fill the gap in knowledge about the effects and side effects of these substances on the users.

The findings in our studies appear to support the ban of cathinone derivatives as this thesis has focused on the characterization and pharmacokinetics of cathinone derivatives, which showed that the products purchased as mephedrone derivatives contain various novel substances within a single product. These substances were associated with a risk of severe poisoning or even death, which provides new challenges in clinical and forensic toxicological practice. *In vitro* metabolism findings can provide information that can be used to predict the *in vivo* metabolic pathways as well as likely pharmacokinetic behaviour within this class of controlled drugs. This could provide an understanding the toxicity risks for these substances.

References

1. Boys, A., J. Marsden, and J. Strang, *Understanding reasons for drug use amongst young people: a functional perspective*. Health Education Research, 2001. **16**(4): p. 457-469.
2. Siegel, R.K., *Intoxication : The universal Drive for Mind-Altering Substances*. 3 ed. 2005: Inner Traditions, Bear & Co.
3. Davies, S., et al., *Purchasing 'legal highs' on the Internet—is there consistency in what you get?* QJM, 2010. **103**(7): p. 489-493.
4. *Single Convention on Narcotic Drugs, 1961*. [cited 2013 16/02/2013]; Available from: http://www.unodc.org/pdf/convention_1961_en.pdf.
5. *Convention on Psychotropic Substances, 1971*. [cited 2013 16/02/2013]; Available from: http://www.unodc.org/pdf/convention_1971_en.pdf.
6. *Convention against the Illicit Traffic in Narcotic Drugs and Psychotropic Substances, 1988*". [cited 2013 16/02/2013]; Available from: http://www.unodc.org/pdf/convention_1988_en.pdf.
7. [cited 2013 16/02/2013]; Available from: <http://webarchive.nationalarchives.gov.uk/http://www.homeoffice.gov.uk/drugs/drugs-law/Class-a-b-c/>.
8. DrugScope. *Drug laws The Misuse of Drugs Act 1971* [cited 2013 16/02/2013]; Available from: <http://www.drugscope.org.uk/resources/drugsearch/drugsearchpages/laws>.
9. *The Misuse of Drugs Regulations 2001*, . 2001 [cited 2013 16/02/2013]; Available from: <http://www.legislation.gov.uk/uksi/2001/3998/made>.
10. Rojek, S., et al., *"Legal highs"—Toxicity in the clinical and medico-legal aspect as exemplified by suicide with bk-MBDB administration*. Forensic science international, (0).
11. Gibbons, S. and M. Zloh, *An analysis of the 'legal high' mephedrone*. Bioorganic & Medicinal Chemistry Letters, 2010. **20**(14): p. 4135-4139.
12. Zawilska, J.B., *"Legal highs" - new players in the old drama*. Curr Drug Abuse Rev, 2011. **4**(2): p. 122-30.

13. Ramsey, J., et al., *Buying 'legal' recreational drugs does not mean that you are not breaking the law*. QJM, 2010. **103**(10): p. 777-783.
14. Coppola, M. and R. Mondola, *Research chemicals marketed as legal highs: The case of pipradrol derivatives*. Toxicology Letters, 2012. **212**(1): p. 57-60.
15. EMCDDA and Europol, *EMCDDA–Europol 2011 Annual Report on the implementation of Council Decision 2005/387/JHA*, 2012: Lisbon.
16. Camilleri, A., et al., *Chemical analysis of four capsules containing the controlled substance analogues 4-methylmethcathinone, 2-fluoromethamphetamine, α -phthalimidopropiophenone and N-ethylcathinone*. Forensic science international, 2010. **197**(1): p. 59-66.
17. Zuba, D., *Identification of cathinones and other active components of 'legal highs' by mass spectrometric methods*. TrAC Trends in Analytical Chemistry, 2012. **32**(0): p. 15-30.
18. Gibbons, S. and M. Zloh, *An analysis of the 'legal high' mephedrone*. Bioorganic & Medicinal Chemistry Letters, 2010. **20**(14): p. 4135-4139.
19. Brandt, S.D., et al., *Analyses of second-generation 'legal highs' in the UK: Initial findings*. Drug Testing and Analysis, 2010. **2**(8): p. 377-382.
20. Hillebrand, J., D. Olszewski, and R. Sedefov, *Legal Highs on the Internet*. Substance Use & Misuse, 2010. **45**(3): p. 330-340.
21. Dick, D. and C. Torrance, *'MixMag Drugs Survey'*, 2010, Mix Mag 225. p. 44-53.
22. Winstock, A., *'The 2011 Mixmag drugs survey'*. Mixmag March 2011.
23. Kalix, P. and O. Braenden, *PHARMACOLOGICAL ASPECTS OF THE CHEWING OF KHAT LEAVES*. Pharmacological Reviews, 1985. **37**(2): p. 149-164.
24. Kalix, P., *Cathinone, an alkaloid from khat leaves with an amphetamine-like releasing effect*. Psychopharmacology, 1981. **74**(3): p. 269-270.
25. Litman, A., et al., *The use of khat. An epidemiological study in two Yemenite villages in Israel*. Culture, medicine and psychiatry, 1986. **10**(4): p. 389-396.
26. Al-Motarreb, A., K. Baker, and K.J. Broadley, *Khat: Pharmacological and medical aspects and its social use in Yemen*. Phytotherapy Research, 2002. **16**(5): p. 403-413.

27. Kalix, P., *Catha edulis, a plant that has amphetamine effects*. Pharmacy World & Science, 1996. **18**(2): p. 69-73.
28. ACMD, *Consideration of the cathinones, 31 March*. Available at: *cathinodes-report-2010.*, A.C.o.t.M.o. Drugs, Editor 2010: London.
29. Deluca, P. and F. Schifano, *The Psychonaut Web Mapping Project 2008-2009*.
30. Ghodse, H., et al., *Drug-related deaths in the UK: annual report 2010*, 2010, International Centre for Drug Policy, St George's University of London: London. p. p.77.
31. Kelly, J.P., *Cathinone derivatives: a review of their chemistry, pharmacology and toxicology*. Drug Test Anal, 2011. **3**(7-8): p. 439-53.
32. Prosser, J.M. and L.S. Nelson, *The toxicology of bath salts: a review of synthetic cathinones*. J Med Toxicol, 2012. **8**(1): p. 33-42.
33. Kavanagh, P., et al., *The characterization of 'legal highs' available from head shops in Dublin (Poster)*. , in *The National Drug Advisory and Drug Treatment Board 2010*: Dublin, Ireland.
34. Cawrse, B.M., et al., *Distribution of Methylone in Four Postmortem Cases*. Journal of Analytical Toxicology, 2012. **36**(6): p. 434-439.
35. Cox, G. and H. Rampes, *Adverse effects of khat: a review*. Advances in Psychiatric Treatment, 2003. **9**(6): p. 456-463.
36. *The Mechanism of Action of amphetamine (low-dose)* , Lundbeck Institute, CNSforum, Educational Resources, Image Bank, http://www.cnsforum.com/imagebank/item/Drug_amphet_low/default.aspx . . [cited 2013 16/02/2013].
37. Al-Motarreb, A., M. Al-Habori, and K.J. Broadley, *Khat chewing, cardiovascular diseases and other internal medical problems: the current situation and directions for future research*. J Ethnopharmacol, 2010. **132**(3): p. 540-8.
38. Drake, P.H., *Khat-chewing in the near east* The Lancet, 1988. **331**(8584): p. 532-533.

39. Sparago, M., et al., *Neurotoxic and pharmacologic studies on enantiomers of the N-methylated analog of cathinone (methcathinone): a new drug of abuse*. J Pharmacol Exp Ther, 1996. **279**(2): p. 1043-52.
40. Elias, L.J. and D.M. Saucier, *Neuropsychology: Clinical and Experimental Foundations*. 2006: Pearson/Allyn & Bacon.
41. Kalix, P., *Effect of the alkaloid (-)-cathinone on the release of radioactivity from rat striatal tissue prelabelled with 3H-serotonin*. Neuropsychobiology, 1984. **12**(2-3): p. 127-9.
42. Pehek, E.A., M.D. Schechter, and B.K. Yamamoto, *Effects of cathinone and amphetamine on the neurochemistry of dopamine in vivo*. Neuropharmacology, 1990. **29**(12): p. 1171-1176.
43. Zelger, J.L., H.X. Schorno, and E.A. Carlini, *Behavioural effects of cathinone, an amine obtained from Catha edulis Forsk.: comparisons with amphetamine, norpseudoephedrine, apomorphine and nomifensine*. Bull Narc, 1980. **32**(3): p. 67-81.
44. Valterio, C. and P. Kalix, *The effect of the alkaloid (-)-cathinone on the motor activity in mice*. Arch Int Pharmacodyn Ther, 1982. **255**(2): p. 196-203.
45. Babayan, E.A., N.K. Barkov, and A.I. Machula, *Mediator mechanisms of cathinone effects on animal behaviour*. Drug Alcohol Depend, 1983. **12**(1): p. 31-5.
46. Nencini, P. and A.M. Ahmed, *Khat consumption: a pharmacological review*. Drug Alcohol Depend, 1989. **23**(1): p. 19-29.
47. Kebede, D., et al., *Khat and alcohol use and risky sex behaviour among in-school and out-of-school youth in Ethiopia*. BMC Public Health, 2005. **5**: p. 109.
48. Widler, P., et al., *Pharmacodynamics and pharmacokinetics of khat: a controlled study*. Clin Pharmacol Ther, 1994. **55**(5): p. 556-62.
49. Brenneisen, R., et al., *Amphetamine-like effects in humans of the khat alkaloid cathinone*. Br J Clin Pharmacol, 1990. **30**(6): p. 825-8.
50. Glennon, R.A., M.D. Schechter, and J.A. Rosecrans, *Discriminative stimulus properties of S(-)- and R(+)-cathinone, (+)-cathine and several structural modifications*. Pharmacol Biochem Behav, 1984. **21**(1): p. 1-3.

51. Nagai, F., R. Nonaka, and K. Satoh Hisashi Kamimura, *The effects of non-medically used psychoactive drugs on monoamine neurotransmission in rat brain*. *European Journal of Pharmacology*, 2007. **559**(2–3): p. 132-137.
52. Calkins, R.F., G.B. Aktan, and K.L. Hussain, *Methcathinone: the next illicit stimulant epidemic?* *J Psychoactive Drugs*, 1995. **27**(3): p. 277-85.
53. Gygi, M.P., J.W. Gibb, and G.R. Hanson, *Methcathinone: an initial study of its effects on monoaminergic systems*. *J Pharmacol Exp Ther*, 1996. **276**(3): p. 1066-72.
54. Belhadj-Tahar, H. and N. Sadeg, *Methcathinone: a new postindustrial drug*. *Forensic Sci Int*, 2005. **153**(1): p. 99-101.
55. Cozzi, N.V. and K.F. Foley, *Methcathinone is a Substrate for the Serotonin Uptake Transporter**. *Pharmacology & Toxicology*, 2003. **93**(5): p. 219-225.
56. de Bie Ra, G.R.M.S.A.P.K.J.L.A.E., *Manganese-induced parkinsonism associated with methcathinone (ephedrone) abuse*. *Archives of Neurology*, 2007. **64**(6): p. 886-889.
57. *RECOMMENDED METHODS FOR THE IDENTIFICATION AND ANALYSIS OF AMPHETAMINE, METHAMPHETAMINE AND THEIR RING-SUBSTITUTED ANALOGUES IN SEIZED MATERIALS*. 2006 [cited 2013 16/02/2013]; Available from: <http://www.unodc.org/pdf/scientific/stnar34.pdf>.
58. Paul, B.D. and K.A. Cole, *Cathinone (Khat) and methcathinone (CAT) in urine specimens: a gas chromatographic-mass spectrometric detection procedure*. *J Anal Toxicol*, 2001. **25**(7): p. 525-30.
59. Brandt, S.D., P.F. Daley, and N.V. Cozzi, *Analytical characterization of three trifluoromethyl-substituted methcathinone isomers*. *Drug Test Anal*, 2012. **4**(6): p. 525-9.
60. McDermott, S.D., et al., *The analysis of substituted cathinones. Part 2: an investigation into the phenylacetone based isomers of 4-methylmethcathinone and N-ethylcathinone*. *Forensic Sci Int*, 2011. **212**(1-3): p. 13-21.
61. Sorensen, L.K., *Determination of cathinones and related ephedrines in forensic whole-blood samples by liquid-chromatography-electrospray tandem*

- mass spectrometry*. J Chromatogr B Analyt Technol Biomed Life Sci, 2011. **879**(11-12): p. 727-36.
62. Ammann, D., et al., *Detection and Quantification of New Designer Drugs in Human Blood: Part 2 – Designer Cathinones*. Journal of Analytical Toxicology, 2012. **36**(6): p. 381-389.
 63. Santali, E.Y., et al., *Synthesis, full chemical characterisation and development of validated methods for the quantification of (±)-4'-methylmethcathinone (mephedrone): A new “legal high”*. Journal of Pharmaceutical and Biomedical Analysis, 2011. **56**(2): p. 246-255.
 64. Mohr, S., M. Taschwer, and M.G. Schmid, *Chiral separation of cathinone derivatives used as recreational drugs by HPLC-UV using a CHIRALPAK® AS-H column as stationary phase*. Chirality, 2012. **24**(6): p. 486-492.
 65. Kamata, H.T., et al., *Metabolism of the recently encountered designer drug, methylone, in humans and rats*. Xenobiotica, 2006. **36**(8): p. 709-723.
 66. Meyer, M.R. and H.H. Maurer, *Metabolism of Designer Drugs of Abuse: An Updated Review*. Current Drug Metabolism, 2010. **11**(5): p. 468-482.
 67. Meyer, M.R., et al., *Beta-keto amphetamines: studies on the metabolism of the designer drug mephedrone and toxicological detection of mephedrone, butylone, and methylone in urine using gas chromatography-mass spectrometry*. Analytical and Bioanalytical Chemistry, 2010. **397**(3): p. 1225-1233.
 68. Pedersen, A.J., et al., *In vitro metabolism studies on mephedrone and analysis of forensic cases*. Drug Testing and Analysis, 2012: p. n/a-n/a.
 69. Maurer, H.H., *Chemistry, pharmacology, and metabolism of emerging drugs of abuse*. Ther Drug Monit, 2010. **32**(5): p. 544-9.
 70. Kamata, H.T., et al., *Metabolism of the recently encountered designer drug, methylone, in humans and rats*. Xenobiotica, 2006. **36**(8): p. 709-23.
 71. Zaitso, K., et al., *Determination of the metabolites of the new designer drugs bk-MBDB and bk-MDEA in human urine*. Forensic science international, 2009. **188**(1-3): p. 131-139.
 72. Mueller, D. and K. Rentsch, *Generation of metabolites by an automated online metabolism method using human liver microsomes with subsequent*

- identification by LC-MS(n), and metabolism of 11 cathinones.* Analytical and Bioanalytical Chemistry, 2012. **402**(6): p. 2141-2151.
73. Mueller, D., et al., *Development of a fully automated toxicological LC-MSⁿ screening system in urine using online extraction with turbulent flow chromatography.* Analytical and Bioanalytical Chemistry, 2011. **400**(1): p. 89-100.
74. Arias, I., et al., *The Liver: Biology and Pathobiology.* 2011: John Wiley & Sons.
75. Block, J. and J.M. Beale, *Wilson & Gisvold's Textbook of Organic Medicinal and Pharmaceutical Chemistry.* 2003: Lippincott Williams & Wilkins,(Chapter 4:p.66).
76. Li, A.P., *Primary Hepatocyte Cultures as an in Vitro Experimental Model for the Evaluation of Pharmacokinetic Drug–Drug Interactions,* in *Advances in Pharmacology*, P.L. Albert, Editor. 1997, Academic Press. p. 103-130.
77. Mudra, D.R. and A. Parkinson, *Preparation of Hepatocytes,* in *Current Protocols in Toxicology.* 2001, John Wiley & Sons, Inc.
78. Rauckman, E.J. and G.M. Padilla, *The Isolated hepatocyte: use in toxicology and xenobiotic biotransformations.* 1987: Academic Press (Chapter 4 : pp.70-72).
79. Patrick, G.L., *An Introduction to Medicinal Chemistry.* 2009: Oxford University Press, USA (Chapter 11: pp.157-163).
80. Gibson, G.G. and P. Skett, *Introduction to Drug Metabolism,* 2001, Nelson Thomas: London. p. 204-214.
81. Gibson, G.G. and P. Skett, *Introduction to Drug Metabolism.* 2001: Nelson Thornes Publishers, pp.196-197.
82. Ramanathan, R., S.K. Chowdhury, and K.B. Alton, *Chapter 10 Oxidative metabolites of drugs and xenobiotics: lc-ms methods to identify and characterize in biological matrices,* in *Progress in Pharmaceutical and Biomedical Analysis*, K.C. Swapan, Editor. 2005, Elsevier. p. 225-276.
83. Levy, G., *Sulfate conjugation in drug metabolism: role of inorganic sulfate.* Fed Proc, 1986. **45**(8): p. 2235-40.

84. Wang, W. and N. Ballatori, *Endogenous Glutathione Conjugates: Occurrence and Biological Functions*. Pharmacological Reviews, 1998. **50**(3): p. 335-356.
85. Lemke, T.L., et al., *Foye's Principles of Medicinal Chemistry*. 2012, Wolters Kluwer Health, p.152.
86. Evans, G., *Phase II enzymes Gary Manchee Maurice Dickins and Elizabeth Pickup*, in *A Handbook of Bioanalysis and Drug Metabolism*. 2004, Taylor & Francis. p. 223.
87. Rouessac, F. and A. Rouessac, *Chemical Analysis: Modern Instrumentation Methods and Techniques*. 2007: John Wiley & Sons.
88. *Getting Started in HPLC*. 2001 [cited 2013 03/05/2013]; Available from: <http://www.lcresources.com/resources/getstart/3c01.htm#top>.
89. Watson, D.G., *Pharmaceutical Analysis a textbook for pharmacy students and pharmaceutical chemists* 2005: Elsevier Limited (Chapter 12:pp.268-269). 190-191.
90. Golkiewicz, W., A. Blazewicz, and D. Matosiuk, *Use of binary and ternary mobile phases in reversed-phase high performance liquid chromatographic separation of chiral compounds*. J Sep Sci, 2004. **27**(4): p. 304-10.
91. Fountain, S.T., *A Mass Spectrometry Primer*, in *Mass spectrometry in Drug Discovery*, D.T. Rossi and M.W. Sinz, Editors. 2002, Marcel Dekker, Inc.: New York. p. 420.
92. Watson, D.G., *The potential of mass spectrometry for the global profiling of parasite metabolomes*. Parasitology, 2010. **137**(9): p. 1409-23.
93. Soares, R., et al., *Mass spectrometry and animal science: Protein identification strategies and particularities of farm animal species*. Journal of Proteomics, 2012. **75**(14): p. 4190-4206.
94. Cohen, L.R.H. and D.T. Rossi, *The LC/MS Experiment*, in *Mass spectrometry in Drug Discovery*, D.T. Rossi and M.W. Sinz, Editors. 2002, Marcel Dekker, Inc.: New York. p. 138-139.
95. *The Interdepartmental Equipment Facility*. 2009 [cited 2013 03/05/2013]; Available from: <http://departments.agri.huji.ac.il/zabam/Polaris-Q.html>.

96. Makarov, A., et al., *Performance evaluation of a hybrid linear ion trap/orbitrap mass spectrometer*. Anal Chem, 2006. **78**(7): p. 2113-20.
97. Scigelova, M. and A. Makarov, *Orbitrap mass analyzer--overview and applications in proteomics*. Proteomics, 2006. **2**: p. 16-21.
98. Makarov, A., et al., *Dynamic range of mass accuracy in LTQ Orbitrap hybrid mass spectrometer*. J Am Soc Mass Spectrom, 2006. **17**(7): p. 977-82.
99. Lee, M.S. and M. Zhu, *Mass Spectrometry in Drug Metabolism and Disposition: Basic Principles and Applications*. 2011, Wiley.
100. Makarov, A. and M. Scigelova, *Coupling liquid chromatography to Orbitrap mass spectrometry*. Journal of Chromatography A, 2010. **1217**(25): p. 3938-3945.
101. Kohl, A., H.-K. Lim, and Y. Huang *Identification of GSH Conjugates Using Accurate Mass Data and MetWorks Software*. 2008
102. Rezai, T., et al. *ToxID Software for the Identification of Analytes in Various LC-MS Based Toxicology Screening Applications*.
103. Korfmacher, W.A., *Using Mass Spectrometry for Drug Metabolism Studies, Second Edition*. 2009: Taylor & Francis, Chapter 3, p.231.
104. Hu, Q., et al., *The Orbitrap: a new mass spectrometer*. J Mass Spectrom, 2005. **40**(4): p. 430-43.
105. Ma, S., S.K. Chowdhury, and K.B. Alton, *Application of mass spectrometry for metabolite identification*. Curr Drug Metab, 2006. **7**(5): p. 503-23.
106. Brazzarola, F., et al., *The mass spectrometric behaviour of fluorinated ephedrines under different protonating conditions*. Il Farmaco, 2003. **58**(1): p. 69-77.
107. Tozuka, Z., et al., *Strategy for structural elucidation of drugs and drug metabolites using (MS)ⁿ fragmentation in an electrospray ion trap*. J Mass Spectrom, 2003. **38**(8): p. 793-808.
108. Ragu, R., S.á. mezoglu, and W. Humphreys, *Metabolite Identification Strategies and Procedures*, in *Using Mass Spectrometry for Drug Metabolism Studies, Second Edition*. 2010, CRC Press. p. 127-203.

109. Schifano, F., et al., *Mephedrone (4-methylmethcathinone; 'meow meow'):* *chemical, pharmacological and clinical issues*. *Psychopharmacology*, 2011. **214**(3): p. 593-602.
110. Meyer, M.R., F.T. Peters, and H.H. Maurer, *Metabolism of the new designer drug mephedrone and toxicological detection of the beta keto designer drugs mephedrone, butylone and methylone in urine*. *Annales de Toxicologie Analytique*, 2009(2): p. 22-23.
111. Dargan, P.I., et al., *The pharmacology and toxicology of the synthetic cathinone mephedrone (4-methylmethcathinone)*. *Drug Testing and Analysis*, 2011. **3**(7-8): p. 454-463.
112. Dickson, A.J., et al., *Multiple-Drug Toxicity Caused by the Coadministration of 4-Methylmethcathinone (Mephedrone) and Heroin*. *Journal of Analytical Toxicology*, 2010. **34**(3): p. 162-168.
113. Wood, D.M., et al., *Recreational use of mephedrone (4-methylmethcathinone, 4-MMC) with associated sympathomimetic toxicity*. *Journal of medical toxicology : official journal of the American College of Medical Toxicology*, 2010. **6**(3): p. 327-30.
114. Torrance, H. and G. Cooper, *The detection of mephedrone (4-methylmethcathinone) in 4 fatalities in Scotland*. *Forensic science international*, 2010. **202**(1-3): p. E62-E63.
115. Deruiter, J., et al., *METHCATHINONE AND DESIGNER ANALOGS - SYNTHESIS, STEREOCHEMICAL ANALYSIS, AND ANALYTICAL PROPERTIES*. *Journal of Chromatographic Science*, 1994. **32**(12): p. 552-564.
116. Jankovics, P., et al., *Identification and characterization of the new designer drug 4'-methylethcathinone (4-MEC) and elaboration of a novel liquid chromatography–tandem mass spectrometry (LC–MS/MS) screening method for seven different methcathinone analogs*. *Forensic science international*, 2011. **210**(1): p. 213-220.
117. Brandt, S.D., et al., *Analysis of NRG 'legal highs' in the UK: identification and formation of novel cathinones*. *Drug Testing and Analysis*, 2011. **3**(9): p. 569-575.

118. Kazakevich, Y.V. and R. LoBrutto, *HPLC for Pharmaceutical Scientists*. 2007: John Wiley & Sons, p.788.
119. Kalendra, D.M. and B.R. Sickles, *Diminished reactivity of ortho-substituted phenacyl bromides toward nucleophilic displacement*. *J Org Chem*, 2003. **68**(4): p. 1594-6.
120. Jacobsen, N.E., *NMR Spectroscopy Explained: Simplified Theory, Applications and Examples for Organic Chemistry and Structural Biology*. . 2007: John Wiley & Sons, Inc.
121. Scott, A.I., *Interpretation of the ultraviolet spectra of natural products*. International series of monographs on organic chemistry v. 7. 1964: Oxford, New York, Pergamon Press.
122. Singh, N., et al., *LC Purity and Related Substances Screening for Mephedrone*. *Journal of Pharmacy and Pharmacology*, 2010. **62**(10): p. 1209-1210.
123. C. Rambabu, S.V.R., A. B. Babu, *Qualitative analysis of mephedrone in bulk and pharmaceutical formulations by reverse phase high performance liquid chromatography*. *Rasayan Journal of Chemistry*, 2010(3): p. 796-799.
124. Wood, D.M., et al., *Case series of individuals with analytically confirmed acute mephedrone toxicity*. *Clinical Toxicology*, 2010. **48**(9): p. 924-927.
125. Maskell, P.D., et al., *Mephedrone (4-Methylmethcathinone)-Related Deaths*. *Journal of Analytical Toxicology*, 2011. **35**(3): p. 188-191.
126. Sorensen, L.K., *Determination of cathinones and related ephedrine in forensic whole-blood samples by liquid-chromatography-electrospray tandem mass spectrometry*. *Journal of Chromatography B-Analytical Technologies in the Biomedical and Life Sciences*, 2011. **879**(11-12): p. 727-736.
127. Wissenbach, D.K., et al., *Drugs of abuse screening in urine as part of a metabolite-based LC-MSⁿ screening concept*. *Analytical and Bioanalytical Chemistry*, 2011. **400**(10): p. 3481-3489.
128. Bell, C., et al., *Development of a rapid LC-MS/MS method for direct urinalysis of designer drugs*. *Drug Testing and Analysis*, 2011. **3**(7-8): p. 496-504.

129. Snyder, L.R., J.J. Kirkland, and J.L. Glajch, *Practical HPLC Method Development*. 1997: John Wiley & Sons, pp.307-395.
130. KONAKANCHI, N., *Application of novel NMR techniques in the determination of illicit drug substances*, in *Strathclyde Institute of Pharmacy and biomedical Science* 2011, University of Strathclyde: University of Strathclyde.
131. Khreit, O.I.G., et al., *Synthesis, full chemical characterisation and development of validated methods for the quantification of the components found in the evolved "legal high" NRG-2*. *Journal of Pharmaceutical and Biomedical Analysis*, 2012. **61**(0): p. 122-135.
132. Meyer, M.R., et al., *New cathinone-derived designer drugs 3-bromomethcathinone and 3-fluoromethcathinone: studies on their metabolism in rat urine and human liver microsomes using GC-MS and LC-high-resolution MS and their detectability in urine*. *Journal of Mass Spectrometry*, 2012. **47**(2): p. 253-262.
133. Brandt, S.D., P.F. Daley, and N.V. Cozzi, *Analytical characterization of three trifluoromethyl-substituted methcathinone isomers*. *Drug Testing and Analysis*, 2012. **4**(6): p. 525-529.
134. Kamleh, A., et al., *Metabolomic profiling using Orbitrap Fourier transform mass spectrometry with hydrophilic interaction chromatography: a method with wide applicability to analysis of biomolecules*. *Rapid Communications in Mass Spectrometry*, 2008. **22**(12): p. 1912-1918.
135. Waters. <http://www.waters.com/waters/nav.htm?cid=513211>. [cited 2013 16/02/2013].
136. Kalendra, D.M. and B.R. Sickles, *Diminished reactivity of ortho-substituted phenacyl bromides toward nucleophilic displacement*. *Journal of Organic Chemistry*, 2002. **68**(4): p. 1594-1596.
137. Moldeus, P., J. Hogberg, and S. Orrenius, *Isolation and use of liver cells*. *Methods Enzymol*, 1978. **52**: p. 60-71.
138. Hayward, M., et al., *Techniques to Facilitate the Performance of Mass Spectrometry: Sample Preparation, Liquid Chromatography, and Non-Mass-*

- Spectrometric Detection*, in *Mass Spectrometry in Drug Metabolism and Disposition*. 2011, John Wiley & Sons, Inc. p. 353-381.
139. Papeleu, P., et al., *Isolation of Rat Hepatocytes*, in *Cytochrome P450 Protocols*, I. Phillips and E. Shephard, Editors. 2006, Humana Press. p. 229-237.
140. Sinz, M.W., *In Vitro Metabolism:Hepatocytes*, in *Handbook of Drug Metabolism*. p. 445-464.
141. Creek, D.J., et al., *Toward Global Metabolomics Analysis with Hydrophilic Interaction Liquid Chromatography–Mass Spectrometry: Improved Metabolite Identification by Retention Time Prediction*. *Analytical Chemistry*, 2011. **83**(22): p. 8703-8710.
142. Frison, G., et al., *Gas chromatography/mass spectrometry determination of mephedrone in drug seizures after derivatization with 2,2,2-trichloroethyl chloroformate*. *Rapid Communications in Mass Spectrometry*, 2011. **25**(2): p. 387-390.
143. Meyer, M.R., et al., *New cathinone-derived designer drugs 3-bromomethcathinone and 3-fluoromethcathinone: studies on their metabolism in rat urine and human liver microsomes using GC-MS and LC-high-resolution MS and their detectability in urine*. *J Mass Spectrom*, 2012. **47**(2): p. 253-62.
144. Castell, J.V. and M.J. Gómez-Lechón, *In Vitro Methods in Pharmaceutical Research*. 1997: Academic Press , pp.137-138.
145. Coundouris, J.A., et al., *Cryopreservation of human adult hepatocytes for use in drug metabolism and toxicity studies*. *Xenobiotica*, 1993. **23**(12): p. 1399-409.
146. Klieber, S., et al., *The use of human hepatocytes to investigate drug metabolism and CYP enzyme induction*. *Methods Mol Biol*, 2010. **640**: p. 295-308.
147. Li, A.P., et al., *Cryopreserved human hepatocytes: characterization of drug-metabolizing activities and applications in higher throughput screening assays for hepatotoxicity, metabolic stability, and drug–drug interaction potential*. *Chemico-Biological Interactions*, 1999. **121**(1): p. 17-35.

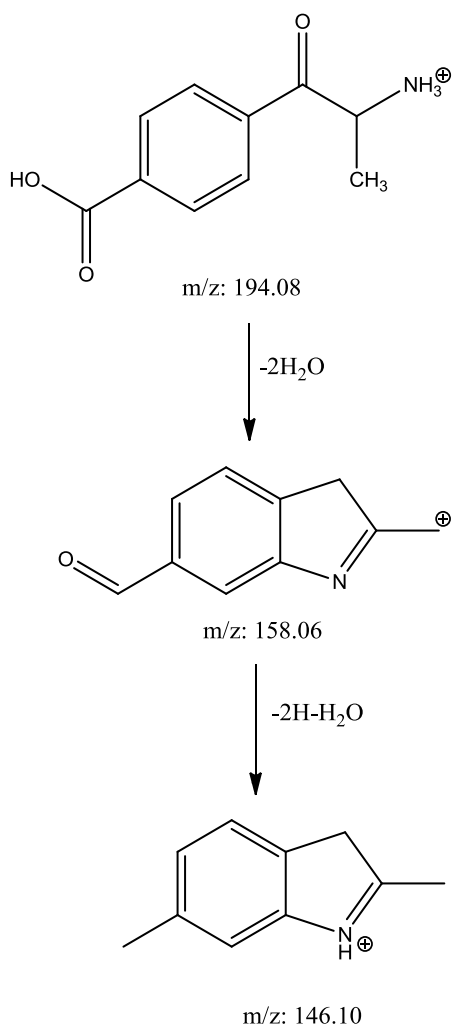
148. Ingelman-Sundberg, M., *Genetic polymorphisms of cytochrome P450 2D6 (CYP2D6): clinical consequences, evolutionary aspects and functional diversity*. Pharmacogenomics J, 2004. **5**(1): p. 6-13.
149. Zanger, U., S. Raimundo, and M. Eichelbaum, *Cytochrome P450 2D6: overview and update on pharmacology, genetics, biochemistry*. Naunyn-Schmiedeberg's Archives of Pharmacology, 2004. **369**(1): p. 23-37.
150. Spina, E., et al., *Relationship between plasma desipramine levels, CYP2D6 phenotype and clinical response to desipramine: a prospective study*. European Journal of Clinical Pharmacology, 1997. **51**(5): p. 395-398.
151. Wuttke, H., et al., *Increased frequency of cytochrome P450 2D6 poor metabolizers among patients with metoprolol-associated adverse effects*. Clin Pharmacol Ther, 2002. **72**(4): p. 429-37.
152. Rau, T., et al., *Effect of the CYP2D6 genotype on metoprolol metabolism persists during long-term treatment*. Pharmacogenetics, 2002. **12**(6): p. 465-72.
153. de la Torre, R., et al., *MDMA (ecstasy) pharmacokinetics in a CYP2D6 poor metaboliser and in nine CYP2D6 extensive metabolisers*. European Journal of Clinical Pharmacology, 2005. **61**(7): p. 551-4.
154. Khreit, O.I.G., et al., *Elucidation of the Phase I and Phase II metabolic pathways of (±)-4'-methylmethcathinone (4-MMC) and (±)-4'-(trifluoromethyl)methcathinone (4-TFMMC) in rat liver hepatocytes using LC-MS and LC-MS2*. Journal of Pharmaceutical and Biomedical Analysis, (0).
155. Seddon, T., I. Michelle, and R.J. Chenery, *Comparative drug metabolism of diazepam in hepatocytes isolated from man, rat, monkey and dog*. Biochemical Pharmacology, 1989. **38**(10): p. 1657-1665.
156. Dettmer, K., P.A. Aronov, and B.D. Hammock, *Mass spectrometry-based metabolomics*. Mass Spectrom Rev, 2007. **26**(1): p. 51-78.

Appendices

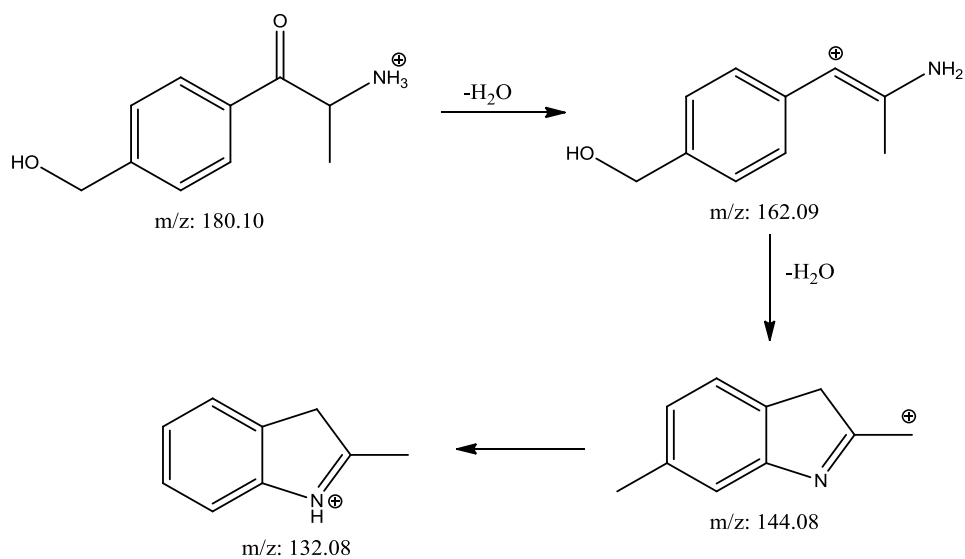
Appendix 1:

Many of these fragmentation pattern interpretations are just putative. They fit with the elemental compositions obtained for the fragments but often do not fit the expected rules of fragmentation.

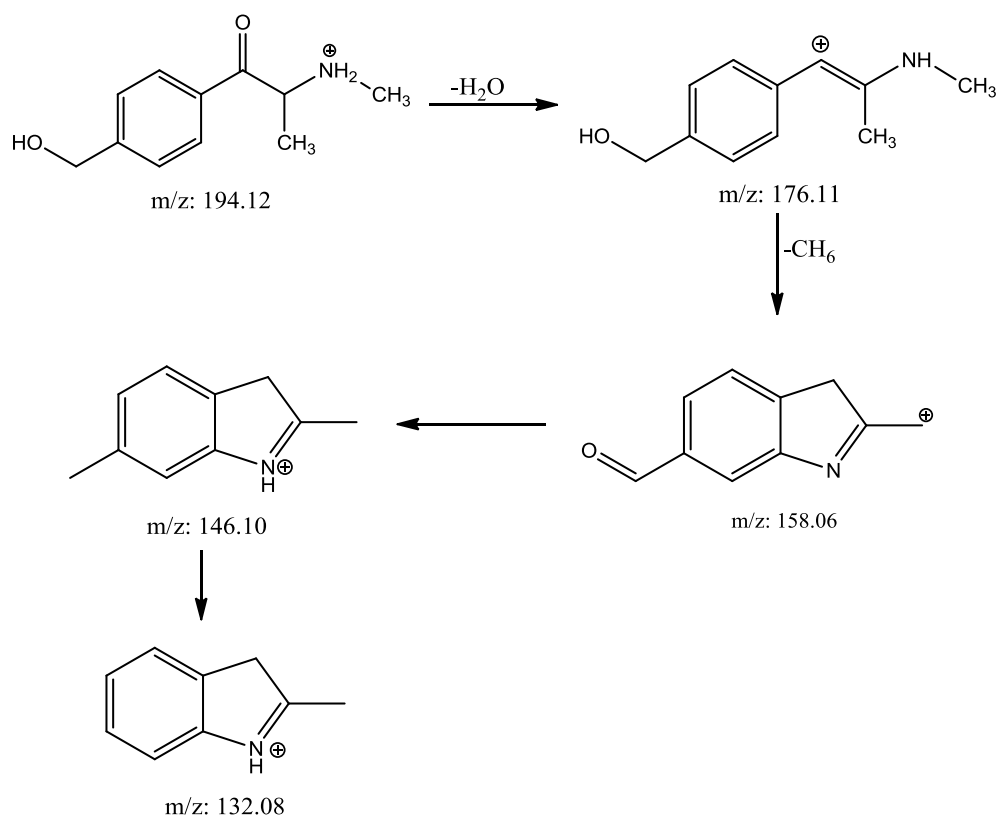
1.1 Scheme for the proposed fragmentation of metabolite13, fragmentation can be formed a conjugated indole.



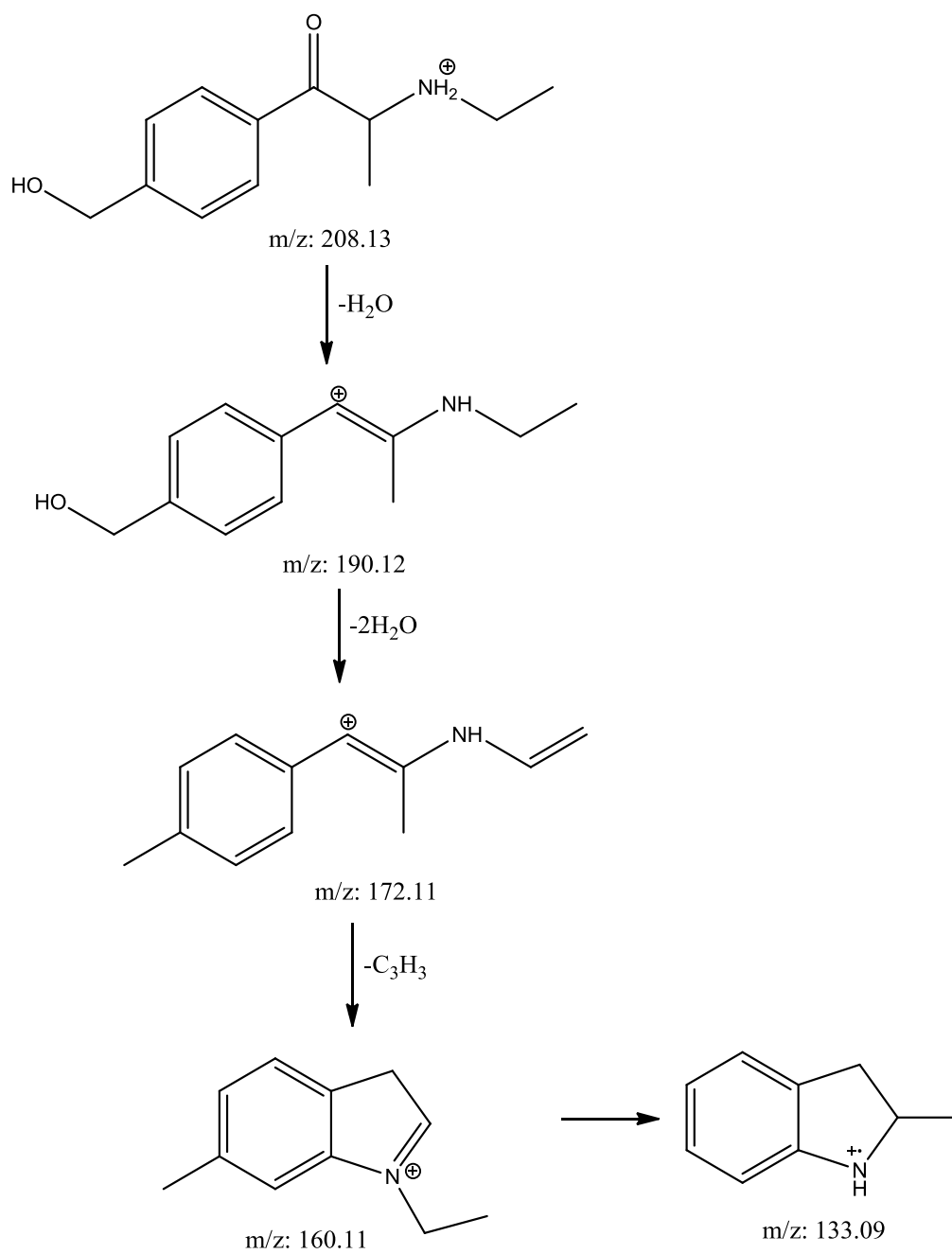
1.2 Scheme for the proposed fragmentation of metabolite14, fragmentation can be formed a conjugated indole.



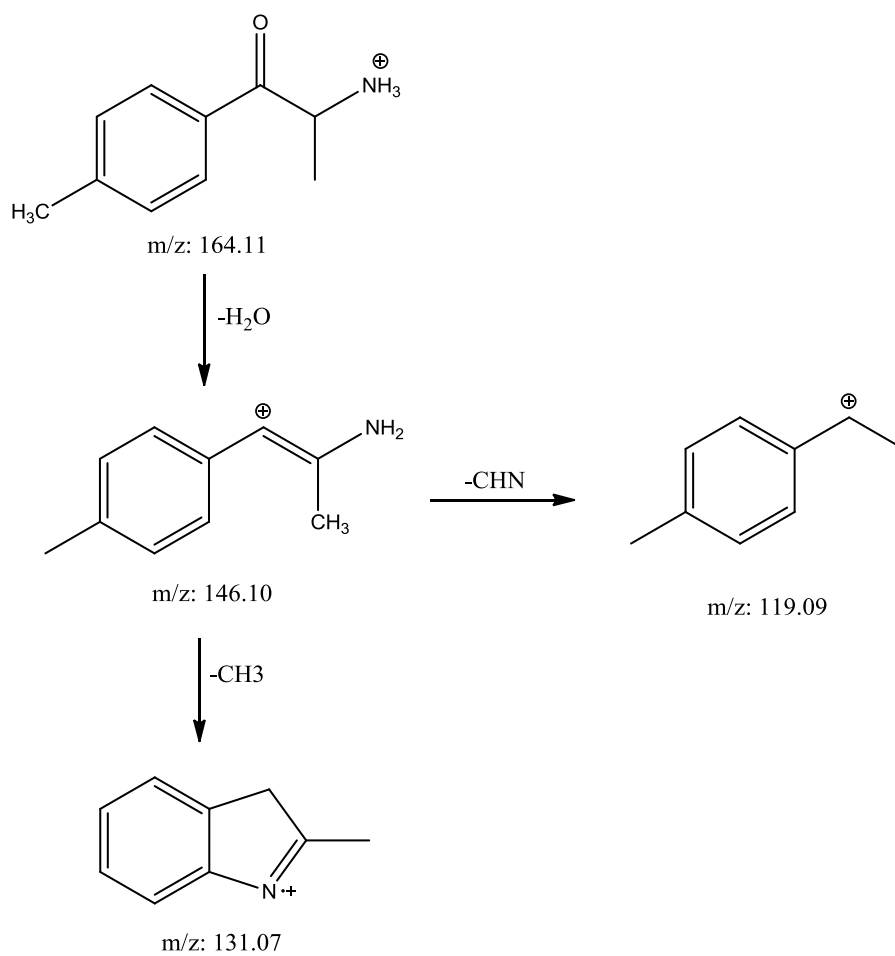
1.3 Scheme for the proposed fragmentation of metabolite16, fragmentation can be formed a conjugated indole.



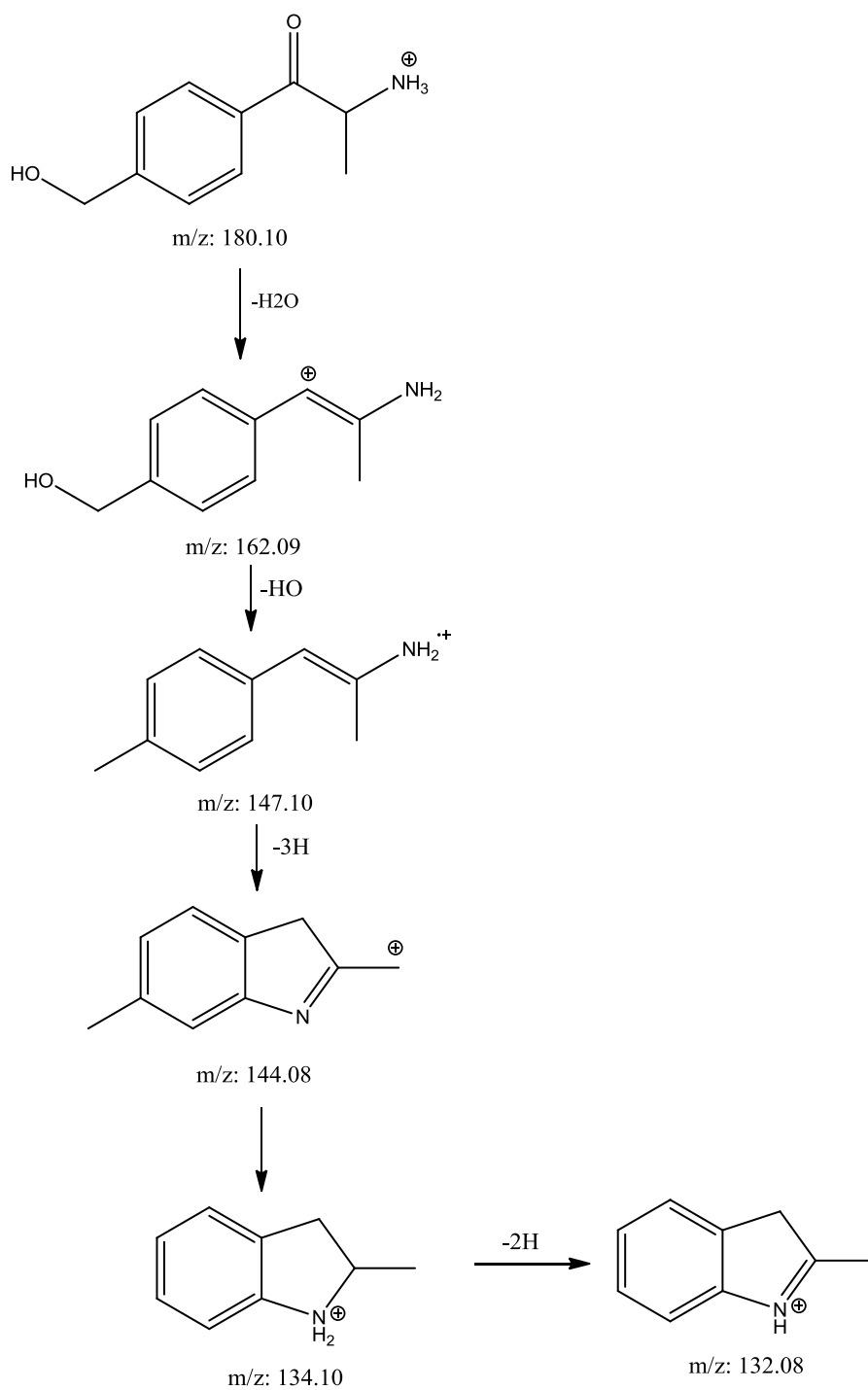
1.4 Scheme for the proposed fragmentation of metabolite35, fragmentation can be formed a conjugated indole.



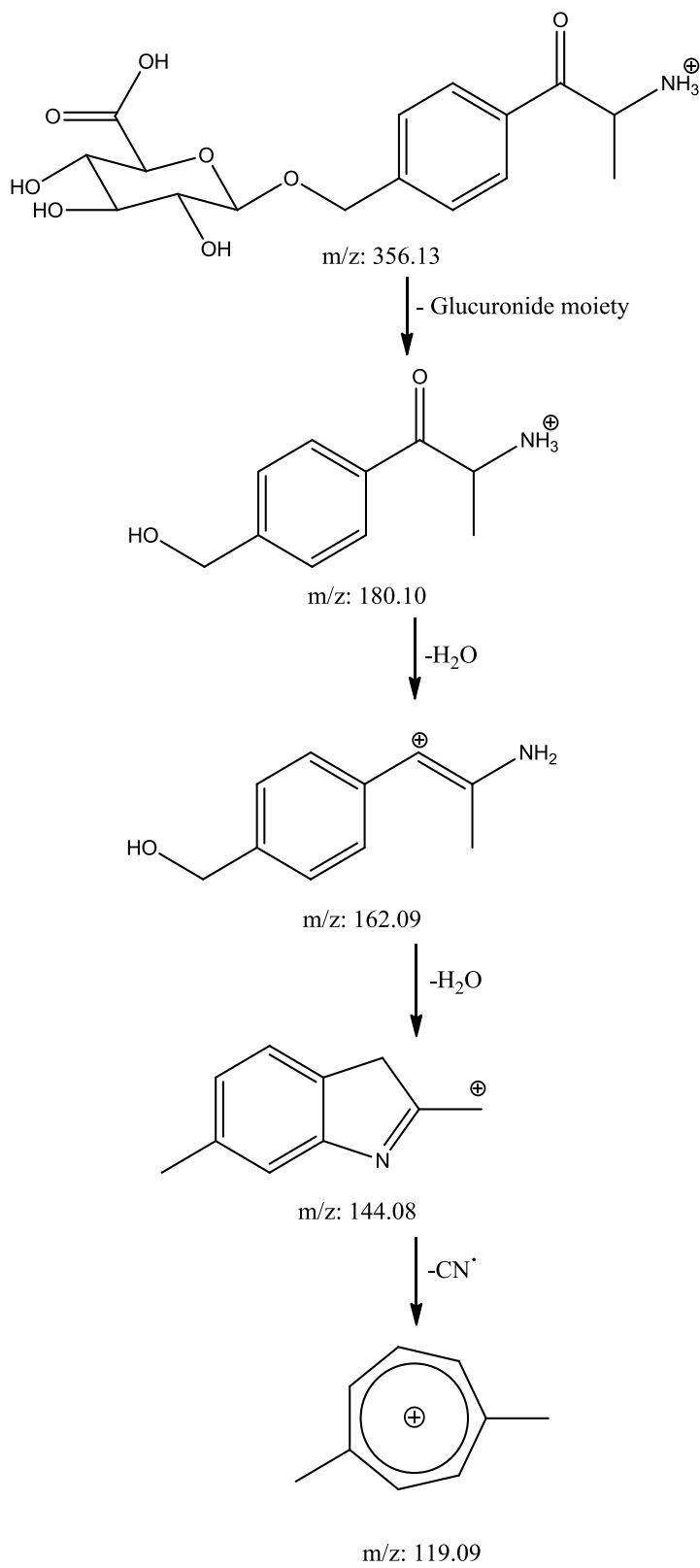
1.5 Scheme for the proposed fragmentation of metabolite36, fragmentation can be formed a conjugated indole.



1.6 Scheme for the proposed fragmentation of metabolite43, fragmentation can be formed a conjugated indole.

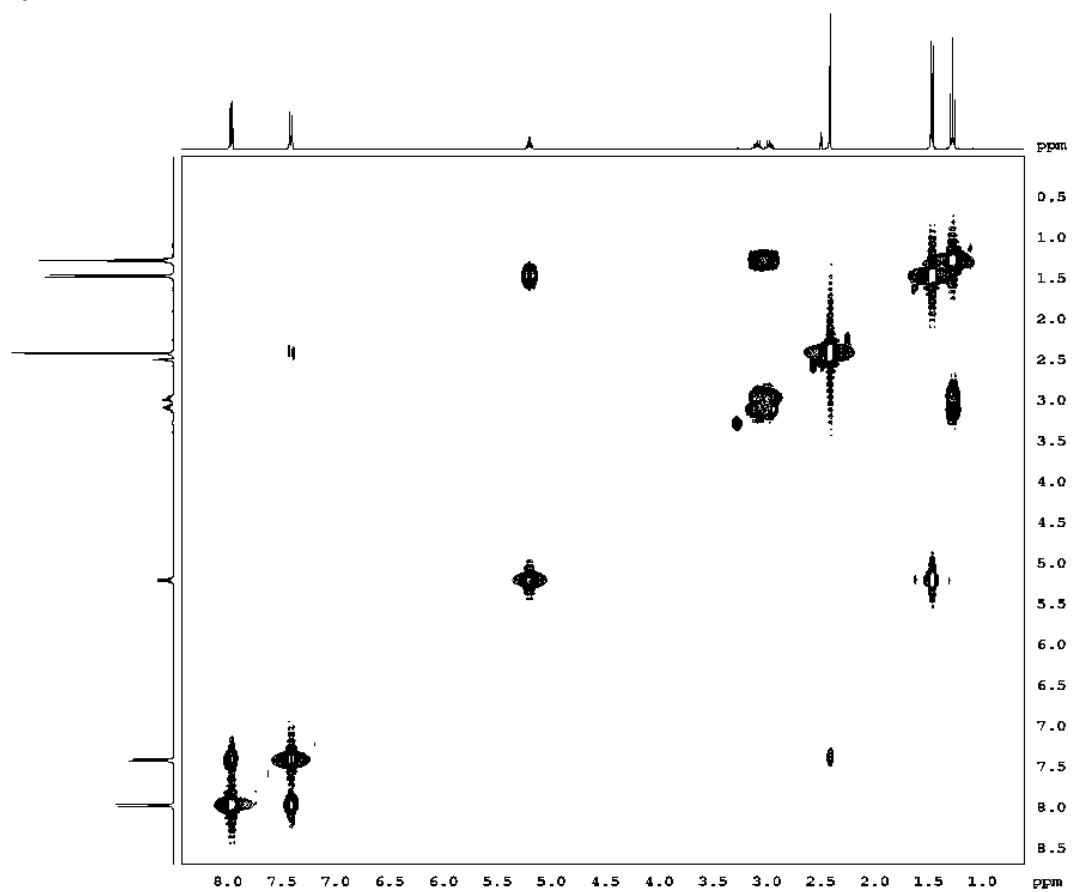


1.7 Scheme for the proposed fragmentation of metabolite48, fragmentation can be formed a conjugated indole.

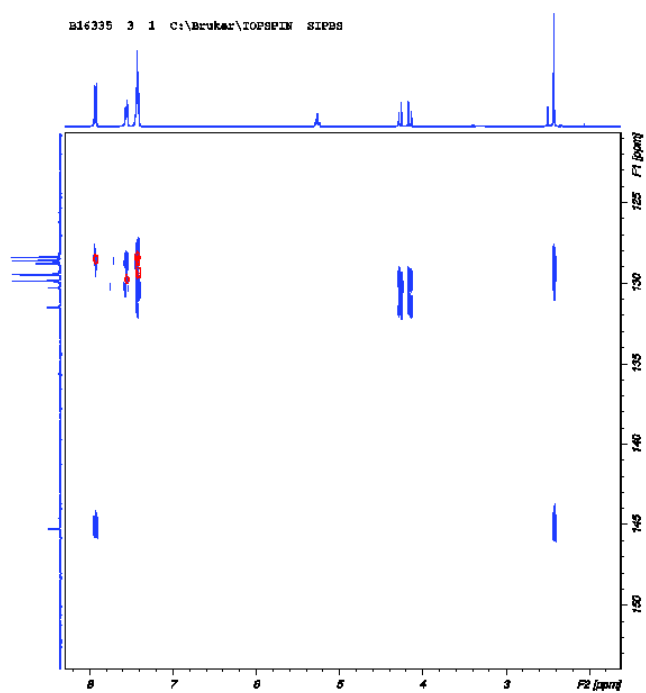


Appendix 2:

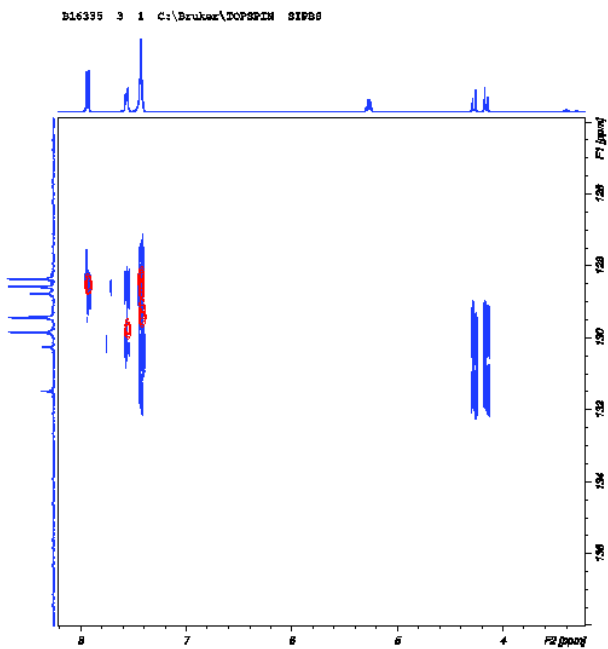
2.1 2D [^1H , ^1H] COSY NMR spectrum of (\pm)-4'-methyl-N-ethylcathinone hydrobromide



2.2 2D [¹H, ¹H] COSY NMR spectrum of (±)-4'-methyl-N-benzylcathinone hydrobromide

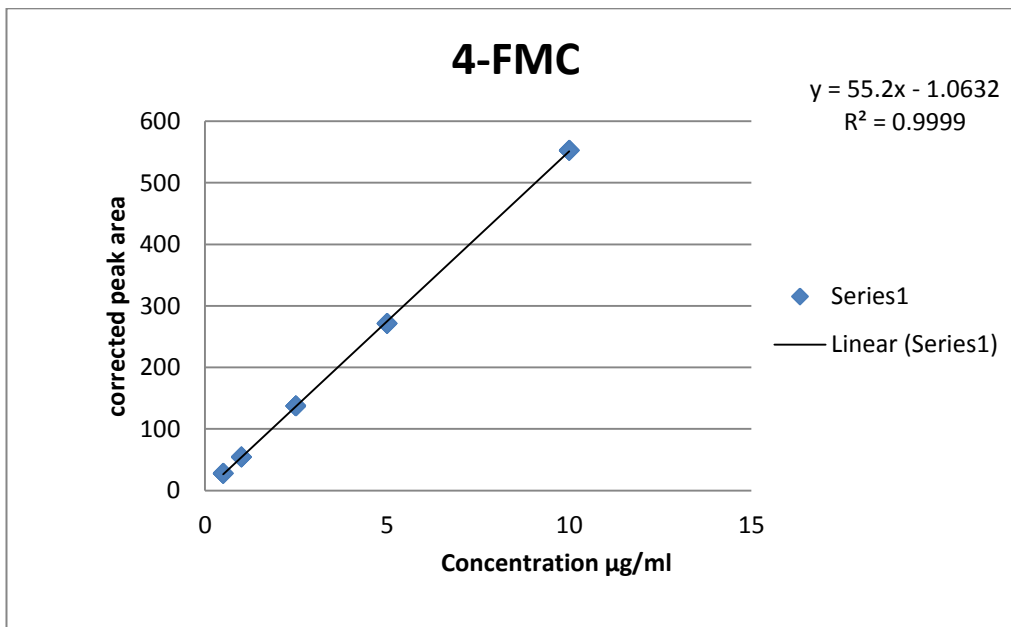


2.3 2D [¹H, ¹H] COSY NMR spectrum (expanded) of (±)-4'-methyl-N-benzylcathinone hydrobromide

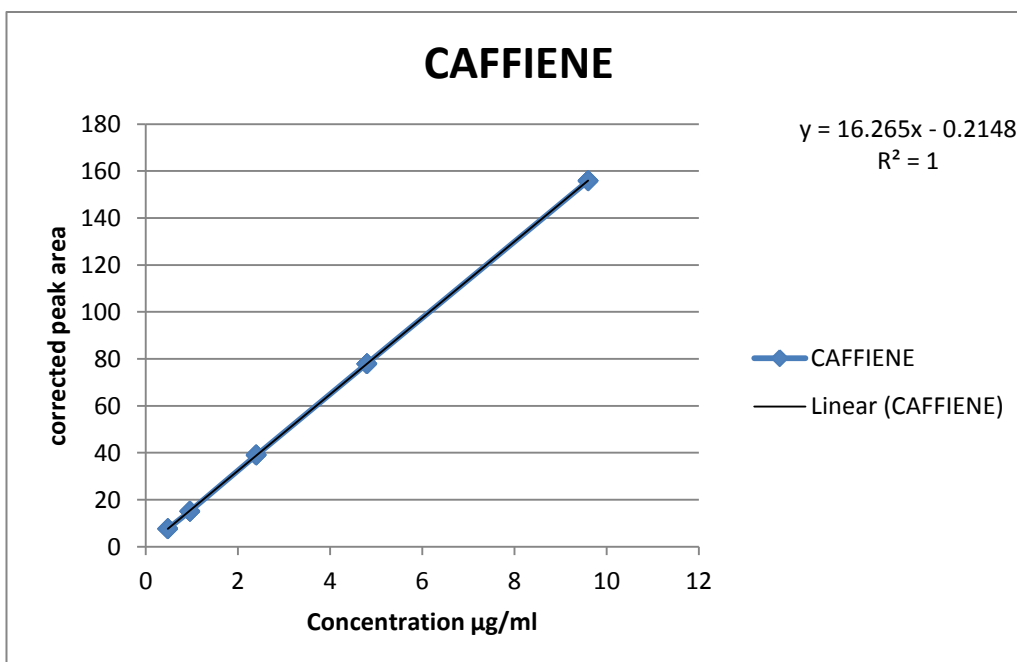


Appendix 3: Calibration curve of common NRG-2 ingredients and adulterants injected six times at different concentrations

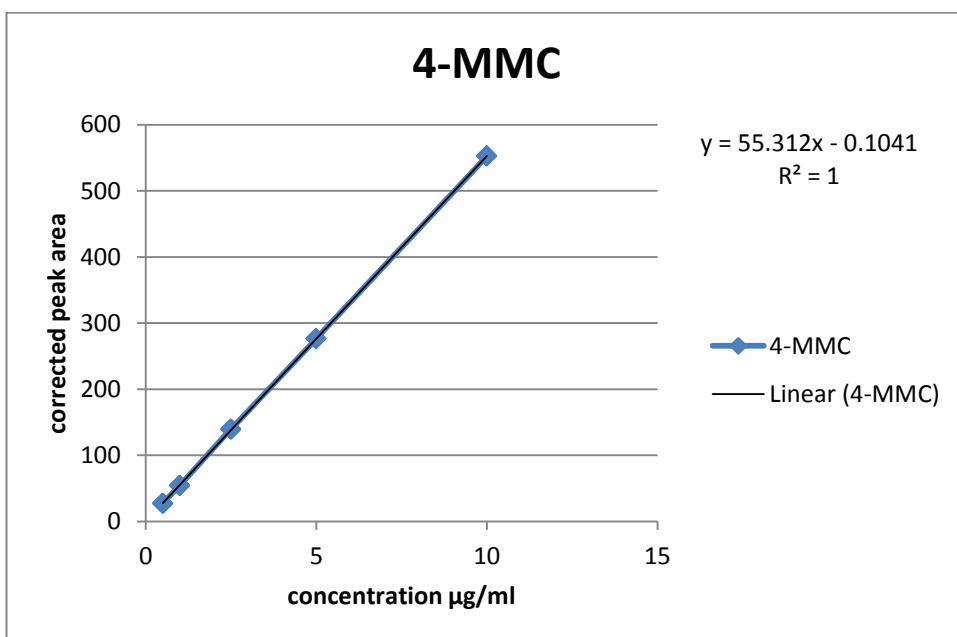
3.1 Calibration curve of 4-FMC (4c) (0.5 – 10 µg/mL)



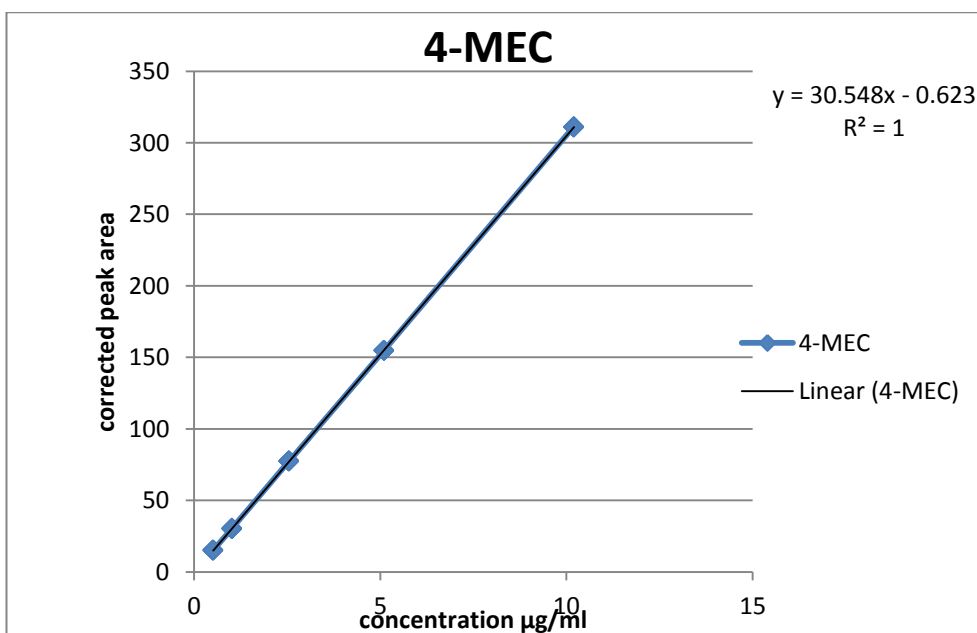
3.2 Calibration curve of caffeine (0.5 – 10 µg/mL)



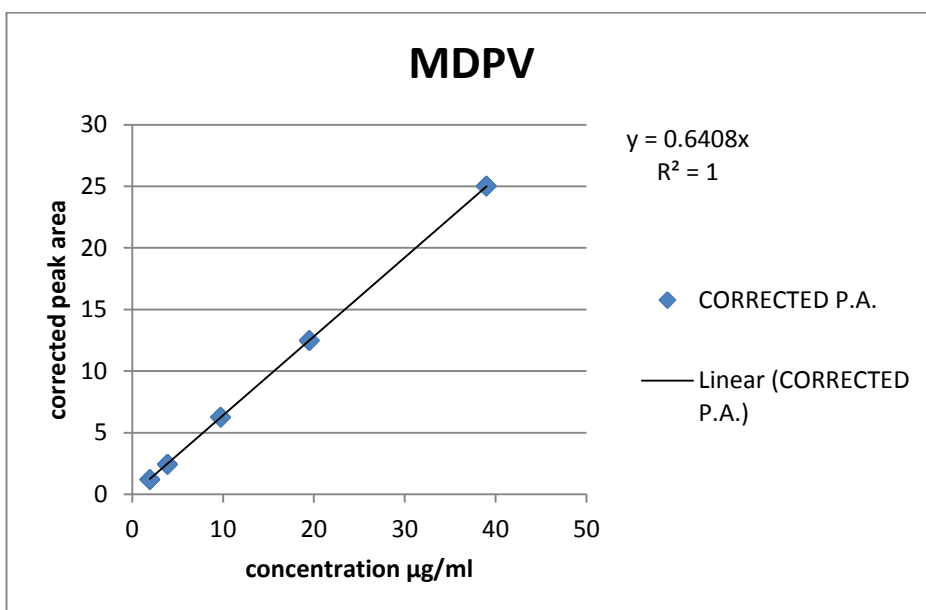
3.3 Calibration curve of 4-MMC (3a) (0.5 – 10 µg/mL)



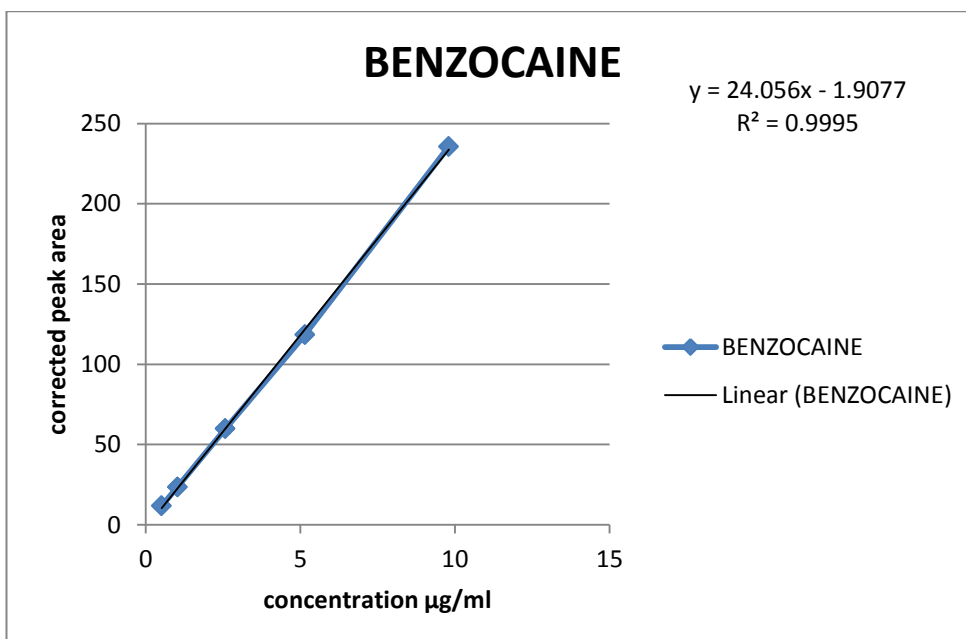
3.4 Calibration curve of 4-MEC (3c) (0.5 – 10 µg/mL)



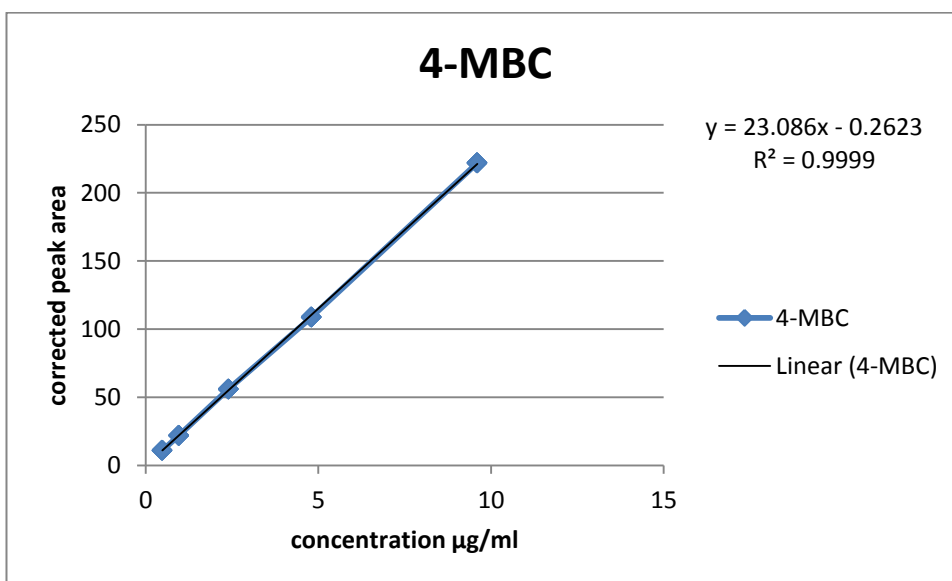
3.5 Calibration curve of MDPV (7c) (2 – 40 µg/mL)



3.6 Calibration curve of benzocaine (0.5 – 10 µg/mL)

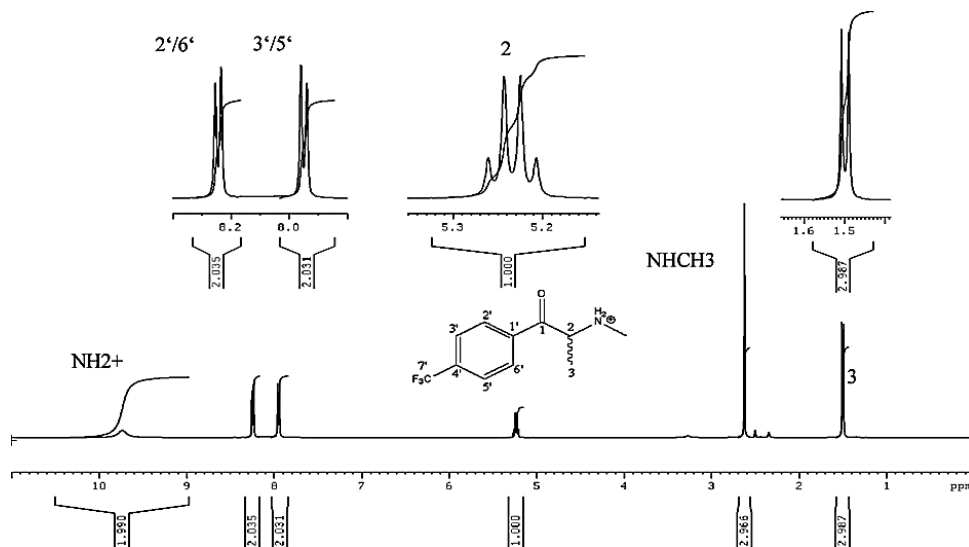


3.7 Calibration curve of 4-MBC (3d) (0.5 – 10 µg/mL)

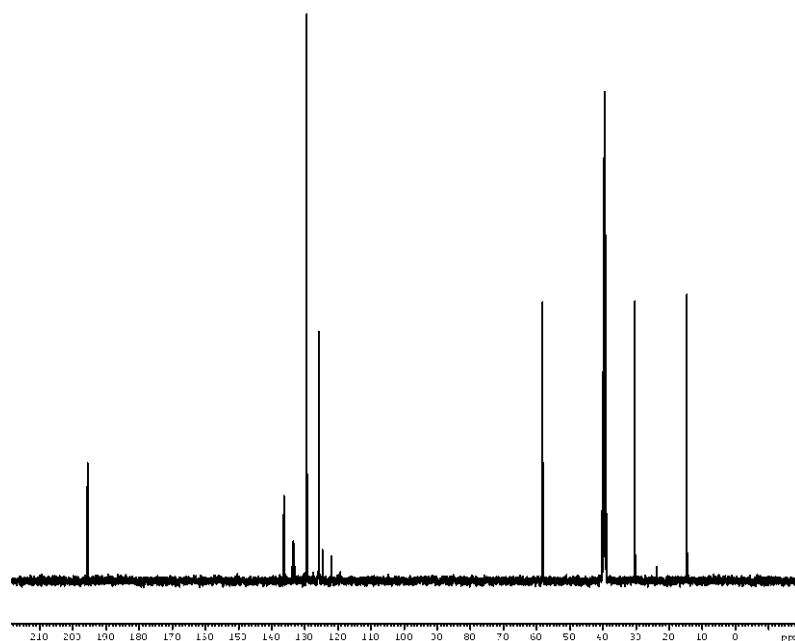


Appendix 4 :

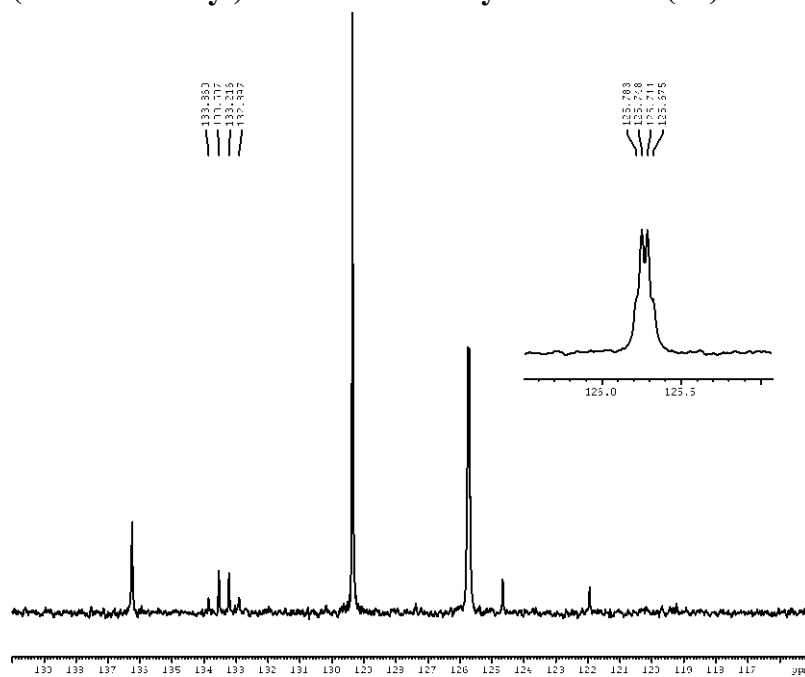
4.1 ^1H -NMR spectrum (d_6 -DMSO, 60 °C) of (\pm)-4'-(trifluoromethyl) methcathinone hydrochloride (3b)



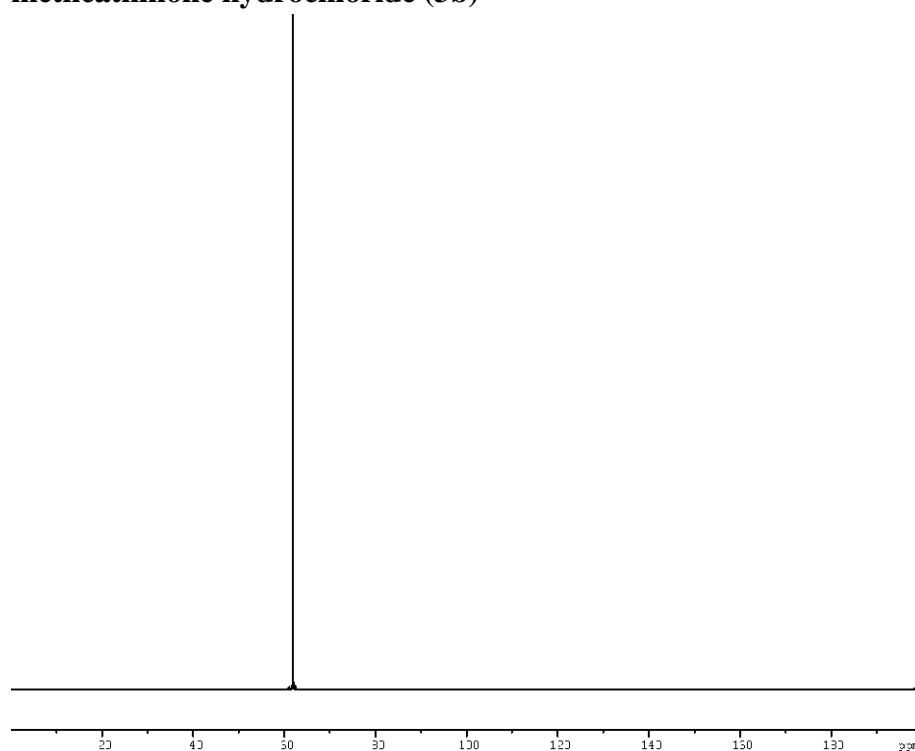
4.2 ^{13}C -NMR spectrum (d_6 -DMSO, 60 °C) of (\pm)-4'-(trifluoromethyl) methcathinone hydrochloride (3b)



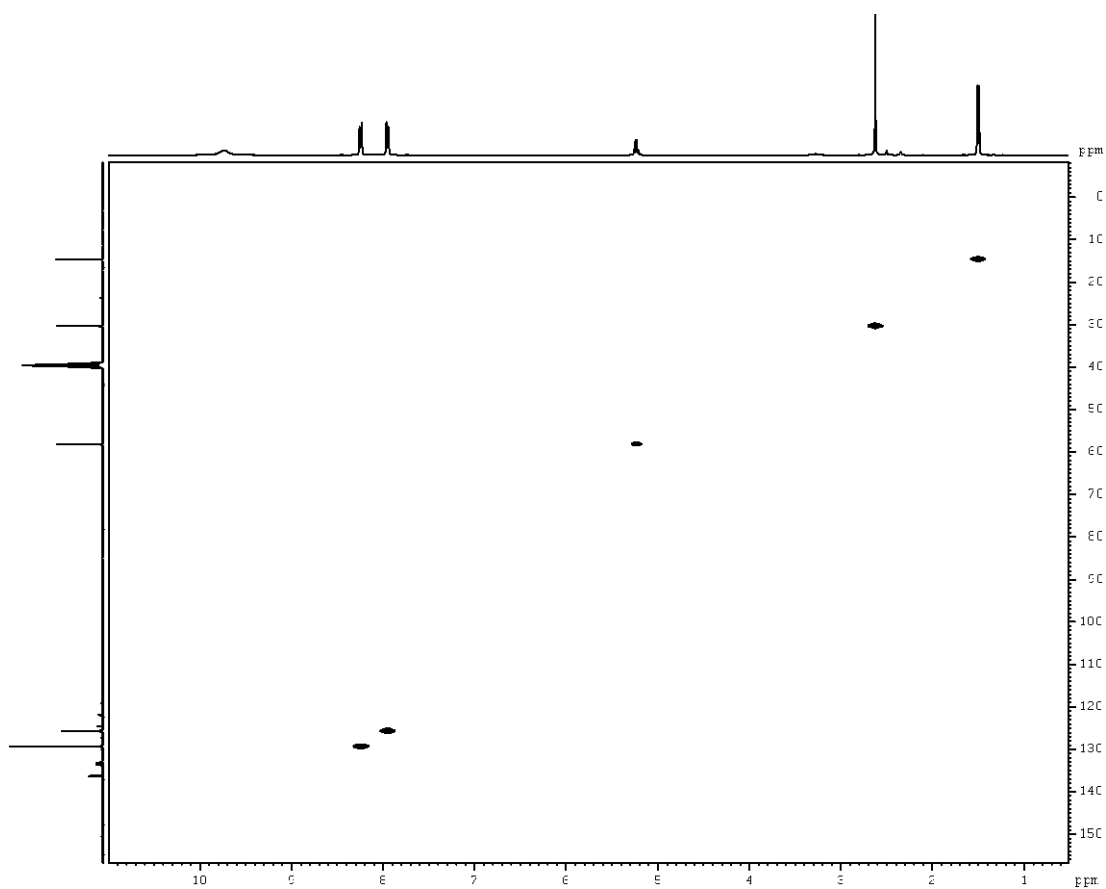
4.3 Expanded ^{13}C -NMR spectrum (d_6 -DMSO, 60 °C, 110 – 140 ppm) of (\pm)-4'-(trifluoromethyl) methcathinone hydrochloride (3b)



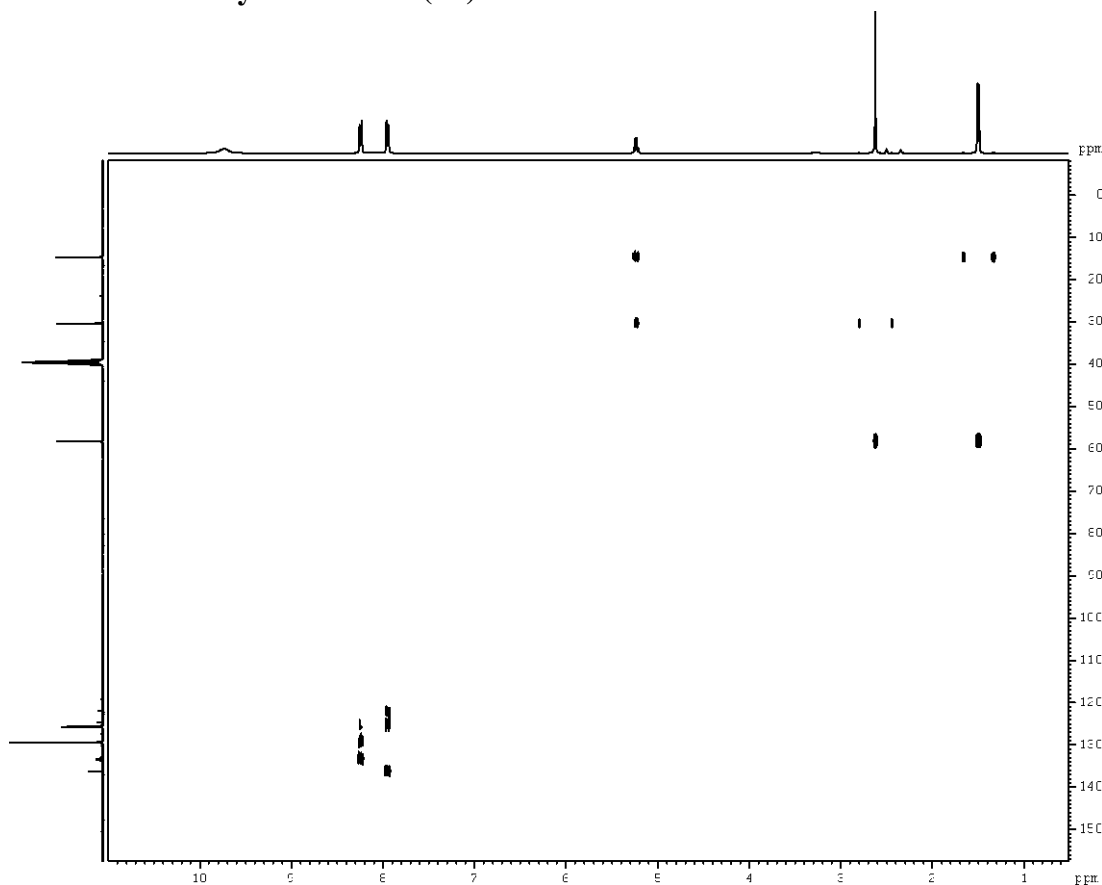
4.4 ^{19}F -NMR spectrum (d_6 -DMSO, 60 °C) of (\pm)-4'-(trifluoromethyl) methcathinone hydrochloride (3b)



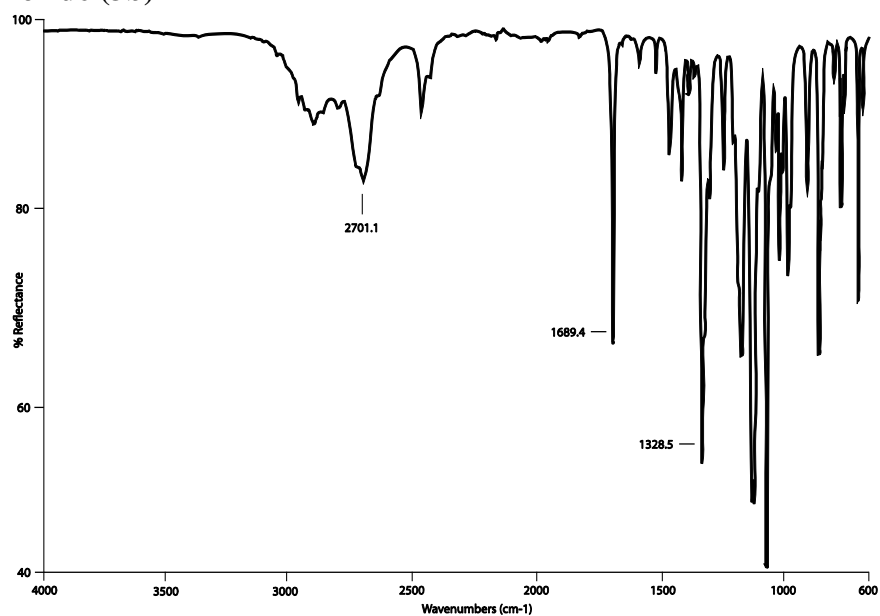
4.5 HSQC spectrum (d_6 -DMSO, 60 °C) of (\pm)-4'-(trifluoromethyl)methcathinone hydrochloride (3b)



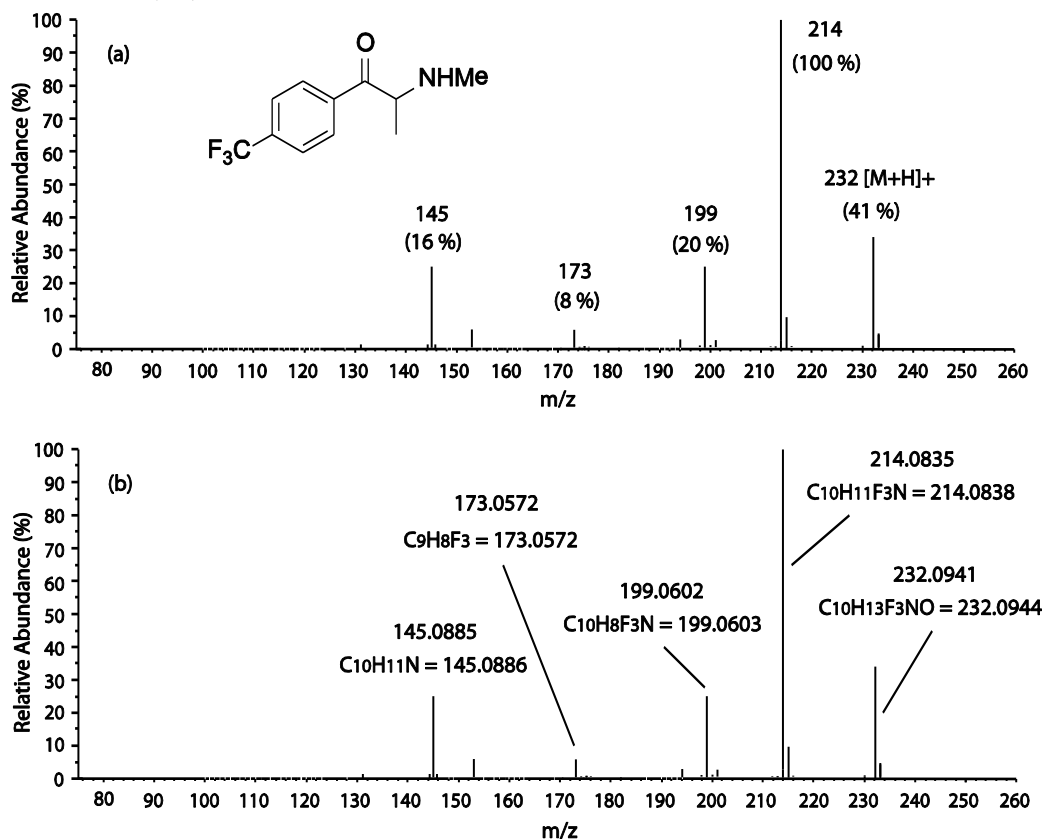
4.6 HMBC spectrum (d_6 -DMSO, 60 °C) of (\pm)-4'-(trifluoromethyl) methcathinone hydrochloride (3b)



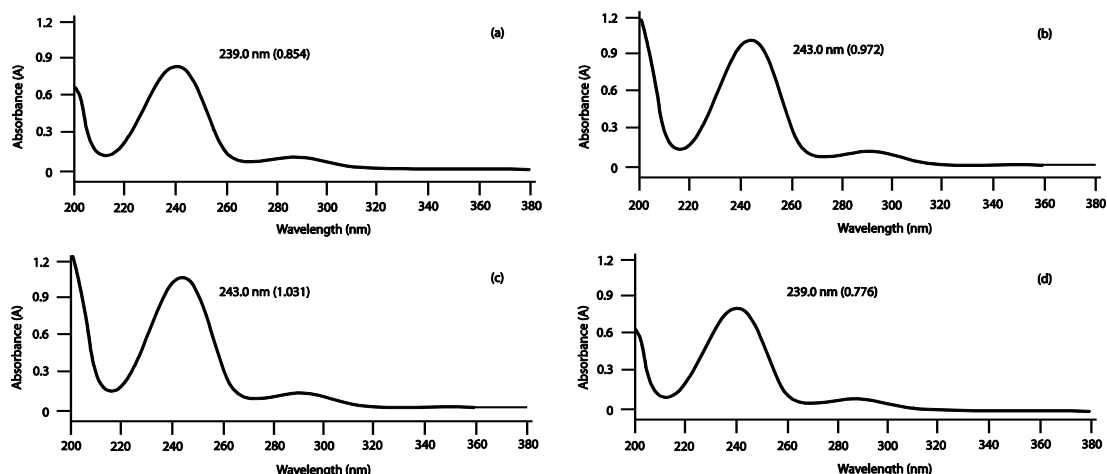
4.7 ATR-FTIR spectrum of (\pm)-4'-(trifluoromethyl) methcathinone hydrochloride (3b)



4.8 (a) LRMS and (b) HRMS spectra of (\pm)-4'-(trifluoromethyl)methcathinone hydrochloride (3b)



4.9 UV spectra of (\pm)-4'-(trifluoromethyl)methcathinone hydrochloride (3b) in (a) EtOH: 3b, c = 2.0 x 10⁻³ g/100 mL; (b) H₂O: 3b, c = 2.0 x 10⁻³ g/100 mL; (c) 0.1 M aqueous HCl: 3b, c = 2.0 x 10⁻³ g/100 mL; (d) 0.1 M aqueous NaOH: 3b, c = 2.0 x 10⁻³ g/100 mL.



Appendix 5

Schematic setup of the perfusion equipment (Obtained from Dr. Mark Jairaj Thesis 2002)

